



MONASH University

Developing Novel Anionic Copolymers and  
Investigation of the Influence of Water Quality  
on their Dissolution and Performance

Vu Huy Dao

*BE(Chem)(Hons) & BSc*

A thesis submitted for the degree of  
Doctor of Philosophy at Monash University in 2019

School of Chemistry  
Faculty of Science  
Monash University

This page is intentionally left blank.

# Copyright Notices

© Vu H. Dao (2019)

I certify that I have made all reasonable efforts to secure copyright permissions for third-party content included in this thesis and have not knowingly added copyright content to my work without the owner's permission.

# Declaration

I hereby declare that this thesis contains no material which has been accepted for the award of any other degree or diploma at any university or equivalent institution and that, to the best of my knowledge and belief, this thesis contains no material previously published or written by another person, except where due reference is made in the text of the thesis.

This thesis includes 2 original papers published in peer reviewed journals and 2 unpublished publications. The core theme of the thesis is *“design and synthesis of novel polymeric materials for flocculation applications in high ionic strength environment”*. The ideas, development and writing up of all the papers in the thesis were the principal responsibility of myself, the student, working within the School of Chemistry in the Faculty of Science under the supervision of Associate Professor Kei Saito and Professor Neil Cameron.

The inclusion of co-authors reflects the fact that the work came from active collaboration between researchers and acknowledges input into team-based research.

In the case of Chapter 1, Chapter 2, Chapter 3, and Chapter 4, my contribution to the work involved the following:

Thesis Chapter	Publication Title	Status	Nature and % of student contribution	Co-author name(s) Nature and % of contribution	Co-author(s), Monash student Y/N
1	Synthesis, properties and performance of organic polymers employed in flocculation applications	Published	80%. Concept, collection of data, and preparation of first draft.	A/Prof. Kei Saito. 10%. Key idea & manuscript editing. Prof. Neil Cameron. 10% Key idea and manuscript editing.	No
2	Synthesis of ultra-high molecular weight ABA triblock copolymers <i>via</i> aqueous RAFT-mediated gel polymerisation, end group modification and chain coupling	Published	80%. Concept, collection of data, and preparation of first draft.	A/Prof. Kei Saito. 10%. Key idea & manuscript editing. Prof. Neil Cameron. 10% Key idea and manuscript editing.	No
3	Enhanced flocculation efficiency in high ionic strength environment by the aid of anionic ABA triblock copolymers	Submitted	65%. Concept, collection of data, and preparation of first draft.	A/Prof. Kei Saito. 10%. Key idea & manuscript editing. Prof. Neil Cameron. 10% Key idea and manuscript editing. Dr Philip Fawell. 6%. Manuscript editing. Dr Krishna Mohanarangam. 6%. Manuscript editing. Mr Kosta Simic. 3%. Input into manuscript.	No
4	Synthesis of UHMW star-shaped AB block copolymers and their flocculation efficiency in high ionic strength environments	Submitted	80%. Concept, collection of data, and preparation of first draft.	A/Prof. Kei Saito. 10%. Key idea & manuscript editing. Prof. Neil Cameron. 10% Key idea and manuscript editing.	No

I have not renumbered sections of submitted or published papers in order to generate a consistent presentation within the thesis.

**Student Signature:**

**Date:** 24/06/2019

The undersigned hereby certify that the above declaration correctly reflects the nature and extent of the student's and co-authors' contributions to this work. In instances where I am not the responsible author I have consulted with the responsible author to agree on the respective contributions of the authors.

**Main Supervisor Signature:**

**Date:** 24/06/2019

# Acknowledgements

The completion of this thesis was only possible due to the help and support of many people. Firstly, I would like to express my sincere gratitude towards my academic supervisors, Associate Professor Kei Saito and Professor Neil Cameron. Thank you both for believing in me and provided me with the opportunity to pursue a PhD. Kei, thank you so much for your enthusiasm, as well as your patience and reassurance you have given every time I have any doubts about the progress of the project. Without your support and scientific guidance, the project wouldn't be where it is today. Neil, thank you so much for your enormous support, as well as the many insightful discussions and suggestions you have given towards the research project. Both of your continuous support, patience, guidance and encouragement throughout the years have shaped me into a professional polymer scientist, and for that I am extremely grateful.

I would also like to extend a thank you to my industry supervisor, Dr Richard Macoun for his time and professional input for the research project. In addition, thank you for your encouragement and recommendation in getting involved with various BASF activities and events. Thank you to Mr Greg Catterall for his continuous support with the PhD project and the C&P GRIP program.

This research was supported by an Australian Government Research Training Program (RTP) Scholarship. For financial support, I would like to acknowledge BASF Australia, the School of Chemistry at Monash University, as well as the Chemicals and Plastics Manufacturing Innovation Network and Training (C&P GRIP) program, supported by Monash University, Chemistry Australia and the Victorian Government of Australia.

Thank you to Professor Antonio Patti for his strong enthusiasm and devotion with the C&P GRIP program. His energetic attitude and passion have made us recognise the importance of industry-university collaborations. Professor Karen Hapgood, Dr Ilija Sutalo, Associate Professor Victoria Haritos, and Dr Gary Annat are also acknowledged for the management of this program. Thank you to Dr Christian Rein

for his professional input throughout the first year of the research project, as well as Mrs Tara Haskell for training me on the cylinder settling test. Thank you to Dr Krishna Mohanarangam and Dr Phillip Fawell for their professional input and support with the FBRM measurements. Thank you to Dr Rico Tabor for his support with the DLS measurements.

The Saito Group and the Patti Group have provided tremendous support to me throughout my PhD project at Monash University. A special thank you to Dr Sepa Nanayakkara for her help with many laboratory-related questions, as well as her assistance and patience during the stressful period of fixing the GPC. In addition, thank you for all of your constant effort in keeping the laboratory a safe and a well-organised environment for us to work in. Thank you to all of my other colleagues, Dr Ahmed Al-Shereiqli, Dr Mustafa Abdalh, Dr Lionel Longé, Dr Temma Carruthers-Taylor, Dr Parijat Ray, Dr Jinhua Dai, Mr Gavin Styles, Dr Timothy Hughes, Ms Sinuo Tan, Mr Yanallah Alqarni, Dr Hussain Bhukya, Dr Roshanak Sepehrifar, Ms Shen Ni Thian, and Dr Ruchi Pal, whom have helped me at some stage throughout my PhD project. The countless dinners and coffee breaks with all of you have made my PhD experience so much more enjoyable and memorable. To the late Dr Ahmed Al-Shereiqli, you were always a special part of our group and will always be in our thoughts.

On a personal note, I would like to thank my mother, Ms Mai Cao, for her constant care, support and encouragement throughout my undergraduate degrees and my PhD. Words cannot simply express how thankful I am for you. Thank you to the rest of my family, Trevor, Joel and Kathy, Jessie and Shane, George and Helen, for being so understanding, and eager to help and support me through different aspects of life. Thank you to all of my close friends, Glenn, Shivam, Brendan, Temma, Jonathan, Albert, Toby and Patrick for being such wonderful people and enormous emotional supports in my life. A special thank you to Glenn for being such a caring and supportive best friend, and always managing to put a smile on my face throughout the difficult periods. This PhD thesis would have been impossible without all of you, so thank you from the bottom of my heart.

# Publications

1. V. H. Dao, N. R. Cameron and K. Saito, "Synthesis, Properties and Performance of Organic Polymers Employed in Flocculation Applications", *Polymer Chemistry*, 2016, **7**, 11-25.
2. V. H. Dao, N. R. Cameron and K. Saito, "Synthesis of Ultra-high Molecular Weight ABA Triblock Copolymers *via* Aqueous RAFT-mediated Gel Polymerisation, End Group Modification and Chain Coupling", *Polymer Chemistry*, 2017, **8**, 6834-6843.
3. V. H. Dao, K. Mohanarangam, P. D. Fawell, K. Simic, N. R. Cameron and K. Saito, "Enhanced Flocculation Efficiency in High Ionic Strength Environment by the aid of Anionic ABA Triblock Copolymers", *Langmuir*, submitted.
4. V. H. Dao, N. R. Cameron and K. Saito, "Synthesis of UHMW Star-shaped AB Block Copolymers and their Flocculation Efficiency in High Ionic Strength Environments", *Macromolecules*, submitted.

## Conference Presentations and Awards

1. V. H. Dao, N. R. Cameron and K. Saito, "Synthesis of High Molecular Weight Diblock Polymers using Aqueous RAFT-mediated Gel Polymerisation", **Warwick 2016 "The Polymer Conference"**, University of Warwick, Coventry, United Kingdom, 11<sup>th</sup>-14<sup>th</sup> July 2016 (poster presentation).
2. V. H. Dao, N. R. Cameron and K. Saito, "Synthesis of High Molecular Weight Diblock Polymers using Aqueous RAFT-mediated Gel Polymerisation", **BASF International Summer Courses 2016**, BASF Headquarter, Ludwigshafen, Germany, 7<sup>th</sup>-12<sup>th</sup> August 2016 (oral and poster presentations).
3. V. H. Dao, N. R. Cameron and K. Saito, "Synthesis of UHMW ABBA Triblock Copolymers using RAFT Polymerisation", **RACI National Centenary Conference**, Melbourne Convention and Exhibition Centre, Melbourne, Australia, 23<sup>rd</sup>-28<sup>th</sup> July 2017 (oral presentation).
4. V. H. Dao, N. R. Cameron and K. Saito, "New Pathway for the Synthesis of Ultra-high Molecular Weight Water-soluble Polymers with Well-controlled Structure", **8<sup>th</sup> International Conference on Green and Sustainable Chemistry (GSC8)**, Melbourne Convention and Exhibition Centre, Melbourne, Australia, 23<sup>rd</sup>-28<sup>th</sup> July 2017 (flash oral and poster presentations).
5. A. F. Patti, G. Catterall and V. H. Dao, "Experiences with the Graduate Research Industry Partnership (GRIP) Model of Innovation – Monash University and BASF", **Surface Coatings Association Australia Conference 2017 (SCAA 2017)**, Watermark Hotel & Spa, Gold Coast, Australia, 6<sup>th</sup>-8<sup>th</sup> September 2017 (joint oral presentation).
6. V. H. Dao, N. R. Cameron and K. Saito, "Design and Synthesis of Ultra-high Molecular Weight ABA Triblock Copolymers", **PolymerVic 2017**, Monash Institute of Pharmaceutical Sciences, Melbourne, Australia, 27<sup>th</sup>-28<sup>th</sup> September 2017 (oral presentation).  
  
Awarded the PolymerVic 2017 prize for Best Oral Presentation by a PhD candidate.

7. V. H. Dao, N. R. Cameron and K. Saito, “Synthesis of Ultra-High Molecular Weight ABA Triblock Copolymers using RAFT Polymerisation, End Group Modification, and Chain Coupling”, **Emerging Polymer Technologies Summit 2017 (EPTS’17)**, RMIT Storey Hall, Melbourne, Australia, 22<sup>nd</sup>-24<sup>th</sup> November 2017 (poster presentation).  
Awarded the EPTS’17 Best Poster Award (First Place).
  
8. V. H. Dao, N. R. Cameron and K. Saito, “Design and Synthesis of Novel Ultra-High Molecular Weight Polymers with Advanced Architectures”, **Macro 2018**, Cairns Convention Centre, Cairns, Australia, 1<sup>st</sup>-5<sup>th</sup> July 2018 (oral presentation).

# Table of Contents

Copyright Notices .....	iii
Declaration .....	iv
Acknowledgements .....	vii
Publications .....	ix
Conference Presentations and Awards.....	x
Table of Contents.....	xii
Abstract .....	xiv
List of Abbreviations .....	xvi
Chapter 1: Introduction, Research Background, and Project Objectives .....	1
1.1. General Overview on Flocculation .....	3
1.2. Review Paper ‘Polymer Chemistry, 2016, 7, 11-25’ .....	7
1.3. Research Background.....	22
1.4. Research Objectives .....	26
1.5. Thesis Outline.....	28
1.6. References .....	30
Chapter 2: Synthesis of Ultra-high Molecular Weight ABA Triblock Copolymers <i>via</i> Aqueous RAFT-mediated Gel Polymerisation, End Group Modification and Chain Coupling .....	35
2.1. General Overview .....	37
2.2. Research Paper ‘Polymer Chemistry, 2017, 8, 6834-6843’ .....	39
2.3. Supporting Information.....	49
2.4. Appendix.....	64

2.4.1. Isolation yields of the ABA triblock copolymers .....	64
2.4.2. Controlled synthesis of an ABA triblock copolymer by RAFT polymerisation .....	64
Chapter 3: Enhanced Flocculation Efficiency in High Ionic Strength Environment by the Aid of Anionic ABA Triblock Copolymers.....	67
3.1. General Overview .....	69
3.2. Research Paper ‘Langmuir, 2019, submitted manuscript’ .....	70
3.3. Supporting Information.....	114
Chapter 4: Synthesis of UHMW Star-shaped AB Block Copolymers and their Flocculation Efficiency in High Ionic Strength Environments .....	117
4.1. General Overview .....	119
4.2. Research Paper ‘Macromolecules, 2019, submitted manuscript’ .....	120
4.3. Supporting Information.....	164
4.4. Appendix.....	171
4.4.1. Synthesis of 4-arm star-shaped copolymers <i>via</i> thiol-ene reactions.....	172
4.4.2. Synthesis of 4-arm star-shaped copolymers <i>via</i> thiol-norbornene reactions.....	175
4.4.3. Synthesis of 4-arm star-shaped copolymers <i>via</i> thiol-epoxy reactions .....	179
Chapter 5: Conclusions and Outlooks .....	185
5.1. Project Conclusions.....	187
5.2. Project Outlooks.....	190

# Abstract

Flocculation is a common process used in numerous industrial applications to separate suspended colloidal particles from solution efficiently. The addition of a polymeric flocculating agent leads to contact between the particles *via* polymer bridging, which destabilise the colloidal suspension, hence allowing for faster sedimentation. The excess presence of multivalent cations has a detrimental effect on the flocculation efficiency of anionic polymeric flocculants, due to the shielding of the active anionic functionality. In addition, this interaction can also lead to precipitation of the polymers in some extreme cases.

The primary focus of this research project was to develop novel anionic polymers that have improved solubility and strong flocculation efficiency in high ionic strength environments. It was hypothesised that the anionic polymer would be more stable in high ionic strength environments if its anionic functionalities are distributed in a well-defined manner rather than arbitrarily across the polymer chain (a typical characteristic of commercial flocculants). Consequently, two different types of architecture of ABA triblock copolymers and star-shaped AB block copolymers were targeted; where the terminal A blocks are anionic blocks derived from acrylic acid (AA), and the centre or core B block is a non-ionic block derived from acrylamide (AM).

Eight different ABA triblock copolymers (**ABA1** – **ABA8**) and six different 4-arm star-shaped block copolymers (**4A-BA1** – **4A-BA6**) were successfully synthesised. The ABA triblock copolymers were synthesised in a three-stage process. The first two stages involved the polymerisation of AA to form the anionic blocks (molecular weights ranging from 5.21 to 173 kDa;  $\bar{D} < 1.20$ ), followed by chain extension with AM to form a series of AB diblock copolymers (molecular weights of approximately 500 kDa;  $\bar{D} < 1.50$ ). This was achieved using an aqueous RAFT-mediated gel polymerisation technique. The third stage involved an aminolysis process, where the thiocarbonylthio moiety on the polymer chain was converted into thiol, which spontaneously coupled under oxidative environment to form the desired ultra-high molecular weight (UHMW) ABA triblock copolymers (molecular weights of approximately 1 MDa,  $\bar{D} <$

1.70). The star-shaped block copolymers were synthesised using the same aqueous RAFT-mediated gel polymerisation technique, this time with the aid of a 4-arm star RAFT chain transfer agent.

Prior to flocculation analysis, three different control polymers (homopolymer of AA, **PAA**; homopolymer of AM; **PAM**, and random copolymer of AA and AM, **RAB**) were synthesised. RAB possessed a similar architecture compared to that of current commercial flocculants and thus was created for direct flocculation comparison with the block copolymers. High ionic strength kaolin clay slurry with three concentrations of  $\text{Ca}^{2+}$  (0.05 M, 0.10 M, and 0.50 M) were employed for flocculation testings *via* cylinder settling tests and turbulent pipe flow. While the flocculation efficiency of RAB diminished rapidly in high ionic strength environments, the ABA triblock copolymers and the star-shaped block copolymers remained stable, induced relatively faster settling rates and were able to clarify the solution efficiently, particularly at the highest concentration of  $\text{Ca}^{2+}$ . With further developments and flocculation testings, these well-defined novel block copolymers have high potentials to be implemented into current industrial applications of flocculation.

# List of Abbreviations

AA	Acrylic acid
ABA	ABA triblock copolymers of AA and AM
ADP	Aqueous dispersion polymerization
Ag	Agar
AM	Acrylamide
Amp	Amylopectin
AMPS	2-Acrylamido-2-methyl-1-propanesulfonic acid
APS	Ammonium persulfate
APS/SFS	APS and SFS redox initiation system
ATRP	Atom transfer radical polymerisation
Bar	Barley
Cas	Casein
CC	Corn cob
CD	Charge density
Cell	Cellulose
CETCTP	3-((((1-carboxyethyl)thio)carbonothioyl)thio)propanoic acid
CMC	Carboxymethyl cellulose
CMCs	Carboxymethyl chitosan
CMG	Carboxymethyl guar gum
CMI	Carboxymethyl inulin
CMS	Carboxymethyl starch
CMT	Carboxymethyl tamarind
CPAM	Cationic polyacrylamide
CRG	Conventional redox grafting

Cs	Chitosan
CSA	AM grafted crosslinked starch
CSt	Crosslinked starch
CSX	Sodium xanthate grafted crosslinked starch
CTA	Chain transfer agent
Đ	Dispersity
DAC	Acryloyloxyethyl trimethyl ammonium chloride
DADMAC	Diallyldimethylammonium chloride
DEP	Diethyl phthalate
Dex	Dextran
DLS	Dynamic light scattering
DMA	<i>N,N</i> -dimethylacrylamide
DMC	Methacryloyloxyethyl trimethyl ammonium chloride
DMF	<i>N,N</i> -dimethylformamide
DOP	Dioctyl phthalate
Dxt	Dextrin
EDL	Electrical double layer
EP	Emulsion polymerization
ESI	Electronic supplementary information
FBRM	Focused beam reflectance measurement
FRP	Free radical polymerization
GG	Guar gum
GGh	Gum ghatti
Gly	Glycogen
GPC	Gel permeation chromatography
GRR	Gamma ray radiation

HPMC	Hydroxypropyl methyl cellulose
IEP	Inverse emulsion polymerization
In	Inulin
kCr	k-carrageenan
KGM	Konjac glucomannan
MA	Methyl acrylate
Macro-CTA	Macro chain transfer agent
MAPMS	Methacryloxypropyl trimethoxy silane
MFRP	Micellar free radical polymerization
MMA	Methyl methacrylate
$M_n$	Number-average molecular weight
$M_{n,th}$	Theoretical number-average molecular weight
MWA	Microwave assisted
MWI	Microwave initiated
NIPAM	<i>N</i> -isopropylacrylamide
NMR	Nuclear magnetic resonance
NVF	<i>N</i> -vinylformamide
NVP	<i>N</i> -vinylpyrrolidone
Oat	Oatmeal
PAA	Polyacrylic acid
PAM	Polyacrylamide
P-Cell	Phosphorylated cellulose
P-Dex	Phosphorylated dextran
PEO	Polyethylene oxide
Psy	Psyllium
Pul	Pullulan

RAB	Control random copolymer of AA and AM
RAFT	Reversible addition–fragmentation chain transfer
RDRP	Reversible deactivation radical polymerization
R <sub>H</sub>	Hydrodynamic radius
RI	Refractive index
SA	Sodium alginate
SAB	Star-shaped block copolymers of AA and AM
Sal	Salep
SEC	Size exclusion chromatography
SET-LRP	Single-electron transfer living radical polymerisation
SFS	Sodium formaldehyde sulfoxylate dihydrate
SI	Supporting information
St	Starch
SX	Sodium xanthate
T.o.P	Type of polymerization
TKP	Tamarind kernel polysaccharide
UHMW	Ultra-high molecular weight
UV	Ultraviolet
UVI	Ultraviolet irradiation
VTMS	Vinyl trimethoxy silane
Xyl	Xylan
4A-A	4-arm star-shaped polymers of AA
4A-BA	4-arm star-shaped block copolymers of AA and AM
4A-CTA	4-arm star-shaped chain transfer agent

This page is intentionally left blank.

# Chapter 1

Introduction, Research Background, and Project Objectives

This page is intentionally left blank.

# Chapter 1

## Introduction, Research Background, and Project Objectives

---

### 1.1. General Overview on Flocculation

Industrial processes typically generate large quantities of wastewater and effluents. These waste streams as well as other internal process streams can contain significant amount of finely dispersed solids, metal ions, organic and inorganic particles, and other impurities.<sup>1,2</sup> Such colloidal particles and impurities are small in size and typically carry a surface charge, which render them to strong surface phenomena caused by repulsion forces such as water solvation layer and electrical charge.<sup>3</sup> Water molecules have a tendency to adsorb onto the hydrophilic surfaces to form solvation layers and hence reduce the overall agglomeration potential.<sup>3, 4, 5</sup> Interaction between hydrophobic surfaces is also difficult due to the electrostatic repulsion forces associated with the similarity in surface charges, which arose from charge transfer between the suspended particle and the aqueous phase, or from defect within the crystal lattice of the particle.<sup>3</sup> These overall repulsion forces would prevent colloidal particles from close proximity interaction with one another. This consequently hinders particle-particle attraction forces from taking effect, and thus establishes a stable colloidal suspension over a prolonged period of time.<sup>3, 6, 7</sup> Therefore, an efficient technology is often required to promote fast and cost-effective solid-liquid separation of these colloidal particles from the wastewater or process streams.

Amongst many solid-liquid separation processes, flocculation is commonly used in a wide range of industrial applications, including but not limited to mining and minerals processing, wastewater treatment, pulp and paper production, agriculture, medicinal applications, petroleum, textile industry, oil recovery, and biotechnology.<sup>1, 4, 6, 8, 9, 10, 11, 12</sup> The majority of flocculants used in industrial applications are synthetic organic polymers based on polyacrylamide (PAM) and its derivatives.<sup>9</sup> The terms flocculant

## Chapter 1

or flocculating agent also cover other widely used natural polymers such as starch, chitosan, alginates, cellulose, gums and glues.<sup>2, 3</sup> Industrial applications of flocculation often employ two main methods: coagulation-flocculation and direct flocculation.<sup>2</sup> Coagulation-flocculation often involves the use of inorganic metal salts as the coagulant and long chain organic polymers as the flocculant. In direct flocculation, only high molecular weight polymers are utilised to reduce treatment time and overall cost of the process.<sup>2</sup> Coagulation and flocculation are comparatively different processes; however, misinterpretation between these two methods often occurs. Coagulation utilises metal salts or low molecular weight polymers to destabilise colloidal suspension through electrostatic interaction.<sup>3, 4</sup> In contrast to coagulation, flocculation requires high molecular weight polymers to adsorb and form bridges between colloidal particles to destabilise the solid suspension.<sup>3</sup>

Commercial flocculants are often used in three distinct categories of application: clarification, thickening, and dewatering.<sup>10</sup> These applications are primarily categorised based on the quality of solids output from the process. Clarification involves the removal of suspended solids at low concentration from an aqueous solution. The main objective of clarification is to prevent downstream interference by suspended solid particles, particularly when the water quality has a significant importance to the particular process.<sup>8</sup> Clarification is regularly employed in minerals processing, treatment of potable and non-potable water, as well as treatment of municipal sewage and industrial effluents.<sup>10, 11</sup> Thickening is employed when the concentration of suspended solid particles in solution is higher compared to that of clarification. In thickening, suspended solids and water separation occurs based on a difference in density, and the liquid is recovered from the upper surface of the thickener; whereas the concentrated solids slurry is removed from the bottom of a typical thickener.<sup>8</sup> Thickeners are commonly found in minerals processing applications, as well as treatment of communal and industrial wastewaters.<sup>10</sup> Dewatering is the removal of water from an aqueous solution, where the main aim is to concentrate the solid content. Therefore, dewatering takes higher priority on the quality of the solids extracted compared to the recovery of the liquors.<sup>8</sup> Dewatering covers solid-liquid separation processes such as centrifugation and filtration (deep bed, vacuum and pressure filtrations) and has many applications in

## Chapter 1

mineral processing, paper industry, wastewater treatment and biotechnology.<sup>8,10</sup> A general laboratory demonstration of a colloidal suspension before and after flocculation is shown in Figure 1.1 below.

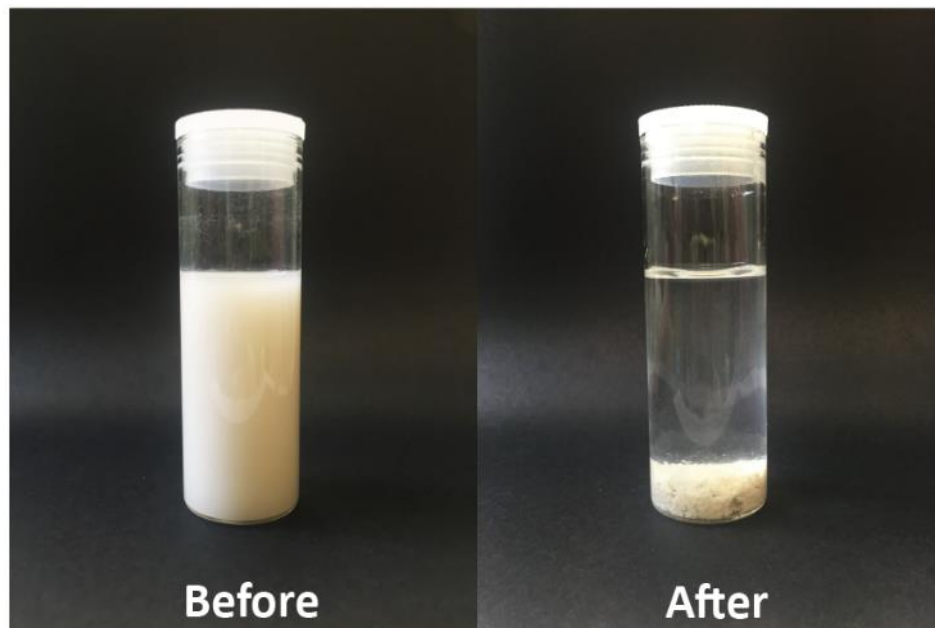


**Figure 1.1.** Images taken of a colloidal clay suspension before (left) and after (right) the flocculation process.

Chapter 1 is partially a review paper titled “Synthesis, properties and performance of organic polymers employed in flocculation applications”, which was published in *Polymer Chemistry* in 2015.

In this paper, the synthesis technique and flocculation efficiency of several newly developed organic polymeric flocculants were summarised and reported. In addition, a brief description on the four main types of flocculants (non-ionic, cationic, anionic, and amphoteric), as well as the mechanisms of flocculation were also discussed. The majority of recent flocculation studies had directed their focus towards the modification of various natural polymers to enhance their shelf life and flocculation efficiency. This would potentially allow these novel polymers to have comparable properties to the current commercial ones, whilst maintaining their biodegradable characteristics.<sup>1</sup> Several natural polysaccharides were employed in these studies, which included starches, hydroxypropyl methyl cellulose, chitosan, gums, agar, sodium alginate, dextran, dextrin, k-carrageenan, inulin, psyllium,

## Chapter 1

oatmeal, barley, and tamarind kernel polysaccharide.<sup>1</sup> Grafting of various monomers onto these polysaccharides backbone were often done through the conventional redox grafting method or the microwave assisted/initiated method. Gamma ray initiated polymerisation, ultraviolet initiated polymerisation, free radical polymerisation, emulsion polymerisation, and inverse emulsion polymerisation were also used to produce the grafted polysaccharides.

The grafted polymers in this review were observed to be in agreement with the *Brostow, Pal and Singh Model of Flocculation*.<sup>13, 14</sup> This model indicated that grafted polymers with larger hydrodynamic radius would have higher flocculation efficiency. In addition, another model developed by the same group, the *Singh's Easy Approachability Model* stated that grafted polymers should have superior flocculation efficiency compared to the original unmodified natural polymer.<sup>13, 14</sup> This is attributed to the grafted polymers having a comb-like structure, allowing the side chains to extend into the aqueous environment to capture solid colloidal particles with significantly higher efficiency.<sup>1, 13</sup> Hydrophobic monomers such as methacryloxypropyl trimethoxysilane,<sup>15</sup> vinyltrimethoxysilane,<sup>16</sup> butylacrylate,<sup>17, 18, 19</sup> and dimethylbenzyl aminoethyl acrylate chloride<sup>20</sup> were incorporated into the polymer chains to enhance the flocculation efficiency. Utilisation of hydrophobic monomers resulted in an increase in the average length of the polymer chain, which subsequently enabled better interaction between the hydrophobic segments and the solid particles.<sup>1</sup> The use of hydrophobic functional groups such as -SiOH also allowed for crosslinking between the molecular chains, which resulted in a complex three dimensional network and thus allowing for better containment of the colloidal particles.<sup>1, 15, 16</sup> Some of the polymers reported in the review article have shown comparable or even better flocculation efficiency compared to some of the current commercial flocculants, and thus with further research, these polymers exhibit strong potentials as efficient and sustainable flocculating agents in the near future.

## 1.2. Review Paper 'Polymer Chemistry, 2016, 7, 11-25'

Cite this: *Polym. Chem.*, 2016, 7, 11

## Synthesis, properties and performance of organic polymers employed in flocculation applications

Vu H. Dao,<sup>a</sup> Neil R. Cameron\*<sup>b,c</sup> and Kei Saito\*<sup>a</sup>

Flocculation is a common technique that is widely used in many industrial applications to promote solid-liquid separation processes. The addition of a polymeric flocculant allows for the destabilization of suspended colloidal particles, and thus significantly increases their sedimentation rate. Polymeric flocculants are generally divided into four categories, which include non-ionic, cationic, anionic, and amphoteric polymers. This minireview article summarises important information on the recent design and synthesis of polymeric materials from these four categories. In addition, their properties and flocculation efficiency are also presented and discussed.

Received 29th September 2015,  
Accepted 31st October 2015

DOI: 10.1039/c5py01572c

www.rsc.org/polymers

### 1. Introduction

Over the past few decades, a higher demand for industrial products has led to a significant increase in generation rate of industrial effluents. The wastewater coming from these indus-

trial processes contains large quantities of finely dispersed solids, organic and inorganic particles, as well as metal ions and other impurities.<sup>1,2</sup> Separation and removal of these particles is challenging due to their small particle size and the presence of surface charges, which create interparticle repulsion, and thus a stable colloidal suspension is established over an extended period of time.<sup>3-5</sup> Amongst numerous solid-liquid separation processes, flocculation is commonly used to promote and optimize solid-liquid separation of colloidal suspensions in many industrial processes, such as mining and mineral processing, wastewater treatment, pulp and paper processing, and biotechnology.<sup>6</sup>

<sup>a</sup>School of Chemistry, Monash University, Clayton, VIC 3800, Australia.

E-mail: kei.saito@monash.edu; Tel: +61 3 9905 4600; Fax: +61 3 9905 8501

<sup>b</sup>Department of Materials Science and Engineering, Monash University, Clayton, VIC 3800, Australia. E-mail: neil.cameron@monash.edu; Tel: +61 3 9902 0774<sup>c</sup>School of Engineering, University of Warwick, Coventry, CV4 7AL, UK

Vu H. Dao

Vu Dao received his Bachelor of Engineering (Honours) and Bachelor of Science from Monash University, Australia, in 2014. His major areas of study were in the fields of Chemical Engineering and Chemistry. He is currently undertaking his PhD studies in polymer chemistry, under the supervision of Dr Kei Saito and Professor Neil Cameron at Monash University. His research interests are

focused on the design and synthesis of novel polymeric materials for usage in a wide range of industrial applications.



Neil R. Cameron

Neil Cameron undertook his BSc and PhD at the University of Strathclyde in Glasgow. Following two post-doctoral periods, first in Eindhoven then at Heriot Watt University, he was appointed as a Lecturer (Assistant Professor) at Durham University in 1997. In 2005 he was promoted to Reader (Associate Professor) and in October 2008 he took up the position of Professor of Bioactive Chemistry in the same department. In Sep-

tember 2014 he became the Monash Warwick Professor of Polymer Materials based at Monash University (Australia) and the University of Warwick (UK). His research is focused on the preparation of novel polymeric materials, with particular emphasis on scaffolds for tissue engineering, self-assembling polypeptides, peptide-synthetic polymer hybrids and sugar-containing polymers (glycopolymers).

### 1.1. Type of flocculants

The term flocculant generally includes both natural and synthetic water-soluble polymers, and the latter has gained tremendous interest from industry due to their ability to create strong and large solid aggregates, allowing for the solid flocs to be easily removed from the wastewater.<sup>6</sup> In addition, these flocculants are highly cost efficient due to their low dosage requirement and easy handling process.<sup>7,8</sup> However, as synthetic flocculants are usually non-biodegradable, the majority of recent studies have extensively focused on combining the best properties of both synthetic and natural polymers, to potentially create environmentally friendly flocculants, while having longer shelf life and higher efficiency compared to traditional natural flocculants.<sup>2</sup> The term flocculation efficiency used in this review refers to a polymer's ability to induce optimal flocculation, and this factor is typically evaluated based on two main factors: clarity of the upper flow and settlement rate of the flocculated particles.<sup>9</sup>

Polymeric flocculants are typically classified based on their ionic character: non-ionic, cationic, anionic and amphoteric.<sup>2</sup> Commercial flocculants are often based on polyacrylamide (PAM) and its derivatives since acrylamide (AM) is one of the most reactive monomers to undergo radical polymerization, thus allowing ultra-high molecular weight polymers to be built easily.<sup>5</sup> In addition, AM is cost effective and highly soluble in water (2150 g L<sup>-1</sup> at 30 °C).<sup>5</sup> Apart from PAM, non-ionic flocculants are also based on polyethylene oxide (PEO), polyvinyl alcohol and polyvinylpyrrolidone.<sup>6</sup> Cationic flocculants are often based on polydiallyldimethylammonium chloride, cationic polyacrylamide (CPAM) and polyethylene imine, and most anionic flocculants are homopolymers or AM copolymers of ammonium or alkali metal salts of acrylic acid (AA).<sup>1,6</sup> Anionic monomers such as methacrylic acid and 2-acrylamido-2-methyl-1-propanesulfonic acid (AMPS) are also often used in copolymerization with AM to produce anionic flocculants.<sup>1</sup>



Kei Saito

Dr Kei Saito is currently a Lecturer at the School of Chemistry, Faculty of Science, Monash University, Australia. He received his BEng. (2000), MEng. (2002) and Ph.D. (2004) degrees from Waseda University, Tokyo, Japan. From 2004–2005, he was a Research Associate at the 21COE Centre for Practical Nano-Chemistry, Department of Applied Chemistry, Waseda University, Japan. From 2005–2007, he was a Postdoctoral fellow, at

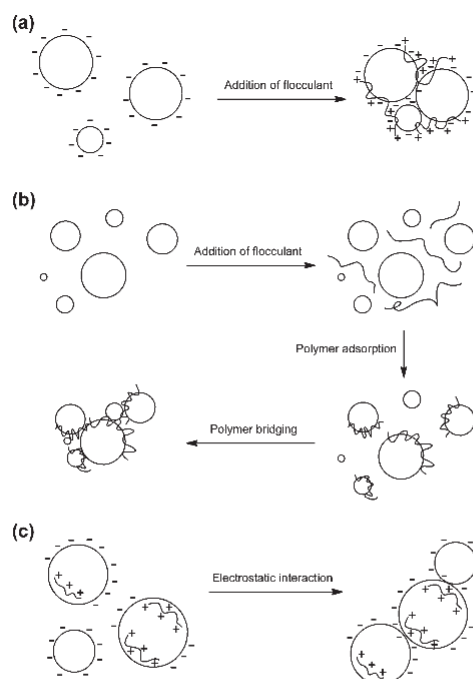
the Centre for Green Chemistry, University of Massachusetts Lowell, USA. His research interests are in developing new synthesis and production methods for novel sustainable/environment benign polymeric materials.

Amphoteric polymers contain both cationic and anionic functional groups, and have recently emerged as promising candidates for flocculation applications.

### 1.2. Mechanisms of flocculation

Numerous mechanisms for flocculation have been studied and reported in various literatures; the most common of which include charge neutralization, polymer bridging and electrostatic patch.<sup>1–3,6,8</sup> Charge neutralization is most effective when the polymer has an opposite charge to that of the colloidal particles.<sup>6</sup> This therefore allows for neutralization of the particle's surface charge, and hence destabilizes the colloidal suspension to promote agglomeration.<sup>1</sup> Numerous practical cases have shown that hydrophobic colloidal particles and other impurities commonly have negatively charged surface, and therefore cationic polymers favour charge neutralization as the main flocculation mechanisms.<sup>2</sup>

When a long chain polymer is added into the colloidal suspension, adsorption of the polymer onto the surface of the contaminant occurs through hydrogen bonding, electrostatic interaction, van der Waals forces, or chemical bonding.<sup>1</sup> Polymer bridging is most effective when the polymer has a linear structure and a high molecular weight.<sup>2,8</sup> Once adsorbed, extensive elongation of the dangling polymer chains into the aqueous environment allow for interaction and polymer bridging between contaminant particles, which would



Scheme 1 Schematic representation of colloidal suspension flocculation by: (a) charge neutralization, (b) polymer adsorption and bridging, and (c) electrostatic patch.

then induce flocculation.<sup>8</sup> As different types of polymer adsorb differently, ionic strength can also have a major impact on the effectiveness of polymer bridging.<sup>8</sup>

Electrostatic patch mechanism occurs when a lower molecular weight polymer with high charge density and opposite charge as the colloidal particles is used. The high charge density allows the polymeric chain to be readily adsorbed onto weakly charged negative surface.<sup>3,8</sup> This then induces localised charge reversal on each particle, thereby allowing 'patches' or localised areas with opposite charge between different particles to interact and form flocs.<sup>2</sup> The schematic views of these mechanisms are outlined in Scheme 1.

### 1.3. Aim and scope of the review

The present review article will present and summarize important information on the synthesis of organic polymers that were tested as flocculants in recent studies. This review is arranged into four main sections based on the ionic characteristics of these flocculants. It is aimed to provide a summary and quick insight into recent developments on the design and synthesis of polymeric flocculants. In addition, the important properties and flocculation efficiency of these polymers are also presented and discussed.

## 2. Non-ionic flocculants

Polymers are considered as non-ionic flocculants if they contain less than 1% of charged functional groups.<sup>10</sup> This almost-neutral overall charge arises from a small degree of hydrolysis that can occur during the synthesis of the polymer.<sup>8</sup> Non-ionic polymers are commonly used as flocculants in mineral processing, as well as the treatment of industrial effluents and potable wastewater.<sup>1,3</sup>

Table 1 provides a summary of the polymerization technique and the flocculation testing medium for non-ionic polymeric flocculants 1–26.

### 2.1. Modified starch

Graft copolymerization of natural polysaccharides such as starch has become an important foundation for the development of polymeric materials with applications across many fields of science and technology.<sup>11</sup> Several research groups have attempted to synthesize grafted polysaccharides in order to improve the flocculation efficiency of the respective natural biopolymer. Sen *et al.* reported the synthesis of polymer 1 by grafting PAM onto carboxymethyl starch using both a conventional redox grafting (CRG) method and a microwave initiated (MWI) method.<sup>12</sup> Similarly, a recent study conducted by Mishra *et al.* reported microwave assisted (MWA) synthesis of PAM grafted natural starch to produce polymer 2.<sup>11</sup> All of these methods involved the initial formation of free radicals on the polysaccharide backbone prior to the polymerization of the monomer (Scheme 2).<sup>11,12</sup> The same notation used in Scheme 2 will be used for subsequent natural polymers in this review article. MWI/MWA synthesis of both polymers 1 and 2

**Table 1** Summary of the polymerization technique and the testing medium of non-ionic polymeric materials which were utilised as flocculating agents in previous studies

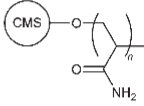
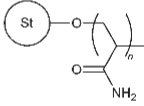
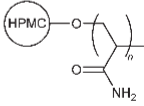
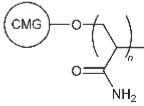
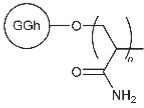
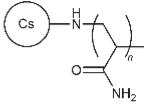
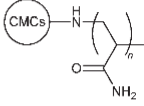
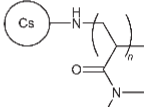
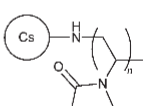
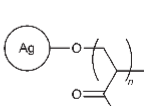
Entry	Polymer structure <sup>a</sup>	T.o.P <sup>b</sup>	Testing medium	Ref.
1		CRG MWI	Municipal sewage wastewater	12
2		MWA	0.25 wt% kaolin suspension	11
3		FRP	0.25 wt% kaolin suspension; 0.25 wt% iron ore suspension; mine wastewater	14
4		CRG MWA	Municipal sewage wastewater; 0.25 wt% kaolin suspension; methylene blue solution	18, 19
5		MWA	Municipal sewage wastewater; 0.25 wt% kaolin suspension	20
6		GRR	0.25 wt% kaolin suspension	21
7		CRG	0.10 wt% kaolin suspension	23
8		FRP	1 wt% coal fine suspension	22
9		FRP	1 wt% coal fine suspension	24
10		CRG MWA	Municipal sewage wastewater; 0.25 wt% kaolin suspension	25, 26

Table 1 (Contd.)

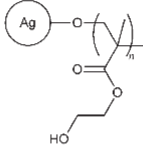
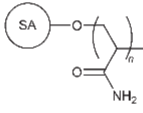
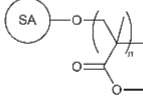
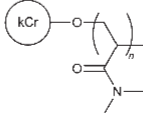
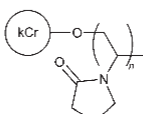
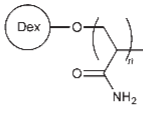
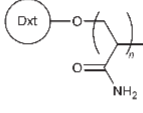
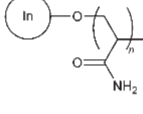
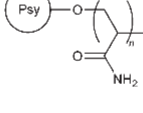
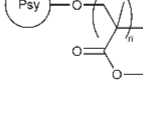
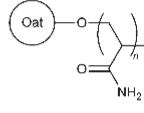
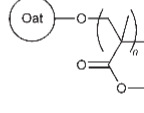
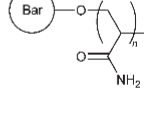
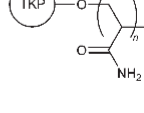
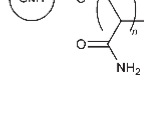
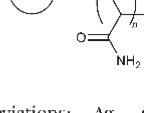
Entry	Polymer structure <sup>a</sup>	T.o.P. <sup>b</sup>	Testing medium	Ref.
11		MWI MWA	Municipal sewage wastewater; 0.25 wt% kaolin suspension; 1 wt% coal fine suspension; river water	27, 28
12		CRG	0.25 wt% kaolin suspension; dyeing wastewater	29, 30
13		MWA	1 wt% coal fine suspension	31
14		FRP	1 wt% coal fine suspension	32
15		FRP	1 wt% coal fine suspension	33
16		CRG	1 wt% kaolin suspension	34
17		MWA	3 wt% kaolin suspension	35
18		MWA	1 wt% coal fine suspension	36
19		MWI	0.25 wt% kaolin suspension; 1 wt% coal fine suspension	37
20		MWA	0.25 wt% kaolin suspension	38

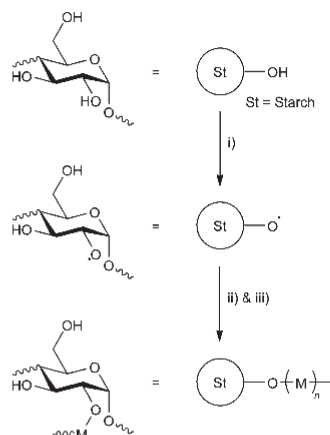
Table 1 (Contd.)

Entry	Polymer structure <sup>a</sup>	T.o.P. <sup>b</sup>	Testing medium	Ref.
21		CRG	Municipal sewage wastewater; 0.25 wt% kaolin suspension; 1 wt% coal fine suspension; 1 wt% iron ore suspension	39
22		CRG	Municipal sewage wastewater; 0.25 wt% kaolin suspension	40
23		CRG	1 wt% coal fine suspension	41
24		CRG MWI MWA	Municipal sewage wastewater; textile industry wastewater; 0.25 wt% kaolin suspension	42, 43
25		CRG	0.25 wt% kaolin suspension	44
26		MWI	1 wt% coal fine suspension	45

<sup>a</sup>Abbreviations: Ag, agar; Bar, barley; Cas, casein; CMCs, carboxymethyl chitosan; CMG, carboxymethyl guar gum; CMS, carboxymethyl starch; CMT, carboxymethyl tamarind; Cs, chitosan; Dex, dextran; Dxt, dextrin; GGh, gum ghatti; HPMC, hydroxypropyl methyl cellulose; In, inulin; kCr, k-carrageenan; Oat, oatmeal; Psy, psyllium; SA, sodium alginate; St, starch; TKP, tamarind kernel polysaccharide. <sup>b</sup>Type of polymerization (T.o.P) abbreviations: CRG, conventional redox grafting; FRP, free radical polymerization; GRR, gamma ray radiation; MWA, microwave assisted; MWI, microwave initiated.

was shown to be quicker, more reliable and reproducible compared to the CRG method. In addition, this method produced higher quality copolymer products with higher molecular weight, thereby higher flocculation efficiency was observed.<sup>11,12</sup>

Polymers **1** and **2** were also shown to have better flocculation efficiency compared to carboxymethyl starch and natural starch, respectively.<sup>11,12</sup> These results were in agreement with Singh's Easy Approachability Model.<sup>7,13</sup> This model stated that grafted polysaccharides have superior performance in comparison to its respective unmodified polysaccharide due to them having a "comb" like structure, which allowed the



**Scheme 2** Example mechanistic pathway for the synthesis of starch graft copolymer via: (i) formation of free radical on the polysaccharide backbone, (ii) propagation of monomer M, and (iii) termination of graft copolymerization.

grafted chains to further approach and capture metallic and non-metallic contaminants at a significantly higher efficiency.<sup>13</sup>

### 2.2. Modified cellulose

A few studies have directed their focus on modifying cellulose-based materials to develop high performance water-soluble polymeric flocculants. For example, PAM chains were grafted onto a hydroxypropyl methyl cellulose (HPMC) backbone using free radical polymerization (FRP) with multiple reaction parameters to generate different grades of polymer **3**.<sup>14</sup> A particular grade of **3** was found to be much more effective as a flocculant compared to the rest, as well as unmodified HPMC and synthetic PAM, due to its high percentage of grafting and large hydrodynamic radius.<sup>14</sup> This was in agreement with a flocculation model previously developed by the same group (*Brostow, Pal and Singh Model of Flocculation*), which suggested that a large radius of gyration would correspond to high flocculation efficiency.<sup>15</sup> In addition, the type of grafted synthetic polymer can affect the solvency of the original natural polymer.<sup>16</sup> For example, poly(methyl acrylate) grafted onto cellulose showed significantly lower affinity towards polar solvents. This was ascribed to blockage of hydroxyl groups which shielded active sites from interacting with hydrophilic solvents.<sup>16</sup>

### 2.3. Modified gum

Guar gum and its derivatives such as carboxymethyl guar gum are versatile naturally-occurring polymers with various applications in the oil and textile industries.<sup>17</sup> Minimal attention was directed towards using modified guar gum as flocculant until Pal *et al.* and Adhikary *et al.* introduced the synthesis of polymer **4** by using both the CRG and MWA methods.<sup>18,19</sup> Apart from guar gum, flocculation efficiency of grafted gum

ghatti was also investigated by Rani *et al.* where AM was used to produce polymeric flocculant **5**.<sup>20</sup> As expected, **4** and **5** demonstrated better flocculation efficiency than their original polysaccharides, especially when the MWA method was used. In addition to other advantageous factors, compared to CRG, grafting with microwave irradiation does not generate the free radical by chain opening of the polysaccharide backbone; therefore the product polymer retains its rigidity, allowing for further extension of the PAM chains into the aqueous solution to capture more contaminants.<sup>18</sup>

### 2.4. Modified chitosan

Chitosan is considered to be a biodegradable and non-toxic material.<sup>21</sup> In spite of this, chitosan is only readily soluble in acidic solution due to its strong inter- and intramolecular hydrogen bonding, and therefore there are restrictions in exploiting it for industrial applications such as flocculation.<sup>21,22</sup> Chitosan and carboxymethyl chitosan's solubility and flocculation efficiency have been improved by multiple research groups, through grafting of PAM,<sup>21,23</sup> *N,N*-dimethylacrylamide (DMA),<sup>22</sup> and *N*-vinylpyrrolidone (NVP),<sup>24</sup> to synthesize polymers **6–9**. In contrast to previous grafting approaches, **6** was synthesized using a gamma ray radiation (GRR) method due to its high efficiency and low level of contaminations by chemical initiators.<sup>21</sup> Both **8** and **9** were synthesized by FRP in acetic acid using potassium peroxydisulfate and potassium bromate as initiators, respectively.<sup>22,24</sup>

### 2.5. Other modified natural polymers

Apart from starch, cellulose, gum and chitosan, previous studies had also focused on the synthesis and flocculation efficiency of various synthetic polymers grafted onto other polysaccharides such as agar (**10**, **11**),<sup>25–28</sup> sodium alginate (**12**, **13**),<sup>29–31</sup> k-carrageenan (**14**, **15**),<sup>32,33</sup> dextran (**16**),<sup>34</sup> dextrin (**17**),<sup>35</sup> inulin (**18**),<sup>36</sup> psyllium (**19**, **20**),<sup>37,38</sup> oatmeal (**21**, **22**),<sup>39,40</sup> barley (**23**),<sup>41</sup> tamarind kernel polysaccharide (**24**),<sup>42,43</sup> carboxymethyl tamarind (**25**),<sup>44</sup> In addition to these polysaccharides, Sinha *et al.* conducted a graft polymerization of an amphiphilic protein, casein, to produce polymer **26**.<sup>45</sup> Various monomers including AM, DMA, NVP, 2-hydroxyethylmethacrylate, and methyl methacrylate (MMA) were used in these studies for the synthesis of grafted polysaccharide polymers. An optimum dosage was often observed for each of the polymeric flocculants.<sup>25,27</sup> This behaviour was ascribed to the polymer bridging mechanism associated with flocculation. Beyond the optimum dosage, there is insufficient space for polymer bridging between particles, which leads to a reduction in flocculation efficiency.<sup>25,27</sup>

It is difficult to present an accurate comparison between these non-ionic flocculants, as well as subsequent cationic, anionic and amphoteric flocculants mentioned in this review article. Flocculation is a complex process and the flocculation efficiency is significantly dependent on a variety of factors, including but not limited to pH and ionic strength of the solution, agitation rate, particle size, charge density, molecular

weight and dosage of the polymer.<sup>10,46,47</sup> In addition, the mineral composition, and type and addition sequence of the flocculating agents also play an important role in successful destabilization of the colloidal particles.<sup>9</sup> Any attempt at comparing these flocculants against one another would be inadequate as there are many inconsistencies in flocculation performance analysis across different studies.

### 3. Cationic flocculants

Water-soluble cationic polymers are typically categorised into three groups: ammonium, sulfonium and phosphonium quaternaries.<sup>10</sup> Cationic polymers can bind strongly to negatively charged particles, and thus these polymers are often used in a wide range of industrial applications. These include wastewater and sludge treatment, paper production industry, oily water clarification, textile industry, paint manufacturing, dairy processing, and biotechnology.<sup>1,3,10</sup>

Table 2 provides a summary of the polymerization technique and the flocculation testing medium for cationic polymeric flocculants 27–59.

#### 3.1. Synthetic acrylamide-based copolymers

There are very few commercially available monomers with cationic functional groups due to problems associated with accessibility and/or stability.<sup>48</sup> Quaternary ammonium is one of the most commonly reported cationic structures amongst these groups. Therefore, cationic flocculants are often developed based on copolymerization between AM and monomers containing quaternary ammonium functional groups.<sup>48</sup> Methacryloyloxyethyl trimethylammonium chloride (DMC) and acryloyloxyethyl trimethylammonium chloride (DAC) are two of the most known comonomers used alongside AM to produce CPAM for flocculation purposes.<sup>49</sup>

Shang *et al.* developed a hydrophobically modified cationic terpolymer consisted of AM, DMC and methacryloxypropyl trimethoxysilane (MAPMS).<sup>50</sup> Terpolymer 27 was synthesized from these monomers by inverse emulsion polymerization (IEP) to allow for adequate dissolution of the hydrophobic monomer.<sup>50</sup> In addition, IEP is an advantageous polymerization technique which produces polymers with high MW and high solid content.<sup>48</sup> The easy handling of the inverse latexes also allow for a simple post-treatment process.<sup>48,50</sup> For cationic flocculants, charge neutralization is hypothesized as the major mechanism.<sup>2</sup> Therefore, an increase in the dosage of 27 led to better flocculation due to neutralization of the negative charges on the particle surface. However, excess dosing of the flocculant resulted in restabilization of the colloidal suspension, where the overall particle surface charge changed from negative to positive.<sup>50</sup> Apart from 27, numerous research groups have also directed their attention towards developing and utilizing hydrophobically modified cationic polymers as flocculants. Cationic terpolymers 28–32 were synthesized through copolymerization between AM and various monomers, including diallyldimethylammonium chloride

**Table 2** Summary of the polymerization technique and the testing medium of cationic polymeric materials which were utilised as flocculating agents in previous studies

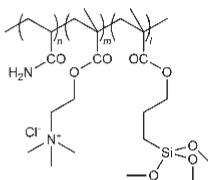
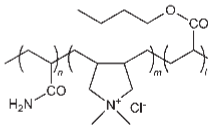
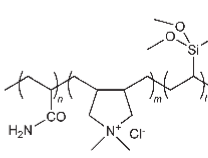
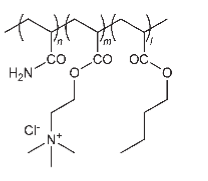
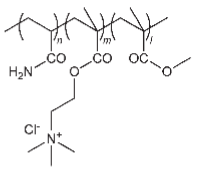
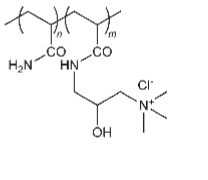
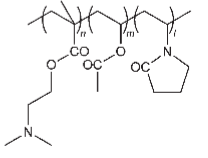
Entry	Polymer structure <sup>a</sup>	T.o.P <sup>b</sup>	Testing medium	Ref.
27		IEP	Reactive brilliant red X-3B dye; 0.10 wt% kaolin suspension	50
28		MFRP	Oily wastewater	51
29		IEP	Reactive brilliant red X-3B dye	52
30		UVI	Textile sewage sludge; waste-activated sludge	53, 54
31		ADP	Oily wastewater	55
32		ADP	0.25 wt% kaolin suspension	56, 57
33		FRP	River water	58

Table 2 (Contd.)

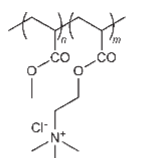
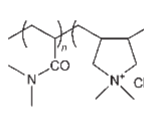
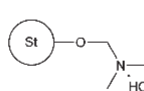
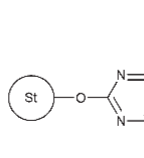
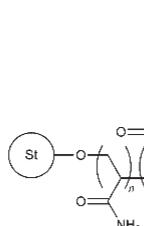
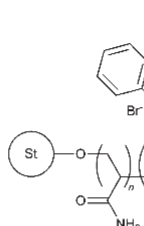
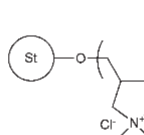
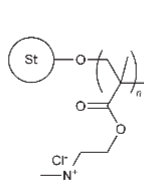
Entry	Polymer structure <sup>a</sup>	T.o.P <sup>b</sup>	Testing medium	Ref.
34		EP	Clay slurry; municipal biological sludge; polymer plant sludge; refinery wastewater	5
35		FRP	0.30 wt% bentonite solution; 2 wt% suspension of animal slurries	59
36		N/A	Reactive brilliant red KE-3B dye	60
37		N/A	C.I. reactive red 141 dye; C.I. acid blue 341 dye; C.I. acid red 1 dye	61
38		FRP	Refinery wastewater; paper mill wastewater	62
39		GRR	0.60 wt% kaolin suspension	63
40		FRP	Municipal sewage and sludge; 2 wt% kaolin suspension	64–66
41		FRP	0.25 wt% kaolin suspension	67

Table 2 (Contd.)

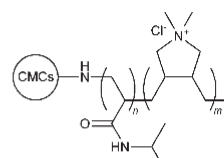
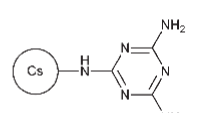
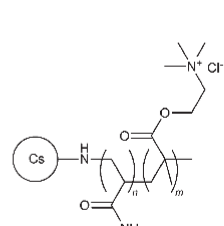
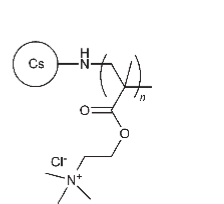
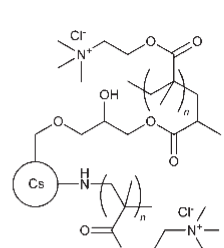
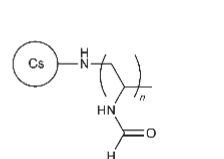
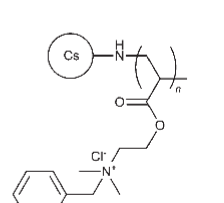
Entry	Polymer structure <sup>a</sup>	T.o.P <sup>b</sup>	Testing medium	Ref.
42		FRP	Synthetic copper and/or tetracycline wastewaters	68
43		N/A	Synthetic copper and/or tetracycline wastewaters	69
44		GRR	0.25 wt% kaolin suspension	70
45		GRR FRP	0.10 wt% and 0.25 wt% kaolin suspensions; pulp mill wastewater; kaolin – humic acid solution	71–73
46		CRG	C.I. reactive orange 5 dye; C.I. reactive blue 19 dye	74
47		FRP	1 wt% coal fine suspension	75
48		CRG	Oily wastewater	76

Table 2 (Contd.)

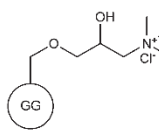
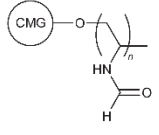
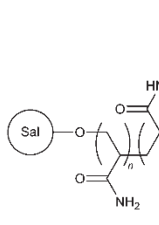
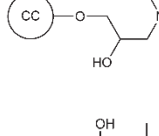
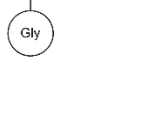
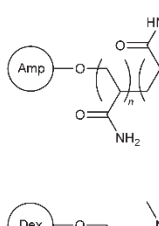
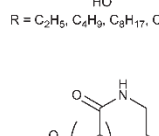
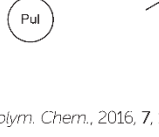
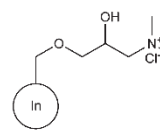
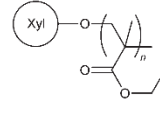
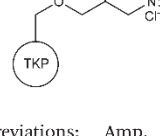
Entry	Polymer structure <sup>a</sup>	T.o.P <sup>b</sup>	Testing medium	Ref.
49		N/A	Chlorella sp. CB4 microalgae; chlamydomonas sp. CRP7 microalgae	77
50		FRP	1 wt% coal fine suspension	17
51		FRP	Cement suspension	78
52		N/A	0.25 wt% kaolin suspension; Alexandrium tamarense algae	79, 80
53		N/A	0.25 wt% iron ore suspension	81
54		FRP	0.25 wt% kaolin suspension	82
55		N/A	0.10 wt% clay suspension	83
56		FRP	0.10 wt% clay suspension	84

Table 2 (Contd.)

Entry	Polymer structure <sup>a</sup>	T.o.P <sup>b</sup>	Testing medium	Ref.
57		N/A	Fresh water green algae	85
58		FRP	Reactive orange 16 dye	86
59		N/A	Textile industry wastewater	87

<sup>a</sup> Abbreviations: Amp, amylopectin; CC, corn cob; CMCs, carboxymethyl chitosan; CMG, carboxymethyl guar gum; Cs, chitosan; GG, guar gum; Gly, glycogen; In, inulin; Pul, pullulan; Sal, salep; St, starch; TKP, tamarind kernel polysaccharide; Xyl, xylan. <sup>b</sup> Type of polymerization (T.o.P) abbreviations: ADP, aqueous dispersion polymerization; CRG, conventional redox grafting; EP, emulsion polymerization; FRP, free radical polymerization; GRR, gamma ray radiation; IEP, inverse emulsion polymerization; MFRP, micellar free radical polymerization; N/A, not applicable; UVI, ultraviolet irradiation.

(DADMAC),<sup>51,52</sup> vinyltrimethoxysilane (VTMS),<sup>52</sup> butylacrylate (BA),<sup>51,53,54</sup> DAC,<sup>53,54</sup> DMC,<sup>55</sup> MMA,<sup>55</sup> and acryloylamino-2-hydroxypropyl trimethylammonium chloride.<sup>56,57</sup>

The presence of MAPMS in 27 and VTMS in 29 was observed to impose a positive effect on the flocculation efficiency. Hydrolysis of the SiOCH<sub>3</sub> functional group generated SiOH moieties, which lead to crosslinking between the molecular chains (Fig. 1).<sup>50,52</sup> This subsequently enhanced the chain length and built three dimensional networks, thus allowing for better capture and containment of the contaminant particles. However, a decrease in water solubility of the polymers was observed when the ratios of MAPMS and VTMS were increased.<sup>50,52</sup> Other hydrophobic monomers such as BA can reportedly increase the flocculation efficiency of a polymer. This was ascribed to higher intrinsic viscosity caused

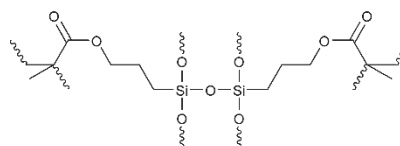


Fig. 1 Example showing crosslinked structure of MAPMS groups on terpolymer 27.

by the number of hydrophobic segments and their respective average length within the polymeric chain.<sup>53</sup> This subsequently allows for better interactions between the hydrophobic segments and the solid contaminants.<sup>49,53,54</sup>

### 3.2. Synthetic acrylamide-free copolymers

Although PAM is one of the chemicals with the largest production volume, the high toxicity associated with AM is of environmental and human health concerns. It is a challenging process to design and develop non-AM-based flocculants with similar performance and cost compared to the current commercial ones.<sup>5</sup> Nasr *et al.* developed a cationic terpolymer **33** which consisted of dimethylaminoethyl methacrylate, NVP and vinyl acetate.<sup>58</sup> Another cationic polymer **34** based on the emulsion copolymerization between methyl acrylate (MA) and DAC was synthesized by Lu *et al.*<sup>5</sup> More recently, the flocculation efficiency of a cationic copolymer **35** consisting of only DMA and DADMAC was reported by Abdiyev *et al.*<sup>59</sup>

P(MA-*co*-DAC) **34** with 55% charge density (CD) was compared to a P(AM-*co*-DAC) sample with the same CD (widely used for flocculation of biological sludge).<sup>5</sup> The results obtained showed that **34** had good water solubility and comparable or slightly better performance against the AM-based polymer at various concentrations.<sup>5</sup> Therefore this would potentially allow **34** to be a comparable competitor to AM-based flocculants, as well as being more beneficial for having less strict environmental regulations.<sup>5</sup>

### 3.3. Cationically-modified polysaccharides

Cationic starches are commonly used in wastewater treatment, paper production, textile industry, oil drilling, and the cosmetic industry. These biodegradable materials are classified into graft copolymerized starch, esterified starch, and etherified starch.<sup>60</sup> Jiang *et al.* and Shi *et al.* recently reported the synthesis of cationic flocculants **36** and **37**, based on the etherification of starch with methylene dimethylamine hydrochloride and 2,4-bis(dimethylamino)-6-chloro-[1,3,5]-triazine, respectively.<sup>60,61</sup> Both polymers were found to be effective in flocculation and removal of anionic dyestuffs from wastewater.<sup>60,61</sup> Flocculation efficiency of cationic graft copolymerized starches (**38–41**) were also reported by multiple research groups where different monomers were employed, including AM,<sup>62,63</sup> DAC,<sup>62</sup> allyltriphenylphosphonium bromide,<sup>63</sup> DADMAC,<sup>64–66</sup> and DMC.<sup>67</sup>

Chitosan and its derivatives are prominent biopolymers for this category due to its high cationic charge density from the presence of the amino groups.<sup>2</sup> Recent studies conducted by Yang and coworkers introduced temperature-responsive polymers **42** and **43** for flocculation of copper and tetracycline from wastewater.<sup>68,69</sup> Multiple other studies have reported the grafting of DMC onto chitosan backbone to produce polymers **44–46**.<sup>70–73</sup> However, in polymer **46**, the chitosan backbone was also modified by ring-opening reaction with glycidyl methacrylate prior to the graft polymerization process.<sup>74</sup> Apart from DMC, monomers such as *N*-vinyl formamide (NVF), and dimethyl acryloyloxyethyl benzyl ammonium chloride were

grafted onto chitosan to develop cationic polymers **47** and **48**, respectively.<sup>75,76</sup>

Cationic moieties such as *N*-3-chloro-2-hydroxypropyl trimethylammonium chloride, *N*-alkyl-*N,N*-dimethyl-*N*-2-hydroxypropyl ammonium chloride, 3-acrylamidopropyl trimethylammonium chloride, 3-methacryloylaminopropyl trimethylammonium chloride, NVF and DMC were used in modification of many different polysaccharides, including guar gum (**49**),<sup>77</sup> carboxymethyl guar gum (**50**),<sup>17</sup> salep (**51**),<sup>78</sup> corn cob (**52**),<sup>79,80</sup> glycogen (**53**),<sup>81</sup> amylopectin (**54**),<sup>82</sup> dextran (**55**),<sup>83</sup> pullulan (**56**),<sup>84</sup> inulin (**57**),<sup>85</sup> xylan (**58**),<sup>86</sup> and tamarind kernel polysaccharide (**59**).<sup>87</sup>

## 4. Anionic flocculants

The majority of commercial anionic flocculants contain carboxylate and sulfonate ions as the anionic functional group, and this can range from 1 to 100% of the monomer units.<sup>10</sup> Anionic polymers are most commonly used as flocculants in mineral processing applications.<sup>1,3</sup> Optimal flocculation is possible due to strong ionic interaction between the active anionic groups on the polymer chain and the divalent cations (primarily calcium and magnesium) available on the suspended particles.<sup>1</sup> Apart from mineral processing, anionic polymers can also be used in the treatment of municipal wastewaters and sludges, tanning industry, paper production, foundries and metal working, sugar processing, and gravel washing.<sup>1,3,10</sup>

Table 3 provides a summary of the polymerization technique and the flocculation testing medium for anionic polymeric flocculants **60–72**.

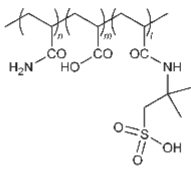
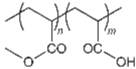
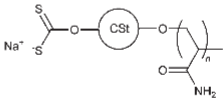
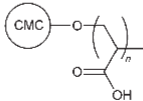
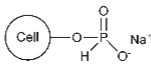
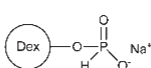
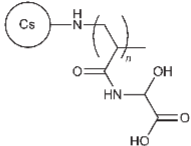
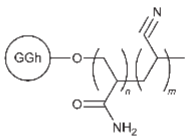
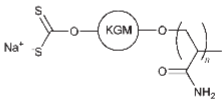
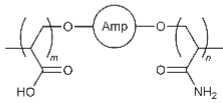
### 4.1. Synthetic acrylamide-based copolymers

Commercial anionic flocculants are often synthesized based on the copolymerization between AM and anionic monomers such as AA and AMPS.<sup>1</sup> All three of these monomers were employed to synthesize terpolymer **60** *via* ultraviolet irradiation (UVI) polymerization.<sup>88–90</sup> With respect to other types of initiation, UVI is an environmentally friendly and easily operated process. In addition, it has other advantages, including higher MW products, less initiator consumption, and faster reaction at lower reaction temperature.<sup>53,54,88</sup> Terpolymer **60**'s flocculation efficiency was tested in diethyl phthalate (DEP), dioctyl phthalate (DOP) simulated wastewater, and dewatering of waste sludge.<sup>88–90</sup> Better flocculation efficiency was observed in the sludge dewatering experiment for terpolymer **60**, when compared to a commercial PAM sample. The results showed that the filter cake moisture content was decreased from 94.6% to 65.1% by terpolymer **60** while only 72.8% was achieved when the commercial PAM sample was used.<sup>88</sup>

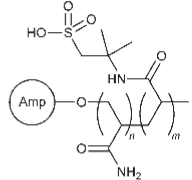
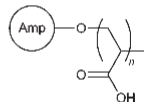
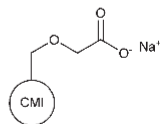
### 4.2. Synthetic acrylamide-free copolymers

The same research group which synthesized AM-free cationic flocculant **34** also developed an anionic derivative using MA as

**Table 3** Summary of the polymerization technique and the testing medium of anionic polymeric materials which were utilised as flocculating agents in previous studies

Entry	Polymer structure <sup>a</sup>	T.o.P <sup>b</sup>	Testing medium	Ref.
60		UVI	Waste sludge; DEP and DOP simulated wastewaters	88–90
61		EP	Clay slurry	5
62		CRG	5 wt% kaolin suspension with Cu <sup>2+</sup> ions	91, 92
63		MWI	River water	93
64		N/A	ZnO suspension; Fe <sub>2</sub> O <sub>3</sub> (hematite) suspension	94
65		N/A	ZnO suspension; Fe <sub>2</sub> O <sub>3</sub> (hematite) suspension	94
66		FRP	1 wt% coal fine suspension	95
67		FRP	50 ppm kaolin solution	96
68		CRG	CuCl <sub>2</sub> solution	97
69		FRP	0.25 wt% iron ore suspension	98

**Table 3** (Contd.)

Entry	Polymer structure <sup>a</sup>	T.o.P <sup>b</sup>	Testing medium	Ref.
70		CRG	1 wt% kaolin suspension	99
71		FRP	Mining industry wastewater; 5 wt% iron ore suspension; 5 wt% manganese suspension; 5 wt% kaolin suspension	100
72		N/A	Municipal sewage wastewater; 0.25 wt% kaolin suspension	101

<sup>a</sup> Abbreviations: Amp, amylopectin; Cell, cellulose; CMC, carboxymethyl cellulose; CMI, carboxymethyl inulin; Cs, chitosan; CST, crosslinked starch; Dex, dextran; GGh, gum ghatti; KGM, Konjac glucomannan; St, starch. <sup>b</sup> Type of polymerization (T.o.P) abbreviations: CRG, conventional redox grafting; EP, emulsion polymerization; FRP, free radical polymerization; MWI, microwave initiated; N/A not applicable; UVI, ultraviolet irradiation.

a non-ionic comonomer.<sup>5</sup> Polymeric flocculant **61** was also synthesized *via* the emulsion polymerization (EP) method, with AA employed as the anionic comonomer. This polymer was able to reduce the turbidity of the clay suspension by a hundredfold with only 2 ppm dosage.<sup>5</sup> In addition, this polymer exhibited comparable flocculation performance to a commercial PAM sample (with slightly higher intrinsic viscosity and lower CD). However, its solvency in water is not as high as AM-based polymers due to relatively poorer solubility of MA.<sup>5</sup>

#### 4.3. Anionically-modified polysaccharides

Chang *et al.* reported the development of a crosslinked starch-based flocculant with PAM and sodium xanthate (SX) grafted onto its backbone.<sup>91</sup> The flocculation efficiency of polymer **62** was tested based on turbidity reduction as well as removal of Cu<sup>2+</sup> ions in kaolin suspension.<sup>91,92</sup> SX-grafted crosslinked starch (CSX) and AM-grafted crosslinked starch (CSA) were also synthesized separately in this study for flocculation comparison purposes. CSA was observed to have significantly lower Cu<sup>2+</sup> removal rate compared to **62** and CSX; whereas CSX showed only slightly lower Cu<sup>2+</sup> removal rate with respect to **62**.<sup>91</sup> The studies also concluded that the presence of high solution turbidity and Cu<sup>2+</sup> ions in the simulated wastewater

complemented each other. The xanthate functional group on the flocculant underwent complexation with  $\text{Cu}^{2+}$  ions to form precipitates, which were observed to be entrained by large flocs as they settled down and *vice versa* for fine suspended solid particles.<sup>91,92</sup> In addition,  $\text{Cu}^{2+}$  ions also neutralized the negative charges on the suspended solids, which decreased the repulsion between the particles and the polymeric chains, hence enhanced the flocculation efficiency.<sup>91</sup>

Mishra *et al.* reported another modified polysaccharide **63**, this time, focused on polyacrylic acid grafted onto carboxymethyl cellulose by MWI synthesis.<sup>93</sup> Recent work by Ghimici and Suflet tested the flocculation efficiency of phosphorylated derivatives of cellulose (P-Cell) **64** and dextran (P-Dex) **65** in zinc oxide and hematite suspensions.<sup>94</sup> The results obtained from this study showed that P-Dex performed better in zinc oxide suspension compared to P-Cell. In addition, P-Dex showed significantly better flocculation performance in hematite fines suspension compared to unmodified dextran.<sup>94</sup>

A non-traditional anionic monomer was used by Yadav *et al.* in the synthesis of chitosan-based polymer **66**. This was achieved by graft copolymerization of 2-acrylamidoglycolic acid onto a chitosan backbone by the FRP method.<sup>95</sup> Apart from starch, cellulose and chitosan, grafted polysaccharides based on gum ghatti (**67**),<sup>96</sup> Konjac glucomannan (**68**),<sup>97</sup> and amylopectin (**69–71**),<sup>98–100</sup> and carboxymethyl inulin (**72**)<sup>101</sup> were also reported in recent studies.

## 5. Amphoteric flocculants

Amphoteric polymers contain both cationic and anionic functional groups and currently have little uses as flocculants in industrial applications.<sup>1</sup> However, these polymers have recently proved to be promising candidates for flocculation in the near future due to the positive properties attributed to both cationic and anionic functional groups.

Table 4 provides a summary of the polymerization technique and the flocculation testing medium for amphoteric polymeric flocculants **73–82**.

### 5.1. Synthetic copolymers

Polymeric chelating agents have gained recent attention as flocculants in the treatment of heavy metal wastewater.<sup>102</sup> Interaction between the anionic groups on these agents and heavy metal ions can lead to precipitation and formation of small flocs, as demonstrated by flocculant **62** and **68**. In addition, the presence of metal ions allows for possible cross-linking between polymer chains, thus enabling small flocs to combine and form larger flocs.<sup>102</sup> However, steric hindrance and spatial mismatch problems associated with polymeric chelating agents can result in formation of loose flocs and therefore poor flocculation performance is often observed.<sup>102</sup>

Liu *et al.* reported multiple studies on the development of an amphoteric chelating polymer in an attempt to tackle this problem.<sup>102–104</sup> Amphoteric polymer **73** was synthesized *via*

**Table 4** Summary of the polymerization technique and the testing medium of amphoteric polymeric materials which were utilised as flocculating agents in previous studies

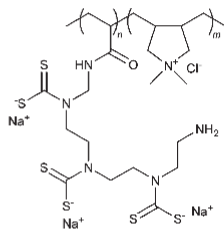
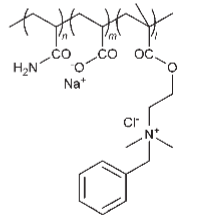
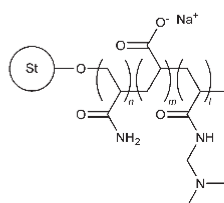
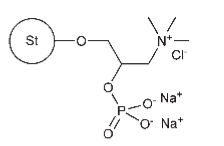
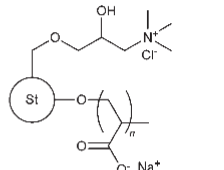
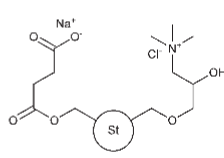
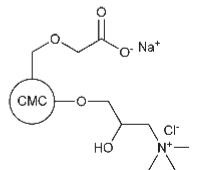
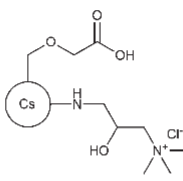
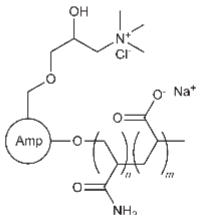
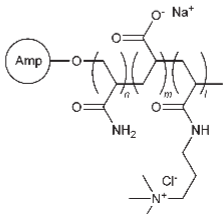
Entry	Polymer structure <sup>a</sup>	T.o.P. <sup>b</sup>	Testing medium	Ref.
73		FRP	Simulated heavy metal wastewater ( $\text{Cu}^{2+}$ , $\text{Cd}^{2+}$ , $\text{Pb}^{2+}$ , $\text{Zn}^{2+}$ or $\text{Ni}^{2+}$ ions)	102–104
74		FRP	1 wt% montmorillonite suspension	105
75		IEP	Dyeing wastewater; paper mill wastewater; refinery wastewater	108
76		MWI	Methyl violet solution	109
77		FRP	0.10 wt% kaolin suspension; 0.10 wt% hematite suspension	106
78		N/A	6 wt% kaolin suspension	112
79		N/A	0.25 wt% kaolin suspension	107

Table 4 (Contd.)

Entry	Polymer structure <sup>a</sup>	T.o.P. <sup>b</sup>	Testing medium	Ref.
80		N/A	Algal turbid water	110
81		MWA	5 wt% iron ore suspension; 3 wt% kaolin suspension; methylene blue solution	111
82		FRP	0.25 wt% kaolin suspension	82

<sup>a</sup> Abbreviations: Amp, amylopectin; CMC, carboxymethyl cellulose; Cs, chitosan; St, starch. <sup>b</sup> Type of polymerization (T.o.P) abbreviations: IEP, inverse emulsion polymerization; FRP, free radical polymerization; MWA, microwave assisted; MWI, microwave initiated; N/A, not applicable.

three main reaction sequences: FRP to form a copolymer between DADMAC and AM; grafting of triethylenetetramine onto the polymer sidechain; and xanthogenation reaction with carbon disulfide.<sup>102</sup> The flocculation efficiency of chelating polymer 73 was subsequently tested with simulated wastewater that contained various heavy metal ions, including  $\text{Cu}^{2+}$ ,  $\text{Cd}^{2+}$ ,  $\text{Pb}^{2+}$ ,  $\text{Zn}^{2+}$  or  $\text{Ni}^{2+}$ .<sup>102–104</sup> The results from these studies indicated that chelation–flocculation efficiency was at its maximum when the molar ratio of  $\text{–CSS}^-$  to the heavy metal ions ( $\text{Cd}^{2+} > \text{Cu}^{2+} > \text{Pb}^{2+} > \text{Ni}^{2+} > \text{Zn}^{2+}$ ) was approximately 2:1.<sup>103</sup> As expected, the heavy metal ions removal rate increased with higher pH levels, and the flocs produced were observed to be highly stable at low concentration of acid.<sup>103</sup> The chelation–flocculation mechanism was improved by the presence of positive charges from DADMAC units within the polymer chain. This was ascribed to the neutralization of excess negative flocs caused by steric hindrance and spatial mismatch that occurred during chelation.<sup>102,103</sup> In addition, these positive charges also interacted with negative charges on

other flocs which resulted in the formation of thicker and denser flocs.<sup>103</sup>

More recently, an amphoteric hydrophobically-modified flocculant 74 was prepared by copolymerization of AM, AA and dimethylbenzyl aminoethyl acrylate chloride.<sup>105</sup> This flocculant was shown to have comparable performance to commercial CPAM and better performance than anionic PAM in montmorillonite simulated wastewater. The effect of  $\text{Na}^+$ ,  $\text{Ca}^{2+}$ ,  $\text{Zn}^{2+}$  and  $\text{Al}^{3+}$  ions were also tested and the results showed that 74 exhibited high salt tolerance with possible potential applications in high-salinity wastewater.<sup>105</sup>

## 5.2. Modified polysaccharides

Most modified polysaccharide studies so far have mainly directed their focus on non-ionic, cationic or anionic-based polymers. Amphoteric polysaccharides have gained recent interest from various research groups due to their beneficial characteristics obtained from the presence of both cationic and anionic moieties, as well as the positive flocculation properties associated with grafted branches.<sup>106</sup> In addition, these types of polymers can also behave as effective flocculating agents across a wide range of pH levels.<sup>107</sup>

Song *et al.* synthesized an amphoteric starch-based polymer 75, and its flocculation efficiency in various types of wastewater was shown to be better in comparison to CPAM, hydrolytic PAM and amphoteric PAM that were used in the study.<sup>108</sup> Another study incorporated non-conventional cationic quaternary ammonium and anionic phosphate moieties onto a starch backbone to develop polymer 76.<sup>109</sup> A common trend was observed in subsequent amphoteric polysaccharide studies, where either etherification or graft copolymerization, or a combination of both were employed to introduce separate cationic and anionic groups onto the polysaccharide backbone.<sup>106,107,110–112</sup> Apart from starch-based polymers 75–78, other studies have also synthesized amphoteric carboxymethyl cellulose (79),<sup>107</sup> chitosan (80),<sup>110</sup> and amylopectin (81, 82).<sup>82,111</sup>

## 6. Future challenges for flocculation

It is clear from this review that the environmental problems associated with current commercially available synthetic flocculation are of great concerns. Only very few of the current industrial processes utilize starch, dextran, carboxymethyl cellulose, guar gum, and chitosan-based polymers for flocculation purposes.<sup>3,10</sup> The majority of the flocculation studies mentioned in this review have combined synthetic and natural polymers together through graft copolymerization. Although this is a positive step towards the synthesis of ‘greener’ flocculants, further studies are required to push the limit of these polymers when it comes to their biodegradability and flocculation efficiency. This would potentially result in greater interests from industries that have the ability to commercialize these polymers for flocculation applications.

The flocculation efficiency of many polymers decreases with an increase in salt content. This is a result of a reduction in the hydrodynamic radius due to the interaction between the salt and the active functional groups on the polymer chain, rendering the polymer impaired or inactive for flocculation.<sup>105</sup> As this interaction is unavoidable, flocculation in high salinity substrates remains a difficult challenge to overcome.

The synthesis of hydrophobically-modified polymeric flocculants is also challenging due to issues associated with the insolubility of hydrophobic monomers in water.<sup>50</sup> This drawback could therefore complicate the synthesis process. In addition, hydrophobically-modified polymers are less soluble in water compared to the conventional polymeric flocculants, and thus their positive properties can be irrelevant if they are poorly soluble in aqueous substrates.

## 7. Conclusions

In this review, we have described the synthesis techniques and flocculation efficiency associated with several non-ionic (1–26, cationic (27–59), anionic (60–72) and amphoteric (73–82) polymers, and a summary of each type of polymeric flocculant is presented in Tables 1–4, respectively. The development of synthetically-modified polysaccharide-based materials was observed to be of significant research interest recently due to their aforementioned biodegradable characteristics compared to synthetic flocculants. In addition, the flocculation efficiency of these modified polymers was better with respect to their original unmodified polysaccharide. This was in agreement with *Singh's Easy Approachability Model* and the *Brostow, Pal and Singh Model of Flocculation*. Synthetic polymeric flocculants have been the minor focus of recent studies due to the current abundance of commercially available synthetic flocculants. However, most synthetic flocculants were observed to be hydrophobically-modified as this can enhance the interaction between the polymer chain and the solid contaminants. The polymeric materials reported in this paper have shown comparable or better flocculation efficiency compared to the current commercial ones, and thus have strong potential as efficient flocculating agents in the near future.

## Acknowledgements

We would like to thank the Chemicals and Plastics Manufacturing Innovation Network and Training Program, supported by Monash University, the Plastics and Chemicals Industries Association (PACIA) and the Victorian Government.

## Notes and references

- 1 H. Burkert and J. Hartmann, in *Ullmann's Encyclopedia of Industrial Chemistry*, Wiley-VCH Verlag GmbH & Co. KGaA, Federal Republic of Germany, 2000, vol. 15, pp. 199–210.

- 2 C. S. Lee, J. Robinson and M. F. Chong, *Process Saf. Environ. Prot.*, 2014, **92**, 489–508.
- 3 G. M. Moody, in *Handbook of Industrial Water Soluble Polymers*, ed. P. A. Williams, John Wiley & Sons, Oxford, The United Kingdom, 2008, pp. 134–173.
- 4 M. S. Nasser and A. E. James, *Sep. Purif. Technol.*, 2006, **52**, 241–252.
- 5 L. Lu, Z. Pan, N. Hao and W. Peng, *Water Res.*, 2014, **57**, 304–312.
- 6 J. Gregory and S. Barany, *Adv. Colloid Interface Sci.*, 2011, **169**, 1–12.
- 7 R. P. Singh, G. P. Karmakar, S. K. Rath, N. C. Karmakar, S. R. Pandey, T. Tripathy, J. Panda, K. Kanan, S. K. Jain and N. T. Lan, *Polym. Eng. Sci.*, 2000, **40**, 46–60.
- 8 B. Bolto and J. Gregory, *Water Res.*, 2007, **41**, 2301–2324.
- 9 E. Sabah and I. Cengiz, *Water Res.*, 2004, **38**, 1542–1549.
- 10 T. Tripathy and B. R. De, *J. Phys. Sci.*, 2006, **10**, 93–127.
- 11 S. Mishra, A. Mukul, G. Sen and U. Jha, *Int. J. Biol. Macromol.*, 2011, **48**, 106–111.
- 12 G. Sen, R. Kumar, S. Ghosh and S. Pal, *Carbohydr. Polym.*, 2009, **77**, 822–831.
- 13 R. P. Singh, in *Polymers and Other Advanced Materials: Emerging Technologies and Business Opportunities*, ed. P. N. Prasad, J. E. Mark and T. J. Fai, Springer US, New York, The United States of America, 1995, pp. 227–249.
- 14 R. Das, S. Ghorai and S. Pal, *Chem. Eng. J.*, 2013, **229**, 144–152.
- 15 W. Brostow, S. Pal and R. P. Singh, *Mater. Lett.*, 2007, **61**, 4381–4384.
- 16 V. K. Thakur, M. K. Thakur and R. K. Gupta, *Carbohydr. Polym.*, 2013, **98**, 820–828.
- 17 M. M. Mishra, D. K. Mishra, P. Mishra and K. Behari, *Carbohydr. Polym.*, 2015, **115**, 776–784.
- 18 S. Pal, S. Ghorai, M. K. Dash, S. Ghosh and G. Udayabhanu, *J. Hazard. Mater.*, 2011, **192**, 1580–1588.
- 19 P. Adhikary, S. Krishnamoorthi and R. P. Singh, *J. Appl. Polym. Sci.*, 2011, **120**, 2621–2626.
- 20 P. Rani, G. Sen, S. Mishra and U. Jha, *Carbohydr. Polym.*, 2012, **89**, 275–281.
- 21 J.-P. Wang, Y.-Z. Chen, S.-J. Zhang and H.-Q. Yu, *Bioresour. Technol.*, 2008, **99**, 3397–3402.
- 22 J. Tripathy, D. K. Mishra, M. Yadav and K. Behari, *Carbohydr. Polym.*, 2010, **79**, 40–46.
- 23 Z. Yang, B. Yuan, X. Huang, J. Zhou, J. Cai, H. Yang, A. Li and R. Cheng, *Water Res.*, 2012, **46**, 107–114.
- 24 A. Srivastava, D. K. Mishra and K. Behari, *Carbohydr. Polym.*, 2010, **80**, 790–798.
- 25 S. Mishra, G. Sen, G. U. Rani and S. Sinha, *Int. J. Biol. Macromol.*, 2011, **49**, 591–598.
- 26 G. U. Rani, S. Mishra, G. Sen and U. Jha, *Carbohydr. Polym.*, 2012, **90**, 784–791.
- 27 G. U. Rani, S. Mishra, G. Pathak, U. Jha and G. Sen, *Int. J. Biol. Macromol.*, 2013, **61**, 276–284.
- 28 G. Sen, G. U. Rani and S. Mishra, *Front. Chem. Sci. Eng.*, 2013, **7**, 312–321.

- 29 K. Xu, X. Xu, Z. Ding and M. Zhou, *China Part.*, 2006, **4**, 60–64.
- 30 T. Tripathy and R. P. Singh, *J. Appl. Polym. Sci.*, 2001, **81**, 3296–3308.
- 31 P. Rani, S. Mishra and G. Sen, *Carbohydr. Polym.*, 2013, **91**, 686–692.
- 32 D. K. Mishra, J. Tripathy and K. Behari, *Carbohydr. Polym.*, 2008, **71**, 524–534.
- 33 M. M. Mishra, A. Sand, D. K. Mishra, M. Yadav and K. Behari, *Carbohydr. Polym.*, 2010, **82**, 424–431.
- 34 S. Krishnamoorthi, P. Adhikary, D. Mal and R. P. Singh, *J. Appl. Polym. Sci.*, 2010, **118**, 3539–3544.
- 35 S. Pal, T. Nasim, A. Patra, S. Ghosh and A. B. Panda, *Int. J. Biol. Macromol.*, 2010, **47**, 623–631.
- 36 R. Rahul, U. Jha, G. Sen and S. Mishra, *Carbohydr. Polym.*, 2014, **99**, 11–21.
- 37 G. Sen, S. Mishra, G. U. Rani, P. Rani and R. Prasad, *Int. J. Biol. Macromol.*, 2012, **50**, 369–375.
- 38 S. Mishra, S. Sinha, K. P. Dey and G. Sen, *Carbohydr. Polym.*, 2014, **99**, 462–468.
- 39 S. Bharti, S. Mishra and G. Sen, *Carbohydr. Polym.*, 2013, **93**, 528–536.
- 40 S. Bharti, S. Mishra, L. V. Narendra, T. Balaraju and K. Balraju, *Desalin. Water Treat.*, 2015, 1–16.
- 41 G. Sen, S. Mishra, K. Prasad Dey and S. Bharti, *J. Appl. Polym. Sci.*, 2014, **131**, 41046.
- 42 S. Ghosh, G. Sen, U. Jha and S. Pal, *Bioresour. Technol.*, 2010, **101**, 9638–9644.
- 43 S. Ghosh, U. Jha and S. Pal, *Bioresour. Technol.*, 2011, **102**, 2137–2139.
- 44 G. Sen and S. Pal, *Macromol. Symp.*, 2009, **277**, 100–111.
- 45 S. Sinha, S. Mishra and G. Sen, *Int. J. Biol. Macromol.*, 2013, **60**, 141–147.
- 46 J. M. Henderson and A. D. Wheatley, *Coal Prep.*, 1987, **4**, 1–49.
- 47 J. M. Henderson and A. D. Wheatley, *J. Appl. Polym. Sci.*, 1987, **33**, 669–684.
- 48 W. Jaeger, J. Bohrisch and A. Laschewsky, *Prog. Polym. Sci.*, 2010, **35**, 511–577.
- 49 Z. Abdollahi, M. Frounchi and S. Dadbin, *J. Ind. Eng. Chem.*, 2011, **17**, 580–586.
- 50 H. Shang, J. Liu, Y. Zheng and L. Wang, *J. Appl. Polym. Sci.*, 2009, **111**, 1594–1599.
- 51 Z. L. Yang, B. Y. Gao, C. X. Li, Q. Y. Yue and B. Liu, *Chem. Eng. J.*, 2010, **161**, 27–33.
- 52 H. Shang, Y. Zheng and J. Liu, *J. Appl. Polym. Sci.*, 2011, **119**, 1602–1609.
- 53 H. Zheng, Y. Sun, C. Zhu, J. Guo, C. Zhao, Y. Liao and Q. Guan, *Chem. Eng. J.*, 2013, **234**, 318–326.
- 54 H. Zheng, Y. Sun, J. Guo, F. Li, W. Fan, Y. Liao and Q. Guan, *Ind. Eng. Chem. Res.*, 2014, **53**, 2572–2582.
- 55 T. Lü, D. Qi, H. Zhao and Y. Cheng, *Polym. Eng. Sci.*, 2015, **55**, 1–7.
- 56 L.-J. Wang, J.-P. Wang, S.-J. Yuan, S.-J. Zhang, Y. Tang and H.-Q. Yu, *Chem. Eng. J.*, 2009, **149**, 118–122.
- 57 L.-J. Wang, J.-P. Wang, S.-J. Zhang, Y.-Z. Chen, S.-J. Yuan, G.-P. Sheng and H.-Q. Yu, *Sep. Purif. Technol.*, 2009, **67**, 331–335.
- 58 H. E. Nasr, A. A. Farag, S. M. Sayyah and S. H. Samaha, *J. Dispersion Sci. Technol.*, 2010, **31**, 427–437.
- 59 K. Z. Abdiyev, Z. Toktarbay, A. Z. Zhenissova, M. B. Zhursumbaeva, R. N. Kainazarova and N. Nuraje, *Colloids Surf., A*, 2015, **480**, 228–235.
- 60 Y. Jiang, B. Ju, S. Zhang and J. Yang, *Carbohydr. Polym.*, 2010, **80**, 467–473.
- 61 Y. Shi, B. Ju and S. Zhang, *Carbohydr. Polym.*, 2012, **88**, 132–138.
- 62 H. Song, *Carbohydr. Polym.*, 2010, **82**, 768–771.
- 63 W. Song, Z. Zhao, H. Zheng and G. Wang, *Water Sci. Technol.*, 2013, **68**, 1778–1784.
- 64 S. Lv, T. Sun, Q. Zhou, J. Liu and H. Ding, *Carbohydr. Polym.*, 2014, **103**, 285–293.
- 65 M. A. A. Razali and A. Ariffin, *Appl. Surf. Sci.*, 2015, **351**, 89–94.
- 66 M. A. A. Razali, H. Ismail and A. Ariffin, *Ind. Crops Prod.*, 2015, **65**, 535–545.
- 67 J.-P. Wang, S.-J. Yuan, Y. Wang and H.-Q. Yu, *Water Res.*, 2013, **47**, 2643–2648.
- 68 Z. Yang, S. Jia, N. Zhuo, W. Yang and Y. Wang, *Chemosphere*, 2015, **141**, 112–119.
- 69 S. Jia, Z. Yang, W. Yang, T. Zhang, S. Zhang, X. Yang, Y. Dong, J. Wu and Y. Wang, *Chem. Eng. J.*, 2016, **283**, 495–503.
- 70 J.-P. Wang, Y.-Z. Chen, Y. Wang, S.-J. Yuan, G.-P. Sheng and H.-Q. Yu, *RSC Adv.*, 2012, **2**, 494–500.
- 71 J.-P. Wang, Y.-Z. Chen, X.-W. Ge and H.-Q. Yu, *Chemosphere*, 2007, **66**, 1752–1757.
- 72 J.-P. Wang, Y.-Z. Chen, S.-J. Yuan, G.-P. Sheng and H.-Q. Yu, *Water Res.*, 2009, **43**, 5267–5275.
- 73 Z. Yang, H. Li, H. Yan, H. Wu, H. Yang, Q. Wu, H. Li, A. Li and R. Cheng, *J. Hazard. Mater.*, 2014, **276**, 480–488.
- 74 X. Jiang, K. Cai, J. Zhang, Y. Shen, S. Wang and X. Tian, *J. Hazard. Mater.*, 2011, **185**, 1482–1488.
- 75 D. K. Mishra, J. Tripathy, A. Srivastava, M. M. Mishra and K. Behari, *Carbohydr. Polym.*, 2008, **74**, 632–639.
- 76 T. Lü, H. Zhao, D. Qi and Y. Chen, *Adv. Polym. Technol.*, 2015, **0**, 21502.
- 77 C. Banerjee, S. Ghosh, G. Sen, S. Mishra, P. Shukla and R. Bandopadhyay, *Carbohydr. Polym.*, 2013, **92**, 675–681.
- 78 A. Pourjavadi, S. M. Fakoorpoor and S. H. Hosseini, *Carbohydr. Polym.*, 2013, **93**, 506–511.
- 79 Y. Pang, Y. Ding and B. Sun, *Procedia Environ. Sci.*, 2013, **18**, 602–609.
- 80 Y. Pang, Y. Ding, J. Chen and W. Gong, *Agric. Sci.*, 2013, **4**, 23–28.
- 81 S. Pal, D. Mal and R. P. Singh, *Colloids Surf., A*, 2006, **289**, 193–199.
- 82 K. Kumar, P. Adhikary, N. C. Karmakar, S. Gupta, R. P. Singh and S. Krishnamoorthi, *Carbohydr. Polym.*, 2015, **127**, 275–281.
- 83 L. Ghimici and M. Nichifor, *Bioresour. Technol.*, 2010, **101**, 8549–8554.

- 84 L. Ghimici, M. Constantin and G. Fundueanu, *J. Hazard. Mater.*, 2010, **181**, 351–358.
- 85 R. Rahul, S. Kumar, U. Jha and G. Sen, *Int. J. Biol. Macromol.*, 2015, **72**, 868–874.
- 86 S. Wang, Q. Hou, F. Kong and P. Fatehi, *Carbohydr. Polym.*, 2015, **124**, 229–236.
- 87 S. Pal, S. Ghosh, G. Sen, U. Jha and R. P. Singh, *Int. J. Biol. Macromol.*, 2009, **45**, 518–523.
- 88 J. Ma, H. Zheng, M. Tan, L. Liu, W. Chen, Q. Guan and X. Zheng, *J. Appl. Polym. Sci.*, 2013, **129**, 1984–1991.
- 89 J. Ma, H. Zheng, X. Tang, W. Chen, W. Xue, Y. Liao, Q. Guan and Y. Liao, *Appl. Mech. Mater.*, 2013, **361**, 726–729.
- 90 H. Zheng, J. Ma, C. Zhu, Z. Zhang, L. Liu, Y. Sun and X. Tang, *Sep. Purif. Technol.*, 2014, **123**, 35–44.
- 91 Q. Chang, X. Hao and L. Duan, *J. Hazard. Mater.*, 2008, **159**, 548–553.
- 92 X. Hao, Q. Chang and X. Li, *J. Appl. Polym. Sci.*, 2009, **112**, 135–141.
- 93 S. Mishra, G. Usha Rani and G. Sen, *Carbohydr. Polym.*, 2012, **87**, 2255–2262.
- 94 L. Ghimici and D. M. Suflet, *Sep. Purif. Technol.*, 2015, **144**, 31–36.
- 95 M. Yadav, A. Sand and K. Behari, *Int. J. Biol. Macromol.*, 2012, **50**, 1306–1314.
- 96 H. Mittal, R. Jindal, B. S. Kaith, A. Maity and S. S. Ray, *Carbohydr. Polym.*, 2014, **114**, 321–329.
- 97 J. Duan, Q. Lu, R. Chen, Y. Duan, L. Wang, L. Gao and S. Pan, *Carbohydr. Polym.*, 2010, **80**, 436–441.
- 98 S. Pal and A. Pal, *Polym. Bull.*, 2012, **69**, 545–560.
- 99 P. Adhikary and S. Krishnamoorthi, *J. Appl. Polym. Sci.*, 2012, **126**, E313–E318.
- 100 A. K. Sarkar, N. R. Mandre, A. B. Panda and S. Pal, *Carbohydr. Polym.*, 2013, **95**, 753–759.
- 101 R. Rahul, U. Jha, G. Sen and S. Mishra, *Int. J. Biol. Macromol.*, 2014, **63**, 1–7.
- 102 L. Liu, J. Wu, Y. Ling, X. Li and R. Zeng, *J. Appl. Polym. Sci.*, 2013, **127**, 2082–2094.
- 103 L. Liu, J. Wu, X. Li and Y. Ling, *Sep. Purif. Technol.*, 2013, **103**, 92–100.
- 104 L. Liu, Y. Li, X. Liu, Z. Zhou and Y. Ling, *Spectrochim. Acta, Part A*, 2014, **118**, 765–775.
- 105 C. Liu, B. Hong, K. Xu, M. Zhang, H. An, Y. Tan and P. Wang, *Polym. Bull.*, 2014, **71**, 3051–3065.
- 106 Z. Yang, H. Wu, B. Yuan, M. Huang, H. Yang, A. Li, J. Bai and R. Cheng, *Chem. Eng. J.*, 2014, **244**, 209–217.
- 107 H. Kono and R. Kusumoto, *React. Funct. Polym.*, 2014, **82**, 111–119.
- 108 H. Song, D. Wu, R.-Q. Zhang, L.-Y. Qiao, S.-H. Zhang, S. Lin and J. Ye, *Carbohydr. Polym.*, 2009, **78**, 253–257.
- 109 Q. Lin, S. Qian, C. Li, H. Pan, Z. Wu and G. Liu, *Carbohydr. Polym.*, 2012, **90**, 275–283.
- 110 C. Dong, W. Chen and C. Liu, *Bioresour. Technol.*, 2014, **170**, 239–247.
- 111 R. P. Singh, S. Pal, V. K. Rana and S. Ghorai, *Carbohydr. Polym.*, 2013, **91**, 294–299.
- 112 E. Lekniute, L. Peciulyte, R. Klimaviciute, J. Bendoraitiene and A. Zemaitaitis, *Colloids Surf., A*, 2013, **430**, 95–102.

### 1.3. Research Background

Mining and minerals processing is one of the world's leading chemical industries with a high and continually growing demand. This industry generates up to thousands of tonnes of process streams and effluent streams daily at each site, and therefore innovation in solid-liquid separation process is a critical factor for the economic and environmental sustainability.<sup>8</sup> The selection of a flocculant for mining applications is difficult due to the complexity associated with the interaction between the flocculant and the solid particles, as well as the characteristic of the aqueous effluents.<sup>8</sup> Table 1.1 below outlines a few general guidelines for selection of optimal polymers based on various aqueous substrates.

**Table 1.1. General guidelines for the selection of the optimal type of flocculant in mining applications.<sup>8</sup>**

Quality of substrate	Type of flocculant
Acidic (E.g. Copper, zinc, nickel leach slurries)	Non-ionic or low anionic (less than 15 mol%) polymeric flocculants
Neutral (E.g. Coal tailings, sand and gravel effluents)	Mid-range anionic (15-45 mol%) polymeric flocculants
Highly alkaline (E.g. Alumina refinery effluents)	Highly anionic (larger than 45 mol%) polymeric flocculants

From this general guidelines, non-ionic and anionic polymeric flocculants are observed to be frequently used in mining applications. Non-ionic flocculants typically contain a small amount of anionic groups, ranging from approximately 1 to 3% of overall ionisable functional groups. This almost-neutral overall charge is attributed to a small degree of hydrolysis occurring during preparation and synthesis of the polymers.<sup>21</sup> Some examples of non-ionic flocculants are PAM, polyvinyl alcohol, polyvinyl pyrrolidone, and polyethylene oxide (PEO) (Figure 1.2a).<sup>9</sup> Polymerisation between acrylamide (AM) and acrylic acid (AA) or its sodium salt is a common method used to synthesise anionic flocculant. Alternatively, other

## Chapter 1

monomers such as methacrylic acid and 2-acrylamido-2-methyl-1-propane sulfonic acid (AMPS) can also be utilised to prepare a wide range of copolymers and terpolymers (Figure 1.2b).<sup>8, 9, 21, 22</sup>

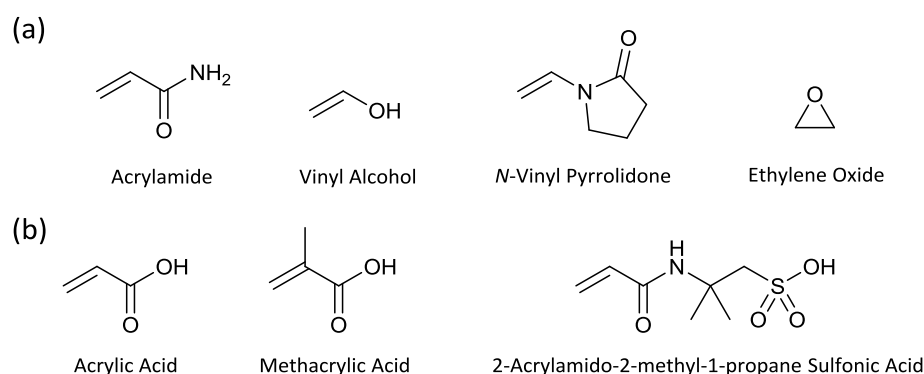


Figure 1.2. Chemical structures of commonly used monomers for the synthesis of (a) non-ionic and (b) anionic flocculants.

Flocculation performance is dependent on several factors, acting individually or collectively. Salinity, pH, agitation rate, and the flocculant's characteristics such as charge density, molecular weight, and concentration are a few of the many factors regulating the flocculation efficiency.<sup>3, 23, 24</sup> Therefore, various factors along with environmental considerations must be analysed prior to the selection of a flocculant for a particular industrial application. Flocculation efficiency is often evaluated based on the quality of the recovered water and the settlement rate of the flocs. Previous studies have shown that there is a great difficulty in achieving high settling rate and high water quality simultaneously, as there are many variables that could affect the performance of a flocculant.<sup>25</sup> However, the trade-off between the overflow's clarity and the settlement rate of the flocs is often tolerated, depending on the type of industrial application where flocculation is employed.

Recent mineral processing practices had directly employed seawater as the aqueous medium due to its natural abundance and ability to increase flocculation efficiency. A comparison between saline and freshwater tailings performed by Ji *et al.* showed a significantly higher quantity of Na<sup>+</sup>, K<sup>+</sup>, Mg<sup>2+</sup>, Ca<sup>2+</sup>, and other heavy metals such as iron, nickel, copper, selenium and strontium.<sup>23</sup> Although there had been advances in mineral flotation using saline water, the knowledge on the influence of salinity is still limited.<sup>23, 26</sup> Multiple studies performed by Ji *et al.*, Kim *et al.*, and Portela *et al.* demonstrated an

## Chapter 1

increase in the settling rate and/or a decreased in the turbidity as the salinity increased.<sup>23, 26, 27</sup> With an optimal increase in the salt concentration, the electrical double layer was compressed, which consequently destabilise the suspension to promote efficient flocculation.<sup>23, 28</sup> Rogan stated that this was only accurate for low ionic strength solutions (ionic strength less than 0.01) where the polymer elongated and expanded due to intramolecular electrostatic repulsion.<sup>29</sup> With high salinity solution (ionic strength more than 0.10), the presence of dissolved salts shielded active groups on the polymer, resulted in a condensed conformation of the flocculant.<sup>29, 30, 31</sup> Consequently, this imposed a negative impact on the solvency, bridging efficiency, viscosity and dispersion capability of the polymer.<sup>29, 32</sup>

Mining-impacted water often contains high quantity of divalent cations such as  $\text{Ca}^{2+}$  and  $\text{Mg}^{2+}$ . Although these cations had been known improve flocculation through various enhancement of the adsorption process.<sup>8, 33, 34, 35</sup> A few studies had found that high levels of dissolved calcium and magnesium salts inflicted detrimental effects on the properties and efficiency of a flocculant itself.<sup>32</sup> Liu *et al.* determined that the recovery rate of bottom concentrate following flocculation was lower in hard water compared to that of soft water.<sup>36</sup> This was attributed to the competitive attachment of  $\text{Ca}^{2+}$  and  $\text{Mg}^{2+}$  on the active sites of the flocculants, thereby resulted in poor adsorption of polymer onto the suspended particles. In addition, with respect to monovalent cations, cations with higher valency were shown to have greater effects on the settling rate of the bottom concentrate.<sup>36</sup>

Witham *et al.* also claimed divalent cations ( $\text{Ca}^{2+}$  and  $\text{Mg}^{2+}$ ) inflicted a negative effect on the flocculant efficiency in a dilute solution, with  $\text{Ca}^{2+}$  being more dominant compared to  $\text{Mg}^{2+}$ .<sup>32</sup> The settling rate was observed to approach a plateau when the concentration of  $\text{Ca}^{2+}$  was increased. Furthermore, there was a larger influence on the settling rate when high charge density anionic flocculants was used compared to a low anionic flocculant.<sup>32</sup> However, there was a conflict between the results obtained by Witham *et al.* and older studies conducted by Henderson and Wheatley, which showed the presence of cations ( $\text{Na}^+$ ,  $\text{K}^+$ ,  $\text{Ca}^{2+}$ ,  $\text{Mg}^{2+}$ ,  $\text{Zn}^{2+}$ ,  $\text{Cu}^{2+}$ ,  $\text{Pb}^{2+}$ ,  $\text{Al}^{3+}$ , and  $\text{Fe}^{3+}$ ) only imposed significant effects on concentrated solution (30% w/v) of flocculant and not the diluted solution (0.2% w/v).<sup>32, 37, 38</sup> Witham *et al.* suggested

## Chapter 1

that the reason for this conflict in results was due to excessive shear effects in batch testings performed in the older studies, which lead to loss of sensitivity in flocculation.<sup>32</sup>

Multivalent cations were also known to interact with the carboxylate functional group on the polymer chain, which lead to precipitation and formation of insoluble polyacrylate species.<sup>39</sup> The results from a study conducted by Boisvert *et al.* claimed out of the three cations used ( $\text{Ca}^{2+}$ ,  $\text{Mg}^{2+}$ , and  $\text{Ba}^{2+}$ ),  $\text{Ba}^{2+}$  had the highest affinity to form polymeric complexes through interactions with the acrylate group, subsequently followed by  $\text{Ca}^{2+}$  and  $\text{Mg}^{2+}$ , respectively. The formation of insoluble species was concluded to be dependent on the hydration energy; a stronger interaction between the polymer and the cation was observed when the cation possessed a lower hydration energy, and vice versa.<sup>39</sup>

In a comparison between  $\text{Na}^+$  and  $\text{Ca}^{2+}$ , Huber stated  $\text{Ca}^{2+}$  ion binding to polyacrylate was much stronger compared to that of  $\text{Na}^+$ .<sup>40</sup> This was explained by the higher degree of neutralisation in  $\text{Ca}^{2+}$ , which pointed to additional intramolecular bridging ( $\text{COO}^- - \text{Ca}^{2+} - \text{OOC}$ ) and thus resulted in a higher propensity for precipitate formation. When the binding capacity of the polymer was exceeded, the interaction between  $\text{Ca}^{2+}$  and polyacrylate resulted in precipitation of insoluble calcium polyacrylate salts.<sup>40</sup> Similar findings were obtained by Peng and Di44, which indicated deterioration in flocculant efficiency caused by two  $\text{Ca}^{2+}$  species ( $\text{Ca}^{2+}$  ion and  $\text{CaOH}^+$  ion, with  $\text{Ca}^{2+}$  ion being the predominant species) to form  $(\text{COO})_2\text{Ca}$  and  $-\text{COOCa}(\text{OH})$ , respectively.<sup>41</sup> The binding caused a change in polymer conformation due to weaken repulsive forces between anionic functional groups, which eventually lead to precipitation and formation of insoluble hydroxyl complexes.<sup>41</sup> Therefore, it is evident that the interaction between multivalent cations and the anionic functional groups on the polymer chain is unavoidable and remains a difficult challenge to overcome.

### 1.4. Research Objectives

This industry-based research project is a collaboration between Monash University and BASF Australia, with a primary focus on the development of novel anionic polymers with potential flocculation applications in mining and minerals processing. As mentioned previously, mining-impacted water with significantly high ionic content can have a negative effect on the flocculation efficiency of the anionic flocculants. The interactions between multivalent cations and the anionic functional groups on the polymer chain would lead to shielding of these active groups and hence a condensed polymer conformation (Figure 1.3a). In addition, intramolecular crosslinking associated with the multivalent cations could lead to the formation of insoluble polyacrylate species. Consequently, this interaction renders the anionic polymers inefficient or inactive for the flocculation process. Therefore, to address this challenge and narrow the research gap, the main objective of this research project is to design and develop novel anionic polymers with improved stability in high ionic strength environments, whilst still exhibiting a comparable or better flocculation efficiency compared to the current commercial flocculants.

To address this research objective, the first part of this project was aimed towards the synthesis, purification, and characterisation of a series of ultra-high molecular weight (UHMW) ABA triblock copolymers and star-shaped AB block copolymers. The A and B blocks represent anionic and non-ionic blocks derived from AA and AM, respectively. The second part of the project involves the flocculation efficiency analysis of the aforementioned copolymers, with direct comparison to control copolymers bearing similar molecular weights that are also representative of current commercial flocculants. To the best of our knowledge, the use of ABA triblock and star-shaped block copolymers as industrial flocculants is a novel concept, particularly in high ionic strength environment. Very little work in the field has directly focused on exploiting the architecture of the copolymers in general for flocculation analysis. In addition, none have used the controlled radical polymerisation techniques outlined in this thesis to create advanced polymers for employment as flocculants.

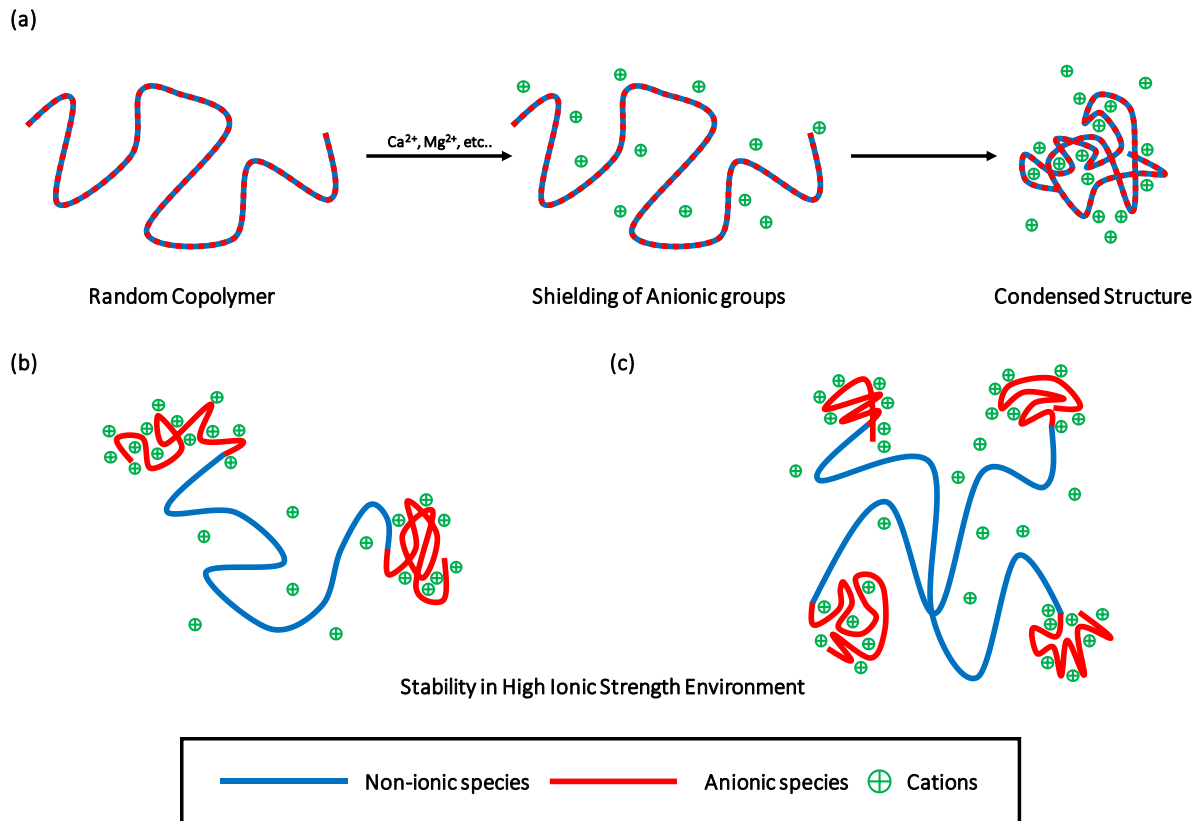


Figure 1.3. Illustration showing (a) the negative effects of multivalent cations on random copolymer in high ionic strength environment, and conversely the stability of (b) ABA triblock and (c) star-shaped block architectures.

Due to the precise architecture of these UHMW ABA triblock and star-shaped block copolymers, the interactions between the multivalent cations within the aqueous environment and the polymeric chain would be reduced and localised to the anionic terminals (Figure 1.3b and c, respectively). The highly water-soluble non-ionic B block at the centre of the chain would stabilise the overall solubility of the polymer even if the terminal anionic blocks were compromised by multivalent cations. Consequently, these polymers were hypothesised to have better solubility in high ionic strength environment compared to commercial anionic flocculants, which typically exhibit random copolymer architecture. The unique properties obtained from these polymers would have the potential to address the problems associated with poor flocculation efficiency observed in high ionic strength environments.

## Chapter 1

### 1.5. Thesis Outline

**Chapter 1** of the thesis provides a general overview on the field of flocculation, mechanisms of flocculation, and its applications. In addition, this chapter also includes a review paper which outlined the synthesis technique and flocculation efficiency of several newly developed organic polymeric flocculants. The review paper is titled *“Synthesis, properties and performance of organic polymers employed in flocculation applications”* and it is separated into four main sections to depict the four main types of flocculants: non-ionic, cationic, anionic, and amphoteric. The last section of this chapter explains the research background, which focuses on the negative impact that multivalent cations have on the flocculation efficiency of anionic flocculants, and consequently how this challenge can be addressed through the main objectives of this research project.

**Chapter 2** is a research paper titled *“Synthesis of ultra-high molecular weight ABA triblock copolymers via aqueous RAFT-mediated gel polymerisation, end group modification and chain coupling”*. This paper described a three-step synthetic pathway to create a series of UHMW ABA triblock copolymers (**ABA1 – ABA8**). This was initially achieved through a sequential RAFT-mediated gel polymerisation technique to synthesise the UHMW AB diblock copolymers derived from AA and AM monomers. The final stage involved the end-group modification of these polymers *via* an aminolysis process to allow for spontaneous chain coupling under oxidative environment, which led to the formation of the UHMW ABA triblock copolymers.

**Chapter 3** is a submitted manuscript titled *“Enhanced flocculation efficiency in high ionic strength environment by the aid of anionic ABA triblock copolymers”*. This paper described the use of the aforementioned ABA triblock copolymers (**ABA1 – ABA8**) in Chapter 2 to flocculate high ionic strength kaolin clay slurries at three different  $\text{Ca}^{2+}$  concentrations of 0.05 M, 0.10 M, and 0.50 M. The flocculation efficiency of these ABA triblock copolymers was compared against three control polymers with similar molecular weight: homopolymer of AA (**PAA**), homopolymer of AM (**PAM**), and random copolymer of

## Chapter 1

AA and AM (**RAB**). Two different methodologies of flocculation involving cylinder settling tests and turbulent pipe flow with focused beam reflectance measurement were employed. The former was used to analyse the flocculation efficiency, whilst the latter was employed to understand the flocculation mechanism and aggregate profile.

**Chapter 4** is a submitted manuscript titled “*Synthesis of UHMW star-shaped AB block copolymers and their flocculation efficiency in high ionic strength environments*”. The first part of this manuscript focused on the synthesis and characterisation of a series of UHMW 4-arm star-shaped block copolymers (**4A-BA1 – 4A-BA6**). The second part employed these star-shaped block copolymers for flocculation analysis in high ionic strength kaolin slurries (0.05 M, 0.10 M, and 0.50 M). Cylinder settling test was employed as the main methodology to determine the flocculation efficiency. Similarly to Chapter 3, the flocculation efficiency of these star-shaped copolymers were directly compared against the control polymers **PAA**, **PAM**, and **RAB**. The final part of this chapter also outlines the attempts in creating 4-arm star-shaped block copolymers based on the existing AB diblock copolymers described in Chapter 2.

**Chapter 5** concludes the thesis by providing a summary of the main scientific findings obtained from this research project. In addition, this chapter also provides practical suggestions that this research project could take on in the future to further narrow the research gap and address the research problem in a more efficient manner.

## 1.6. References

1. Dao, V. H.; Cameron, N. R.; Saito, K. Synthesis, properties and performance of organic polymers employed in flocculation applications. *Polym. Chem.* **2016**, *7*, 11-25.
2. Lee, C. S.; Robinson, J.; Chong, M. F. A review on application of flocculants in wastewater treatment. *Process Saf. Environ. Prot.* **2014**, *92* (6), 489-508.
3. Moss, N. Flocculation: Theory and Application. *Mine and Quarry Journal* **1979**, *7* (5), 57-61.
4. Tripathy, T.; De, B. R. Flocculation: A New Way to Treat the Waste Water. *J. Phys. Sci.* **2006**, *10*, 93-127.
5. Shaw, D. J. *Introduction to Colloid and Surface Chemistry*; Elsevier 1992. p 306.
6. Rabiee, A.; Zeynali, M. E.; Baharvand, H. Synthesis of High Molecular Weight Partially Hydrolyzed Polyacrylamide and Investigation on its Properties. *Iran. Polym. J.* **2005**, *14* (7), 603-608.
7. Hunter, R. J. *Foundation of Colloid Science*; Oxford University Press 2001.
8. Moody, G. M. Chapter 6: Polymeric Flocculants. In *Handbook of Industrial Water Soluble Polymers*, Williams, P. A., Ed.; John Wiley & Sons: Oxford, The United Kingdom, 2008, pp 134-173.
9. Gregory, J.; Barany, S. Adsorption and flocculation by polymers and polymer mixtures. *Adv. Colloid Interface Sci.* **2011**, *169* (1), 1-12.
10. Burkert, H.; Hartmann, J. Flocculants. In *Ullmann's Encyclopedia of Industrial Chemistry*; Wiley-VCH Verlag GmbH & Co. KGaA: Federal Republic of Germany, 2000; Vol. 15, pp 199-210.
11. Kurenkov, V. F. Chapter 3: Acrylamide Polymers. In *Handbook of Engineering Polymeric Materials*, Cheremisinoff, P., Ed.; CRC Press, 1997, pp 61-72.

## Chapter 1

12. Records, A.; Sutherland, K. Chapter 5: Flocculation. In *Decanter Centrifuge Handbook*, Records, A.; Sutherland, K., Eds.; Elsevier, 2001, pp 215-241.
13. Singh, R. P. Advanced Turbulent Drag Reducing and Flocculating Materials Based on Polysaccharides. In *Polymers and Other Advanced Materials: Emerging Technologies and Business Opportunities*, Prasad, P. N.; Mark, J. E.; Fai, T. J., Eds.; Springer US: New York, The United States of America, 1995, pp 227-249.
14. Singh, R. P.; Karmakar, G. P.; Rath, S. K.; Karmakar, N. C.; Pandey, S. R.; Tripathy, T.; Panda, J.; Kanan, K.; Jain, S. K.; Lan, N. T. Biodegradable Drag Reducing Agents and Flocculants Based on Polysaccharides: Materials and Applications. *Polym. Eng. Sci.* **2000**, *40* (1), 46-60.
15. Shang, H.; Liu, J.; Zheng, Y.; Wang, L. Synthesis, Characterization, and Flocculation Properties of Poly(acrylamide-methacryloxyethyltrimethyl Ammonium Chloride-Methacryloxypropyltrimethoxy Silane). *J. Appl. Polym. Sci.* **2009**, *111* (3), 1594-1599.
16. Shang, H.; Zheng, Y.; Liu, J. Synthesis in Inverse Emulsion and Decolorization Properties of Hydrophobically Modified Cationic Polyelectrolyte. *J. Appl. Polym. Sci.* **2011**, *119* (3), 1602-1609.
17. Yang, Z. L.; Gao, B. Y.; Li, C. X.; Yue, Q. Y.; Liu, B. Synthesis and characterization of hydrophobically associating cationic polyacrylamide. *Chem. Eng. J.* **2010**, *161* (1–2), 27-33.
18. Zheng, H.; Sun, Y.; Guo, J.; Li, F.; Fan, W.; Liao, Y.; Guan, Q. Characterization and Evaluation of Dewatering Properties of PADB, a Highly Efficient Cationic Flocculant. *Ind. Eng. Chem. Res.* **2014**, *53* (7), 2572-2582.
19. Zheng, H.; Sun, Y.; Zhu, C.; Guo, J.; Zhao, C.; Liao, Y.; Guan, Q. UV-initiated polymerization of hydrophobically associating cationic flocculants: Synthesis, characterization, and dewatering properties. *Chem. Eng. J.* **2013**, *234* (0), 318-326.

## Chapter 1

20. Liu, C.; Hong, B.; Xu, K.; Zhang, M.; An, H.; Tan, Y.; Wang, P. Synthesis and application of salt tolerance amphoteric hydrophobic associative flocculants. *Polym. Bull.* **2014**, *71* (12), 3051-3065.
21. Bolto, B.; Gregory, J. Organic polyelectrolytes in water treatment. *Water Res.* **2007**, *41* (11), 2301-2324.
22. Ma, J.; Zheng, H.; Tang, X.; Chen, W.; Xue, W.; Liao, Y.; Guan, Q.; Liao, Y. Research on flocculation behavior in diethyl phthalate removal from water by using anionic flocculants P(AM-AA-AMPS). *Appl. Mech. Mater.* **2013**, *361*, 726-729.
23. Ji, Y.; Lu, Q.; Liu, Q.; Zeng, H. Effect of solution salinity on settling of mineral tailings by polymer flocculants. *Colloids Surf. A: Physicochem. Eng. Aspects* **2013**, *430*, 29-38.
24. Pillai, J. Flocculants and Coagulants: The Keys to Water and Waste Management in Aggregate Production. *Naperville, IL: Nalco Company (Stone Review)* **1997**, 1-6.
25. Sabah, E.; Cengiz, I. An evaluation procedure for flocculation of coal preparation plant tailings. *Water Res.* **2004**, *38* (6), 1542-1549.
26. Portela, L. I.; Ramos, S.; Teixeira, A. T. Effect of salinity on the settling velocity of fine sediments of a harbour basin. *J. Coast. Res.* **2013**, *65*, 1188-1193.
27. Kim, M.; Kim, S.; Kim, J.; Kang, S.; Lee, S. Factors affecting flocculation performance of synthetic polymer for turbidity control. *J. Agric. Chem. Environ.* **2013**, *2* (1), 16-21.
28. Ritvo, G.; Dassa, O.; Kochba, M. Salinity and pH effect on the colloidal properties of suspended particles in super intensive aquaculture systems. *Aquaculture* **2003**, *218* (1), 379-386.
29. Rogan, K. R. The variations of the configurational and solvency properties of low molecular weight sodium polyacrylate with ionic strength. *Colloid. Polym. Sci.* **1995**, *273* (4), 364-369.

## Chapter 1

30. Mortimer, D. A. Synthetic Polyelectrolytes - A Review. *Polym. Int.* **1991**, 25 (1), 29-41.
31. Kay, P. J.; Treloar, F. E. The Intrinsic Viscosity of Poly(acrylic acid) at Different Ionic Strengths: Random Coil and Rigid Rod Behaviour. *Die Makromolekulare Chemie* **1974**, 175 (11), 3207-3223.
32. Witham, M. I.; Grabsch, A. F.; Owen, A. T.; Fawell, P. D. The effect of cations on the activity of anionic polyacrylamide flocculant solutions. *Int. J. Miner. Process.* **2012**, 114-117, 51-62.
33. Sabah, E.; Erkan, Z. E. Interaction mechanism of flocculants with coal waste slurry. *Fuel* **2006**, 85 (3), 350-359.
34. Mpofu, P.; Addai-Mensah, J.; Ralston, J. Influence of hydrolyzable metal ions on the interfacial chemistry, particle interactions, and dewatering behavior of kaolinite dispersions. *J. Colloid Interface Sci.* **2003**, 261 (2), 349-359.
35. Sworska, A.; Laskowski, J. S.; Cymerman, G. Flocculation of the Syncrude fine tailings: Part I. Effect of pH, polymer dosage and Mg<sup>2+</sup> and Ca<sup>2+</sup> cations. *Int. J. Miner. Process.* **2000**, 60 (2), 143-152.
36. Liu, W.; Sun, W.; Hu, Y. Effects of water hardness on selective flocculation of diasporic bauxite. *Trans. Nonferrous. Met. Soc. China.* **2012**, 22 (9), 2248-2254.
37. Henderson, J. M.; Wheatley, A. D. Factors affecting the efficient flocculation of tailings by polyacrylamides. *Coal. Prep* **1987**, 4 (1-2), 1-49.
38. Henderson, J. M.; Wheatley, A. D. Factors Effecting a Loss of Flocculation Activity of Polyacrylamide Solutions: Shear Degradation, Cation Complexation, and Solution Aging. *J. Appl. Polym. Sci.* **1987**, 33 (2), 669-684.
39. Boisvert, J.-P.; Malgat, A.; Pochard, I.; Daneault, C. Influence of the counter-ion on the effective charge of polyacrylic acid in dilute condition. *Polymer* **2002**, 43 (1), 141-148.

## Chapter 1

40. Huber, K. Calcium-Induced Shrinking of Polyacrylate Chains in Aqueous Solution. *J. Phys, Chem* **1993**, *97* (38), 9825-9830.
41. Peng, F. F.; Di, P. Effect of Multivalent Salts - Calcium and Aluminum on the Flocculation of Kaolin Suspension with Anionic Polyacrylamide. *J. Colloid Interface Sci.* **1994**, *164* (1), 229-237.

# Chapter 2

Synthesis of Ultra-high Molecular Weight ABA Triblock Copolymers *via*  
Aqueous RAFT-mediated Gel Polymerisation, End Group Modification and Chain Coupling

This page is intentionally left blank.

# Chapter 2

## Synthesis of Ultra-high Molecular Weight ABA Triblock Copolymers *via* Aqueous RAFT-mediated Gel Polymerisation, End Group Modification and Chain Coupling

---

### 2.1. General Overview

Chapter 2 is a journal paper titled “*Synthesis of ultra-high molecular weight ABA triblock copolymers via aqueous RAFT-mediated gel polymerisation, end group modification and chain coupling*”, which was published in Polymer Chemistry in 2017.

In this chapter, the design and synthesis of a series of UHMW ABA triblock copolymers derived from AA and AM monomers were investigated and hereby discussed. A simple two-stage aqueous RAFT-mediated gel polymerisation technique was initially used to synthesise high molecular weight AB diblock copolymers with low dispersities ( $\mathcal{D} < 1.50$ ). The use of said gel polymerisation method in combination with a redox initiation system allowed for the rapid chain propagation of water-soluble monomers under low reaction temperatures (below ambient). However, poor propagation efficiency was observed when RAFT polymerisation was once again employed to integrate the third A block into the polymer chain. Alternatively, these AB diblock copolymers were subsequently used in the final aqueous aminolysis stage where the thiocarbonylthio terminal was converted to thiol functionality, which spontaneously coupled under oxidative condition to form disulfide bridges between the AB diblock copolymers to produce the final UHMW ABA triblock copolymers (**ABA1** – **ABA8**). The overall schematic for this three-stage synthetic process is shown in Figure 2.1.

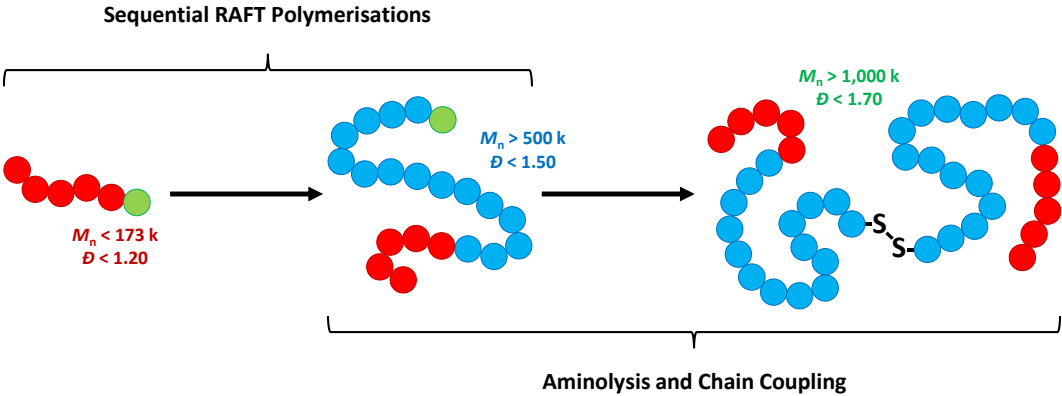
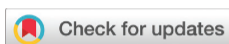


Figure 2.1. Overall schematic for the synthesis of the UHMW ABA triblock copolymers.



Cite this: *Polym. Chem.*, 2017, 8, 6834

## Synthesis of ultra-high molecular weight ABA triblock copolymers *via* aqueous RAFT-mediated gel polymerisation, end group modification and chain coupling†

Vu H. Dao, <sup>a</sup> Neil R. Cameron <sup>\*b,c</sup> and Kei Saito <sup>\*a</sup>

The synthesis of ultra-high molecular weight (UHMW) polymers using reversible deactivation radical polymerisation techniques remains a challenge and has been the centre of attention only in a limited number of studies. Although UHMW polymers were synthesised in these research studies, the complexity in architecture has mainly been limited to linear homopolymers and AB diblock copolymers. We hereby report a new pathway to synthesise UHMW ABA triblock copolymers using a combination of reversible addition–fragmentation chain transfer (RAFT) polymerisation, end-group modification by aminolysis and chain coupling. A simple aqueous RAFT-mediated gel polymerisation technique was initially employed to synthesise high molecular weight AB diblock copolymers with low dispersities ( $D < 1.50$ ). The use of the said gel polymerisation method in combination with a redox initiation system allowed for the rapid chain propagation of water-soluble monomers at a low reaction temperature of 20 °C. These polymers were subsequently treated by aminolysis to convert the chain end into a thiol functionality, which spontaneously coupled under oxidative conditions to form a disulfide bridge between the AB diblock copolymers to produce the final UHMW ABA triblock copolymers ( $M_{n,SEC} > 1000k$ ;  $D < 1.70$ ).

Received 21st August 2017,  
Accepted 18th October 2017

DOI: 10.1039/c7py01410d

rsc.li/polymers

### Introduction

Reversible deactivation radical polymerization (RDRP) has gained tremendous attention from the polymer research community as it can produce polymers with precise molecular weights, diverse architectures and narrow dispersities. However, the design and synthesis of ultra-high molecular weight (UHMW) polymers ( $M_n > 500k$ ) using RDRP techniques remain a challenge and have been reported only in a few isolated studies.<sup>1–3</sup> UHMW polymers are extensively used in many industrial applications including, but not limited to, oil recovery, hydraulic fracturing, mining and mineral processing, paper production, waste water treatment and biotechnology.<sup>1,4</sup>

Well-defined UHMW polymers have previously been synthesised by atom transfer radical polymerisation (ATRP),<sup>5–11</sup> single-electron transfer living radical polymerisation (SET-LRP),<sup>12–14</sup> and reversible addition–fragmentation chain

transfer (RAFT)<sup>1–3,11,15–17</sup> polymerisation. However, the methodologies employed to synthesise these polymers often required the use of environmentally unfriendly organic solvents, metal catalysts or high reaction pressures. For instance, pressures of up to 9 kbar were used by both Arita *et al.*<sup>8</sup> and Rzayev *et al.*<sup>15</sup> to synthesise well-controlled poly(methyl methacrylate) with  $M_n$  of up to 3600k. Mueller *et al.*<sup>9</sup> was able to synthesise polystyrene with  $M_n$  of 1030k at a pressure of 6 kbar. Well-defined polyacrylonitrile with  $M_n$  of 1030k was synthesised by Huang *et al.*<sup>10</sup> within just 2 hours at a pressure of 5 kbar. Some recent studies however reported the synthesis of well-defined UHMW acrylamido-based polymers *via* fast and simple aqueous RAFT polymerisations without the need for a high pressure or a metal catalyst.<sup>1–3</sup> Read *et al.*<sup>1</sup> were able to produce acrylamido-based polymers with molecular weights of 1000k by using the redox initiation pair ammonium persulfate (APS) and sodium formaldehyde sulfoxylate (SFS) under gel polymerisation conditions. Gel polymerisation is a type of homogeneous aqueous polymerisation process that utilises a high monomer concentration in combination with an optimised initiation profile that would favour fast reaction kinetics at low temperatures. At this high monomer concentration, the reaction mixture typically forms a non-covalent gel rapidly throughout the polymerisation, and hence the name.<sup>1,18</sup> Another study conducted by Carmean *et al.*<sup>2</sup> pushed the limit

<sup>a</sup>School of Chemistry, Monash University, Clayton, VIC 3800, Australia.

E-mail: kei.saito@monash.edu; Fax: +613 9905 8501; Tel: +61 3 9905 4600

<sup>b</sup>Department of Materials Science and Engineering, Monash University, Clayton, VIC 3800, Australia. E-mail: neil.cameron@monash.edu; Tel: +61 3 9902 0774

<sup>c</sup>School of Engineering, University of Warwick, Coventry, CV4 7AL, UK

† Electronic supplementary information (ESI) available. See DOI: 10.1039/c7py01410d

further by utilising photopolymerisation to produce poly(dimethylacrylamide) with a molecular weight of 8570k, which is the highest value reported to date.

Although UHMWs were achieved in these studies, the complexity in architecture has primarily been limited to homopolymers, statistical copolymers, and AB diblock copolymers. Read *et al.*<sup>1</sup> reported the synthesis of an AB diblock copolymer ( $M_n = 1020k$ ), where the A and B blocks were derived from *N*-isopropylacrylamide (NIPAM) and dimethylacrylamide (DMA), respectively. Carmean *et al.*<sup>2</sup> were able to produce another AB diblock copolymer with a higher molecular weight ( $M_n = 2670k$ ), where both blocks were derived from DMA. To the best of our knowledge, only one recent study conducted by Despax *et al.*<sup>3</sup> has reported the synthesis of ABA triblock copolymers polymerised from DMA and NIPAM but the molecular weight of these polymers was only up to 500k. Therefore, the ability to develop different polymers with advanced architectures and higher molecular weights ( $M_n > 1000k$ ) could potentially give rise to a whole new class of materials with unique properties.<sup>2</sup> This next stage of development in well-controlled UHMW polymers could be achieved by exploiting the end-group removal and modification process of RAFT polymers.

The conversion of a thiocarbonylthio group into a thiol in the presence of nucleophiles or ionic reducing agents is one of the most widely reported techniques of end-group modification for RAFT polymers.<sup>19</sup> Thiol-terminated polymers can subsequently undergo spontaneous disulfide coupling under an oxidative environment.<sup>20</sup> Primary or secondary amines are most commonly used for this, in a process referred to as aminolysis.<sup>21</sup> Disulfide linkages formed by chain coupling have high resistance towards moisture, ozone, weathering, as well as oil and most of the organic solvents.<sup>22</sup> In addition, the disulfide linkages formed can be cleaved in the presence of reducing agents, such as zinc dust and acetic acid, or tris(2-carboxyethyl)phosphine.<sup>19</sup> The cleavable feature of these disulfide linkages as well as their high tolerance to harsh conditions could prove to be advantageous in a multitude of industrial applications.

In this work, we have synthesised a series of novel UHMW water-soluble ABA triblock copolymers with  $M_n > 1000k$  ( $D < 1.70$ ), where the A and B blocks were derived from acrylic acid (AA) and acrylamide (AM), respectively. Copolymers based on AA and AM have many uses in industries that are also in alignment to those that employ UHMW polymers. Some examples include agriculture, waste water treatment, mining, oil drilling, cosmetics, personal care products, paints and detergents.<sup>23</sup> In addition, the electrolytic nature of AA in well-defined block copolymers can be tuned at different pH values and ionic strengths to allow for desirable amphiphilic properties.<sup>24</sup> In comparison to previous studies, these ABA triblock copolymers based on AA and AM are the first of their kind with such high molecular weights and low dispersities. In addition, this is the first report of UHMW ABA triblock copolymers with molecular weights above 1000k.

Under gel polymerisation conditions, we employed a water-soluble monofunctional trithiocarbonate chain transfer agent

(CTA), 3-(((1-carboxyethylthio)carbonothioyl)thio)propanoic acid (CETCTP), in combination with an ammonium persulfate and sodium formaldehyde sulfoxylate redox initiating system (APS/SFS) to synthesise the initial AB diblock copolymers. Poor blocking efficiency was observed when RAFT polymerisation was initially used to incorporate the third A block into the polymer chain. Therefore, this problem was addressed with a simple aminolysis and chain end coupling stage using *n*-butylamine, where the AB diblock copolymers were converted into the desired UHMW ABA triblock copolymers with a molecular weight above 1000k. These ABA triblock copolymers are the first of their kind with such high molecular weights and low dispersities.

## Experimental section

### Materials

Prior to use, acrylic acid (AA; Aldrich, 99%) was pre-treated with basic aluminium oxide (Acros Organics) to remove the radical inhibitor monomethyl ether hydroquinone. Acrylamide (AM; Sigma, 99%), 3-(((1-carboxyethylthio)carbonothioyl)thio)propanoic acid (CETCTP; Boron Molecular, 90%), ammonium persulfate (APS; Sigma-Aldrich, 98%), sodium formaldehyde sulfoxylate dihydrate (SFS; Aldrich, 98%), *n*-butylamine (Sigma-Aldrich, 99.5%), sodium hydroxide (Merck, 99%), sodium nitrate (Merck, 99.9%), sodium bicarbonate (Merck, 99.9%), *N,N*-dimethylformamide (DMF; Ajax FineChem, 99.9%), water (deionised and Milli-Q grade), and deuterium oxide (Merck, 99.9%) were used as received without further purification.

### General procedure for the RAFT polymerisation of AA or AM

In a typical RAFT polymerisation experiment, an 8 M aqueous solution of AA or AM, the required amount of the CTA and water were initially charged in an ampule (refer to the ESI†). DMF (0.3 mL) was also added to the reaction mixture as an internal standard. The polymerisation mixture was then deoxygenated by argon bubbling for 30 minutes and maintained at 20 °C in a thermostated water bath. Stock solutions of APS and SFS were prepared accordingly and deoxygenated in the same manner. Once the deoxygenation process was complete, the required amount of APS was carefully injected into the ampule and the reaction mixture was further bubbled with argon for another 5 minutes. This was immediately followed by the injection of SFS in an equimolar amount relative to APS (refer to the ESI†), and another 5 minutes of argon bubbling was applied. The reaction was left to proceed under a flow of argon for 24 hours. At this point, the monomer conversion was analysed by <sup>1</sup>H NMR spectroscopy by comparing the disappearance of one of the monomer's vinyl peaks (dd, 1H, 5.80–6.00 ppm) with respect to that of DMF (s, 1H, 7.95 ppm). The polymer was then purified by dialysis and freeze-dried to give a yellow or white powder. Once dried, the molecular weight and dispersity were measured by size exclusion chromatography (SEC).

### General procedure for the aminolysis reactions

In a typical aminolysis experiment, 50 mg of the AB diblock copolymer was dissolved in 10 mL of water. If required, the pH of the solution was adjusted to approximately 8 using 0.1 M sodium hydroxide solution. The solution was bubbled with oxygen gas for 30 minutes to promote an oxidative environment. This was followed by the injection of the optimal amount of *n*-butylamine (refer to the ESI†). The reaction mixture was stirred and maintained at 50 °C in a closed system where the molecular weight and dispersity were directly monitored by SEC over a period of 24 hours. For UV-Vis measurements, the aminolysis reactions were repeated until the appropriate reaction time was reached, and the final polymer produced was separated from the excess *n*-butylamine by dialysis and freeze-dried to give a yellow/white powder.

### Purification and freeze-drying of the polymer samples

The synthesised polymers were purified using SnakeSkin dialysis tubing, made of regenerated cellulose, with a molecular weight cut-off of 3.5k. Once purified, the polymers were freeze-dried using a Labconco FreeZone Benchtop Freeze Dry system.

### Nuclear magnetic resonance (NMR) spectroscopy

<sup>1</sup>H NMR spectra were recorded at 400 MHz using a Bruker DRX 400 spectrometer in deuterium oxide (D<sub>2</sub>O).

### Size exclusion chromatography (SEC)

Molecular weight and dispersity measurements were performed using a Tosoh High Performance EcoSEC HLC-8320GPC System, which comprised of an autosampler, a vacuum degasser, a dual flow pumping unit, a Bryce-type refractive index (RI) detector, a UV detector set at 280 nm, a TSKgel SuperH-RC reference column, and three TSKgel PW<sub>XL</sub> columns (TSKgel G5000PW<sub>XL</sub>, TSKgel G6000PW<sub>XL</sub> and TSKgel MPW<sub>XL</sub>) connected in series. The analytical columns were calibrated with a series of polyacrylic acid (PAA) standards ranging from 106 to 1520k. The eluent used was deionised water with 0.1 M NaNO<sub>3</sub> and 0.1 M NaHCO<sub>3</sub> (pH ≈ 8.3) at 40 °C and at a flow rate of 1.0 mL min<sup>-1</sup>.

### UV-Vis spectroscopy

All UV-Vis measurements were performed using a Shimadzu UV-1800 UV Spectrophotometer.

### Determination of monomer conversion

The monomer conversion (*p*) was calculated from <sup>1</sup>H NMR data using eqn (1):

$$\text{Conversion } (p) = \frac{[M]_0 - [M]_t}{[M]_0} = \frac{\int M_0 - \int M_t}{\int M_0} \quad (1)$$

where [M]<sub>0</sub> and [M]<sub>t</sub> are the concentrations of the monomer at time 0 and time *t*, respectively; and ∫M<sub>0</sub> and ∫M<sub>t</sub> are the corrected integrals (based on DMF) for a vinyl proton (5.70 ppm) of the monomer at time 0 and time *t*, respectively.

### Calculation of the theoretical molecular weight (*M*<sub>n,th</sub>)

The theoretical number-average molecular weight (*M*<sub>n,th</sub>) of the polymers was determined using eqn (2):

$$M_{n,th} = \frac{[M]_0}{[CTA]_0} \times p \times M_M + M_{CTA} \quad (2)$$

where [M]<sub>0</sub> and [CTA]<sub>0</sub> are the initial concentrations of the monomer and the CTA in mol L<sup>-1</sup>, respectively; *p* is the monomer conversion as determined by eqn (1), and *M*<sub>M</sub> and *M*<sub>CTA</sub> are the molecular weights of the monomer and the CTA, respectively.

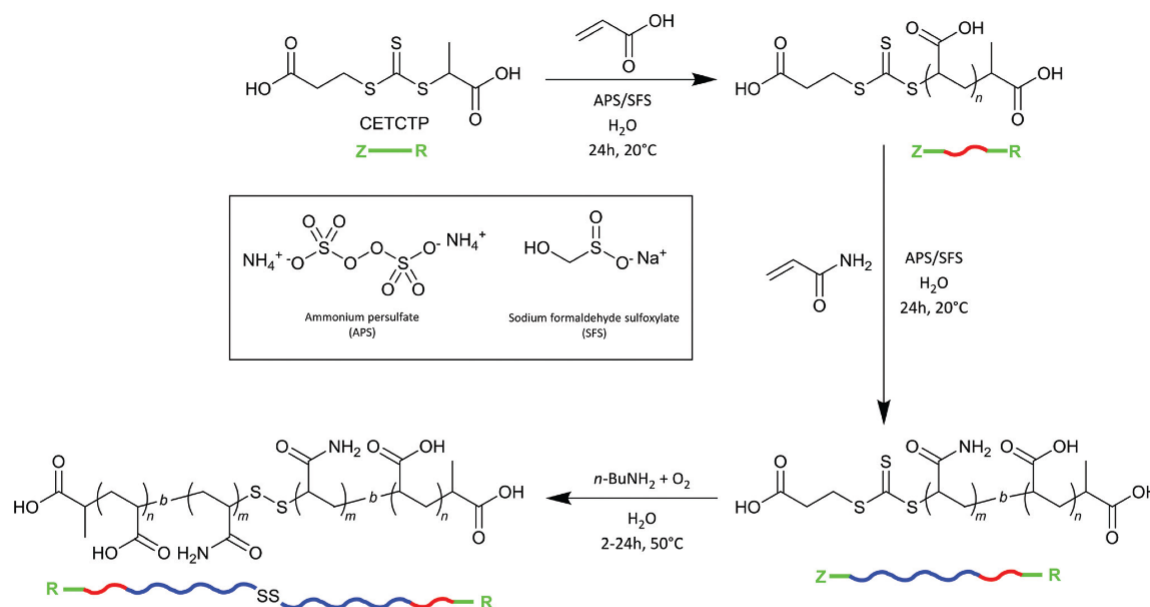
## Results and discussion

### Initial screening experiments for the synthesis of the A block

The synthesis of the UHMW ABA triblock copolymers was performed in three main steps: the initial synthesis of the A block by the polymerisation of AA, the formation of the B block by chain extension with AM, and lastly the aminolysis of the AB diblock copolymers using nucleophilic *n*-butylamine (Scheme 1). Prior to the synthesis of the A blocks, a series of screening experiments were conducted to determine the polymerisation conditions that would allow for an optimal increase in the molecular weight while also maintaining an adequate control over the dispersity. There are several factors that could affect the outcome of the polymerisation, including, but not limited to, the type and concentration of the monomer, the type of RAFT agent, the redox initiation system, temperature, pressure, time, the ratio between the RAFT agent and the initiators, and the ratio between the oxidant and reductant initiator pair.<sup>25–28</sup> These screening tests have the potential to reveal certain trends in the data, and therefore possibly allow the optimal conditions to be identified.

CETCTP,<sup>29</sup> a trithiocarbonate RAFT agent, was selected as the CTA due to its water-solubility and compatibility with AA and AM.<sup>25–34</sup> High monomer concentrations will favour fast reaction kinetics and optimised initiation in the gel polymerisation process and therefore the initial concentration of the monomers was maintained at approximately 33 wt%.<sup>1,35,36</sup> This initial screening test involved the polymerisation of AA, targeting a molecular weight of 200k, at two different reaction temperatures (10 °C and 20 °C) and six different ratios of CETCTP to the redox initiators (ranging from 4:1:1 to 20:1:1, maintaining an equimolar ratio between APS and SFS). The molecular weights and dispersities of the polymers obtained were assessed by SEC after 24 hours of polymerisation and compared for the determination of the optimal reaction temperature and the [CETCTP]:[APS]:[SFS] ratio (Fig. 1).

The data obtained from SEC indicated that polymerisations conducted at a temperature of 20 °C resulted in higher molecular weight polymers compared to those conducted at 10 °C. Consequently, these molecular weights are closer to the targeted value of 200k. The highest molecular weight was obtained at a [CETCTP]:[APS]:[SFS] ratio of 6:1:1. Low dispersities (*D* < 1.20) were obtained for all polymerisations from



**Scheme 1** Overall reaction strategy for the synthesis of UHMW ABA triblock copolymers using sequential RAFT-mediated gel polymerisation of AA and AM monomers, and subsequently the end-group modification of the thiocarbonylthio functionality via aminolysis. The RAFT polymerisations were performed in water at 20 °C with APS and SFS acting as the redox initiation pair. The aminolysis process was also performed in water at 50 °C with *n*-butylamine being employed as the nucleophilic reagent.

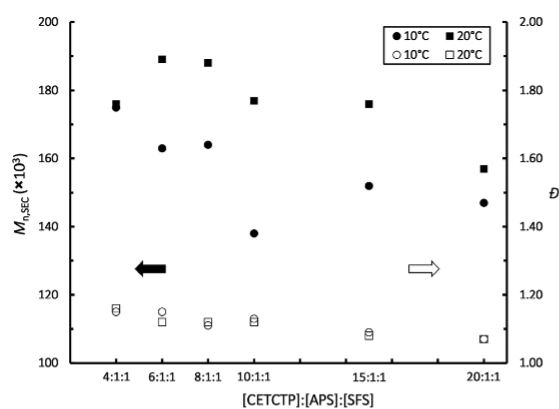


**Fig. 1** SEC data obtained from the screening polymerisations of AA, with target molecular weight of 200k, conducted at two reaction temperatures (10 °C and 20 °C) and six [CETCTP]:[APS]:[SFS] ratios (ranging from 4:1:1 to 20:1:1) for 24 hours.

this screening test, which indicated good control across the range of the [CETCTP]:[APS]:[SFS] ratios employed. Another trend was observed where the dispersity decreased as the [CETCTP]:[APS]:[SFS] ratio increased. This was attributed to the lower flux of radicals and hence better control over the molecular weight distribution of the polymers was observed.<sup>37</sup> However, this decrease in the concentration of initiators also led to a drop in the molecular weight due to slower polymeris-

ation kinetics.<sup>36,37</sup> Therefore a reaction temperature of 20 °C and a [CETCTP]:[APS]:[SFS] ratio of 6:1:1 were chosen as the optimal conditions for the synthesis of the initial A blocks.

#### Synthesis of the A blocks by polymerisation of AA

Once the optimal conditions for the synthesis of the initial A blocks were established, the polymerisations of AA were performed with eight different target molecular weights (Table 1). Polymers A1 to A5 were intended to have molecular weights ranging from 10 to 50k with an increment of 10k, while subsequent polymers had a higher increment of 50k, up until the target value of 200k for polymer A8. The purpose of synthesising the A blocks with varying molecular weights was to determine their effect on the efficiency of the subsequent chain extension and chain coupling stages.

From the <sup>1</sup>H NMR data, high monomer conversions (74–85%) were obtained for all of the eight reactions listed in Table 1. Lower monomer conversion was achieved for polymers with smaller target molecular weights (polymers A1 to A3). This was attributed to the retardation in reaction kinetics due to the elevated concentration of CETCTP.<sup>25,38</sup> As expected, these conversions were shown to have a direct correlation with the resultant molecular weights. The molecular weight values obtained by SEC for all the eight A blocks were in close agreement with the theoretical molecular weights. In addition, the dispersities of these polymers remained below 1.20, which were in agreement with the results obtained in the screening test. Therefore, no further optimisation was required for this step.

**Table 1** Summary of  $^1\text{H}$  NMR and SEC data obtained for the synthesis of the initial A blocks polymerised from AA

Entry	$\text{DP}_{\text{target}}^a$	Monomer conversion <sup>b</sup> (%)	$M_{n,\text{th}}^c$ ( $\times 10^3$ )	$M_{n,\text{SEC}}^d$ ( $\times 10^3$ )	$\mathcal{D}^d$
A1	139	74	7.67	5.21	1.18
A2	278	74	15.1	11.8	1.17
A3	416	79	23.9	20.9	1.18
A4	555	84	33.8	33.9	1.17
A5	694	83	41.8	45.7	1.16
A6	1390	84	84.4	84.8	1.14
A7	2080	80	120	118	1.15
A8	2780	85	171	173	1.14

<sup>a</sup> Polymerisations were performed with an initial AA concentration of  $4.63 \text{ mol L}^{-1}$  and a [CETCTP]:[APS]:[SFS] ratio of 6:1:1 at  $20^\circ\text{C}$  for 24 hours (refer to the ESI†). <sup>b</sup> Monomer conversion was determined by  $^1\text{H}$  NMR spectroscopy with DMF as an internal standard, according to eqn (1) (refer to the Experimental section). <sup>c</sup> Theoretical molecular weight was calculated according to eqn (2) (refer to the Experimental section). <sup>d</sup> Molecular weight data were determined using aqueous SEC calibrated with PAA standards (refer to the Experimental section).

The SEC traces of all the eight polymers (Fig. 2a) were monomodal, which further proved that the polymerisations were well controlled under the optimal reaction conditions selected. A linear increase in the molecular weight was also observed as the reaction progressed. An example of this linear relationship between the molecular weight and the monomer conversion is shown in Fig. 2b for the RAFT polymerisation of AA, targeting a molecular weight of 50k. These polymers were directly purified by dialysis and freeze dried prior to use as the macro-CTA for the next RAFT polymerisation stage.

#### Optimisation and synthesis of the AB diblock copolymers

The second stage involves the chain extension of the A blocks, described in Table 1, with AM to form a series of UHMW AB diblock copolymers. The reaction conditions required for this

process were yet to be established, thus further screening reactions were required in order to achieve an optimal increase in the molecular weight and maintain a low dispersity. Synthesis of the final UHMW ABA triblock copolymers with a molecular weight of 1000k was desired. Therefore the main objective of these screening reactions was to determine the optimal conditions to synthesise the AB diblock copolymers with molecular weights greater than 500k, while also maintaining low dispersities. In addition, it was hypothesised that each macro-CTA would exhibit different characteristics with regard to chain conformation, steric hindrance and viscosity, which would affect the reaction kinetics. Therefore, performing an array of reaction conditions would prove to be beneficial. Consequently, polymers A1 to A8 were subjected to RAFT polymerisations at  $20^\circ\text{C}$  for 24 hours with an initial [macro-CTA]:[APS]:[SFS] ratio of 6:1:1, with the varying factor being the initial monomer to macro-CTA ratio, or targeted degree of polymerisation ( $\text{DP}_{\text{target}}$ ). Three different ratios ranging from 28 100 to 56 300 were initially targeted (Tables S5 and S6 in the ESI†).

The SEC data for this set of polymerisations showed several trends (refer to the ESI† for the comprehensive results obtained by  $^1\text{H}$  NMR and SEC). There was a decrease in the molecular weight of the AB diblock copolymers as a higher molecular weight macro-CTA was used. However, a drop in the dispersity of the polymer was also observed. In addition, the overall molecular weight generally increased with a higher  $\text{DP}_{\text{target}}$ . This increment was at times insignificant even with a two-fold elevation in the  $\text{DP}_{\text{target}}$ . These results demonstrated that there was a limitation on the degree of chain growth based on the length of the macro-CTA. This was clearly evidenced by the significant drop in monomer conversion with a higher molecular weight macro-CTA. For instance, at a  $\text{DP}_{\text{target}}$  of 28 100, the monomer conversion dropped from 77% to 16% when macro-CTAs A1 and A8 were employed, respectively

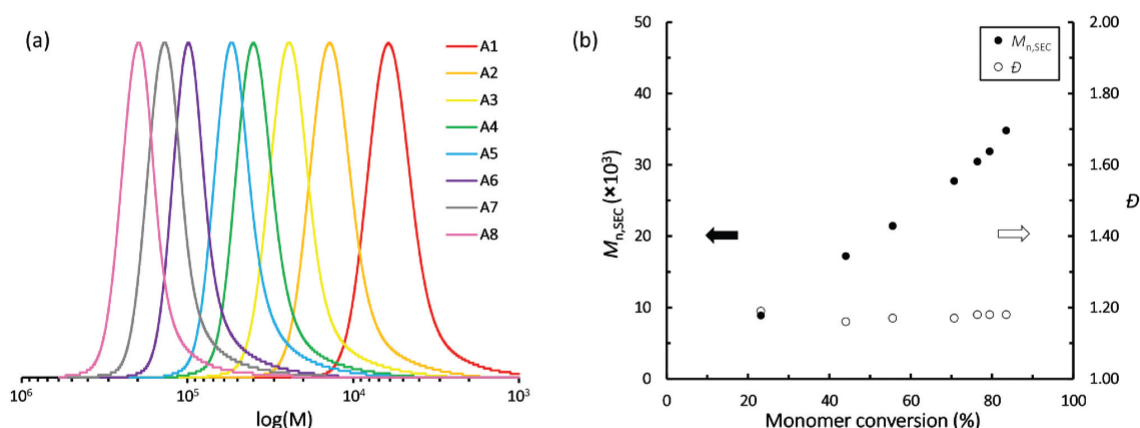


**Fig. 2** (a) Overlay of chromatograms obtained by using SEC for polymers A1 to A8 obtained from the polymerisation of AA, with target molecular weights ranging from 10 to 200k; (b) an example plot showing a linear increase in the measured molecular weight data for the RAFT polymerisation of AA, with target molecular weight of 50k.

(Table S5 in the ESI<sup>†</sup>). A similar decline was also observed when using other DP<sub>target</sub>.

PAA and its derivatives contain several carboxylic acid functionalities that can partially dissociate in water. The conformational change in these polyelectrolytes in solution remains complex and depends on several factors.<sup>39</sup> PAA has been shown to exhibit conformational changes based on the pH at high molecular weight ( $M_n > 16.5k$ ).<sup>40</sup> Below this molecular weight, PAA maintains an extended coil conformation despite changes in the pH. A transformation from an extended coil to a condensed globular structure would further cause steric hindrance at the active chain end, particularly for long chain polymers.<sup>41</sup> In addition to this, the hydrophobic or hydrophilic interactions between the carboxyl groups on the PAA chains and other polymer chains can significantly alter the overall conformation.<sup>39</sup> Therefore, macro-CTAs of PAA with longer chain length are more susceptible to kinetics retardation. These macro-CTAs also possess higher viscosity with longer chain length. High viscosity also correlates with the reduction in random termination as it is a diffusion-controlled process.<sup>42</sup> With longer chain length, the drastic drop in segmental and translational diffusion rates results in a reduction in the chain–chain interaction, and hence a deceleration in the termination process.<sup>2</sup> Consequently, this effect possibly contributed to the drop in the dispersity when higher molecular weight macro-CTAs were used.

Five well-controlled AB diblock copolymers (AB1 to AB5) were initially synthesised from five different macro-CTAs (polymers A1 to A5, respectively) (Table 2). This was achieved under different DP<sub>target</sub> and the resultant molecular weights of these polymers ranged from approximately 500 to 550k ( $D < 1.50$ ). As for the AB diblock copolymers produced from macro-CTAs A6 to A7, the final molecular weights were inadequate for the subsequent aminolysis stage ( $M_{n,SEC} < 500k$ ), even with a high DP<sub>target</sub> of 56 300 (Table S6 in the ESI<sup>†</sup>). From previous screening polymerisation results, it was seen that there was typically a trade-off between the molecular weight and the dispersity based on the variation in the [CTA]:[APS]:[SFS] ratios. A higher molecular weight was often obtained when a lower [CTA]:[APS]:[SFS] ratio (*i.e.* higher flux of radicals) was used.

However, a broader molecular weight distribution also coincides with this trend, and *vice versa*. Consequently, further polymerisations were conducted using polymers A6 to A8 as the macro-CTAs. This time, the DP<sub>target</sub> was increased to 70 300, and the [macro-CTA]:[APS]:[SFS] ratio was decreased to approximately 5:1:1. As expected, the combination of a higher targeted chain length and higher flux of radicals facilitated the successful synthesis of the AB diblock copolymers AB6 to AB8 (Table 2). The molecular weights of these polymers varied from approximately 582 to 641k and were thus deemed to be satisfactory for aminolysis.

### Synthesis of the UHMWABA triblock copolymers

An initial control experiment was performed using only RAFT polymerisation for the second chain extension step from AA to form an UHMWABA triblock copolymer. The purpose of this reaction was to determine the blocking efficiency of this second chain extension stage, particularly when an UHMW macro-CTA is employed. A derivative similar to polymer AB-1 ( $M_n = 626k$ ,  $D = 1.46$ ) was used as the macro-CTA for this polymerisation with a DP<sub>target</sub> of approximately 31 300 and a [macro-CTA]:[APS]:[SFS] ratio of 6:1:1 (refer to Table S3 in the ESI<sup>†</sup>). A poor chain growth was observed, where the final monomer conversion and molecular weight were 4% and  $M_n = 566k$  ( $D = 1.80$ ), respectively. The final molecular weight after chain extension was lower due to a broader molecular weight distribution, which indicated poor control over the polymerisation. In addition, a large fraction of the monomer remained unreacted; thus, in this study, the use of only RAFT polymerisation to synthesise UHMWABA triblock copolymers was considered to be unsatisfactory. To overcome this problem, aminolysis and chain coupling were employed as an alternative.

The final stage involved the aminolysis of the eight AB diblock copolymers by *n*-butylamine. This would allow for the spontaneous coupling of the modified thiol groups under oxidative conditions to form the desired UHMWABA triblock copolymers. Polymer AB1 was initially subjected to several aminolysis reactions to determine the most optimal conditions required. Factors such as the quantity and structure of the

Table 2 Summary of optimised <sup>1</sup>H NMR and SEC data for the formation of the B blocks by chain extension with AM

Entry	Macro-CTA	$M_{n,SEC}$ of macro-CTA ( $\times 10^3$ )	DP <sub>target</sub> <sup>a</sup>	[Macro-CTA]:[APS]:[SFS] <sup>a</sup>	Monomer conversion <sup>b</sup> (%)	$M_{n,th}$ <sup>c</sup> ( $\times 10^3$ )	$M_{n,SEC}$ <sup>d</sup> ( $\times 10^3$ )	$D^d$
AB1	A1	5.21	28 100	6:1:1	77	1540	557	1.49
AB2	A2	11.8	42 200	6:1:1	67	2020	542	1.44
AB3	A3	20.9	42 200	6:1:1	70	2120	502	1.39
AB4	A4	33.9	56 300	6:1:1	55	2230	537	1.32
AB5	A5	45.7	56 300	6:1:1	51	2090	513	1.21
AB6	A6	84.8	70 300	5:1:1	48	2480	602	1.50
AB7	A7	118	70 300	5:1:1	40	2120	641	1.36
AB8	A8	173	70 300	5:1:1	27	1520	582	1.23

<sup>a</sup> Polymerisations were performed with an initial AM concentration of 4.69 mol L<sup>-1</sup> at 20 °C for 24 hours (refer to the ESI). <sup>b</sup> Monomer conversion was determined by <sup>1</sup>H NMR spectroscopy with DMF as an internal standard, according to eqn (1) (refer to the Experimental section). <sup>c</sup> Theoretical molecular weight was calculated according to eqn (2) (refer to the Experimental section). <sup>d</sup> Molecular weight data were determined using aqueous SEC calibrated with PAA standards (refer to the Experimental section).

nucleophilic reagent, nature of the solvent, temperature, and concentration of the initial polymer have significant influences on the reaction rates.<sup>43</sup> *N*-Butylamine was chosen as the aminolysis reagent due to its miscibility with water. Two initial AB diblock copolymer concentrations were employed, 0.5 and 1.0 wt%. Previous aminolysis reactions typically employ a 5–20 fold molar excess of *n*-butylamine to thiocarbonylthio end-groups.<sup>44–48</sup> However, initial trials indicated that these ratios were insufficient, where the molecular weight remained the same after aminolysis. This was possibly attributed to the long polymer chain of the AB diblock copolymers restricting the nucleophilic attack, particularly in the presence of a minimal amount of *n*-butylamine. Therefore, three different excess ratios ranging from 2000 to 200 000 fold of *n*-butylamine were employed. These reactions were monitored using SEC for 24 hours and compared against each other (refer to the ESI† for the detailed plots showing an increase in the molecular weight of the polymer **AB1** under different aminolysis conditions).

The SEC data showed a distinctive increase in the molecular weight when comparing different excess ratios of *n*-butylamine. A higher ratio corresponded to a larger increase in the molecular weight and *vice versa*. However, the dispersity of these polymers also increased as the reaction progressed. As for the two different initial AB diblock copolymer concentrations used, a larger increase in the molecular weight was obtained for the lower concentration. Therefore the most optimal ratio of *n*-butylamine to thiocarbonylthio functionality was determined to be 20 000 with an initial polymer concentration of 0.5 wt%. After 6 hours of aminolysis, the molecular weight of the polymer **AB1** increased from 557 to 1050k (polymer **ABA1**), with a corresponding dispersity increase from 1.49 to 1.67 (Table 3). The same conditions were applied to polymers **AB2** to **AB8** (refer to the ESI† for the SEC data). As expected, the molecular weights and dispersities of all the seven AB diblock copolymers increased as the reactions progressed. However, the increase in the molecular weights was generally observed to be smaller for polymers with the longer A block, and *vice versa*. For instance, the molecular weight of polymer **AB8** increased to only 662k after 6 hours, which was

significantly less than the increase observed in polymer **AB1**. From this set of reactions, two more satisfactory ABA triblock copolymers (**ABA2** and **ABA3**) were obtained at reaction times of 8 and 12 hours, respectively (Table 3). *N*-Butylamine is a weak organic base which would interact with the carboxylic acid functionalities on the polymer chain of the AB diblock copolymers. Consequently, this could reduce the desired interaction between the *n*-butylamine and the thiocarbonylthio group, resulting in a lesser increase in the molecular weight, as observed with the longer A block.

To counteract this problem, the aminolysis procedures with a 20 000-fold excess of *n*-butylamine were reattempted under the same reaction conditions with a higher pH (approximately 8.0) compared to their unadjusted original pH of 4.0–4.5. The interaction between primary and secondary amines and the thiocarbonylthio groups is significantly dependent on the pH of the solution. The rate of aminolysis should increase with an increase in the pH.<sup>49</sup> Consequently, the quantity of *n*-butylamine required for the aminolysis of the AB diblock copolymers could possibly be reduced with the addition of a base. However, the SEC data obtained for the aminolysis at pH 8 indicated otherwise. The increase in the molecular weight for all the eight AB diblock copolymers was relatively lower compared to when the reactions were performed at lower pH (refer to Table S8 in the ESI†). In addition, as the reaction progressed, the dispersities of these polymers increased by larger increments at higher pH, which led to a drop in the  $M_n$  from the initial increase by the 24-hour mark. The molecular weights of these polymers did not reach the target value of 1000k at any stage during the reaction. The hydrolytic stability of the thiocarbonylthio groups is compromised at a high pH as the C=S bond is less stable compared to the C=O bond.<sup>49,50</sup> As such, the partial hydrolysis of the thiocarbonylthio functionality on the polymer chains was suspected to be the reason for the slow increase in the molecular weight and the increase in dispersity, which was also exacerbated at a high reaction temperature of 50 °C. Therefore increasing the pH of the solution to decrease the amount of *n*-butylamine was not a suitable solution.

**Table 3** Summary of the aminolysis conditions employed in the synthesis of the final UHMWABA triblock copolymers

Entry	AB diblock copolymer	$M_{n,SEC}$ of AB diblock copolymer ( $\times 10^3$ )	[BuNH <sub>2</sub> ]:[C=S] <sup>a</sup>	[BuNH <sub>2</sub> ]:[COOH] <sup>b</sup>	Reaction time (h)	$M_{n,SEC}$ ( $\times 10^3$ ) <sup>c</sup>	$D^c$
<b>ABA1</b>	<b>AB1</b>	557	20 000 : 1	278 : 1	6	1050	1.67
<b>ABA2</b>	<b>AB2</b>	542	20 000 : 1	122 : 1	8	1010	1.68
<b>ABA3</b>	<b>AB3</b>	502	20 000 : 1	69 : 1	12	1000	1.67
<b>ABA4</b>	<b>AB4</b>	537	131 000 : 1	278 : 1	6	1050	1.59
<b>ABA5</b>	<b>AB5</b>	513	176 000 : 1	278 : 1	24	967	1.53
<b>ABA6</b>	<b>AB6</b>	602	654 000 : 1	556 : 1	2	1170	1.59
<b>ABA7</b>	<b>AB7</b>	641	911 000 : 1	556 : 1	4	1210	1.49
<b>ABA8</b>	<b>AB8</b>	582	1 330 000 : 1	556 : 1	24	1000	1.46

<sup>a</sup> Molar excess ratio of *n*-butylamine to thiocarbonylthio groups. <sup>b</sup> Molar excess ratio of *n*-butylamine to the carboxylic acid functionalities on the polymer chain of the AB diblock copolymers. <sup>c</sup> Molecular weight data were determined using aqueous SEC calibrated with PAA standards (refer to the Experimental section).

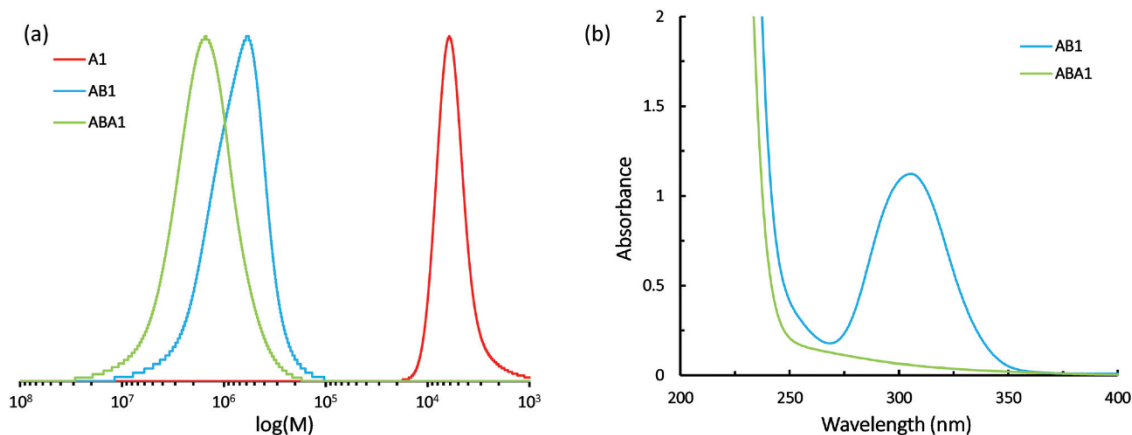


Fig. 3 (a) An example overlay of chromatograms obtained by using SEC showing changes in molecular weight for polymers **A1**, **AB1** and **ABA1**; (b) typical UV-Vis spectrum showing the changes in the absorbance of the thiocarbonylthio peak before and after the aminolysis process.

The next solution was to increase the amount of *n*-butylamine such that the ratio between the amine and carboxyl groups is 278 : 1 (Table S9 in the ESI†). This value corresponds to the base to acid ratio employed in the aminolysis of the polymer **AB1**. At this ratio, polymers **AB4** and **AB5** were successfully converted to polymers **ABA4** and **ABA5** after 6 and 24 hours, respectively (Table 3). This ratio was then doubled to 556 : 1 for the remaining three AB diblock copolymers to allow for a faster and larger increase in the molecular weight (Table S10 in the ESI†). Consequently, polymers **ABA6** to **ABA8** were successfully produced after 2, 4 and 24 hours of aminolysis, respectively (Table 3). The steady increase in the dispersity of all the eight AB diblock copolymers as the reaction progressed could be explained by the presence of unreacted polymer chains, leading to a broader distribution as the molecular weight increased over time. In addition to this, the presence of pre-existing dead polymer chains and inactive AB diblock copolymers due to hydrolysis could also contribute to this broadening effect. However, the fraction of these polymer chains is considered to be insignificant compared to the fraction of ABA triblock copolymers produced in this step. This was evaluated by the molecular weight distribution obtained by SEC, as well as by UV-vis measurements.

An example overlay of the SEC traces for polymers **A1**, **AB1** and **ABA1** is shown in Fig. 3a, showing distinctive changes in the molecular weight throughout the three main reaction stages (refer to the ESI† for the SEC data of the remaining polymers reported in this study). UV-vis measurements were also performed on the polymer samples before and after the aminolysis process. Fig. 3b shows a typical UV-vis spectrum of the AB diblock copolymer and the corresponding ABA triblock copolymer. In this example, polymer **AB1** has a strong absorbance at approximately 300–310 nm which is attributed to the presence of the thiocarbonylthio group.<sup>21</sup> After the aminolysis process, the reduction of this peak was observed for polymer

**ABA1**. Similar UV-vis measurements were obtained for the remaining AB diblock and ABA triblock copolymers.

## Conclusions

The synthesis of eight different UHMW ABA triblock copolymers was performed successfully in three separate reaction stages. The first stage involved the RAFT-mediated gel polymerisation of AA to form eight different A blocks with  $M_{n,SEC}$  ranging from 5.21 to 173k ( $D < 1.20$ ). These polymers were subsequently used as the macro-CTA for the second stage which involved the formation of the B blocks by chain extension from AM. The molecular weight of the macro-CTA had a significant impact on the growth of the B block. Under the same reaction conditions, less efficient chain extension of the B block was observed for macro-CTAs with a higher molecular weight. Therefore, combinations of different  $DP_{target}$  and  $[macro-CTA]:[APS]:[SFS]$  ratios were employed for different macro-CTAs to promote better chain extension efficiency. Consequently, eight AB diblock copolymers with satisfactory molecular weights ( $M_{n,SEC} > 500k$ ) were synthesised while dispersities remained relatively low ( $D < 1.50$ ). The final stage involved the aminolysis of the AB diblock copolymers. This process converted the terminal thiocarbonylthio groups into thiols, which spontaneously coupled to form the UHMW ABA triblock copolymers. This coupling process was more challenging with respect to the size of the A block. Polymers with a longer A block showed a slower increase in the molecular weight and this was attributed to the unfavourable interaction between the *n*-butylamine and the carboxylic acid functionalities. Consequently, different optimal concentrations of *n*-butylamine were utilised to successfully synthesise the desired UHMW ABA triblock polymers, with  $M_{n,SEC}$  ranging from 967 to 1210k ( $D < 1.70$ ).

## Conflicts of interest

There are no conflicts to declare.

## Acknowledgements

Financial support from BASF Australia Ltd, as well as the Chemicals and Plastics Manufacturing Innovation Network and Training program, supported by Monash University, Chemistry Australia and the Victorian Government of Australia, is acknowledged.

## Notes and references

- E. Read, A. Guinaudeau, D. James Wilson, A. Cadix, F. Violleau and M. Destarac, *Polym. Chem.*, 2014, **5**, 2202–2207.
- R. N. Carmean, T. E. Becker, M. B. Sims and B. S. Sumerlin, *Chemistry*, 2017, **2**, 93–101.
- L. Despax, J. Fitremann, M. Destarac and S. Harriison, *Polym. Chem.*, 2016, **7**, 3375–3377.
- V. H. Dao, N. R. Cameron and K. Saito, *Polym. Chem.*, 2016, **7**, 11–25.
- L. Xue, U. S. Agarwal and P. J. Lemstra, *Macromolecules*, 2002, **35**, 8650–8652.
- B. W. Mao, L. H. Gan and Y. Y. Gan, *Polymer*, 2006, **47**, 3017–3020.
- R. W. Simms and M. F. Cunningham, *Macromolecules*, 2007, **40**, 860–866.
- T. Arita, Y. Kayama, K. Ohno, Y. Tsujii and T. Fukuda, *Polymer*, 2008, **49**, 2426–2429.
- L. Mueller, W. Jakubowski, K. Matyjaszewski, J. Pietrasik, P. Kwiatkowski, W. Chaladaj and J. Jureczak, *Eur. Polym. J.*, 2011, **47**, 730–734.
- Z. Huang, J. Chen, L. Zhang, Z. Cheng and X. Zhu, *Polymers*, 2016, **8**, 59.
- J. K. D. Mapas, T. Thomay, A. N. Cartwright, J. Ilavsky and J. Rzaev, *Macromolecules*, 2016, **49**, 3733–3738.
- V. Percec, T. Guliashvili, J. S. Ladislav, A. Wistrand, A. Stjernedahl, M. J. Sienkowska, M. J. Monteiro and S. Sahoo, *J. Am. Chem. Soc.*, 2006, **128**, 14156–14165.
- G. Lligadas and V. Percec, *J. Polym. Sci., Part A: Polym. Chem.*, 2008, **46**, 2745–2754.
- N. H. Nguyen, X. Leng and V. Percec, *Polym. Chem.*, 2013, **4**, 2760–2766.
- J. Rzaev and J. Penelle, *Angew. Chem., Int. Ed.*, 2004, **43**, 1691–1694.
- J. Xu, K. Jung, A. Atme, S. Shanmugam and C. Boyer, *J. Am. Chem. Soc.*, 2014, **136**, 5508–5519.
- N. P. Truong, M. V. Dussert, M. R. Whittaker, J. F. Quinn and T. P. Davis, *Polym. Chem.*, 2015, **6**, 3865–3874.
- M. Destarac, A. Guinaudeau, S. Mazieres and J. Wilson, *United States Pat*, 2013/0267661, 2013.
- G. Moad, E. Rizzardo and S. H. Thang, *Polym. Int.*, 2011, **60**, 9–25.
- R. W. Lewis, R. A. Evans, N. Malic, K. Saito and N. R. Cameron, *Polym. Chem.*, 2017, **8**, 3702–3711.
- H. Willcock and R. K. O'Reilly, *Polym. Chem.*, 2010, **1**, 149–157.
- G. Odian, *Principles of Polymerization*, Wiley, 4th edn, 2004.
- U. Capasso Palmiero, A. Chovancová, D. Cuccato, G. Storti, I. Lacik and D. Moscatelli, *Polymer*, 2016, **98**, 156–164.
- I. Chaduc, A. Crepet, O. Boyron, B. Charleux, F. D'Agosto and M. Lansalot, *Macromolecules*, 2013, **46**, 6013–6023.
- G. Moad, E. Rizzardo and S. H. Thang, *Aust. J. Chem.*, 2005, **58**, 379–410.
- G. Moad, E. Rizzardo and S. H. Thang, *Aust. J. Chem.*, 2006, **59**, 669–692.
- G. Moad, E. Rizzardo and S. H. Thang, *Aust. J. Chem.*, 2009, **62**, 1402–1472.
- G. Moad, E. Rizzardo and S. H. Thang, *Aust. J. Chem.*, 2012, **65**, 985–1076.
- R. Wang, C. L. McCormick and A. B. Lowe, *Macromolecules*, 2005, **38**, 9518–9525.
- R. Wang and A. B. Lowe, *J. Polym. Sci., Part A: Polym. Chem.*, 2007, **45**, 2468–2483.
- G. Qi, C. W. Jones and F. J. Schork, *Macromol. Rapid Commun.*, 2007, **28**, 1010–1016.
- G. Qi, B. Eleazer, C. W. Jones and F. J. Schork, *Macromolecules*, 2009, **42**, 3906–3916.
- L. Ouyang, L. Wang and F. J. Schork, *Macromol. Chem. Phys.*, 2010, **211**, 1977–1983.
- L. Ouyang, L. Wang and F. J. Schork, *Macromol. React. Eng.*, 2011, **5**, 163–169.
- D. J. Currie, F. S. Dainton and W. S. Watt, *Polymer*, 1965, **6**, 451–453.
- M. R. Hill, R. N. Carmean and B. S. Sumerlin, *Macromolecules*, 2015, **48**, 5459–5469.
- D. J. Keddie, *Chem. Soc. Rev.*, 2014, **43**, 496–505.
- G. Moad, R. T. A. Mayadunne, E. Rizzardo, M. Skidmore and S. H. Thang, in *Advances in Controlled/Living Radical Polymerization*, American Chemical Society, 2003, vol. 854, pp. 520–535.
- J. Li and K. Zhao, *J. Phys. Chem. B*, 2013, **117**, 11843–11852.
- T. Swift, L. Swanson, M. Geoghegan and S. Rimmer, *Soft Matter*, 2016, **12**, 2542–2549.
- F. M. Calitz, M. P. Tonge and R. D. Sanderson, *Macromolecules*, 2003, **36**, 5–8.
- C. Herfurth, P. Malo de Molina, C. Wieland, S. Rogers, M. Gradzielski and A. Laschewsky, *Polym. Chem.*, 2012, **3**, 1606–1617.
- M. Deletre and G. Levesque, *Macromolecules*, 1990, **23**, 4733–4741.
- C.-W. Chang, E. Bays, L. Tao, S. N. S. Alconcel and H. D. Maynard, *Chem. Commun.*, 2009, 3580–3582.
- X.-P. Qiu and F. M. Winnik, *Macromol. Rapid Commun.*, 2006, **27**, 1648–1653.
- F. Segui, X.-P. Qiu and F. M. Winnik, *J. Polym. Sci., Part A: Polym. Chem.*, 2008, **46**, 314–326.

## Chapter 2

### Polymer Chemistry

### Paper

- 47 X.-P. Qiu and F. M. Winnik, *Macromolecules*, 2007, **40**, 872–878.
- 48 Y.-M. Ma, D.-X. Wei, H. Yao, L.-P. Wu and G.-Q. Chen, *Biomacromolecules*, 2016, **17**, 2680–2690.
- 49 D. B. Thomas, A. J. Convertine, R. D. Hester, A. B. Lowe and C. L. McCormick, *Macromolecules*, 2004, **37**, 1735–1741.
- 50 G. Levesque, P. Arsène, V. Fanneau-Bellenger and T.-N. Pham, *Biomacromolecules*, 2000, **1**, 400–406.

## 2.3. Supporting Information

Electronic Supplementary Information

### Synthesis of Ultra-High Molecular Weight ABA Triblock Copolymers via Aqueous RAFT-mediated Gel Polymerisation, End Group Modifications and Chain Coupling

Vu H. Dao,<sup>a</sup> Neil R. Cameron,<sup>\*b,c</sup> and Kei Saito<sup>\*a</sup>

---

#### Table of Contents

Materials.....	2
<b>SYNTHETIC PROCEDURES</b>	
Synthesis of Polymers A1 to A8 by RAFT Polymerisation of AA.....	2
Synthesis of Polymers AB1 to AB8 by RAFT Polymerisation of AM.....	3
Controlled Synthesis of an ABA Triblock Copolymer by RAFT Polymerisation.....	4
Aminolysis of AB Diblock Copolymers AB1 to AB8.....	5
<b>SCREENING REACTIONS</b>	
Screening Polymerisations for the Synthesis of the AB Diblock Copolymers.....	6
Screening Reactions for the Aminolysis of AB Diblock Copolymer AB1.....	7
Screening Reactions for the Aminolysis of AB Diblock Copolymers AB2 to AB8.....	9
Screening Reactions for the Aminolysis of AB Diblock Copolymers AB1 to AB8 at pH 8.....	10
Aminolysis Reactions with a [BuNH <sub>2</sub> ]:[COOH] ratios of 278:1 and 556:1.....	11
<b>OVERLAY OF SEC CHROMATOGRAMS</b>	
SEC Chromatograms of A Block Polymers, AB Diblock and ABA Triblock Copolymers.....	12

---

<sup>a</sup> School of Chemistry, Monash University, Clayton, VIC 3800, Australia. E-mail: kei.saito@monash.edu; Tel: +61 3 9905 4600; Fax: +61 3 9905 8501.

<sup>b</sup> Department of Materials Science and Engineering, Monash University, Clayton, VIC 3800, Australia. E-mail: neil.cameron@monash.edu; Tel: +61 3 9902 0774.

<sup>c</sup> School of Engineering, University of Warwick, Coventry, CV4 7AL, United Kingdom

## Materials

Acrylic acid (AA, Aldrich, 99%) was pre-treated with basic aluminium oxide (Acros Organics) to remove the radical inhibitor monomethyl ether hydroquinone (MEHQ) prior to use. Acrylamide (AM, Sigma, 99%), 3-(((1-carboxyethyl)thio)-carbonothioyl)thio)propanoic acid (CETCTP, Boron Molecular, 90%), ammonium persulfate (APS, Sigma-Aldrich, 98%), sodium formaldehyde sulfoxylate dihydrate (SFS, Aldrich, 98%), *n*-butylamine (Sigma-Aldrich, 99.5%), sodium nitrate (Merck, 99.9%), sodium bicarbonate (Merck, 99.9%), *N,N*-dimethylformamide (DMF, Ajax FineChem, 99.9%), water (deionised and Milli-Q grades), deuterium oxide (Merck, 99.9%) were used as received without further purification.

### Synthesis of Polymers A1 to A8 by RAFT Polymerisation of AA

The homopolymers of AA (polymers **A1** to **A8**) were synthesised according to the general procedure outlined in the main manuscript. The quantities of monomer, RAFT reagent, internal standard, solvent, and initiators employed for the synthesis of these polymers are detailed in Table 1.

**Table S1. Quantities of reagents and solvent used in the synthesis of polymers A1 to A8.**

	Polymer Entry							
	A1	A2	A3	A4	A5	A6	A7	A8
AA	5.78 mL <sup>a</sup> 46.3 mmol							
CETCTP	84.8 mg 0.333 mmol	42.4 mg 0.167 mmol	28.3 mg 0.111 mmol	21.2 mg 0.083 mmol	17.0 mg 0.067 mmol	8.50 mg 0.033 mmol	2.83 mL <sup>b</sup> 0.022 mmol	2.12 mL <sup>b</sup> 0.017 mmol
DMF	0.30 mL <sup>c</sup>							
H <sub>2</sub> O	2.10 mL	3.16 mL	3.52 mL	3.69 mL	3.80 mL	4.01 mL	1.26 mL	2.00 mL
APS	1.27 mL <sup>d</sup> 0.056 mmol	634 μL <sup>d</sup> 0.028 mmol	423 μL <sup>d</sup> 0.019 mmol	317 μL <sup>d</sup> 0.014 mmol	254 μL <sup>d</sup> 0.011 mmol	127 μL <sup>d</sup> 0.006 mmol	85 μL <sup>d</sup> 0.004 mmol	63 μL <sup>d</sup> 0.003 mmol
SFS	856 μL <sup>e</sup> 0.056 mmol	428 μL <sup>e</sup> 0.028 mmol	285 μL <sup>e</sup> 0.019 mmol	214 μL <sup>e</sup> 0.014 mmol	171 μL <sup>e</sup> 0.011 mmol	86 μL <sup>e</sup> 0.006 mmol	57 μL <sup>e</sup> 0.004 mmol	43 μL <sup>e</sup> 0.003 mmol

<sup>a</sup> An 57.6 wt% (8 M) stock solution of AA was prepared and utilised for the synthesis of all polymers A1 to A8. <sup>b</sup> A 0.2 wt% stock solution of RAFT agent CETCTP was prepared and utilised for the synthesis of polymers A7 and A8. <sup>c</sup> DMF was used as an internal standard for monitoring of monomer conversion. <sup>d</sup> A 1.0 wt% stock solution of APS was prepared and utilised for the synthesis of all polymers A1 to A8. <sup>e</sup> A 1.0 wt% stock solution of SFS was prepared and utilised for the synthesis of all polymers A1 to A8.

### Synthesis of Polymers AB1 to AB8 by RAFT Polymerisation of AM

The AB diblock copolymers of AA and AM (polymers **AB1** to **AB8**) were also synthesised according to the general procedure outlined in the main manuscript. Note that the synthesis of each AB diblock copolymer employed the same numbered A block as the macro chain transfer agent (macro-CTA). For example, polymer **A1** was used as the macro-CTA for the synthesis of polymer **AB1**. The quantities of monomer, RAFT reagent, internal standard, solvent, and initiators employed for the synthesis of these polymers are detailed in Table 2.

Table S2. Quantities of reagents and solvent used in the synthesis of polymers AB1 to AB8

	Polymer Entry							
	AB1	AB2	AB3	AB4	AB5	AB6	AB7	AB8
AA	5.86 mL <sup>a</sup> 46.9 mmol							
CTA	8.7 mg 1.67 μmol	13.1 mg 1.11 μmol	23.2 mg 1.11 μmol	28.2 mg 0.83 μmol	38.1 mg 0.83 μmol	56.5 mg 0.67 μmol	78.7 mg 0.67 μmol	115 mg 0.67 μmol
DMF	0.30 mL <sup>b</sup>							
H <sub>2</sub> O	4.13 mL	4.13 mL	4.13 mL	4.13 mL	4.13 mL	4.13 mL	4.13 mL	4.13 mL
APS	7 μL <sup>c</sup> 0.28 μmol	4 μL <sup>c</sup> 0.19 μmol	4 μL <sup>c</sup> 0.19 μmol	3 μL <sup>c</sup> 0.14 μmol				
SFS	5 μL <sup>d</sup> 0.28 μmol	3 μL <sup>d</sup> 0.19 μmol	3 μL <sup>d</sup> 0.19 μmol	2 μL <sup>d</sup> 0.14 μmol				

<sup>a</sup> An 56.9 wt% (8 M) stock solution of AM was prepared and utilised for the synthesis of all polymers AB1 to AB8. <sup>b</sup> DMF was used as an internal standard for monitoring of monomer conversion. <sup>c</sup> A 1.0 wt% stock solution of APS was prepared and utilised for the synthesis of all polymers AB1 to AB8. <sup>d</sup> A 1.0 wt% stock solution of SFS was prepared and utilised for the synthesis of all polymers AB1 to AB8.

### Controlled Synthesis of an ABA Triblock Copolymer by RAFT Polymerisation

A controlled experiment was performed to synthesise an ABA triblock copolymer using only RAFT polymerisation. A similar derivative of AB diblock copolymer **AB1** ( $M_n = 626$  k,  $\bar{D} = 1.46$ ) was used as the macro-CTA for the second chain extension stage with AA to see whether the chain would grow efficiently. The quantities of monomer, macro-CTA, solvent, and initiators employed for this reaction is detailed in Table 3.

Table S3. Quantities of reagents and solvent used in the second chain extension stage using RAFT polymerisation.

AA	Macro-CTA	DMF	H <sub>2</sub> O	APS	SFS
5.78 mL <sup>a</sup> 46.3 mmol	0.928 g 1.48 μmol	0.30 mL <sup>b</sup>	4.19 mL	6 μL <sup>c</sup> 0.25 μmol	4 μL <sup>d</sup> 0.25 μmol

<sup>a</sup> An 57.6 wt% (8 M) stock solution of AA was prepared and utilised for this chain extension step. <sup>b</sup> DMF was used as an internal standard for monitoring of monomer conversion. <sup>c</sup> A 1.0 wt% stock solution of APS was prepared and utilised for this reaction. <sup>d</sup> A 1.0 wt% stock solution of SFS was prepared and utilised for this reaction.

The polymerisation was conducted for 24 hours and the final monomer conversion was determined to be approximately 4%. The final molecular weight ( $M_n$ ) of the polymer was analysed with SEC and determined to be 566 k ( $\bar{D} = 1.80$ ). An overlay of the SEC traces for the A block, the AB diblock copolymer and the ABA triblock copolymer from this polymerisation is shown in Figure 1 below.

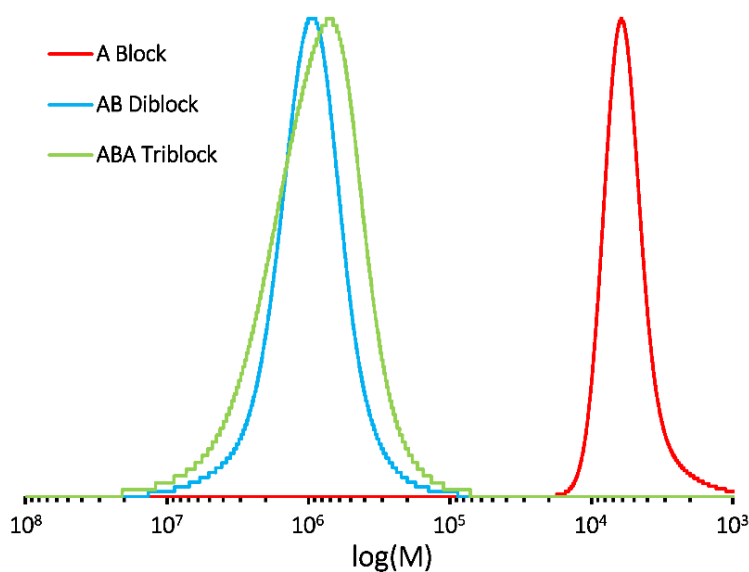


Figure S 1. Overlay of SEC chromatograms for the A block, AB diblock and ABA triblock copolymers from the second chain extension step using only RAFT polymerisation.

**Aminolysis of AB Diblock Copolymers AB1 to AB8**

AB diblock copolymers **AB1** to **AB8** were subjected to aminolysis using *n*-butylamine as the nucleophilic reagent according to the general procedure outlined in the main manuscript. The final optimised quantities of *n*-butylamine used for the aminolysis reactions are shown in Table 4.

Table S4. Quantities of *n*-butylamine in the synthesis of polymers ABA1 to ABA8

	Polymer Entry							
	ABA1	ABA2	ABA3	ABA4	ABA5	ABA6	ABA7	ABA8
Polymer Concentration	50 mg of the AB Diblock Copolymer in 10 mL of H <sub>2</sub> O (0.5 wt%)							
[BuNH <sub>2</sub> ]: [C=S] Ratio	20,000:1	20,000:1	20,000:1	131,000:1	176,000:1	654,000:1	911,000:1	1,330,000:1
[BuNH <sub>2</sub> ]: [COOH] Ratio	278:1	122:1	69:1	278:1	278:1	556:1	556:1	556:1
V( <i>n</i> -BuNH <sub>2</sub> ) (mL)	0.177	0.182	0.197	1.20	1.70	5.40	7.00	11.3
Reaction Time (h)	6	8	12	6	24	2	4	24

### Screening Polymerisations for the Synthesis of the AB Diblock Copolymers

Each of the macro-CTA (polymers **A1** to **A8**) were initially subjected to polymerisation at 20°C for 24 hours, with three initial monomer to macro-CTA ratios ( $DP_{\text{target}}$ ) ranging from 28,100 to 56,300. The ratios between the macro-CTA and the redox initiators were initially maintained at 6:1:1. The monomer conversion (obtained by  $^1\text{H}$  NMR) and the SEC data for these screening polymerisations are shown in Table 5 and Table 6.

Table S5. Monomer conversions obtained from the initial screening polymerisations of the AB diblock copolymers.

Macro-CTA	$M_{n,\text{SEC}}$ of Macro CTA ( $\times 10^3$ )	$DP_{\text{target}}$		
		28,100	42,200	56,300
A1	5.21	77%	73%	63%
A2	11.8	61%	67%	41%
A3	20.9	65%	70%	46%
A4	33.9	68%	57%	55%
A5	45.7	49%	54%	51%
A6	84.8	52%	51%	47%
A7	118	18%	18%	22%
A8	173	16%	20%	15%

Monomer conversion was determined by  $^1\text{H}$  NMR at the 24 hours mark with DMF as the internal standard.

Table S6. SEC data obtained from the initial screening polymerisations of the AB diblock copolymers.

Macro-CTA	$M_{n,\text{SEC}}$ of Macro-CTA ( $\times 10^3$ )	$DP_{\text{target}}$					
		28,100		42,200		56,300	
		$M_{n,\text{SEC}}$ ( $\times 10^3$ )	$\bar{D}$	$M_{n,\text{SEC}}$ ( $\times 10^3$ )	$\bar{D}$	$M_{n,\text{SEC}}$ ( $\times 10^3$ )	$\bar{D}$
A1	5.21	557	1.49	705	1.65	610	1.63
A2	11.8	403	1.31	542	1.44	517	1.24
A3	20.9	355	1.33	502	1.39	490	1.20
A4	33.9	336	1.36	456	1.22	537	1.32
A5	45.7	311	1.22	352	1.31	513	1.21
A6	84.8	291	1.24	359	1.30	440	1.36
A7	118	221	1.19	279	1.21	370	1.27
A8	173	252	1.20	304	1.22	306	1.21

Molecular weight and dispersity data were determined using aqueous SEC calibrated with PAA standards.

### Screening Reactions for the Aminolysis of AB Diblock Copolymer AB1

Six different aminolysis reactions were initially performed on AB diblock copolymer AB1. Two polymer concentrations (0.5 and 1.0 wt%) were used. Three different molar excess ratios of *n*-butylamine to the thiocarbonylthio groups ranging from 2,000 to 200,000 were employed. The changes in molecular weight and dispersity of polymer AB1 were monitored by SEC and these results are shown in Figure 2 to Figure 4.

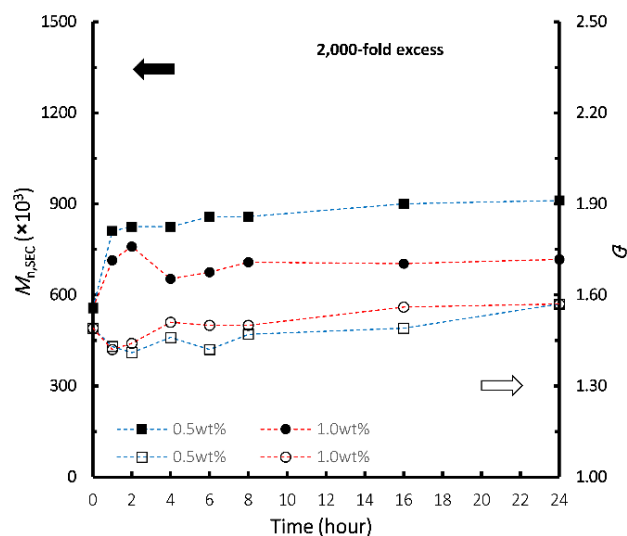


Figure S2. SEC data for the aminolysis of polymer AB1 at 0.5 and 1.0 wt% using an *n*-butylamine excess of 2,000-fold.

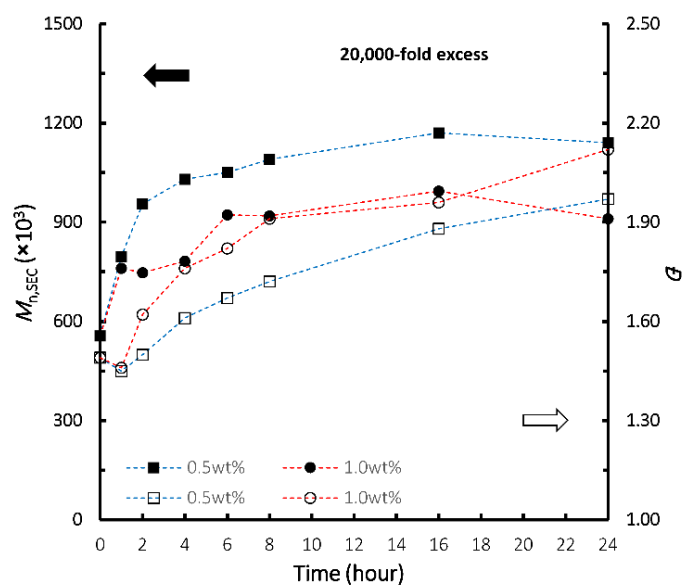


Figure S3. SEC data for the aminolysis of polymer AB1 at 0.5 and 1.0 wt% using an *n*-butylamine excess of 20,000-fold.

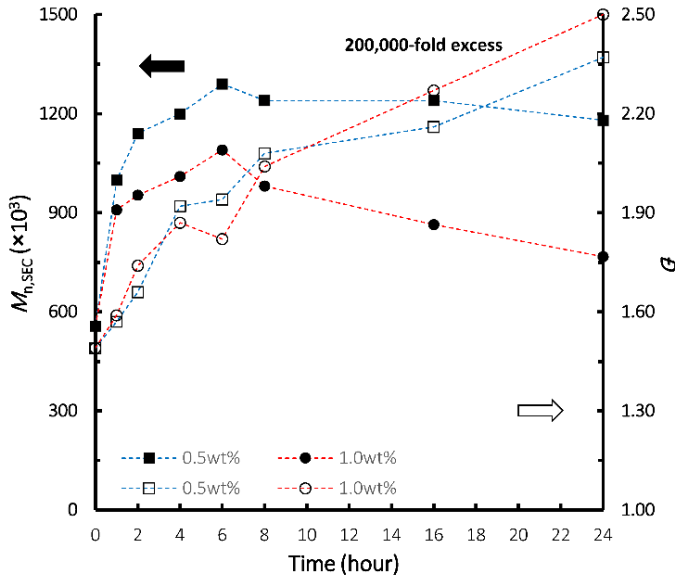


Figure S4. SEC data for the aminolysis of polymer AB1 at 0.5 and 1.0 wt% using an *n*-butylamine excess of 200,000-fold.

### Screening Reactions for the Aminolysis of AB Diblock Copolymers AB2 to AB8

AB diblock copolymers **AB2** to **AB8** were subjected to aminolysis reactions with an initial concentration of 0.5 wt%. The ratio of *n*-butylamine to thiocarbonylthio functionality was maintained at 20,000. SEC was used to monitor the molecular weight growth over 24 hours. The changes in molecular weight and dispersity for polymers **AB2** to **AB8** is detailed in Table 7.

Table S7. SEC data for the aminolysis of polymer AB2 to AB8 using an *n*-butylamine excess of 20,000-fold.

Reaction Time (hour)	$M_{n,SEC} (\times 10^3) / D$						
	AB2	AB3	AB4	AB5	AB6	AB7	AB8
0	542 1.44	502 1.39	537 1.32	513 1.21	602 1.51	641 1.36	582 1.23
6	937 1.65	943 1.59	880 1.45	733 1.30	938 1.99	853 1.74	662 1.50
8	1,000 1.68	960 1.61	879 1.53	749 1.33	889 2.15	813 1.79	666 1.56
10	1,070 1.69	979 1.61	925 1.52	768 1.34	1,110 1.88	741 2.08	708 1.51
12	1,050 1.76	1,000 1.67	945 1.53	815 1.36	989 2.12	776 2.00	703 1.59
14	1,090 1.77	936 1.76	970 1.55	801 1.37	1,090 2.14	835 1.98	651 1.64
16	1,090 1.82	1,020 1.74	990 1.59	810 1.41	874 2.45	841 1.98	668 1.64
24	1,160 1.78	1,030 1.70	991 1.60	801 1.40	961 2.50	852 2.14	704 1.70

Molecular weight and dispersity data were determined using aqueous SEC calibrated with PAA standards.

### Screening Reactions for the Aminolysis of AB Diblock Copolymers AB1 to AB8 at pH 8

AB diblock copolymers **AB1** to **AB8** were subjected to aminolysis reactions with an initial concentration of 0.5wt%. The initial pH of these reaction mixtures ranged from approximately 4.0 to 4.5 depending on the chain length of the A blocks. The pH of these reaction mixtures was adjusted to approximately 8 using sodium hydroxide solution. The ratio of *n*-butylamine to thiocarbonylthio functionality was once again maintained at 20,000 for comparison between low pH and high pH. SEC was used to monitor the molecular weight growth over 24 hours. The changes in molecular weight and dispersity for polymers **AB1** to **AB8** is detailed in Table 8.

Table S8. SEC data for the aminolysis of polymer AB1 to AB8 at pH 8 using an *n*-butylamine excess of 20,000-fold.

Reaction Time (hour)	$M_{n,SEC} (\times 10^3) / \bar{D}$							
	AB1	AB2	AB3	AB4	AB5	AB6	AB7	AB8
0	557 1.49	542 1.44	502 1.39	537 1.32	513 1.21	602 1.51	641 1.36	582 1.23
6	883 1.78	912 1.63	829 1.59	816 1.49	722 1.31	949 2.03	823 1.83	672 1.54
8	952 1.81	933 1.72	898 1.67	881 1.58	732 1.36	927 2.12	847 1.83	732 1.52
10	965 1.98	857 1.94	843 1.53	952 1.53	779 1.33	853 2.43	782 1.99	630 1.61
12	919 2.04	965 1.90	879 1.72	819 1.69	740 1.40	849 2.43	776 2.01	675 1.57
14	924 2.16	943 1.92	758 1.95	789 1.72	789 1.40	812 2.20	772 1.99	612 1.66
16	937 2.23	898 1.99	968 1.82	887 1.72	739 1.44	997 2.30	774 2.31	636 1.72
24	797 2.38	852 2.16	795 2.04	782 1.84	759 1.46	763 2.67	694 2.27	632 1.76

Molecular weight and dispersity data were determined using aqueous SEC calibrated with PAA standards.

### Aminolysis Reactions with a [BuNH<sub>2</sub>]:[COOH] ratios of 278:1 and 556:1

AB diblock copolymers **AB2** to **AB8** were once again subjected to aminolysis reactions with an initial concentration of 0.5 wt%. This time, the ratio of *n*-butylamine to carboxylic functionality on the A blocks was maintained at approximately 278:1 for all polymers. SEC was used to monitor the molecular weight growth over 24 hours. The changes in molecular weight and dispersity for polymers **AB2** to **AB8** is detailed in Table 9.

Table S9. SEC data for the aminolysis of polymer AB2 to AB8 at 0.5 wt% using an [BuNH<sub>2</sub>]:[COOH] ratio of 278:1.

Reaction Time (hour)	$M_{n,SEC} (\times 10^3) / \mathcal{D}$						
	AB2	AB3	AB4	AB5	AB6	AB7	AB8
0	542 1.44	502 1.39	537 1.32	513 1.21	602 1.51	641 1.36	582 1.23
6	999 1.71	1,050 1.73	1,050 1.59	862 1.36	1,370 1.95	1,020 2.05	955 1.50
24	1,170 1.99	966 2.18	1,110 1.85	967 1.53	1,060 3.09	1,030 2.36	867 1.93

Molecular weight and dispersity data were determined using aqueous SEC calibrated with PAA standards.

Lastly, AB diblock copolymers AB6 to AB8 were subjected to another set of aminolysis reactions at 0.5 wt% and a [BuNH<sub>2</sub>]:[COOH] ratio of 556:1. SEC was used to monitor the molecular weight growth over 24 hours. The changes in molecular weight and dispersity for polymers AB6 to AB8 is detailed in Table 10.

Table S10. SEC data for the aminolysis of polymer AB6 to AB8 at 0.5 wt% using an [BuNH<sub>2</sub>]:[COOH] ratio of 556:1.

Reaction Time (hour)	$M_{n,SEC} (\times 10^3) / \mathcal{D}$		
	AB6	AB7	AB8
0	602 1.51	641 1.36	582 1.23
2	1,170 1.59	866 1.60	745 1.24
4	1,360 1.70	1,210 1.49	836 1.27
6	1,440 1.83	1,340 1.54	872 1.29
24	1,600 2.15	1,250 1.80	1,000 1.46

Molecular weight and dispersity data were determined using aqueous SEC calibrated with PAA standards.

**SEC Chromatograms of A Block Polymers, AB Diblock and ABA Triblock Copolymers**

The overlays of SEC traces for the A blocks (A2 to A8), their corresponding AB diblock copolymers (AB2 to AB8) and ABA triblock copolymers (ABA2 to ABA8) are shown in Figure 5 to Figure 11.

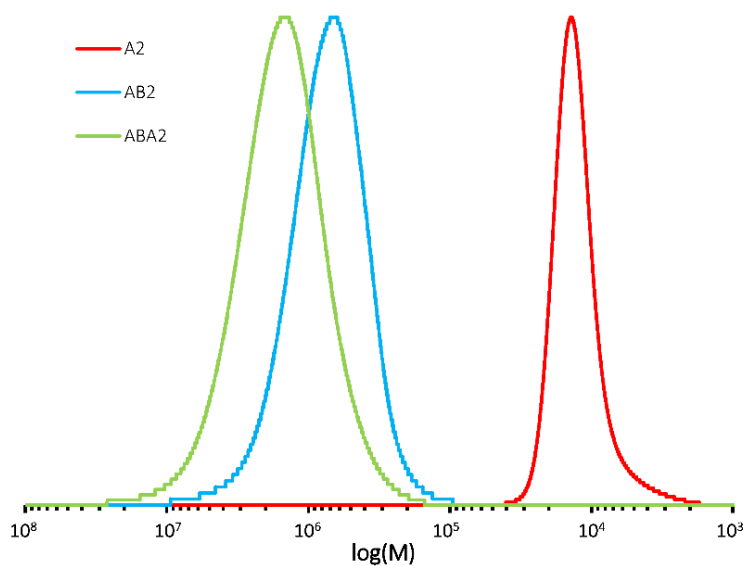


Figure S5. Overlay of SEC chromatograms for polymers A2, AB2 and ABA2.

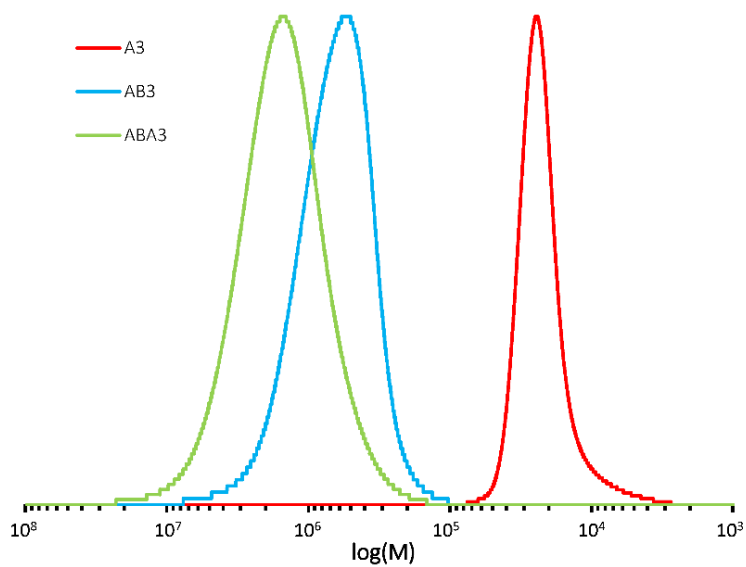


Figure S6. Overlay of SEC chromatograms for polymers A3, AB3 and ABA3.

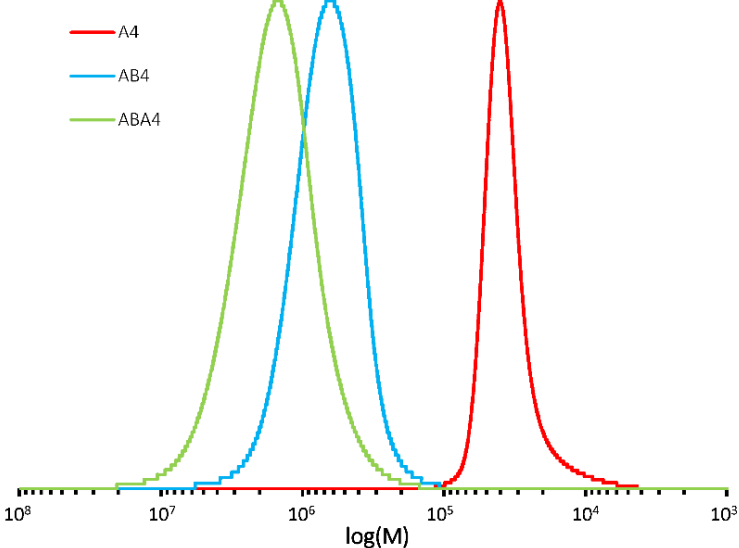


Figure S7. Overlay of SEC chromatograms for polymers A4, AB4 and ABA4.

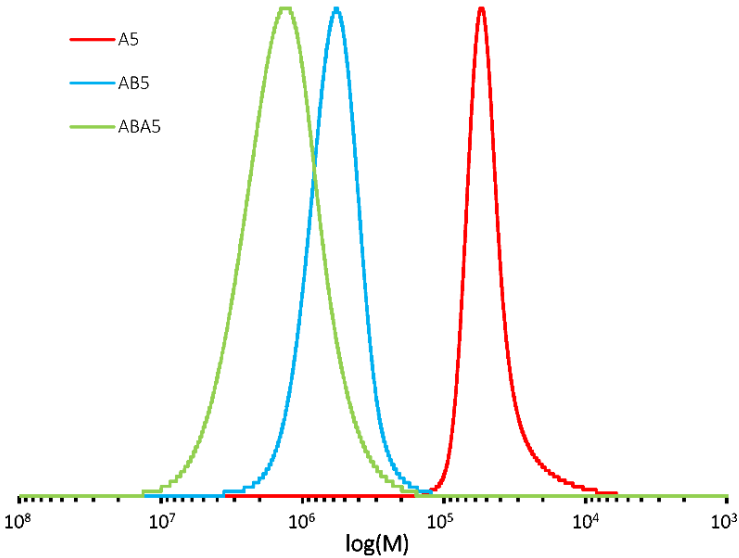


Figure S8. Overlay of SEC chromatograms for polymers A5, AB5 and ABA5.

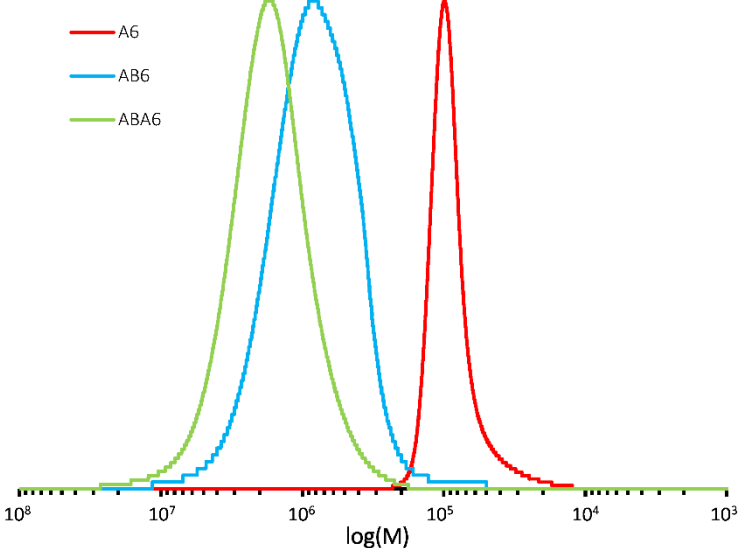


Figure S9. Overlay of SEC chromatograms for polymers A6, AB6 and ABA6.

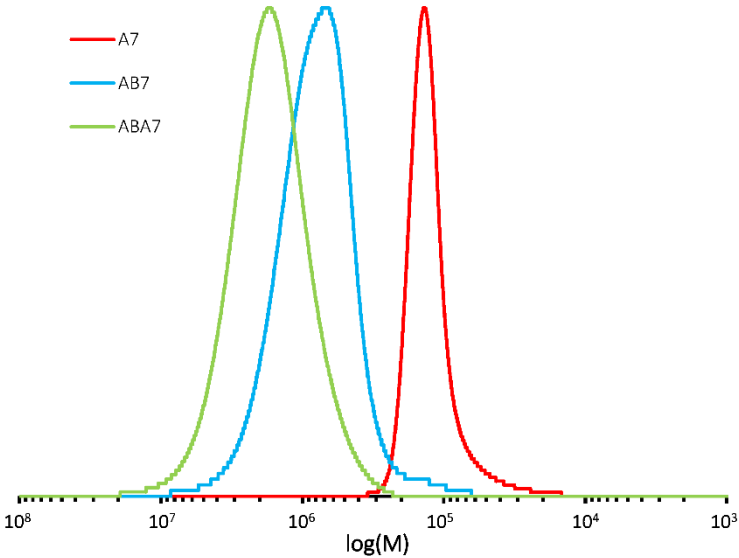


Figure S10. Overlay of SEC chromatograms for polymers A7, AB7 and ABA7.

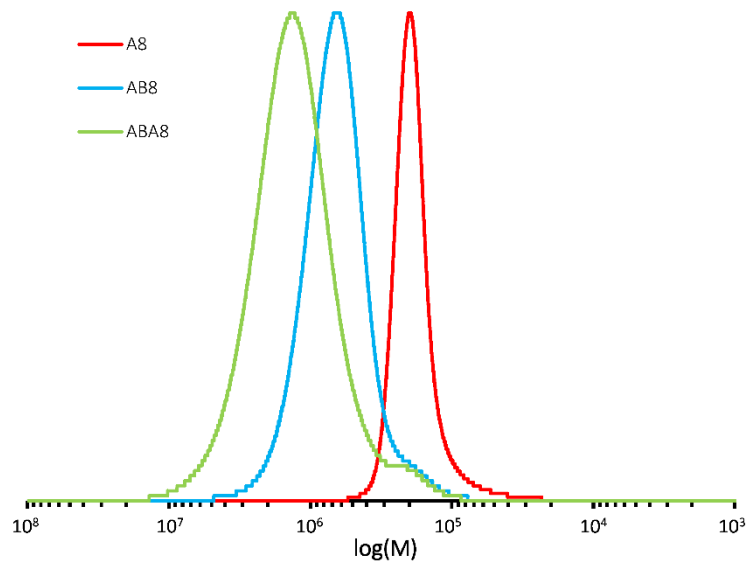


Figure S11. Overlay of SEC chromatograms for polymers A8, AB8 and ABA8.

## 2.4. Appendix

### 2.4.1. Isolation yields of the ABA triblock copolymers

The final isolation yield and mass percentages of the ABA triblock copolymers and their precursor polymers (A block polymers and AB diblock copolymers) are shown in Table 2.1 below.

**Table 2.1. Isolation yields (in mass and weight percentage) of the ABA triblock copolymers and their precursor polymers.**

Entry	A Block Polymers		AB Diblock Copolymers		ABA Triblock Copolymers	
	(g)	(%)	(g)	(%)	(g)	(%)
1	1.7	51	1.2	36	2.5	63
2	1.6	48	0.8	24	2.8	71
3	1.6	49	0.9	27	2.6	65
4	1.8	55	0.8	23	2.7	67
5	1.7	52	0.7	37	2.5	62
6	1.8	54	0.5	15	2.6	65
7	1.6	50	0.5	14	2.8	71
8	1.9	57	0.4	12	2.4	61

### 2.4.2. Controlled synthesis of an ABA triblock copolymer by RAFT polymerisation

Prior to creating the aforementioned ABA triblock copolymers *via* aminolysis and chain coupling, the use of sequential RAFT polymerisation based on the existing AB diblock copolymers was explored. This reaction step involved a chain extension of an existing AB diblock copolymer chain with AA, to form the desired ABA triblock copolymer. An AB diblock copolymer with  $M_n$  of 626 kDa ( $\mathcal{D} = 1.46$ ) was employed as the macro-CTA for this experiment. The targeted degree of polymerisation of AA was approximately 31,300. A [Macro-CTA]:[APS]:[SFS] ratio of 6:1:1 was selected for this polymerisation. However, poor monomer conversion of 4% was obtained and a drop in the  $M_n$  to 566 kDa ( $\mathcal{D} = 1.80$ ) was observed. As mentioned previously, this decrease in the molecular weight was attributed to a broad molecular weight

## Chapter 2

distribution. Along with the low monomer conversion, this indicated a poor control over the polymerisation efficiency. The high molecular weight of the AB diblock macro-CTA had an important role to play in this poor efficiency. The conformation of the polymer chain would lead to steric hindrance at the active thiocarbonylthio functionality, which consequently resulted in inefficient polymerisation. In addition, the large quantity of macro-CTA required to build a small third block onto the polymer chain contributed to the high viscosity of the reaction mixture, which would drastically slow down the diffusion of monomeric species. The combination of slow diffusion rate and steric hindrance of the active site were major factors that led to the low monomer conversion.

This page is intentionally left blank.

# Chapter 3

Enhanced Flocculation Efficiency in High Ionic Strength Environment  
by the Aid of Anionic ABA Triblock Copolymers

This page is intentionally left blank.

# Chapter 3

## Enhanced Flocculation Efficiency in High Ionic Strength Environment by the Aid of Anionic ABA Triblock Copolymers

---

### 3.1. General Overview

Chapter 3 is a manuscript titled “*Enhanced flocculation efficiency in high ionic strength environment by the aid of anionic ABA triblock copolymers*”, which was submitted to Langmuir in 2019.

In this chapter, the UHMW ABA triblock copolymers (**ABA1 – ABA8**) previously synthesised in Chapter 2 were employed to flocculate high ionic strength kaolin clay slurries possessing three different concentrations of  $\text{Ca}^{2+}$  (0.05 M, 0.10 M, and 0.50 M). In addition, three control copolymers (homopolymer of acrylic acid, homopolymer of acrylamide, and random copolymer of acrylic acid and acrylamide) with similar molecular weights were synthesised and also employed as flocculating agents. The architectures of these control copolymers are representative of current commercial flocculants and thus allowed for direct comparison with the ABA triblock copolymers, where the primary focus was placed on the advancement in the architecture.

Flocculation analysis was initially performed by cylinder settling tests. The flocculation efficiency of the ABA triblock copolymers were considered promising as faster settlement rates of the flocculated aggregates were observed, particularly at higher  $\text{Ca}^{2+}$  concentration. In addition, the supernatant turbidity values obtained from the ABA triblock copolymers were relatively lower than that of the control copolymers across all three concentrations of  $\text{Ca}^{2+}$ . Based on these results, focused beam reflectance measurement was utilised as a supplementary method to gain a better understanding of the flocculation mechanism and the aggregate profile.

3.2. Research Paper 'Langmuir, 2019, submitted manuscript'

Enhanced Flocculation Efficiency in High Ionic  
Strength Environment by the aid of Anionic ABA  
Triblock Copolymers

*Vu H. Dao,<sup>a</sup> Krishna Mohanarangam,<sup>b</sup> Phillip D. Fawell,<sup>c</sup> Kosta Simic,<sup>b</sup> Neil R. Cameron,<sup>\*d,e</sup>  
and Kei Saito<sup>\*a</sup>*

<sup>a</sup> School of Chemistry, Monash University, Clayton, VIC 3800, Australia. E-mail:

kei.saito@monash.edu, Tel: + 61 3 9905 4600

<sup>b</sup> CSIRO Mineral Resources, Clayton, VIC 3168, Australia

<sup>c</sup> CSIRO Mineral Resources, Waterford, WA 6152, Australia

<sup>d</sup> Department of Materials Science and Engineering, Monash University, Clayton, VIC 3800,

Australia. E-mail: neil.cameron@monash.edu, Tel: +61 3 9902 0774

<sup>e</sup> School of Engineering, University of Warwick, Coventry, CV4 7AL, United Kingdom

Keywords: flocculation, ABA triblock, FBRM, acrylamide/acrylate, settling, ionic strength

### ABSTRACT

The flocculation efficiency of polyelectrolytes in high ionic strength environment is often affected and reduced due to shielding of the active ionizable functional groups, as well as changes in the surface chemistry of the solid slurry. To address this problem, a series of well-defined novel ABA triblock copolymers were employed for the flocculation of high ionic strength kaolin slurries at three different  $\text{Ca}^{2+}$  concentrations (0.05 M, 0.10 M, and 0.50 M). The primary focus was placed on the advancement in architecture, where the anionic functionalities were localized to the terminal ends. Typical commercial flocculants tend to have anionic functionalities randomly distributed throughout the polymer chain and hence a higher propensity towards condensed conformation and formation of insoluble species. In comparison to a control random copolymer, the ABA triblock copolymers were able to flocculate the kaolin suspension at a faster rate, particularly at the high  $\text{Ca}^{2+}$  concentrations of 0.10 M and 0.50 M. In addition, these polymers had significantly better clarification ability compared to control random copolymer, despite all increments in the  $\text{Ca}^{2+}$  concentration. ABA triblock copolymer architecture may therefore have potential as flocculants in high ionic strength applications.

### INTRODUCTION

Water is one of the most essential resources required for the preservation of life on Earth. However, a continual growth in the population and technologies has led to an increase in the generation of wastewater and industrial effluents over the past few decades. The processes employed to produce potable water from these waste streams require continuous development to satisfy the current demands and increasingly stringent regulations. These waste effluents can contain a large fraction of suspended solid particles, as well as metal ions and micro-organisms.<sup>1</sup>

<sup>2</sup> Removal of the suspended particulates is difficult due to their size and surface charge.<sup>1, 3, 4, 5</sup> This colloidal effect is more significant for clay minerals such as kaolin and bentonite, and thus has caused substantial environmental concerns.<sup>6, 7</sup> Several types of solid-liquid separation processes are utilized in industrial applications to overcome this colloidal effect. Polymer-bridging flocculation, in which fine particles are aggregated to achieve a much larger effective size, is generally the most efficient and feasible process for the separation and removal of colloidal suspensions.<sup>8</sup>

The flocculation process is dependent on a variety of factors, such as the type and concentration of the solid substrate, pH, the type and structure of the polymeric flocculant, as well as the molecular weight and charge density of the polymer.<sup>9, 10, 11, 12</sup> In addition to those mentioned, the ionic strength of the solution had been shown to have a major impact on the flocculation efficiency of a polymer, which is generally evaluated based on the settlement rate of the suspended particles and/or the clarity of the supernatant.<sup>1</sup> Recent practices have directly employed sea water (or diluted sea water) as the aqueous medium in flocculation processes.<sup>10, 13</sup> The tailings in mining and minerals processing also often contain considerable quantities of inorganic ions.<sup>14, 15</sup> This leads to complications when the ions interact with the polyelectrolytes or clay minerals.<sup>8</sup>

At a very low ionic strength, the ionizable functionalities of the polyelectrolyte primarily contributes to elongating the polymer chain to allow for an extended conformation.<sup>16</sup> In addition, these ionizable groups can contribute to polymer adsorption through electrostatic interactions, or salt linkage with metal ions available at the particle surface.<sup>3</sup> As ionic strength increases, the reduction in intramolecular electrostatic repulsion forces allows for more polymer adsorption on the particle surface, which can promote efficient flocculation.<sup>10, 17, 18, 19</sup>

Multiple studies have demonstrated an increase in the settlement rate and/or a decrease in the supernatant turbidity with an increase in the salinity.<sup>10, 20, 21</sup> However, at high ionic strength, the shielding of the active functional groups would result in a condensed polymer conformation that is typically exhibited in the neutral structure of polyacrylamide (PAM).<sup>16, 19, 22, 23</sup> This directly affects both the adsorption and bridging capacity, with the potential to greatly limit flocculation. In addition, the solution viscosity, solvency and dispersion capability of the polymer are also affected, which would subsequently have a direct impact on the flocculant's make-up, transportation, and distribution throughout the colloidal suspension.<sup>16, 19</sup>

Many studies have considered the impact of cations on the flocculation efficiency of acrylamide (AM) and acrylate copolymers.<sup>16, 19, 21, 22, 23, 24, 25</sup> This effect was found to be amplified for multivalent cations such as  $\text{Ca}^{2+}$  and  $\text{Mg}^{2+}$  compared to that of monovalent cations such as  $\text{Na}^+$  and  $\text{K}^+$ .<sup>16, 21, 22</sup> In some cases, precipitation of the polyelectrolyte can occur due to complexation between the cation and the carboxylate functionality.<sup>22, 26, 27</sup> Boisvert *et al.* concluded that the formation of insoluble species from precipitation was dependent on the hydration energy of the cation; a stronger interaction between the polymer and the cation was observed when the cation possessed a lower magnitude hydration energy, and vice versa.<sup>26</sup> Consequently,  $\text{Ca}^{2+}$  was generally found to have stronger effect on the flocculation efficiency compared to that of  $\text{Mg}^{2+}$ .<sup>16, 26</sup> It is quite evident that a high ionic strength environment has a detrimental effect on the flocculation efficiency of a polyelectrolyte. Little work has been done to overcome this problem, as the interaction between the ionizable functional group and the multivalent cation is considered unavoidable.

Commercial polymeric flocculants with ultra-high molecular weight (UHMW) are often synthesized by the copolymerization of AM and its derivatives.<sup>1, 3</sup> The synthesis techniques of

these UHMW polymers typically remain limited to free radical polymerization, and thus have little control over the architecture of the polymer.<sup>3</sup> Consequently, these polymeric flocculants would be more negatively impacted in high ionic strength environment due to the random distribution of ionizable functionalities throughout the polymer chain.

Reversible deactivation radical polymerization (RDRP) techniques have the ability to synthesize polymers with precise molecular weight and advanced architectures, whilst maintaining a good control over the molecular weight distribution. However, the synthesis of UHMW polymers using these techniques remains difficult with only very little advances towards complex architectures.<sup>28</sup> Several studies have reported the synthesis and development of well-defined UHMW polymers using reversible addition-fragmentation chain transfer (RAFT) polymerization,<sup>28, 29, 30, 31, 32, 33, 34, 35</sup> atom transfer radical polymerization (ATRP),<sup>32, 36, 37, 38, 39, 40, 41</sup> and single-electron transfer living radical polymerization (SET-LRP).<sup>42, 43, 44</sup> The majority of these studies have directed their focus towards linear homopolymers and AB diblock copolymers, with one exception being ABA triblock copolymers of dimethylacrylamide and *N*-isopropylacrylamide bearing molecular weight up to 500 kDa.<sup>31</sup>

Recently, our group was able to synthesize a series of UHMW ABA triblock copolymers from acrylic acid (AA) and AM as the A and B blocks, respectively.<sup>28</sup> The lengths of the terminal A block for these eight ABA triblock copolymers were reported to range from 5,210 Da to 173 kDa. These polymers were the first of their kinds with the total overall molecular weight being approximately 1,000 kDa with well-controlled dispersity ( $\bar{D}$ ) remaining below 1.70.<sup>28</sup> In comparison to typical statistical copolymer of AM and AA, these ABA triblock copolymers are hypothesized to have better solubility in high ionic strength environment due to presence of the long and highly water-soluble long B block. In addition, the terminal A blocks would still possibly

allow for elongation of the polymer chain due to electrostatic repulsion, as well as competitive attachment onto the particle surface by hydrogen bonding through the B block even if the anionic functionalities are compromised. Therefore, due to their unique architecture and high molecular weight, these polymers may have strong potential as flocculants, particularly in high ionic strength environments.

In this work, we aim to evaluate the flocculation efficiency of the aforementioned UHMW ABA triblock copolymers on kaolin clay, in high ionic strength environments induced by calcium chloride. Kaolin was selected as it is one of the primary minerals found in wastewater of numerous industrial processes, including but not limited to paint and coatings manufacturing, paper production, rubber, and chemicals productions.<sup>45</sup> In addition, this mineral carries a wide range of other negative risks towards human health, soil and air contamination, and vegetation and wild life.<sup>46</sup> To the best of our knowledge, this is one of the first reported studies employing the use of UHMW polymers with advanced architectures to address the limitations associated with flocculation in high ionic strength environments. The effect of different salt concentrations (0.05 M, 0.10 M and 0.50 M) on the flocculation efficiency (settlement rate and supernatant turbidity) of the ABA triblock copolymers is explored using standard cylinder settling tests. In addition, comparison against control homopolymers and statistical copolymer of AM and AA carrying similar molecular weights is conducted, to allow for a comparison between the ABA triblock architecture and those that are representative of current commercial flocculants.

Cylinder settling tests are routinely used for analysis of the flocculation efficiency and comparison between flocculant products. However, the applied mixing for these tests is not well defined. Settlement rate and supernatant turbidity as efficiency measures give indirect indications of the extent of aggregation. Turbulent pipe flow gives a better view over both the intensity and

duration of mixing between flocculant solutions and a suspension. Focused beam reflectance measurement (FBRM) probe can be utilized in-line to monitor the flocculated aggregate size as a function of flocculant dosage in real time.<sup>47</sup> Cylinder settling tests can be employed as a primary test to determine the flocculation efficiency of a polymer, whilst the turbulent pipe flow approach was utilized as a supplementary test to gain a better understanding of the flocculation mechanisms and the aggregate profile.

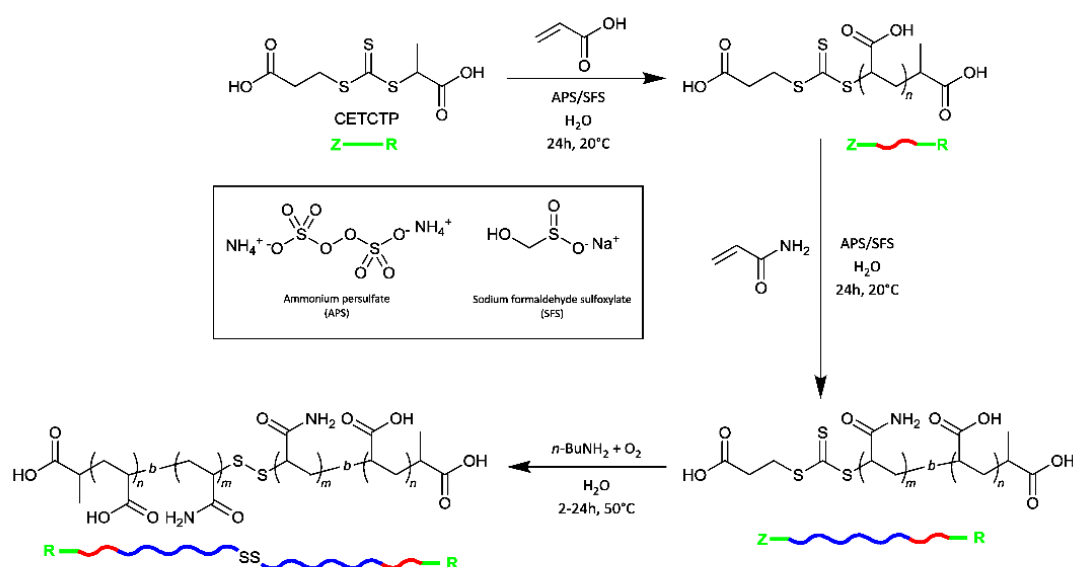
### MATERIALS AND METHODS

**Materials.** The following chemicals were used directly as received without further purification: acrylamide (Sigma, 99%), 3-((((1-carboxyethyl)thio)carbonothioyl)thio)-propanoic acid (Boron Molecular, 90%), ammonium persulfate (Sigma-Aldrich, 98%), sodium formaldehyde sulfoxylate dihydrate (Sigma-Aldrich, 98%), sodium nitrate (Merck, 99.9%), sodium bicarbonate (Merck, 99.9%), *n*-butylamine (Sigma-Aldrich, 99.5%), calcium chloride dihydrate (Merck, 99%), *N,N*-dimethylformamide (Ajax FineChem, 99.9%), and water (Milli-Q and RO grades). Acrylic acid (Aldrich, 99%) was passed through a small column of basic activated aluminium oxide (Acros Organics) and immediately used for polymerizations. Prestige NY kaolin clay (46.7 wt% SiO<sub>2</sub>, 36.1 wt% Al<sub>2</sub>O<sub>3</sub>, 0.8 wt% TiO<sub>2</sub>, 0.9 wt% Fe<sub>2</sub>O<sub>3</sub>, 0.7 wt% CaO, 0.4 wt% MgO, 0.4 wt% K<sub>2</sub>O, and 0.1 wt% Na<sub>2</sub>O) was kindly donated by Sibelco Australia and used as received.

**General Procedure for the Synthesis of the ABA Triblock Copolymers.** The synthetic pathway of the ABA triblock copolymers is outlined in Scheme 1, and these polymer were synthesized in a three-step process based on the procedure previously reported by our group.<sup>28</sup> The first two steps involved the initial RAFT polymerization and subsequent chain extension using AA and AM, respectively. The final step in the synthetic pathway involved the aminolysis of the AB

diblock copolymers to produce the ABA triblock copolymers by spontaneous formation of disulfide linkages.

In a typical RAFT polymerization reaction, the monomer (AA or AM) and the RAFT chain transfer agent were dissolved in Milli-Q water inside a sealable reaction flask. In addition, DMF was employed as the internal standard for subsequent calculation of the monomer conversion by  $^1\text{H}$  NMR. The reaction flask was sealed and subsequently charged with a stream of argon gas. Deoxygenation of the reaction mixture was performed by argon bubbling for 30 minutes. The temperature of the reaction mixture was kept constant at 20°C throughout the process. The initiators (APS and SFS) were then respectively injected into the reaction flask followed by a further 5 minutes of argon bubbling. The reaction was left running under the stream of argon gas for 24 hours. In a typical aminolysis experiment, the AB diblock copolymer was dissolved in water and charged in a sealable reaction flask. To promote an oxidative environment, the reaction mixture was bubbled with pure oxygen for 30 minutes prior to the addition of *n*-butylamine. The reaction was left running under a closed environment at 50°C for up to 24 hours. The polymers were purified by dialysis in water and freeze dried prior to being used in the subsequent stage or flocculation testings. Purification was performed using a SnakeSkin™ dialysis tubing (Thermo Fisher Scientific) with a molecular weight cut-off at 3,500 Da. Freeze drying was performed on a Labconco FreeZone Bench Top Freeze Dry system.



**Scheme 1.** Overall reaction pathway for the synthesis of the UHMW ABA triblock copolymers using sequential RAFT polymerization followed by aminolysis and oxidation of the thiocarbonylthio functionality (Ref. 28 - Reproduced by permission of The Royal Society of Chemistry).

**General Procedure for the Synthesis of the Control Copolymers.** Three different control UHMW polymers with molecular weight roughly 1,000 kDa were employed in this study: homopolymer of AA (**PAA**), homopolymer of AM (**PAM**), and random copolymer of AA and AM (**RAB**; 50 % AA and 50% AM). These control polymers were synthesized using free radical polymerization in a similar methodology with respect to the ABA triblock copolymers. In a typical polymerization reaction, the appropriate amount of monomer(s) were dissolved in Milli-Q water and charged into a sealable reaction flask. The reaction mixture was deoxygenated by argon bubbling for 30 minutes. Aqueous solutions of the initiators (APS and SFS) were respectively injected into the reaction flask and argon bubbling was applied for a further 5 minutes after each injection. The reaction was left running at 20°C for 24 hours under a stream of argon flow. At this

point, the resultant polymer gel was directly freeze dried and ground into smaller particles prior to use as a flocculant.

**Size Exclusion Chromatography (SEC).** Molecular weight distributions of the polymeric flocculants were conducted using a Tosoh High Performance EcoSEC HLC-8320GPC System. Three analytical columns (TSKgel G5000PW<sub>XL</sub>, TSKgel G6000PW<sub>XL</sub>, and TSKgel GMPW<sub>XL</sub>) connected in series and a TSKgel SuperH-RC reference column were employed to analyze the polymers. In addition, the system also comprised of a dual flow pumping unit, a vacuum degasser, an autosampler, a Bryce-type refractive index (RI) detector, a UV detector set at 305 nm, and a TSKgel PW<sub>XL</sub> guard column. The polymers were measured against a series of polyacrylic acid standards with molecular weights ranging from 1 kDa to 1 MDa. Measurements were performed at 40°C with 0.1 M NaNO<sub>3</sub> and 0.1 M NaHCO<sub>3</sub> (pH ≈ 8.3) in deionized water as the eluent (flowrate of 1 mL/min).

**Make-up and Preparation of Polymer for Flocculation Analysis.** Eleven different anionic copolymers (eight ABA triblock copolymers and three control polymers) with similar molecular weights and varying charge densities were synthesized and employed as flocculants for this study. The properties of these polymeric flocculants are summarized in Table 1.

An initial 0.25 wt% stock solution of the polymeric flocculant was prepared by initially wetting the powdered flocculant (0.25 g) with acetone (3 mL) in a 100 mL glass bottle, subsequently followed by the addition of deionized water (97 mL). The mixture was shaken vigorously by hand for 30 seconds to allow for even distribution of the polymer particles and immediately mixed continuously on a benchtop tube roller mixer at 70 RPM for 2 hours. At this point, the resulting solution became clear and homogeneous. This stock solution was further diluted with deionized water and mixed again at 70 RPM for 5 minutes on the roller to make a 0.025 wt% homogeneous

working solution which was used directly for flocculation testings. The working solution was always prepared fresh prior to immediate flocculation testing and discarded at the end of each day whilst the concentrated stock solution was stored under refrigeration when not in use and kept for no longer than one week. The flocculant dosage in this study is expressed as grams of polymer per tonne of dry kaolin solids (g/tds).

**Table 1. Summary of the anionic polymeric flocculants employed in this study**

Abbreviated Name	$M_{n,SEC}$ of A Block (kDa)	Overall $M_{n,SEC}$ (kDa)	$\bar{D}$
PAA	-	1,220	7.73
PAM	-	922	8.63
RAB	-	960	10.4
ABA1	5.21	1,040	1.63
ABA2	11.8	924	1.72
ABA3	20.9	1,140	1.57
ABA4	33.9	1,180	1.48
ABA5	45.7	903	1.40
ABA6	84.8	1,080	1.45
ABA7	118	1,020	1.93
ABA8	173	850	1.62

**Preparation of High Ionic Strength Kaolin Slurry.** For cylinder settling tests, kaolin slurries were prepared fresh daily at the desired solid concentration by adding kaolin clay (3 wt% for cylinder settling tests; 1.5-6 wt% for turbulent pipe flow tests) to deionized water in a 20 L pail. The cation of interest in this study was  $Ca^{2+}$  and therefore high ionic strength environment was

generated by the addition of the appropriate amount of calcium chloride to the bulk slurry in the pail. The slurry was subsequently stirred vigorously using an overhead mechanical stirrer equipped with an impeller blade at a rate of approximately 500 RPM where a vortex was observed. This high intensity stirring was applied for 3 hours to allow for uniform distribution of the clay particle and the cation. After which, the stirring rate was reduced to approximately 250 RPM where a smaller vortex was observed, for a gentle stirring environment during flocculation testing. All flocculation measurements were performed at the natural pH (approximately between 7 and 8) of the high ionic strength slurry.

For continuous flocculation tests, kaolin slurries were also prepared fresh daily at the desired solid concentration by adding kaolin clay to tap water in a 60 L pail. The kaolin slurry was stirred vigorously at 200 RPM using an overhead mechanical stirrer equipped with a large impeller blade so that a vortex was observed. The appropriate quantity of calcium chloride pellets was then slowly added into the slurry. The vigorous stirring was maintained for one hour to allow for homogenization and dissolution of the substrate and the salt, respectively. After which, the same stirring rate was maintained and the kaolin slurry was directly pumped the turbulent pipe flow system with in-line FBRM monitoring.

**Flocculation by Cylinder Settling Tests.** In a typical cylinder batch settling test, the high ionic strength kaolin slurry was transferred to a 1000 mL graduate cylinder (Azlon CT1000P, diameter 6.6 cm, height 44 cm). The temperature of this flocculation process which include the kaolin slurry and the flocculant working solution were unadjusted and maintained at room temperature. A stainless steel plunger was employed for the purpose of mixing and distributing the flocculant throughout the slurry. The diameter of the plunger was 5 cm with five evenly distributed inner radial holes of 1 cm diameter. The plunger was used to mix the slurry vigorously for approximately

5 seconds, which was immediate followed by the addition of the required amount of flocculant. Once added, five plunger strokes were applied to the slurry, where each stroke was considered as both a downward and an upward motion. For good consistency, a metronome was employed to allow for each plunging motion (up or down) to be performed at a rate of 45 BPM. The settlement time of the flocculated particles was measured from when the mud-line passed the starting point at 900 mL mark until it reached the 700 mL mark on the graduated cylinder (total distance of 7 cm). At 20 minutes after the last stroke, approximately 10 mL of the supernatant was taken from the 800 mL mark on the graduated cylinder for turbidity analysis using a Hanna Instruments HI98703-01 Portable Turbidity Meter.

**Continuous Flocculation in Turbulent Pipe Flow.** Continuous flocculation experiments were conducted using a FBRM D600L probe (Mettler-Toledo) and a pipe reactor which consisted of a series of stainless steel pipes. The theories and principles associated with the FBRM technique and chord length distributions in flocculation studies were previously discussed by Heath *et al.* and Owen *et al.*, respectively.<sup>48,49</sup> The coarse (C) electronics mode was employed rather than the fine (F) mode as the slower response with the former increases the probability of larger, highly porous aggregates being measured as a single object. Consequently, the sensitivity of the FBRM would be reduced for particles and fines with sizes below 10  $\mu\text{m}$ .<sup>47</sup> This was deemed to be sufficient for this study. While the probe can measure chord lengths up to 2000  $\mu\text{m}$ , for these experiments chord length distributions were measured between 1 and 1000  $\mu\text{m}$  in 100 channels distributed logarithmically. The chord length distributions are usually presented as line graphs for ease of comparison, but in reality should be column graphs. A volume-weighting is achieved by applying a square-weighting to the chord length distribution.

$$n_{i,2} = n_i M_i^2 \quad (1)$$

where  $n_i$  and  $n_{i,2}$  are the counts and square-weighted counts in a chord channel, respectively, and  $M_i$  is the midpoint of the channel. The mean of this distribution is also derived:

$$\text{Mean square-weighted chord length} = \frac{\sum_{i=1}^k n_i M_i^3}{\sum_{i=1}^k n_i M_i^2} \quad (2)$$

The D600L probe had an outer stainless steel casing of 25 mm in diameter, and a 12 mm diameter flat sapphire window at its tip. Window cleaning was performed regularly to ensure there was minimal adherence of fine particles on the surface, which could affect the final measured size. Therefore, cleaning was repeated prior to each set of measurements until a total background count of less than 150 counts per second was obtained in air.

In previous studies of flocculation kinetics in turbulent pipe flow, the internal diameters of the pipe can range up to 38 mm.<sup>50</sup> Stainless steel pipes may be linked together to achieve a total reactor lengths between 1 and 50 m. However, for the purpose of these flocculation experiments, a small-scale pipe reactor was employed with an internal pipe diameter of 7.7 mm. A straight pipe with a length of 1 m was connected to the inlet of the pipe reactor, which was subsequently followed by a 7 m long helical coil pipe attachment. Each single coil had a total length of 1 m and therefore this section of the pipe reactor incorporated 7 coils. The diameter of each coil was approximately 30 cm. Secondary flow effects can be observed in helical coils,<sup>51</sup> but computational fluid dynamics modelling on this experimental set-up was able to confirm small and negligible effect for the size of coil and low flow velocities employed.<sup>47</sup> An overall schematic of the pipe reactor is shown in Figure S1a in the SI.

The inlet of the pipe reactor was designed to allow for the feed lines (slurry and flocculant) to join and mix together (Figure S1b in the SI). This design consequently allowed for the distance between the point of flocculant addition and the FBRM probe to be well defined. The flocculant feed line had an internal diameter of 3 mm. The outlet of the pipe reactor was a flowcell

measurement chamber which allowed for the insertion of an FBRM probe at a 45° angle to the slurry flow (Figure S1c in the SI). This was carefully designed to ensure that no dead zone exists and the probe window is free of any blockages.

In a typical experiment, water was initially pumped through the system to check for leaks. Subsequently, the kaolin slurry was pumped through the pipe reactor at a volume flowrate of approximately 2.5 L/min until the distributions and main statistics (total counts, mean chord length and mean square-weighted chord length) directly obtained from the FBRM software were stable in real-time. At this point, the flocculant was then pumped through the pipe reactor at an appropriate flowrate so that the final dosage of the flocculant reached the desired values of 17, 33, 50, or 67 g/tds. Chord length distributions between 1 and 1000  $\mu\text{m}$  were measured and recorded instantaneously every 2 seconds. The FBRM results reported were averaged from 20 to 30 measurements when stability was achieved for the condition employed. Unweighted and length square-weighted chord length distributions and a variety of statistics were monitored and recorded by the software in real-time. However, for the purpose of this study, only the mean unweighted chord length and the mean square-weighted chord length were closely examined as a function of flocculant dosage. Once measurements for all the desired dosages and flocculants were performed, the pipe reactor was flushed with water and the FBRM probe window was cleaned prior to the next set of measurements with a different kaolin concentration (1.5, 3, or 6 wt%).

### RESULTS AND DISCUSSION

The UHMW ABA triblock copolymers of AA and AM employed in this study (**ABA1 - ABA8**) were the first of their kind – possessing precise architecture and composition whilst maintaining such high molecular weight and low dispersities.<sup>28</sup> Better flocculation efficiency in high ionic

strength environment was hypothesized for these polymers solely based on the advancement in architecture compared to the current commercial random-type polymeric flocculants. However, it would be misguided to directly compare these ABA triblock copolymers to current available commercial anionic flocculants due to the considerable differences in molecular weight.

In order to primarily focus the difference in architecture, control polymers with similar molecular weight to the ABA triblock copolymers were synthesized. Homopolymers of AA and AM (**PAA** and **PAM**, respectively) were synthesized using free radical polymerization at optimized conditions to achieve a target molecular weight of approximately 1 million. **PAA** and **PAM** were employed as control polymers; in theory, the negative effect of high ionic strength would be more significant towards the flocculation efficiency of the anionic **PAA** compared to the neutral **PAM**. A random copolymer of AA and AM (**RAB**) with similar molecular weights was also synthesized using the same methodology. The architecture of **RAB** is representative of current commercial flocculants commonly applied to clay-based tailings and thus can be directly compared against **ABA1** to **ABA8** in Table 1. This would allow for a comparable analysis, where the advancement in architecture is the most significant factor being considered as a solution to the main research problem.

**Cylinder Settling Test Conditions.** A series of standard cylinder settling tests was initially performed using the three control polymers (**PAA**, **PAM**, and **RAB**) and the eight ABA triblock copolymers (**ABA1** – **ABA8**). Cylinder settling test is one of the most common method employed to study and evaluate flocculation. Nevertheless, there are certain negative connotations associated with this method due to its high level of standard errors typically attributed by poor mixing, and variations in the solid concentrations and testing procedures.<sup>52, 53</sup> The main intention of conducting these tests was to obtain a general guide on the fundamental effect of the multivalent cation and

its concentrations on the flocculation efficiency of these novel polymers. These initial tests would allow for the identification and analysis of various trends amongst the ABA triblock copolymers or between the subject polymers and the control polymers. Therefore, this methodology was deemed to be sufficient for the initial stage of flocculation in this study.

Cylinder settling tests were conducted using kaolin slurry, with calcium chloride added to create a high ionic strength environment. The kaolin slurry was initially maintained at a solid concentration of 3 wt% throughout. Three different calcium chloride concentrations of 0.05 M, 0.10 M, and 0.50 M were targeted. The large increments in the concentration of  $\text{Ca}^{2+}$  allow for any significant changes or trends in the flocculation efficiency of the anionic flocculants to be observed. Solutions of the polymeric flocculants were introduced into the slurry at four different dosages ranging from approximately 17 to 67 g/tds, and the flocculation efficiency determined. Effort was made during cylinder settling testing to reduce the standard errors by having the same operator, accurate solid and salt concentrations, and consistent quantity and rate of plunger strokes throughout.

Figure 1 shows a proposed schematic for the flocculation mechanism of the ABA triblock copolymers, where the terminal anionic A blocks are responsible for bridging via salt linkages with cations on the surface of the particles, whilst the neutral B block is able to bridge *via* hydrogen bonding.

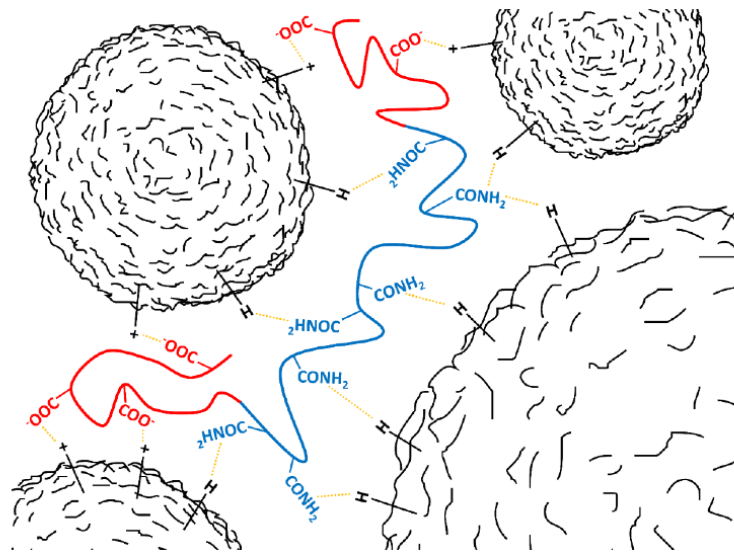


**Figure 1.** Schematic for the flocculation mechanism of the ABA triblock copolymers where the A and B blocks adsorb onto the surface of the colloidal particles *via* salt linkages and hydrogen bonding, respectively.

**Effect of  $\text{Ca}^{2+}$  on Settlement Rate.** The settlement rates of all 11 polymers as a function of dosage are shown in Figure 2. The most efficient strategy to assess these flocculation efficiency plots is to track the changes associated with polymer **RAB** (blue solid line with circle markers) whilst comparing it to the ABA triblock copolymers (dashed lines with square markers).

At the lowest  $\text{Ca}^{2+}$  concentration of 0.05 M (Figure 2a), **RAB** remained effective in flocculating in the kaolin suspension. Increments in dosage resulted in considerably larger increases in settlement rate compared to the ABA triblock copolymers. With the exception of **ABA7**, the overall settlement rates of the ABA triblock copolymers were lower compared to **RAB**, particularly at the highest dosage of 67 g/tds. This first set of data indicated that **RAB** was somewhat unaffected by the concentration of  $\text{Ca}^{2+}$  targeted, and its settlement rate would in all likelihood be superior compared to the ABA triblock copolymers if higher dosages were

employed. Note that **PAM** consistently gave lower settlement rates at all dosages, reflecting the more coiled conformation of the non-ionic polymer. The settlement rates were marginally lower for **PAA** flocculation, with adsorption via salt linkages possibly being less effective of the influence of such adsorption being limited by a degree of polymer complexation.

A two-fold increase in the concentration of  $\text{Ca}^{2+}$  to 0.10 M led to a substantial drop in the settlement rate for **RAB** (Figure 2b). At this concentration, the settlement rates achieved with **RAB** were now observed to be inferior compared to polymers **ABA4** to **ABA7**. Concurrently to this decline in activity, the settlement rates obtained from the ABA triblock copolymers remained in a similar range where no notable changes were observed. This stability in settlement rates was observed yet again when the concentration of  $\text{Ca}^{2+}$  was further increased five-fold from 0.10 M. This indicated that the flocculation efficiency of the ABA triblock copolymers remained relatively unaffected by the changes in the ionic strength, contrary to that of **RAB**. At the highest  $\text{Ca}^{2+}$  concentration of 0.50 M (Figure 2c), the overall settlement rates obtained with **RAB** were lower than all of the eight ABA triblock copolymers. The polymer **RAB** went from being initially better than seven of the ABA triblock copolymers to being the most compromised by the ten-fold increase in  $\text{Ca}^{2+}$  concentration.

Any further increase in  $\text{Ca}^{2+}$  concentration from 0.50 M would perhaps result in similar settlement rates being observed from flocculation with both **RAB** and **PAM**. This is attributed to the near-complete shielding of the anionic groups on **RAB**, leading to a pseudo-PAM structure and hence a condensed polymer conformation that is typically observed in unmodified **PAM**.<sup>16</sup> A closer observation showed minimal changes in the settlement rates with **PAM** across all three  $\text{Ca}^{2+}$  concentrations. These results were expected, as the neutral amide functionality on the polymer backbone would be unaffected by the cations present in the solution. Slight increases in settlement

rates were generally observed for **PAM** and the ABA triblock copolymers when the  $\text{Ca}^{2+}$  concentration was increased. High concentration of multivalent cations would lead to compression of the electrical double layer (EDL), which destabilized the unflocculated colloidal suspension and hence assisted with the subsequent flocculation process.

In contrast to **PAM**, the settlement rates obtained from **PAA** flocculation were significantly influenced by the presence of calcium cations. A notable drop in the settlement rates were observed with stronger ionic strength, until a near-plateau response curve was observed at 0.50 M  $\text{Ca}^{2+}$ , indicating effective deactivation as a flocculant. These results were expected, as anionic functionalities across the entire polymer chain would interact with the cations available in the kaolin slurry, and hence heightened negative effects at higher ionic strength.

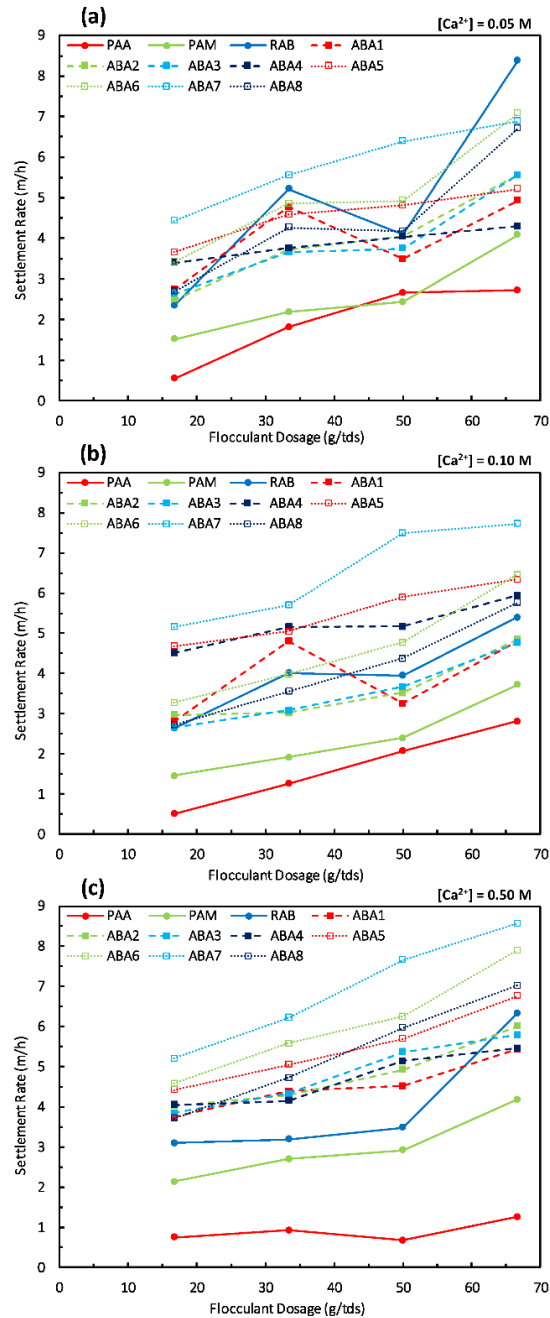


**Figure 2.** Settlement rate of kaolin slurry (3 wt%) as a function of flocculant dosage for the ABA triblock copolymers (ABA1 – ABA8) and the control polymers (PAA, PAM and RAB) obtained by standard cylinder settling tests with varying  $Ca^{2+}$  concentrations at (a) 0.05 M, (b) 0.10 M, and (c) 0.50 M.

Based on the settlement rates obtained from the control polymers alone, it would be concluded that polymers with higher fraction of anionic functionalities were more susceptible to undesirable interactions with multivalent cations. However, examination of the measured settlement rates from just the ABA triblock copolymers indicated the opposite. Longer A blocks for these polymers generally corresponded to faster settlement rates. Overall, **ABA5** to **ABA8** were able to flocculate the kaolin suspension at a faster rate, particularly at the highest  $\text{Ca}^{2+}$  concentration of 0.50 M. At each concentration of  $\text{Ca}^{2+}$ , the settlement rate was observed to decrease once the A block passed a threshold molecular weight. For all three concentrations of  $\text{Ca}^{2+}$  employed, **ABA7** with the second longest A blocks was able to induce flocs with the highest settlement rates in comparison to that of **ABA8**. The overall molecular weights of **ABA7** and **ABA8** were determined by SEC to be 1,020 kDa and 850 kDa, respectively. Therefore, although **ABA8** had a higher concentration of anionic functionalities in comparison to **ABA7**, its lower molecular weight was the main factor for the slight reduction in flocculation efficiency. Relatively inferior settlement rates obtained from using **ABA1** to **ABA4** can be attributed to the lower concentration of anionic functionalities present, which led to inadequate polymer chain elongation and consequently resulted in inefficient polymer-particle bridging. This effect was amplified particularly in high ionic strength environment due to shielding of the active anionic groups. Nevertheless, these differences in the settlement rates amongst the ABA triblock copolymers were very minor across all three concentrations of  $\text{Ca}^{2+}$ .

**Effect of  $\text{Ca}^{2+}$  on Supernatant Turbidity.** The supernatant turbidity of the kaolin suspension was measured consistently at the 20 minutes mark after the addition and homogenization of the polymeric flocculant. Turbidity results obtained with 11 polymers as a function of dosage are shown in Figure 3, presented in the exact same format to those for the settlement rates for ease of

examination. Lower turbidity values (lower NTU) are desirable as this indicates that the polymeric flocculants are more efficient at clarifying the supernatant.

At the lowest  $\text{Ca}^{2+}$  concentration of 0.05 M, it could be clearly observed that all eight ABA triblock copolymers were able to induce much lower turbidity compared to **RAB**, and the control polymers **PAA** and **PAM**. For example, the turbidity obtained from using **ABA2** at a dosage of 50 g/tds was very low at only 15 NTU, whilst values obtained from **RAB** ranged from 80 to 110 NTU across all the four dosages employed. Similar results were also observed for the two higher concentrations of  $\text{Ca}^{2+}$ , where the ABA triblock copolymers consistently produced supernatants with the lowest turbidity values, followed by **PAM**, **RAB**, and **PAA**, respectively. These results essentially indicated that the clarification performance of all eight ABA triblock copolymers were considerably better than **RAB**, irrespective of the concentration of  $\text{Ca}^{2+}$ . Given that little work had been done on the flocculation efficiency of well-defined ABA triblock copolymers, the exact reason behind this phenomenon in turbidity remained unclear.

A closer examine at the supernatant turbidity results did not show any obvious trends amongst the ABA triblock copolymers. All eight ABA triblock copolymers produced similar performance, particularly at the two lowest  $\text{Ca}^{2+}$  concentration of 0.05 M and 0.10 M. At the highest concentration of 0.50 M, the differences in the results obtained for the ABA triblock copolymers were slightly more significant and noticeable. Unlike the results obtained for the settlement rates, a threshold was not observed in the molecular weight the A block to reach the lowest supernatant turbidity. Across the three different concentrations of salt used, turbidity results obtained using ABA triblock copolymers with long terminal A blocks were slightly higher compared to those with shorter A blocks. This was in agreement with the previous comparison between polymers **PAM**, **RAB** and **PAA**. Despite being compromised by the high quantity of salt within the solution,

the performance of these ABA triblock polymers with regards to the supernatant turbidity remained promising throughout all three different  $\text{Ca}^{2+}$  concentrations.

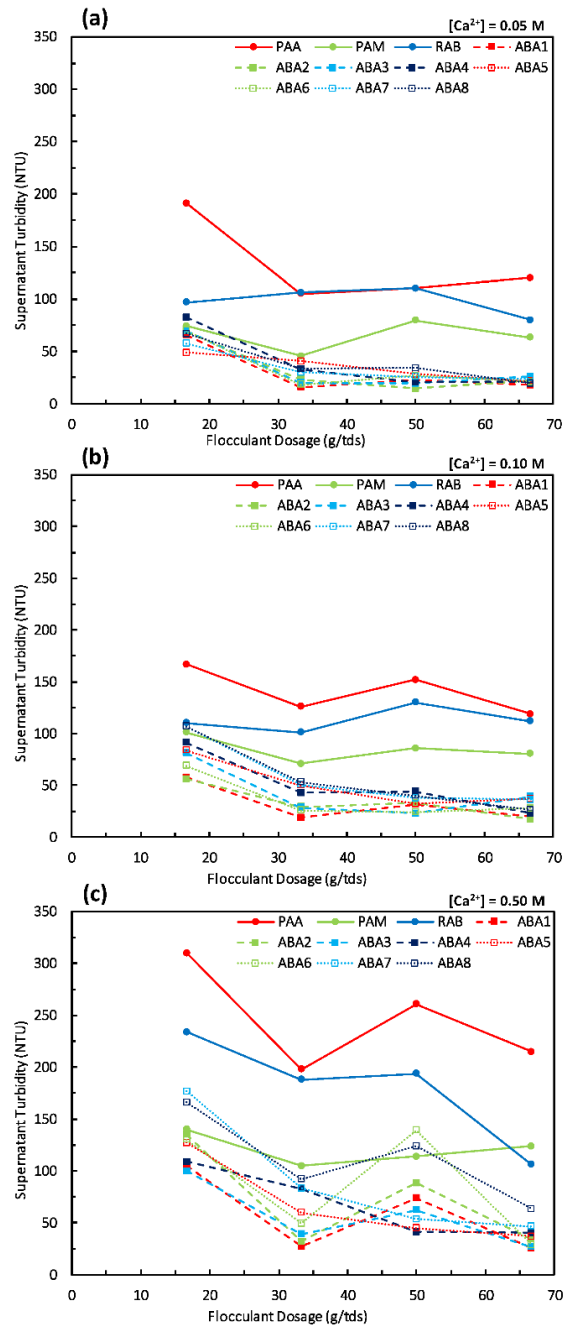


**Figure 3.** Supernatant turbidity of kaolin slurry (3 wt%) as a function of flocculation dosage for the ABA triblock copolymers (ABA1 – ABA8) and the control polymers (PAA, PAM and RAB) obtained by standard cylinder settling tests with varying  $Ca^{2+}$  concentrations at (a) 0.05 M, (b) 0.10 M, and (c) 0.50 M.

**Measuring Aggregate Dimensions in Real-time by FBRM.** Polymer comparisons from batch cylinder testing inevitably involves performance measures made on the products of a series of partially overlapping steps. These include the distribution of the polymer solution through the slurry, adsorption of the polymer to particle surfaces during this mixing step, subsequent aggregate growth (with possible concurrent breakage) and the likelihood of additional aggregate growth occurring in the milder shear conditions after plunger mixing has ceased. The latter steps represent the well-known concept of ‘tapered shear’, with the conditions considered most conducive for optimal aggregation involve a short duration of higher shear to favour reagent distribution and initial aggregate growth, followed by reduced shear that then enables larger aggregates to be formed.<sup>49, 54</sup>

A pipe reactor was employed in conjunction with an FBRM probe to provide in-line monitoring of the flocculated aggregate size while under turbulence. This supplement methodology was employed to gain a better understanding of the aggregate profile due to the unique supernatant turbidity results. However, these tests were not considered as the primary mean to determine the flocculation efficiency of the polymeric flocculants, as the cylinder settling tests alone were sufficient. The mean shear rate examined ( $1270 \text{ s}^{-1}$ ) ensures that conditions remained turbulent throughout all testing and matches that used with this experimental configuration previously,<sup>47</sup> with the fixed reaction time (9.2 s) considered to definitely be after any dosed polymer has been well mixed through the slurry flow.

To appreciate how the FBRM chord length distributions respond to flocculation, it is useful to first examine results obtained separately for a kaolin slurry flocculated with a commercial anionic flocculant (BASF Magnafloc® 336) at a very low ionic strength, in this case  $0.03 \text{ M Ca}^{2+}$  is added to ensure stable dispersion of the kaolin particles. This flocculant has a nominal molecular weight

in excess of 15 MDa, i.e. more than an order of magnitude higher than **RAB**. Figure 4 shows chord length distributions obtained from pipe flocculation at different dosages, contrasted to results for the unflocculated kaolin slurry. The unweighted chord length distributions (Figure 4a) offer sensitivity to the number of particles or aggregates within the slurry, and as increasing dosages of flocculant are introduced, aggregation leads to the distribution reducing in intensity and shifting to larger chord lengths. The flocculated distributions can display some bimodal character, particularly at the lower dosages, with shoulders or peaks at short chord lengths ( $<10\ \mu\text{m}$ ), indicative of some fines not being captured in aggregates.

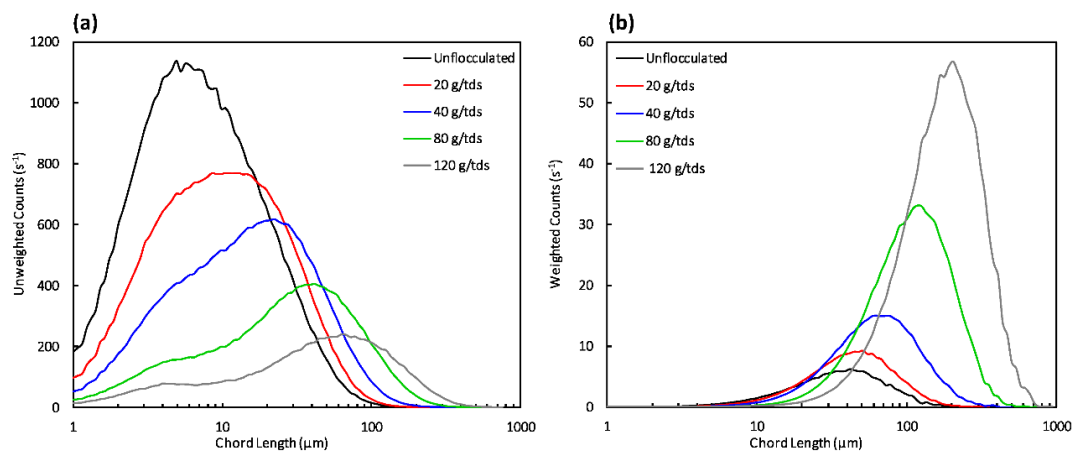


**Figure 4.** (a) Unweighted and (b) length square-weighted chord length distributions for the flocculation of 2 wt% kaolin slurry with BASF Magnafloc® 336 (reaction time 9 s, mean shear rate  $1270\ \text{s}^{-1}$ ).

Large aggregates provide only a small number of counts to such distributions. The length square-weighted chord length distributions (Figure 4b) represent a volume-weighting and better reflect the extent of aggregation, although any fines then essentially become invisible. With each increment in dosage, the volume-weighted peak shifted to larger sizes and a higher intensity.

Previous studies have shown the sizes attained can be limited by the solids concentration and the applied shear conditions.<sup>49</sup> The importance of considering both unweighted and volume-weighted distributions towards fully understanding a flocculation response can therefore be seen.

Based on the results obtained from the cylinder settling tests, the most prominent differences between the ABA triblock copolymers and **RAB** were observed at the highest  $\text{Ca}^{2+}$  concentration of 0.50 M. **ABA7** was one of the top performing flocculants amongst the ABA triblock copolymers and was therefore selected for direct comparison against **RAB** in continuous pipe flow flocculation, with the aggregate chord length distributions determined in real-time as a function of flocculant dosage at three different solids concentrations in 0.50 M  $\text{Ca}^{2+}$  (Figure 5). Similar to the cylinder settling tests, four dosages ranging from 17 to 67 g/tds were employed. The axes for the unweighted and square weight counts in each plot were kept constant to allow for ease of analysis and direct comparison between the two polymers **ABA7** and **RAB**.

Comparison of the unweighted chord length distributions for the unflocculated kaolin distributions in Figure 5 shows that the presence of 0.50 M  $\text{Ca}^{2+}$  clearly induces a level of aggregation. While the shift in size is not large (the mean unweighted chord length rose from 46  $\mu\text{m}$  to 51  $\mu\text{m}$  across the dosage range), it would still represent a substantial reduction in the available surface area exposed to the dosed polymers, and in part explains why polymeric flocculants with a molecular weight of 1 MDa were able to induce sedimentation rates larger than 5 m/h at quite low dosages. The unflocculated distributions in Figure 5 also display an increase in counts as the kaolin concentration is raised, although it should be noted that FBRM counts will rarely give a linear relationship with concentration.<sup>48</sup>

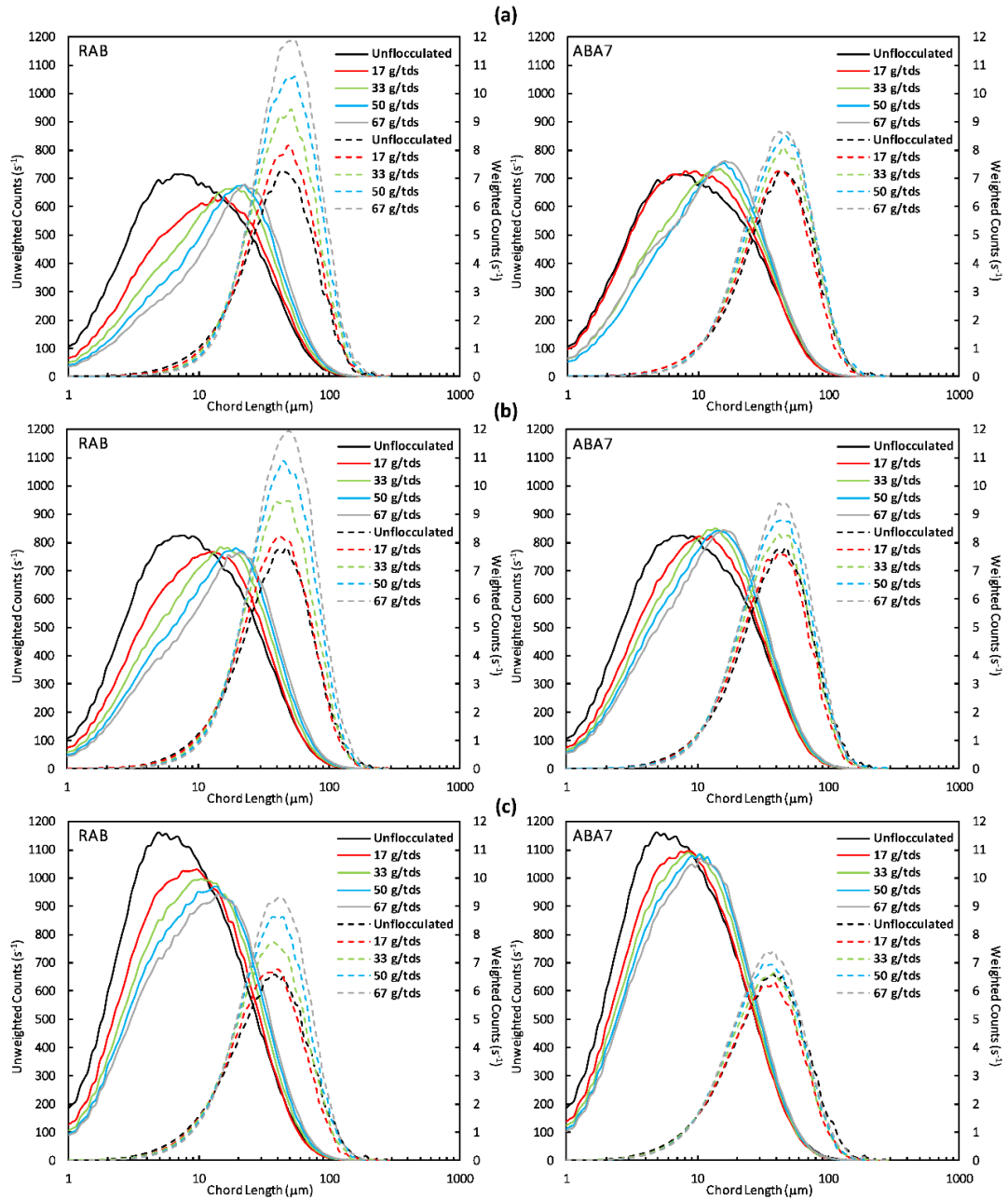


**Figure 5.** Unweighted (solid lines) and length square-weighted (dashed lines) chord length distributions for the flocculation of kaolin slurry with 0.50 M  $\text{Ca}^{2+}$  using polymers **RAB** and **ABA7** (reaction time 9.2 s, mean shear rate  $1270 \text{ s}^{-1}$ ) at varying solid concentrations of (a) 1.5 wt%, (b) 3 wt%, and (c) 6 wt%.

Figure 5b represents the unweighted (solid lines) and length square-weighted (dashed lines) chord length distributions for the flocculation of 3 wt% kaolin slurries containing 0.50 M  $\text{Ca}^{2+}$ , matching the cylinder setting conditions in Figure 3c. Immediately obvious is that the magnitude and form of the observed responses to the applied dosages are very different from Figure 5. There is still a reduction in the unweighted counts but they remain high, with only small shifts to longer chord lengths. The peaks in the length square-weighted distributions do not shift at all (consistently around 45  $\mu\text{m}$ ), instead just increasing in intensity. Together, these observations are consistent with the polymers increasing the capture of the finest particles within the slurries into small aggregates, but the size of such aggregates that can be attained is limited by the polymer molecular weight and the applied shear.

The chord length distributions for **RAB** flocculation of 3 wt% kaolin (Figure 5b) showed distinct changes with each increment in the flocculant dosage. In the case of **ABA7**, the response to dosage followed a similar general trend, but the change with each increment was slightly smaller. However, while the unweighted distributions did shift towards larger chord lengths, there was a greater growth in counts at approximately 20  $\mu\text{m}$  at the expense of the higher counts seen in the 30 – 80  $\mu\text{m}$  range with **RAB**. As a consequence, applying a length square-weighting to these distributions led to much smaller peak increases with dosage when compared to **RAB**.

To gain a better understanding of these responses, the above experiments at 3 wt% kaolin were repeated with the same flocculants and dosages at a lower (1.5 wt% in Figure 5a) and higher (6 wt% in Figure 5c) solids concentration, still maintaining a  $\text{Ca}^{2+}$  concentration of 0.50 M. At 1.5 wt%, the trends for each dosage increment for both flocculants were effectively identical to those observed at 3 wt% kaolin. At 6 wt%, the unweighted counts were still reduced with increasing dosage, but to a much smaller degree, and it can be seen that the peak in the unweighted chord

length distributions were closer to 10  $\mu\text{m}$ , compared to 20  $\mu\text{m}$  at 1.5 and 3.0 wt%. This reflects the highly porous nature of the aggregates formed with the plate-like kaolin particles, leading to a very high effective volume fraction at quite low solids concentrations.<sup>49</sup> The efficient distribution of the polymers throughout the slurry becomes more difficult at higher solids concentration.

An important observation is that the peak in the volume-weighted chord length distributions did not shift for any kaolin solids concentration for flocculation with **ABA7** or **RAB** at any dosage. This indicated that the limitation in aggregate size under the applied shear conditions is a consequence of the polymer molecular weight than the solids concentration, the latter a common factor for higher molecular weight polymers.<sup>47</sup>

**Implications.** It is important to emphasize that the two different experimental methods represent different aspects of the flocculation process. The cylinder settling tests determined the flocculation efficiency of the polymeric flocculants through settlement rate and supernatant turbidity. The pipe reactor method provided a supplementary snapshot of the aggregate profile to further understand the unique characteristics of the ABA triblock copolymers. Furthermore, in regards to the aggregation profile, the former essentially provides a snapshot of the aggregation state under turbulent shear conditions, whereas the latter represents not only the initial turbulent mixing of polymer and initiation of aggregation, but also the subsequent further aggregate growth that takes place under milder shear.

For commercial anionic flocculants, it has been noted that the initial dissolution of powder products in solutions containing even low concentrations of  $\text{Ca}^{2+}$  severely impacts upon their activity.<sup>16</sup> While the dilution of optimally-prepared flocculants into  $\text{Ca}^{2+}$  solutions immediately prior to dosing did have a detrimental effect, the diluted flocculant solutions could still form small aggregates and the restriction in activity only prevented larger sizes being attained. This may

provide a useful insight into how flocculation progresses with the ABA triblock architecture and under which conditions its advantages may be fully realized.

Figure 6a represents how the solution conformation of a conventional flocculant similar in composition to **RAB** may be restricted by complex formation with  $\text{Ca}^{2+}$ , thereby reducing the potential for particle bridging.<sup>55</sup> In Figure 6b, this is also shown in terms of how the adsorbed conformation on a surface may be affected, with a high  $\text{Ca}^{2+}$  concentration limited the extension away from the surface of polymer tails that provide the capacity to bridge between particles. The decline in settlement rates observed for flocculation with **RAB** in Figure 3c is then likely to be due a significant reduction in further aggregate growth under reduced shear immediately after the last plunger stroke.

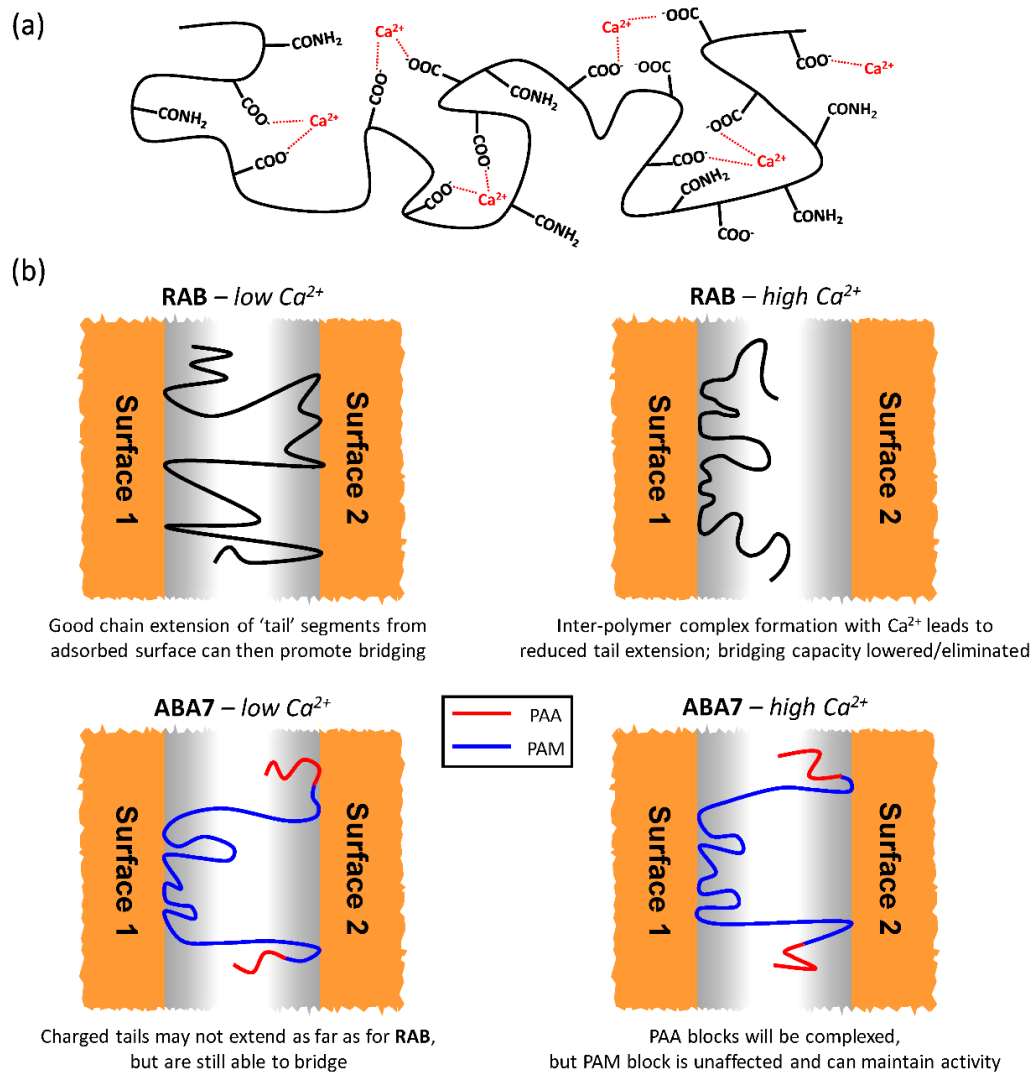


**Figure 6.** Schematic representation of (a) how the solution conformation of a random copolymer of AA and AM would be restricted by complexation with  $Ca^{2+}$ ; and a plausible mechanism for (b) how high concentrations of  $Ca^{2+}$  are postulated to impact on the activity of conventional anionic and ABA triblock copolymers.

In contrast, the non-ionic block within **ABA7** may lead to a flatter overall adsorbed conformation at a low  $Ca^{2+}$  concentration with the anionic tails ensuring there is some extension away from the

adsorbed surface. At a high  $\text{Ca}^{2+}$  concentration there will inevitably be complexation of the anionic tail blocks, but they remain a minor proportion of the full polymer chain length, and the nearest non-ionic sections remain away from the adsorbed surface and able to then provide bridging. Consequently, this characteristic led to decent settlement rates observed throughout the cylinder settling tests. In addition, based on the flow reactor results, the ABA triblock copolymers were more selective towards capturing the fine particles within the slurry, thus resulted in very low turbidity values across all three concentrations of  $\text{Ca}^{2+}$  employed. This characteristic is atypical of commercial polymeric flocculants and was proven to be beneficial towards clarifying the supernatant.

It can therefore be seen that the ABA triblock architecture can maintain flocculation efficiency despite a high level of multivalent cation within a slurry. This demonstrates that such polymers may have considerable potential as tailings flocculants when there is a need or a preference to undertake mineral processing in seawater or other highly saline liquors. Of course this would require synthetic procedures to produce higher molecular weights than have been achieved in this study. There is also a need to extend the flocculation studies to establish the impact of using such flocculants on the structure of aggregates formed and how downstream properties (rheology, sediment compaction) may be affected.

## CONCLUSIONS

Eight novel ABA triblock copolymers (**ABA1** – **ABA8**) were employed in the flocculation of high ionic strength kaolin slurries. The performance of polymers were compared against that of three control polymers (**PAA**, **PAM**, and **RAB**) with similar molecular weights to understand how polymer architecture affects flocculation efficiency in high ionic strength environments. Polymer

**RAB** possessed a random copolymer architecture that is representative of current commercial flocculants and thus could be directly compared to the eight polymers bearing well-defined ABA triblock architectures.

A series of cylinder settling tests were performed at three  $\text{Ca}^{2+}$  concentrations (0.05 M, 0.10 M, and 0.50 M), where the settlement rate and the supernatant turbidity were evaluated as a functional of flocculant dosages (ranged from 17 to 67 g/tds). The ABA triblock copolymers were able to consistently flocculate the kaolin slurry to achieve acceptable settlement rates, whereas the performance of **RAB** declined significantly at the highest  $\text{Ca}^{2+}$  concentration of 0.50 M, indicating that it was certainly compromised by the multivalent cations.

Turbulent pipe flocculation with an in-line FBRM probe for real-time monitoring of flocculated aggregate sizes was used to contrast **RAB** with the best performing of the ABA copolymers (**ABA7**) at a high calcium concentration. Both could only form small aggregates under turbulence, a reflection of their relatively low molecular weights. That both could still achieve useful settlement rates is an indication of the importance of additional aggregation that took place during cylinder settling after turbulent mixing - such aggregation for **RAB** was detrimentally affected by higher calcium concentrations, but the ABA copolymers appear largely unaffected. With further development, polymers bearing ABA triblock architecture have strong potential for implementation into current industrial flocculation applications, particularly for high ionic strength environments.

### ASSOCIATED CONTENT

**Supporting Information.** The Supporting Information (SI) is available free of charge on the ACS publication website at DOI: XXXX/XXXXXXXX. Overall schematic of the pipe reactor

employed for the FBRM experiments, inlet design of the pipe reactor, and cross-section of the flowcell measurement chamber at the pipe reactor outlet.

### **AUTHOR INFORMATION**

**Corresponding Author.** \*E-mail: kei.saito@monash.edu. Phone : + 61 3 9905 4600. \*E-mail : neil.cameron@monash.edu. Phone : Tel: +61 3 9902 0774.

**Notes.** The authors declare no competing financial interest.

### **ACKNOWLEDGEMENTS.**

We would like to acknowledge BASF Australia Ltd, and the Chemicals and Plastics Manufacturing Innovation Network and Training program (supported by Monash University, Chemistry Australia and the Victorian Government of Australia) for their financial supports. Dr. Richard Macoun is gratefully acknowledged for his inputs into the research project. Vivek Ravisankar is acknowledged for his assistance in preparing the FBRM experimental set-up. Xin Gao and Ziqi Liu are acknowledged for acquiring the FBRM data for the Magnafloc® 336 sample.

## REFERENCES

1. Dao, V. H.; Cameron, N. R.; Saito, K. Synthesis, properties and performance of organic polymers employed in flocculation applications. *Polym. Chem.* **2016**, *7*, 11-25.
2. Mishra, S.; Usha Rani, G.; Sen, G. Microwave initiated synthesis and application of polyacrylic acid grafted carboxymethyl cellulose. *Carbohydr. Polym.* **2012**, *87* (3), 2255-2262.
3. Moody, G. M. Chapter 6: Polymeric Flocculants. In *Handbook of Industrial Water Soluble Polymers*, Williams, P. A., Ed.; John Wiley & Sons: Oxford, The United Kingdom, 2008, pp 134-173.
4. Nasser, M. S.; James, A. E. The effect of polyacrylamide charge density and molecular weight on the flocculation and sedimentation behaviour of kaolinite suspensions. *Sep. Purif. Technol.* **2006**, *52* (2), 241-252.
5. Lu, L.; Pan, Z.; Hao, N.; Peng, W. A novel acrylamide-free flocculant and its application for sludge dewatering. *Water Res.* **2014**, *57*, 304-312.
6. Akther, S.; Hwang, J.; Lee, H. Sedimentation characteristics of two commercial bentonites in aqueous suspensions. *Clay Minerals* **2008**, *43* (3), 449-457.
7. Lee, K. E.; Teng, T. T.; Morad, N.; Poh, B. T.; Mahalingam, M. Flocculation activity of novel ferric chloride–polyacrylamide (FeCl<sub>3</sub>-PAM) hybrid polymer. *Desalination* **2011**, *266* (1), 108-113.
8. Konduri, M. K. R.; Fatehi, P. Influence of pH and ionic strength on flocculation of clay suspensions with cationic xylan copolymer. *Colloids Surf. A: Physicochem. Eng. Aspects* **2017**, *530*, 20-32.

9. Moss, N. Flocculation: Theory and Application. *Mine and Quarry Journal* **1979**, 7 (5), 57-61.
10. Ji, Y.; Lu, Q.; Liu, Q.; Zeng, H. Effect of solution salinity on settling of mineral tailings by polymer flocculants. *Colloids Surf. A: Physicochem. Eng. Aspects* **2013**, 430, 29-38.
11. Pillai, J. Flocculants and Coagulants: The Keys to Water and Waste Management in Aggregate Production. *Naperville, IL: Nalco Company (Stone Review)* **1997**, 1-6.
12. Sabah, E.; Cengiz, I. An evaluation procedure for flocculation of coal preparation plant tailings. *Water Res.* **2004**, 38 (6), 1542-1549.
13. Greenlee, L. F.; Lawler, D. F.; Freeman, B. D.; Marrot, B.; Moulin, P. Reverse osmosis desalination: Water sources, technology, and today's challenges. *Water Res.* **2009**, 43 (9), 2317-2348.
14. Sabah, E.; Erkan, Z. E. Interaction mechanism of flocculants with coal waste slurry. *Fuel* **2006**, 85 (3), 350-359.
15. Feng, D.; van Deventer, J. S. J.; Aldrich, C. Removal of pollutants from acid mine wastewater using metallurgical by-product slags. *Sep. Purif. Technol.* **2004**, 40 (1), 61-67.
16. Witham, M. I.; Grabsch, A. F.; Owen, A. T.; Fawell, P. D. The effect of cations on the activity of anionic polyacrylamide flocculant solutions. *Int. J. Miner. Process.* **2012**, 114-117, 51-62.
17. Wilkinson, N.; Metaxas, A.; Bricchetto, E.; Wickramaratne, S.; Reineke, T. M.; Dutcher, C. S. Ionic strength dependence of aggregate size and morphology on polymer-clay flocculation. *Colloids Surf. A: Physicochem. Eng. Aspects* **2017**, 529, 1037-1046.

18. Ritvo, G.; Dassa, O.; Kochba, M. Salinity and pH effect on the colloidal properties of suspended particles in super intensive aquaculture systems. *Aquaculture* **2003**, *218* (1), 379-386.
19. Rogan, K. R. The variations of the configurational and solvency properties of low molecular weight sodium polyacrylate with ionic strength. *Colloid. Polym. Sci.* **1995**, *273* (4), 364-369.
20. Kim, M.; Kim, S.; Kim, J.; Kang, S.; Lee, S. Factors affecting flocculation performance of synthetic polymer for turbidity control. *J. Agric. Chem. Environ.* **2013**, *2* (1), 16-21.
21. Liu, W.; Sun, W.; Hu, Y. Effects of water hardness on selective flocculation of diasporic bauxite. *Trans. Nonferrous. Met. Soc. China.* **2012**, *22* (9), 2248-2254.
22. Mortimer, D. A. Synthetic Polyelectrolytes - A Review. *Polym. Int.* **1991**, *25* (1), 29-41.
23. Kay, P. J.; Treloar, F. E. The Intrinsic Viscosity of Poly(acrylic acid) at Different Ionic Strengths: Random Coil and Rigid Rod Behaviour. *Die Makromolekulare Chemie* **1974**, *175* (11), 3207-3223.
24. Seright, R. S.; Campbell, A.; Mozley, P.; Han, P. Stability of Partially Hydrolyzed Polyacrylamides at Elevated Temperatures in the Absence of Divalent Cations. *SPE-121460-PA* **2010**, *15*, 341-348.
25. Ghimici, L.; Constantin, M.; Fundueanu, G. Novel biodegradable flocculating agents based on pullulan. *J. Hazard. Mater.* **2010**, *181* (1-3), 351-358.
26. Boisvert, J.-P.; Malgat, A.; Pochard, I.; Daneault, C. Influence of the counter-ion on the effective charge of polyacrylic acid in dilute condition. *Polymer* **2002**, *43* (1), 141-148.

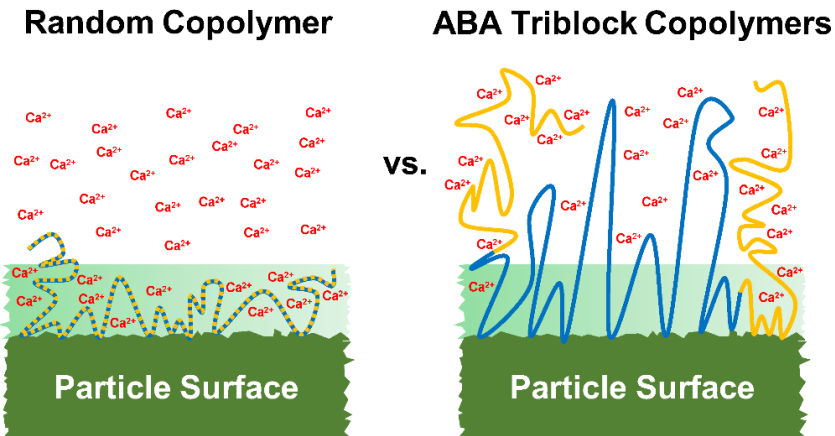
27. Peng, F. F.; Di, P. Effect of Multivalent Salts - Calcium and Aluminum on the Flocculation of Kaolin Suspension with Anionic Polyacrylamide. *J. Colloid Interface Sci.* **1994**, *164* (1), 229-237.
28. Dao, V. H.; Cameron, N. R.; Saito, K. Synthesis of ultra-high molecular weight ABA triblock copolymers via aqueous RAFT-mediated gel polymerisation, end group modification and chain coupling. *Polym. Chem.* **2017**, *8* (44), 6834-6843.
29. Read, E.; Guinaudeau, A.; James Wilson, D.; Cadix, A.; Violleau, F.; Destarac, M. Low temperature RAFT/MADIX gel polymerisation: access to controlled ultra-high molar mass polyacrylamides. *Polym. Chem.* **2014**, *5* (7), 2202-2207.
30. Carmean, R. N.; Becker, T. E.; Sims, M. B.; Sumerlin, B. S. Ultra-High Molecular Weights via Aqueous Reversible-Deactivation Radical Polymerization. *Chem* **2017**, *2* (1), 93-101.
31. Despax, L.; Fitremann, J.; Destarac, M.; Harrisson, S. Low concentration thermoresponsive hydrogels from readily accessible triblock copolymers. *Polym. Chem.* **2016**, *7* (20), 3375-3377.
32. Mapas, J. K. D.; Thomay, T.; Cartwright, A. N.; Ilavsky, J.; Rzyayev, J. Ultrahigh Molecular Weight Linear Block Copolymers: Rapid Access by Reversible-Deactivation Radical Polymerization and Self-Assembly into Large Domain Nanostructures. *Macromolecules* **2016**, *49* (10), 3733-3738.
33. Rzyayev, J.; Penelle, J. HP-RAFT: A Free-Radical Polymerization Technique for Obtaining Living Polymers of Ultrahigh Molecular Weights. *Angew. Chem. Int. Ed.* **2004**, *43* (13), 1691-1694.

34. Xu, J.; Jung, K.; Atme, A.; Shanmugam, S.; Boyer, C. A Robust and Versatile Photoinduced Living Polymerization of Conjugated and Unconjugated Monomers and Its Oxygen Tolerance. *J. Am. Chem. Soc.* **2014**, *136* (14), 5508-5519.
35. Truong, N. P.; Dussert, M. V.; Whittaker, M. R.; Quinn, J. F.; Davis, T. P. Rapid synthesis of ultrahigh molecular weight and low polydispersity polystyrene diblock copolymers by RAFT-mediated emulsion polymerization. *Polym. Chem.* **2015**, *6* (20), 3865-3874.
36. Xue, L.; Agarwal, U. S.; Lemstra, P. J. High Molecular Weight PMMA by ATRP. *Macromolecules* **2002**, *35* (22), 8650-8652.
37. Mao, B. W.; Gan, L. H.; Gan, Y. Y. Ultra high molar mass poly[2-(dimethylamino)ethyl methacrylate] via atom transfer radical polymerization. *Polymer* **2006**, *47* (9), 3017-3020.
38. Simms, R. W.; Cunningham, M. F. High Molecular Weight Poly(butyl methacrylate) by Reverse Atom Transfer Radical Polymerization in Miniemulsion Initiated by a Redox System. *Macromolecules* **2007**, *40* (4), 860-866.
39. Arita, T.; Kayama, Y.; Ohno, K.; Tsujii, Y.; Fukuda, T. High-pressure atom transfer radical polymerization of methyl methacrylate for well-defined ultrahigh molecular-weight polymers. *Polymer* **2008**, *49* (10), 2426-2429.
40. Mueller, L.; Jakubowski, W.; Matyjaszewski, K.; Pietrasik, J.; Kwiatkowski, P.; Chaladaj, W.; Jurczak, J. Synthesis of high molecular weight polystyrene using AGET ATRP under high pressure. *Eur. Polym. J.* **2011**, *47* (4), 730-734.
41. Huang, Z.; Chen, J.; Zhang, L.; Cheng, Z.; Zhu, X. ICAR ATRP of Acrylonitrile under Ambient and High Pressure. *Polymers* **2016**, *8* (3), 59.

42. Percec, V.; Guliashvili, T.; Ladislaw, J. S.; Wistrand, A.; Stjerndahl, A.; Sienkowska, M. J.; Monteiro, M. J.; Sahoo, S. Ultrafast Synthesis of Ultrahigh Molar Mass Polymers by Metal-Catalyzed Living Radical Polymerization of Acrylates, Methacrylates, and Vinyl Chloride Mediated by SET at 25 °C. *J. Am. Chem. Soc.* **2006**, *128* (43), 14156-14165.
43. Lligadas, G.; Percec, V. Ultrafast SET-LRP of methyl acrylate at 25 °C in alcohols. *J. Polym. Sci., Part A: Polym. Chem.* **2008**, *46* (8), 2745-2754.
44. Nguyen, N. H.; Leng, X.; Percec, V. Synthesis of ultrahigh molar mass poly(2-hydroxyethyl methacrylate) by single-electron transfer living radical polymerization. *Polym. Chem.* **2013**, *4* (9), 2760-2766.
45. Zakaria Djibrine, B.; Zheng, H.; Wang, M.; Liu, S.; Tang, X.; Khan, S.; Jimen; #x00E9; z, A. N.; Feng, L. An Effective Flocculation Method to the Kaolin Wastewater Treatment by a Cationic Polyacrylamide (CPAM): Preparation, Characterization, and Flocculation Performance. *International Journal of Polymer Science* **2018**, *2018*, 12.
46. Liimatainen, H.; Sirviö, J.; Sundman, O.; Hormi, O.; Niinimäki, J. Use of nanoparticulate and soluble anionic celluloses in coagulation-flocculation treatment of kaolin suspension. *Water Res.* **2012**, *46* (7), 2159-2166.
47. Grabsch, A. F.; Fawell, P. D.; Adkins, S. J.; Beveridge, A. The impact of achieving a higher aggregate density on polymer-bridging flocculation. *Int. J. Miner. Process.* **2013**, *124*, 83-94.
48. Heath, A. R.; Fawell, P. D.; Bahri, P. A.; Swift, J. D. Estimating Average Particle Size by Focused Beam Reflectance Measurement (FBRM). *Particle & Particle Systems Characterization* **2002**, *19* (2), 84-95.

49. Owen, A. T.; Fawell, P. D.; Swift, J. D.; Labbett, D. M.; Benn, F. A.; Farrow, J. B. Using turbulent pipe flow to study the factors affecting polymer-bridging flocculation of mineral systems. *Int. J. Miner. Process.* **2008**, *87* (3), 90-99.
50. Heath, A. R.; Bahri, P. A.; Fawell, P. D.; Farrow, J. B. Polymer flocculation of calcite: Experimental results from turbulent pipe flow. *AIChE J.* **2006**, *52* (4), 1284-1293.
51. Grundmann, R. Friction diagram of the helically coiled tube. *Chemical Engineering and Processing: Process Intensification* **1985**, *19* (2), 113-115.
52. Owen, A. T.; Fawell, P. D.; Swift, J. D.; Farrow, J. B. The impact of polyacrylamide flocculant solution age on flocculation performance. *Int. J. Miner. Process.* **2002**, *67* (1), 123-144.
53. Farrow, J. B.; Swift, J. D. A new procedure for assessing the performance of flocculants. *Int. J. Miner. Process.* **1996**, *46* (3), 263-275.
54. Nan, J.; He, W. Characteristic analysis on morphological evolution of suspended particles in water during dynamic flocculation process. *Desalin. Water. Treat.* **2012**, *41* (1-3), 35-44.
55. Henderson, J. M.; Wheatley, A. D. Factors Effecting a Loss of Flocculation Activity of Polyacrylamide Solutions: Shear Degradation, Cation Complexation, and Solution Aging. *J. Appl. Polym. Sci.* **1987**, *33* (2), 669-684.

TABLE OF CONTENTS



3.3. Supporting Information

## Supporting Information

# Enhanced Flocculation Efficiency in High Ionic Strength Environment by the aid of Anionic ABA Triblock Copolymers

*Vu H. Dao,<sup>a</sup> Krishna Mohanarangam,<sup>b</sup> Phillip D. Fawell,<sup>c</sup> Kosta Simic,<sup>b</sup> Neil R. Cameron,<sup>\*d,e</sup>  
and Kei Saito<sup>\*a</sup>*

<sup>a</sup> School of Chemistry, Monash University, Clayton, VIC 3800, Australia. E-mail:  
kei.saito@monash.edu, Tel: + 61 3 9905 4600

<sup>b</sup> CSIRO Mineral Resources, Clayton, VIC 3168, Australia

<sup>c</sup> CSIRO Mineral Resources, Waterford, WA 6152, Australia

<sup>d</sup> Department of Materials Science and Engineering, Monash University, Clayton, VIC 3800,  
Australia. E-mail: neil.cameron@monash.edu, Tel: +61 3 9902 0774

<sup>e</sup> School of Engineering, University of Warwick, Coventry, CV4 7AL, United Kingdom

**2 Pages, 1 Figure**

1. Continuous Flocculation in Turbulent Pipe Flow .....S2

### Continuous Flocculation in Turbulent Pipe Flow

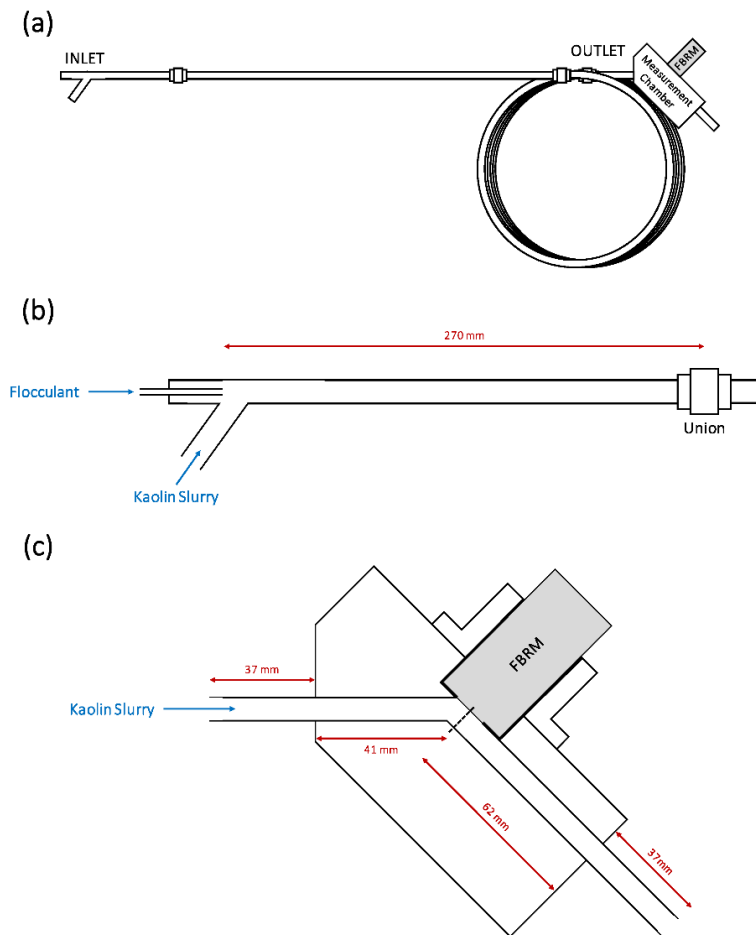


**Figure S1.** (a) Overall schematic of the pipe reactor employed for the FBRM experiments, (b) the inlet design of the pipe reactor showing the addition of the two feed flows (the kaolin slurry and the flocculant), and (c) schematic for the cross-section of the flowcell measurement chamber at the pipe reactor outlet. (b) and (c) were reprinted from ‘The impact of achieving a higher aggregate density on polymer-bridging flocculation’, Grabsch, A. F.; Fawell, P. D.; Adkins, S. J.; Beveridge, A., *Int. J. Miner. Process.* 2013, 124, 83-94, with permission from Elsevier.

This page is intentionally left blank.

# Chapter 4

Synthesis of UHMW Star-shaped AB Block Copolymers  
and their Flocculation Efficiency in High Ionic Strength Environments

This page is intentionally left blank.

# Chapter 4

## Synthesis of UHMW Star-shaped AB Block Copolymers and their Flocculation Efficiency in High Ionic Strength Environments

---

### 4.1. General Overview

Chapter 4 is a manuscript titled “*Synthesis of UHMW Star-shaped AB Block Copolymers and their Flocculation Efficiency in High Ionic Strength Environments*”, which was submitted to *Macromolecules* in 2019.

In this chapter, the synthesis, characterisation, and flocculation of a series of UHMW star-shaped AB block copolymers (**4A-BA1** – **4A-BA6**) were reported. Similarly to the ABA triblock copolymers, the anionic blocks derived from acrylic acid was localised to the terminals of the polymer chain, while the non-ionic block derived from acrylamide remained at the centre. Flocculation analysis was performed in high ionic strength kaolin slurries with three different  $\text{Ca}^{2+}$  concentrations of 0.05 M, 0.10 M, and 0.50 M. The flocculation efficiency of these star-shaped copolymers were evaluated solely by cylinder settling tests. Their settlement rate and supernatant turbidity data were directly compared to the same control polymers (homopolymer of acrylic acid, homopolymer of acrylamide, and random copolymer of acrylic acid and acrylamide) described in Chapter 3. The settlement rates obtained from the star-shaped copolymers were lower compared to those of the control polymers, while the supernatant turbidity values remained relatively low, particularly at high  $\text{Ca}^{2+}$  concentrations. Overall, these star-shaped copolymers showed promising potentials for flocculation applications in high ionic strength environment.

4.2. Research Paper '*Macromolecules*, 2019, submitted manuscript'

Synthesis of UHMW Star-shaped AB Block  
Copolymers and their Flocculation Efficiency in  
High Ionic Strength Environments

*Vu H. Dao,<sup>a</sup> Neil R. Cameron,<sup>\*b,c</sup> and Kei Saito<sup>\*a</sup>*

<sup>a</sup> School of Chemistry, Monash University, Clayton, VIC 3800, Australia. E-mail:

kei.saito@monash.edu, Tel: + 61 3 9905 4600

<sup>b</sup> Department of Materials Science and Engineering, Monash University, Clayton, VIC 3800,

Australia. E-mail: neil.cameron@monash.edu, Tel: +61 3 9902 0774

<sup>c</sup> School of Engineering, University of Warwick, Coventry, CV4 7AL, United Kingdom

Keywords: flocculation, settling, ionic strength, star-shaped, RAFT, acrylamide/acrylate

### **ABSTRACT**

The negative effect of multivalent cations such as  $\text{Ca}^{2+}$  and  $\text{Mg}^{2+}$  on the flocculation efficiency of anionic polymeric flocculants has proven to be a difficult challenge to overcome in recent years. We hereby introduce a new series of ultra-high molecular weight (UHMW) 4-arm star-shaped AB block copolymers, with terminal anionic blocks and a neutral core comprising of polyacrylic acid and polyacrylamide, respectively. These polymers were successfully synthesized using a two-stage aqueous RAFT polymerization process with the aid of a 4-arm star RAFT agent and a redox initiation pair of ammonium persulfate and sodium formaldehyde sulfoxylate. Once synthesized, these polymers were directly used for flocculation analysis where they were compared to a control statistical copolymer of similar molecular weight. The control copolymer was designed to be representative of current commercial flocculants where the anionic functionalities were distributed randomly along the polymer chain, where the negative effects of multivalent cations are heightened. In comparison to the control copolymer, 4-arm star-shaped AB block copolymers exhibited strong stability and flocculation efficiency across the three different  $\text{Ca}^{2+}$  concentrations (0.05 M, 0.10 M and 0.50 M) employed. Fast settlement rates and low supernatant turbidities were obtained when 4-arm star-shaped AB block copolymers were employed, whilst the flocculation efficiency of control copolymer was impacted significantly with the increase in the concentration of  $\text{Ca}^{2+}$ . With further optimization and analysis, these polymers have a strong potential to be implemented in industrial applications of flocculation in the near future.

### **1. INTRODUCTION**

Water-soluble polyelectrolytes play a major role in our everyday life. These polymers are utilized in a wide range of industrial applications, including but not limited to paper production,

composite materials manufacturing, oil recovery, cosmetics, food and nutrition, and wastewater treatment.<sup>1, 2, 3</sup> Polyelectrolytes are key active ingredients in flocculation, an efficient solid-liquid separation process that is often employed in the aforementioned industrial applications.<sup>3, 4</sup> In this process, ultra-high molecular weight (UHMW) water-soluble polymers are utilised to destabilize and remove stable colloidal suspensions from the solution via polymer adsorption, particle-particle bridging, and aggregation.<sup>1, 2, 3, 5</sup> The separation of these colloidal particles can be difficult due to their small size and similar surface charge.<sup>6, 7, 8</sup> Although many other processes are available to address this problem, flocculation is considered one of the most cost-effective and feasible for large scale operations.<sup>4</sup>

Flocculation is a complex process that is dependent on a variety of factors. These factors include various polymer characteristics (charge density, molecular weight, and dosage), shear rate, particle size, ionic strength and pH of the slurry. All of these have been extensively studied and reviewed in previous literature.<sup>9, 10, 11, 12</sup> The effect of the ionic strength on the flocculation efficiency of polymeric flocculants has proven to be a difficult challenge to overcome in recent years. Flocculation is conducted in a wide variety of slurries, ranging from mild conditions such as low salinity fresh water to harsh conditions such as mining-impacted water or high salinity sea water in desalination processes.<sup>3, 10, 13, 14, 15</sup>

The excess ions actively interact with the polymer as well as the solid suspension to adversely affect their flocculation efficiency throughout the flocculation process.<sup>4</sup> The ionizable functionalities distributed along the polyelectrolyte contribute to elongation of the polymeric chain as well as the adsorption onto the surface of the colloidal particles via salt linkage.<sup>6, 16</sup> Excess quantity of monovalent and multivalent ions present within the solution lead to shielding of these functionalities, and hence result in a condensed or coiling polymer conformation.<sup>16, 17, 18, 19</sup> This

directly impacts the viscosity, distribution, adsorption capability, and solubility of the polymer in some severe cases.<sup>16, 17, 19, 20, 21, 22, 23</sup> In addition, high levels of ions can also affect the surface properties of the solid substrate by compressing the electrical double layer (EDL) or by surface charge reversal, which further complicates the flocculation process.

The negative effects of high ionic strength environment on the flocculation efficiency of polyelectrolytes have been extensively analysed in previous studies.<sup>16, 17, 18, 24</sup> Many of these studies directed their focus towards the effect of cations on flocculants bearing anionic functionalities such as carboxylate or sulfonate. These effects were found to be amplified for multivalent cations such as  $\text{Ca}^{2+}$  and  $\text{Mg}^{2+}$  in comparison to monovalent cations such as  $\text{Na}^+$ .<sup>20</sup> Despite the recent advances in understanding the behaviour of these multivalent cations, little work has focused on creating a different type of polymer to address the problems associated with polymer solubility and adsorption capability in high ionic strength environments.

The majority of commercial polymeric flocculants are manufactured by free radical polymerization methodology.<sup>3, 6</sup> This technique is limited in regards to the architecture of the polymer, where ionizable functionalities are primarily distributed randomly along the polymer chain, and thus making the polymer more susceptible towards coiling effects in high ionic strength solution. Reversible deactivation radical polymerization (RDRP) techniques have gained tremendous interest from the polymer science community in recent years due to their ability to create polymers with precise molecular weight and narrow molecular weight distributions, as well as advanced and diverse architectures.<sup>25</sup> However, typical commercial flocculants possess ultra-high molecular weights of up to 20 MDa, where the synthetic capability of RDRP techniques becomes restricted.<sup>26, 27, 28</sup>

Only a few studies have recently employed RDRP techniques such as reversible addition-fragmentation chain transfer (RAFT) polymerization,<sup>26, 27, 28, 29, 30, 31, 32, 33</sup> atom transfer radical polymerization (ATRP),<sup>30, 34, 35, 36, 37, 38, 39</sup> and single-electron transfer living radical polymerization (SET-LRP)<sup>40, 41, 42</sup> to synthesize UHMW polymers. Most of these studies have directed their focus towards the development of well-defined homopolymers or AB diblock copolymers, with a few recent advances in developing ABA triblock copolymers.<sup>26, 29</sup> Despax *et al.* synthesized ABA triblock copolymers comprised of dimethylacrylamide and *N*-isopropylacrylamide with molecular weights up to 500 kDa.<sup>29</sup> Recently, we reported the synthesis of a series of linear UHMW ABA triblock copolymers from acrylic acid (AA) and acrylamide (AM) with molecular weights up to 1 MDa.<sup>26</sup>

In this work, we have employed RAFT polymerization to synthesize a series of UHMW 4-arm star-shaped block copolymers of AA and AM. The high solubility non-ionic block of polyacrylamide (**PAM**) is centralized at the core, while the anionic polyacrylic acid (**PAA**) blocks are localized to the terminal ends. This star-shaped architecture is hypothesized to be better than those of conventional flocculants due to the presence of multiple arms, and hence—potentially higher probability for polymer-particle adsorption and bridging. Ionic activities are localized to the terminal ends, and can minimize disruption towards the flocculation efficiency even if the anionic functionalities were complexed (Figure 1). These polymers were directly employed for flocculation analysis in three different salt solution concentrations (0.05 M, 0.10 M, and 0.50 M). The flocculation efficiency was compared against control homopolymers and a statistical copolymer of AA and AM. This would allow for an adequate comparison with control polymers possessing architecture that is similar to those currently employed in current commercial applications of flocculation.

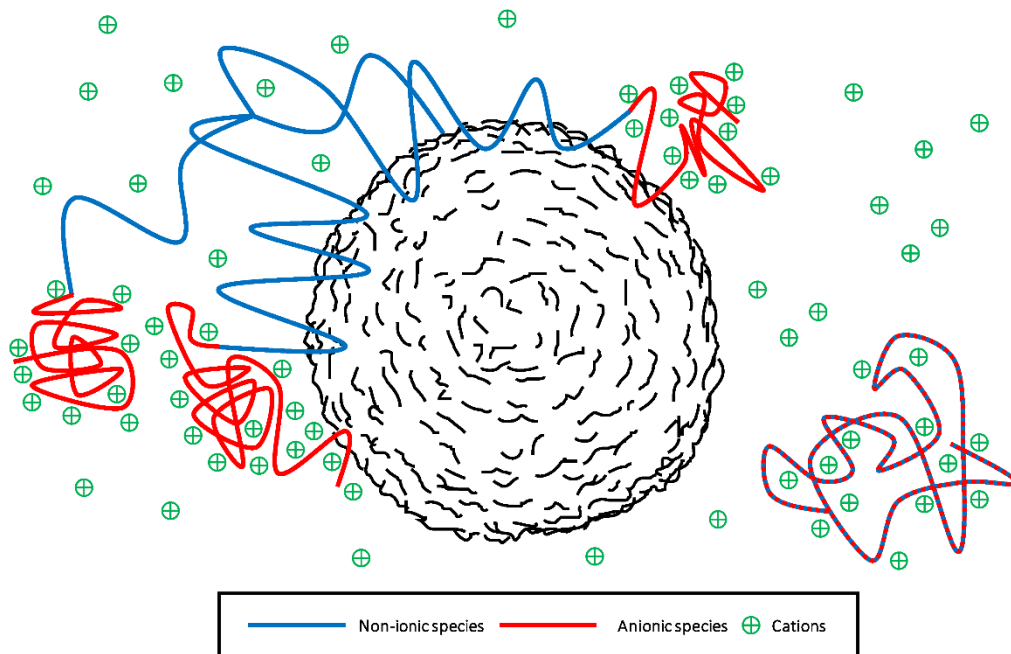


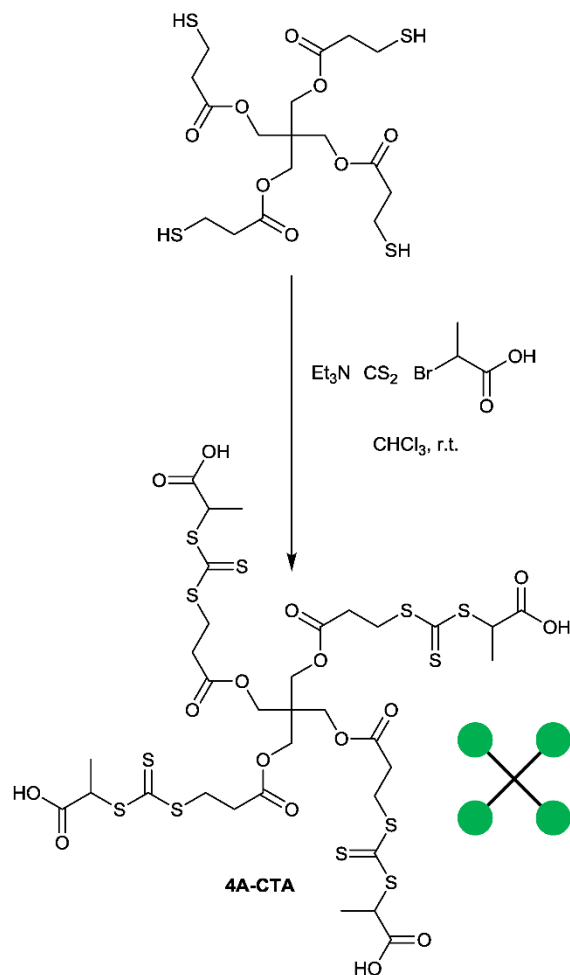
**Figure 1.** Illustration showing the flocculation effectiveness of star-shaped block copolymers in comparison to a conventional flocculant that would be compromised in high ionic strength environment.

## 2. MATERIALS AND METHODS

**2.1. Materials.** The following reagents and solvents were employed in this study: acrylamide (Sigma, 99%), acrylic acid (Aldrich; 99%), pentaerythritol tetrakis(3-mercaptopropionate) (Aldrich, 95%), 2-bromopropionic acid (Aldrich, 99%), triethylamine (Sigma-Aldrich, 99%), carbon disulfide (Sigma-Aldrich, 99%), ammonium persulfate (Sigma-Aldrich, 98%), sodium formaldehyde sulfoxylate dihydrate (Sigma-Aldrich, 98%), sodium nitrate (Merck, 99.9%), sodium bicarbonate (Merck, 99.9%), Prestige NY kaoline clay (donated by Sibelco Australia; 46.7 wt% SiO<sub>2</sub>, 36.1 wt% Al<sub>2</sub>O<sub>3</sub>, 0.8 wt% TiO<sub>2</sub>, 0.9 wt% Fe<sub>2</sub>O<sub>3</sub>, 0.7 wt% CaO, 0.4 wt% MgO, 0.4 wt% K<sub>2</sub>O, and 0.1 wt% Na<sub>2</sub>O), calcium chloride dihydrate (Merck, 99%), hydrochloric acid (Ajax FineChem, 32%), chloroform (Ajax FineChem, 99.8%), *N,N*-dimethylformamide (Ajax

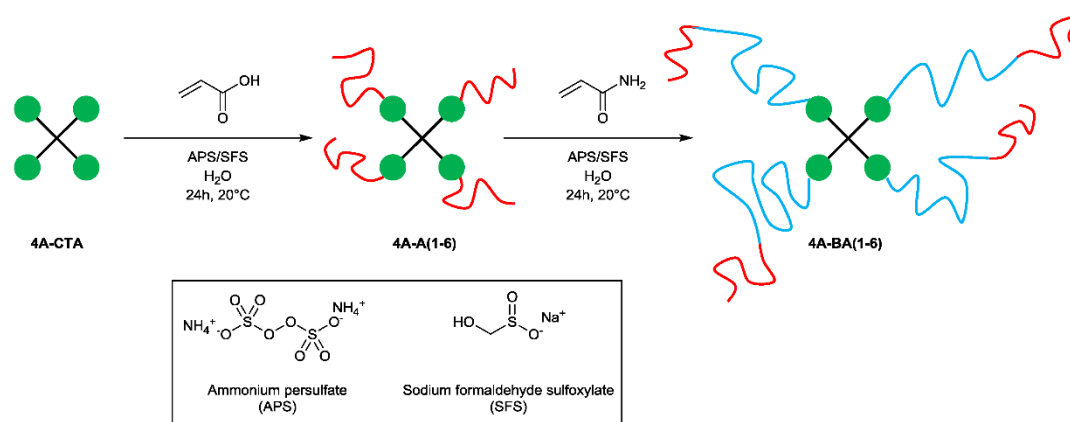
FineChem, 99.9%), and water (RO and Milli-Q grades). All reagents and solvents were used directly as received, except for acrylic acid which was pre-treated with basic activated aluminium oxide (Acros Organics) to remove the radical inhibitor monomethyl ether hydroquinone.

**2.2. Synthesis of 4-arm star RAFT agent 4A-CTA.** The synthetic procedure for the 4-arm star RAFT agent **4A-CTA** (Scheme 1) was performed based on previous protocols reported elsewhere.<sup>43, 44</sup> In a round bottom flask, pentaerythritol tetrakis(3-mercaptopropionate) (2.44 g, 5 mmol) and carbon disulfide (3.04 g, 40 mmol) was mixed in chloroform (15 mL). Triethylamine (4.04 g, 40 mmol) in chloroform (10 mL) was subsequently added dropwise into the magnetically-stirred reaction mixture under ambient conditions. The reaction mixture slowly turned into a yellow solution throughout the addition and the mixture was left stirring for 1 hour. After this, a solution of 2-bromopropionic acid (3.82 g, 25 mmol) dissolved in chloroform (10 mL) was added dropwise into the reaction mixture. After 2 hours, the reaction mixture was poured into an ice-cold solution of 10% HCl, followed by triple extractions with ethyl acetate to obtain a viscous yellow oil. Column chromatography on silica gel with a gradient solvent system going from hexane:ethyl acetate (3:1 v/v) to pure ethyl acetate was employed to obtain the desired compound (4.16 g, 77%).  
<sup>1</sup>H NMR (CDCl<sub>3</sub>) – δ (ppm): 1.62 (12H, -CHCH<sub>3</sub>), 2.80 (8H, -COOCH<sub>2</sub>CH<sub>2</sub>-), 3.61 (8H, -CH<sub>2</sub>CH<sub>2</sub>SC=S-), 4.15 (8H, -COOCH<sub>2</sub>-), 4.80 (4H, -CHCH<sub>3</sub>).



**Scheme 1.** Synthesis pathway of 4-arm star RAFT agent **4A-CTA**.

**2.3. General procedure for the synthesis of 4-arm star-shaped AB block copolymers.** The overall synthetic pathway for the six different 4-arm star-shaped AB block copolymers (**4A-BA1** – **4A-BA6**) is outlined in Scheme 2. These polymers were created through a two-step polymerization procedure, which involved the initial RAFT polymerization of AA, subsequently followed by chain extension with AM.



**Scheme 2.** Overall reaction strategy for the synthesis of the UHMW star-shaped AB block copolymers by a two-step aqueous RAFT polymerization of AA and AM, respectively.

In a typical reaction, the appropriate volume of an 8 M aqueous solution of the monomer (AA or AM) and the RAFT agent **4A-CTA** were initially added into the reaction flask (refer to Tables S1 and S2 in the SI). This mixture was then further diluted topped up with Milli-Q water, and DMF (0.3 mL) was added as the internal standard for subsequent calculation of monomer conversions. In separate flasks, stock solutions APS and SFS were prepared in Milli-Q water. The reaction mixture and both of the APS/SFS stock solutions were deoxygenated by argon bubbling for 30 minutes. Prior to the addition of the initiators, the temperature of the reaction flask was adjusted to 20°C using a thermostated water bath. The appropriate amounts of APS and SFS were respectively injected into the reaction flask with an additional 5 minutes of argon bubbling following each injection (refer to Tables S1 and S2 in the SI). The reaction was then left running at 20°C under an inert argon atmosphere for 24 hours. At the end of each synthetic stage, the resultant polymer was purified to remove undesirable monomers and impurities prior to being used in the next stage.

The purification process was achieved via dialysis performed using a SnakeSkin™ dialysis tubing (Thermo Fisher Scientific) with a molecular weight cut-off at 3,500. Once purified, the polymer was freeze dried in a Labconco FreeZone Bench Top Freeze Dry system. The isolation yields of the star-shaped block copolymers and their precursor are shown in Table 1.

**Table 1. Isolation yields of the star-shaped block copolymers and their precursors.**

Entry	<i>4A-A Polymers</i>		4A-BA Copolymers	
	(g)	(%)	(g)	(%)
1	1.2	36	0.8	24
2	1.3	40	0.6	19
3	1.4	42	0.7	21
4	1.7	51	0.8	25
5	1.5	46	0.7	22
6	1.7	53	0.6	19

**2.4. General procedure for the synthesis of the control polymers.** A homopolymer of AA (**PAA**), a homopolymer of AM (**PAM**), and a random copolymer of AA and AM (**RAB**) were employed as the control polymeric flocculant in this study. In a typical polymerization reaction, the monomer(s) was initially dissolved in Milli-Q water inside a reaction flask. Stock solutions of APS and SFS were also prepared accordingly, and all three solutions were deoxygenated by argon bubbling for 30 minutes prior to the introduction of the initiators into the system. After each addition of APS and SFS into the reaction flask, an additional 5 minutes of argon bubbling was applied. The reaction was left running at 20°C for 24 hours under an inert argon atmosphere once

SFS was added. At this stage, the resultant viscous gel was directly freeze dried and ground into fine particles prior to use for characterizations and flocculation analysis.

**2.5. Preparation of the aqueous polymers for flocculation tests.** The polymers were initially prepared as 0.25 wt% stock solutions in deionized water. This was done by wetting the solid polymer (0.25 g) with acetone (3 mL) and then water (97 mL) in a 100 mL glass bottle. To aid with the distribution of the solid particles, the polymer solution was shaken vigorously by hand for approximately 30 seconds, followed by continuous mixing at 70 RPM using a benchtop tube roller mixer for 2 hours. A 0.025 wt% working solution was then prepared by dilution of this concentrated stock solution once it became clear and homogeneous. The diluted working solution was mixed on the benchtop tube roller at 70 RPM for an additional 15 minutes immediately after dilution and was directly used for flocculation analysis. The dosage of the polymeric flocculants is expressed as grams of polymers per tonne of dry kaolin solids (g/tds). Note that the concentrated stock solution was kept under refrigeration and was reused within a week, whilst the diluted working solution as prepared fresh daily prior to immediate flocculation testings.

**2.6. Make-up of high ionic strength kaolin clay slurry.** The kaolin slurry was prepared for immediate use at 3 wt% by mixing the desired quantity of kaolin clay into deionised water in a 20 L pail. This was followed by the addition of the desired quantity of calcium chloride into the mixture to create a high ionic strength environment with 0.05 M, 0.10 M, or 0.50 M  $\text{Ca}^{2+}$ . Three hours of vigorous mixing at 500 RPM was applied to the mixture with the aid of an overhead mechanical stirrer equipped with an impeller blade. Prior to flocculation tests, the stirring rate was reduced to 250 RPM. The flocculation analysis was conducted at the natural pH of the kaolin slurry, which ranged between the pH of 7 to 8.

**2.7. Cylinder settling tests.** Flocculation testings were conducted in a 1,000 mL graduate cylinder (Azlon CT1000P, diameter 6.6 cm, height 44 cm). The temperature of the working flocculant solution and the kaolin slurry were left unadjusted at room temperature throughout the analysis. A stainless steel plunger (5 cm diameter with five evenly distributed radial holes of 1 cm diameter) was employed as a mixing tool to distribute the flocculant solution throughout the slurry.

In a typical cylinder settling test, the high ionic strength slurry was initially transferred into the cylinder. Once added, the plunger was used to aggressively mix the solution for roughly 5 seconds. The desired quantity of polymeric flocculant was added via a syringe, and this was immediately followed by five strokes of plunging motion. Each stroke consisted of downward and an upward motion. A metronome was employed to maintain a constant mixing rate, where each upward or downward motion was performed at a metronome rate of 45 BPM. Two main factors were considered in the flocculation tests: settlement rate and supernatant turbidity. The settlement time of the aggregate flocs was measured from the 900 mL mark to the 700 mL mark on the cylinder (settling distance of 7 cm). The supernatant turbidity was measured 20 minutes after the final plunger stroke, where 10 mL of the supernatant at the 800 mL mark was taken out as the test sample. Turbidity measurements were performed on a Hanna Instruments HI98703-01 Portable Turbidity Meter.

**2.8. Nuclear magnetic resonance (NMR) spectroscopy.**  $^1\text{H}$  NMR spectroscopy was performed on a 400 MHz Bruker DRX 400 spectrometer in deuterated chloroform ( $\text{CDCl}_3$ ) and deuterium oxide ( $\text{D}_2\text{O}$ ).

**2.9. Size exclusion chromatography (SEC).** A Tosoh High Performance EcoSEC HLC-8320 GPC System consisting of a TSKgel SuperH-RC reference column, a TSKgel PW<sub>XL</sub> guard column, three analytical columns of TSKgel G5000PW<sub>XL</sub>, TSKgel G6000PW<sub>XL</sub>, and TSKgel GMPW<sub>XL</sub>

connected in series, a vacuum degasser, a dual flow pumping system, an autosampler, a Bryce-type refractive index (RI) detector, and a UV detector which was fixed at 305 nm, was employed to analyse the molecular weight and molecular weight distributions of the polymeric flocculants. In addition, a series of PAA standards was employed to calibrate the columns. The molecular weights of these PAA ranged from 1 kDa to 1 MDa. SEC measurements were conducted using 0.1 M NaNO<sub>3</sub> and 0.1 M NaHCO<sub>3</sub> (pH ≈ 8.3) in deionized water heated up to 40°C with as the eluent with a flowrate of 1 mL/min.

**2.10. UV-Vis spectroscopy.** UV-Vis measurements were conducted on a Shimadzu UV-1800 UV Spectrophotometer.

**2.11. Dynamic light scattering (DLS).** Particle size distribution was determined by dynamic light scattering (DLS). DLS measurements was performed using a Malvern Zetasizer Nano ZS by diluting the polymers in deionized water (0.25 wt%) at room temperature. A total of five measurements were conducted and statistics were gathered over 10 minutes per sample.

**2.12. Calculation of monomer conversions.** The monomer conversion (p) was calculated from sing Eqn. 1 based on the <sup>1</sup>H NMR data:

$$\text{Conversion (p)} = \frac{[M]_0 - [M]_t}{[M]_0} = \frac{\int M_0 - \int M_t}{\int M_0} \quad (1)$$

[M]<sub>0</sub> is the initial concentration of the monomer and [M]<sub>t</sub> is the monomer concentration at time t.  $\int M_0$  and  $\int M_t$  are the corresponding corrected integrals at time 0 and time t, respectively. These integrals were corrected based on the internal standard DMF.

**2.13. Determination of theoretical molecular weights ( $M_{n,th}$ ).** The theoretical number-average molecular weight ( $M_{n,th}$ ) of the polymers were calculated using Eqn. 2:

$$M_{n,th} = \frac{[M]_0}{[CTA]_0} \times p \times M_M + M_{CTA} \quad (2)$$

$[M]_0$  and  $[CTA]_0$  are the initial concentrations of the monomer and the chain transfer agent (CTA), respectively. Their corresponding molecular weights are labelled as  $M_M$  and  $M_{CTA}$ , respectively.  $p$  is the monomer conversion as calculated in Eqn. 1.

### 3. RESULTS AND DISCUSSION

**3.1. Reaction conditions for the synthesis of the 4-arm star-shaped AB block (4A-BA) copolymers.** A tetrafunctional trithiocarbonate RAFT agent (**4A-CTA**) was employed as the chain transfer agent for the synthesis of the 4A-BA copolymers. The synthetic procedure for this RAFT agent was adapted from previously published procedures by Mayadunne *et al.* and Boschmann and Vana.<sup>43, 44</sup> Mayadunne *et al.* synthesized a 4-arm star CTA with a benzyl leaving group, whilst Boschmann and Vana introduced a 6-arm star CTA with a methyl acrylate leaving group. Based on these previous studies, **4A-CTA** was designed to be a 4-arm star CTA carrying an acrylic acid leaving group (Scheme 1). The linear monofunctional derivative of **4A-CTA** was previously employed by our group to synthesize the UHMW ABA triblock copolymers due to its water-solubility and compatibility with AA and AM.<sup>26, 45, 46, 47, 48, 49, 50, 51, 52, 53, 54</sup> Consequently, the 4-arm form of this CTA was employed in this study for the same reasons to create UHMW star-shaped block copolymers.

The selection of **4A-CTA** as the RAFT agent meant that the polymerisation is conducted based on the Z-group approach. This approach can be difficult to control due to steric hindrance at the core of the star-shaped molecule, and thus lowering the propagating efficiency. However, this approach was deemed to be more adequate, due to several drawbacks associated with the R-group approach. These drawbacks include star-star coupling, loss of RAFT functionality, and heightened formation of linear chains in the reaction solution, in comparison to the Z-group approach. Another

main driving factors behind the selection of **4A-CTA** was the difficulty associated with synthesizing a suitable water-soluble 4-arm star CTA with the desired R group remaining at the core. As mentioned previously, the linear derivative of **4A-CTA** was employed by our group and showed success in creating UHMW copolymers with high suitability towards AA and AM monomers. It was more efficient synthetically to create the desired 4-arm star RAFT agent with terminal R groups. Therefore, the use of **4A-CTA** and the Z-group approach were deemed to be suitable for this study.

Once synthesized, **4A-CTA** was initially employed as the CTA alongside the redox initiation system APS/SFS for the aqueous RAFT-mediated polymerization of AA. The polymers created from this first stage were subsequently utilized as the macro chain transfer agent (macro-CTA) for the second stage, where the polymer chain was extended with AM to create the desired 4A-BA polymers (Scheme 2). This synthetic procedure allowed for the anionic A blocks to be localized at the terminals, while the non-ionic B block remained at the core of the macromolecule. This was hypothesized to have relatively large hydrodynamic volume in solution due to repulsion of the anionic blocks against one another, and thus extending the polymer chain, which is beneficial towards flocculation applications. If the reverse geometry was employed where the anionic groups remained at the core, this would have minimal effect on the overall hydrodynamic volume, as the terminal non-ionic B blocks would form a condensed structure around the core, like typical conformation of polyacrylamide in solution.<sup>16, 17, 18, 19</sup>

These polymerization reactions are dependent on a wide range of factors, including the initial concentration of the monomer, the type of RAFT agent, the initiation system, the ratio between the CTA and the initiators, reaction time, as well as the temperature and pressure of the reaction.<sup>46, 47, 48, 49</sup> The reaction conditions in this study were chosen based on the previous screening and

polymerization experiments conducted by our group for the synthesis of the UHMW ABA triblock copolymers.<sup>26</sup> The monomer concentration was fixed at a high concentration of 33 wt% to allow for fast reaction kinetics and optimized initiation for the gel polymerization process.<sup>27, 55, 56</sup> The reaction temperature was maintained at 20°C, whilst the ratio between the CTA and the redox initiation pair was kept constant at 6:1:1. Previous results demonstrated that this reaction temperature and the [CTA]:[APS]:[SFS] ratio provided optimal results, where polymers with higher molecular weight and lower dispersity were created.<sup>26</sup> Consequently, the polymerizations were performed stepwise based on the aforementioned conditions to synthesize the desired UHMW 4A-BA copolymers.

**3.2. Initial RAFT polymerization of AA to form star-shaped AA (4A-A) polymers.** The polymerizations of AA were conducted with six different target overall molecular weights ranging from 40 to 240 kDa, with an increment of 40 kDa. These polymers were abbreviated as **4A-A1** to **4A-A6**, where 4A represents 4-arm and A represents the anionic block derived from AA. The differences in the molecular weight of **4A-A1** – **4A-A6** would allow for a comprehensive flocculation analysis of the UHMW 4A-BA copolymers where negative effect of the multivalent Ca<sup>2+</sup> cation on varying levels of anionic functionality can be evaluated. The <sup>1</sup>H NMR and SEC data for this first round of polymerizations are shown in Table 2. The overall monomer conversion ranged from 55 – 71%, where an increasing trend was observed with respect to higher targeted molecular weight.

Kinetics retardation is typically observed in RAFT polymerisations where there is a higher initial concentration CTA, which is required for reactions with lower targeted molecular weight. In the pre-equilibrium period, propagating macroradicals of oligomeric nature attaches onto the thiocarbonylthio moiety to form carbon centered RAFT macroradicals. The high initial

concentration of RAFT agent significantly slows down this pre-equilibrium process, in order to create more oligomeric species.<sup>57</sup> In addition, the termination rate coefficient for smaller radicals is higher compared to that of larger macroradicals.<sup>58, 59</sup> Consequently, higher concentrations of RAFT agent decreases the polymerisation rate in this initial phase, and hence a lower monomer conversion. This effect is common throughout RAFT polymerisation reactions, and is in agreement with the results obtained by this study.

**Table 2. <sup>1</sup>H NMR and SEC data obtained from the initial polymerization of AA.**

Polymer	DP <sub>target</sub> <sup>a</sup>	M <sub>n,target</sub> <sup>a</sup> (kDa)	Monomer conversion <sup>b</sup> (%)	M <sub>n,th</sub> <sup>c</sup> (kDa)	M <sub>n,SEC</sub> <sup>d</sup> (kDa)	Đ <sup>d</sup>
<b>4A-A1</b>	555	41.1	55	23.1	14.7	1.79
<b>4A-A2</b>	1,110	81.1	63	51.5	31.7	1.77
<b>4A-A3</b>	1,670	121	68	82.2	47.9	1.70
<b>4A-A4</b>	2,220	161	70	113	61.5	1.80
<b>4A-A5</b>	2,780	201	68	137	74.8	1.82
<b>4A-A6</b>	3,330	241	71	173	77.5	1.84

<sup>a</sup> The polymerizations were performed with an initial monomer concentration of approximately 4.63 mol L<sup>-1</sup> and a CTA to APS/SFS redox initiators ratio of 6:1:1 at 20°C for 24 hours (refer to Table S1 in the SI). <sup>b</sup> The monomer conversion was calculated based on the <sup>1</sup>H NMR integration of the vinyl proton on the monomer measured at 0 h and 24 h, using DMF as an internal standard (refer to the Experimental Section). <sup>c</sup> The theoretical molecular weight was calculated based on Equation 2 outlined in the Experimental Section. <sup>d</sup> Experimental molecular weight data was determined by aqueous SEC calibrated with PAA standards (refer to the Experimental Section).

Based on these monomer conversion results, the theoretical molecular weights of polymers **4A-A1** – **4A-A6** were calculated to range from approximate 23.1 to 173 kDa. However, the number average molecular weights obtained by SEC ( $M_{n,SEC}$ ) was much lower than the theoretical values. These molecular weights ranged from 14.7 to 77.5 kDa, which were approximately 45 – 60% of

what were theoretically expected. In addition, the dispersity values ( $\mathcal{D}$ ) of these polymers were relatively high for RAFT polymers which potentially indicates uncontrolled reactions. Another reason for this discrepancy in the molecular weight could be compression of the conformation of star-shaped polymers in solution with respect to their linear counterparts.<sup>44</sup> The SEC data obtained for the star-shaped polymers of AA were analysed against a series of linear PAA standards. Consequently, the differences between the experimental SEC results and theoretical molecular weight indicated the successful synthesis of the star-shaped polymers.

A closer examination of the SEC overlays of polymer **4A-A1** – **4A-A6** showed the presence of bimodal distributions, which explained the high dispersity values. This bimodality was less prominent for **4A-A1**, and became more apparent as the molecular weight increased up until **4A-A6**. At this point, both peaks in the molecular weight distribution had similar intensities. The star-shaped copolymers described in this study were synthesized through the Z-group core-first approach. In comparison to the R-group approach, RAFT polymers synthesized by the Z-group approach are less prone to intermolecular star-star coupling as the active thiocarbonylthio moieties remained at the core.<sup>60, 61</sup>

Boschmann and Vana observed similar results when a 6-arm star CTA was employed, which also showed deviation away from the ideal molecular weight distribution.<sup>44</sup> Their study concluded that although star-star coupling by termination is more probable for the R-group approach, star-star coupling by other mechanisms could still be possible for the Z-group approach. The assumption of one active core per polymer molecule for the higher molecular weight peak was unlikely as its UV absorption intensity was stronger compared to its lower molecular weight counterpart.<sup>44</sup> The thiocarbonylthio functionality in RAFT polymers is strongly UV-absorbing between approximately 300-310 nm and thus is easily distinguishable by UV-detection.<sup>62</sup> On the

basis of these findings, Boschmann and Vana suggested a sequence of reactions for the star-star coupling between Z-RAFT polymers. This mechanism entailed the initial intermolecular radical transfer from a growing macroradical to a living star polymer, where this radical potentially allowed for the midchain propagation with the available monomer present in the reaction.<sup>44</sup> Consequently, the propagating radical on the living star polymer now had a higher probability to couple with another living star polymer, which explained the high molecular weight material observed by UV-detection.

Relating this back to the synthesis of **4A-A1** – **4A-A6**, the data obtained by UV detection at a wavelength of 305 nm indicated strong correlation with these previous findings. The molecular weight distributions of **4A-A1** – **4A-A6** obtained by UV-detection also revealed bimodality similarly to those acquired by RI-detection (refer to Figure S1 in the SI). Similar to previous findings, the UV intensity of the higher molecular weight species was stronger compared to the lower molecular weight species. These data evidently indicated that both the high and low molecular materials remained living; where the lower molecular weight peak represented the one core star-shaped polymer, whilst the higher molecular weight peak plausibly represented the star-star coupled product suggested by Boschmann and Vana.<sup>44</sup> Although the architecture of the intended star-shaped RAFT polymers was partially compromised, the star-star coupled material could be beneficial to the flocculation process due to its more complex architecture.

It should also be noted that the SEC data obtained in this study could only be employed as a guide for observing the differences, trends and growths in the molecular weight and its distribution between the polymers. Due to the complex overall structure of these star-shaped polymers, an accurate magnitude of the molecular weight cannot be determined by SEC, particularly due to the lack of star-shaped calibration standards current available for this technique. Therefore, the actual

molecular weights of **4A-A1 – 4A-A6** were estimated to be similar to the theoretically calculated values listed in Table 2, where these polymers were subsequently employed as the macro-CTA for the next chain extension stage with AM.

**3.3. Synthesis of the 4-arm star-shaped AB block (4A-BA) copolymers.** The second step of the polymerization procedure involved the chain extension of the anionic star-shaped polymers **4A-A1 – 4A-A6** with non-ionic AM monomer. The reaction conditions required for this process were designated to be similar to the first set of polymerization reactions, where the monomer concentration, [CTA]:[APS]:[SFS] ratio, and temperature were maintained constant at 33 wt%, 6:1:1, and 20°C, respectively. These polymers were abbreviated as **4A-BA1** to **4A-BA6**, where 4A represents 4-arm, and A and B represent the terminal anionic block and core non-ionic block, respectively. The overall final molecular weights of these 4A-BA copolymers (**4A-BA1 – 4A-BA6**) were targeted to be approximately 1,500 kDa, where the reaction parameters were determined based on the theoretical molecular weights of **4A-A1 – 4A-A6**.

Prior to the selection of this targeted molecular weight, a series of trial and error experiments with three different targeted molecular weights (3,000 kDa, 2,000 kDa, and 1,500 kDa) were conducted to determine the right conditions to achieve a final molecular weight of approximately 1,000 kDa for the 4A-BA copolymers. Different monomer conversions were obtained for each of these three sets of polymerizations, and consequently a target molecular weight of 1,500 kDa led to the synthesis of the six 4A-BA copolymers (**4A-BA1 – 4A-BA6**) with final theoretical molecular weight of approximately 1,000 kDa. The <sup>1</sup>H NMR and SEC data for this set polymerizations are shown in Table 3. The theoretical molecular weights of these 4A-BA copolymers were targeted match up with the control polymers (**PAA**, homopolymer of AA; **PAM**, homopolymer of AM; and **RAB**, random copolymer of AA and AM), to allow for an adequate

comparison in the subsequent flocculation test, where the primary focus was solely directed towards the architecture of the polymers.

**Table 3. <sup>1</sup>H NMR and SEC data obtained from the chain extension with AM.**

Entry	Macro-CTA	$M_{n,th}$ of Macro-CTA (kDa)	$DP_{target}^a$	Monomer conversion <sup>b</sup> (%)	$M_{n,th}^c$ (kDa)	$M_{n,SEC}^d$ (kDa)	$\mathcal{D}^d$
<b>4A-BA1</b>	<b>4A-A1</b>	23.1	21,100	70	1,060	259	3.76
<b>4A-BA2</b>	<b>4A-A2</b>	51.5	21,100	65	1,000	235	3.67
<b>4A-BA3</b>	<b>4A-A3</b>	82.2	21,100	79	1,210	266	3.69
<b>4A-BA4</b>	<b>4A-A4</b>	113	21,100	85	1,300	291	3.29
<b>4A-BA5</b>	<b>4A-A5</b>	137	21,100	88	1,330	262	3.66
<b>4A-BA6</b>	<b>4A-A6</b>	173	21,100	86	1,310	269	3.41

<sup>a</sup> The polymerizations were performed with an initial monomer concentration of approximately 4.69 mol L<sup>-1</sup> and a CTA to APS/SFS redox initiators ratio of 6:1:1 at 20°C for 24 hours (refer to Table S2 in the SI). <sup>b</sup> The monomer conversion was calculated based on the <sup>1</sup>H NMR integration of the vinyl proton on the monomer measured at 0 h and 24 h, using DMF as an internal standard (refer to the Experimental Section). <sup>c</sup> The theoretical molecular weight was calculated based on Equation 2 outlined in the Experimental Section. <sup>d</sup> Experimental molecular weight data was determined by aqueous SEC calibrated with PAA standards (refer to the Experimental Section).

High monomer conversions were obtained for the synthesis of the 4A-BA copolymers. These conversion values ranged from 70-88%, where relatively higher conversions were obtained for the synthesis of **4A-BA4** to **4A-BA6**. These results were unexpected as the previous UHMW block copolymer study indicated that macro-CTA with higher molecular weight were less capable of reaching a high monomer conversion.<sup>26</sup> High molecular weight PAA is more influenced by conformational changes based on the pH, and thus more susceptible to kinetics retardation associated with steric hindrance of the active thiocarbonylthio moieties.<sup>63</sup> This effect would be quite prominent for star-shaped polymers where a condensed globular structure is typical.<sup>44</sup>

However, higher conversion was obtained when higher molecular weight PAA was used. The reason behind this phenomenon is unknown as little work has been done in the field of UHMW star-shaped block copolymers. It was suspected that the electrostatic repulsion forces between the anionic carboxyl groups on the four arms had a role to play in the reaction, where the cumulative repulsion forces on each arm potentially left the active core exposed to radical species. On the contrary to this hypothesis where steric hindrance at the core was a crucial factor, slow reactions kinetic would result in an increase in random termination of radical species. This consequently would result in a high monomer conversion. A closer examination of the SEC data obtained by UV-detection at 305 nm indicated that the final product contained a mixture of the living star-shaped polymer and non-living or dead polymeric species (refer to Figure S2 in the SI). Due to the high molecular weight of the 4A-BA copolymers, the intensity of the UV-detected SEC traces was relatively weak. However, in direct comparison with the RI SEC traces, the presence of a small portion of dead polymeric species was definitively evident. Consequently, both of the aforementioned reasons were believed to contribute to the high monomer conversions obtained.

Further evaluation of the RI-detected SEC traces between the 4A-BA copolymers (**4A-BA1** – **4A-BA6**) and their respective anionic macro-CTA (**4A-A1** – **4A-A6**) showed distinctive growth in the overall molecular weight (Figure 1). The molecular weight distributions of all six macro-CTA **4A-A1** – **4A-A6** changed from a sharp bimodal to a broad multimodal distribution after the chain extension stage. As mentioned previously, SEC traces observed by UV-detection indicated the successful synthesis of the desired living 4A-BA copolymers. However, the product also partially contained other polymeric species. For example, the presence of a low molecular weight shoulder was observed in the SEC traces for all **4A-BA1** – **4A-BA6**. These shoulders were directly aligned with the SEC traces for **4A-A1** – **4A-A6**, which consequently corresponded to non-living

polymeric species produced from the first polymerization step of AA. In addition, the slight multimodal characteristics of the SEC traces indicated the presence of higher molecular weight polymeric species, as well as complex star-star coupled products produced through the mechanisms previously described by Boschmann and Vana.<sup>44</sup> Although the architecture of these undesired species deviated from what was targeted, the SEC traces measured by UV-detection indicated that a large fraction of the final polymeric product was associated with the desired 4A-BA copolymers. Therefore, **4A-BA1 – 4A-BA6** were deemed to be sufficient for subsequent flocculation analysis stage.

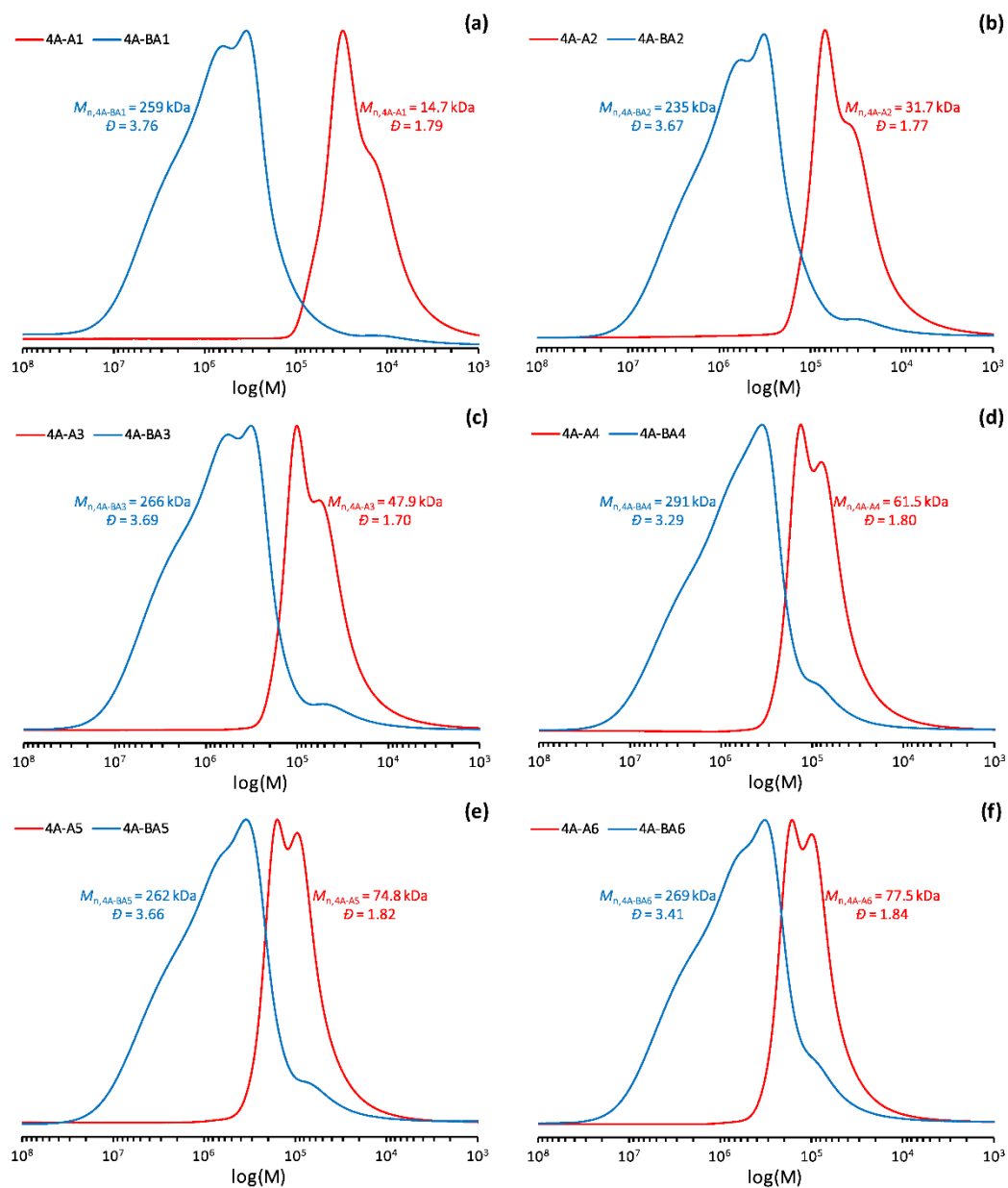


**Figure 1.** Overlay of SEC chromatograms for the macro-CTAs **4A-A1** – **4A-A6** and their respective star-shaped block copolymers **4A-BA1** – **4A-BA6**.

Apart from the data obtained by  $^1\text{H}$  NMR spectroscopy and SEC, the successful synthesis of the 4A-BA copolymers was further confirmed by UV-Vis spectroscopy and dynamic light scattering (DLS) analysis. The overlays of the UV-Vis spectra for the macro-CTAs **4A-A1** – **4A-A6**, as well as the final star-shaped block copolymers **4A-BA1** – **4A-BA6** are shown in Figure 2. Distinctive changes in the UV absorbance of the thiocarbonylthio functionality in macro-CTAs **4A-A1** – **4A-A6** were observed. In contrast to these data, the UV absorbance for **4A-BA1** – **4A-BA6** were found to be approximately the same. At the same mass concentration, higher molecular weight corresponded to a lower molar concentration of the thiocarbonylthio functionality and hence a lower UV absorbance. This explained the high UV absorbance for **4A-A1** and vice versa for the higher molecular weight polymers **4A-A2** – **4A-A6**, respectively. However, **4A-BA1** – **4A-BA6** were targeted to have similar molecular weights, and thus their corresponding UV absorbances were comparable.

In addition to these UV-Vis data, DLS results showed an overall increase in the effective diameter of the star-shaped copolymers in solution, ranging from 267 nm to 443 nm and 745 nm for **4A-A1**, **4A-A4**, and **4A-A6**, respectively. From this it is evident that the 4A-BA polymers form self-assemblies which are detectable by DLS measurements. The DLS results indicated that longer PAA blocks generally gave bigger hydrodynamic volumes possibly due to the electrostatic repulsion of the anionic blocks as mentioned previously.

An aminolysis reaction was also performed on polymer **4A-BA1** to observe changes associated with the molecular weight distribution when the polymer is cleaved at the core. The overlays of the SEC chromatograms of **4A-BA1** before and after the aminolysis process are shown in the SI. This process resulted in an overall molecular weight increase from 259 kDa to 394 kDa. In addition, the molecular weight distribution changed from multimodal and broad signals ( $D = 3.76$ )

to a monomodal and sharp peak ( $\bar{D} = 1.41$ ). Despite the increase in the overall molecular weight, these results are expected as the disappearance of high molecular weight species in the molecular weight distribution was observed after aminolysis. The change from a broad multimodal distribution to a sharp monomodal distribution indicated that cleavage of the core was successful, to produce a series of primary linear chains. However, as the theoretical molecular weight of **4A-BA1** was 1,060 kDa, one would expect the molecular weight of its primary linear chain to be four times lower. In the previous UHMW block copolymer study conducted by our group, it was realized that the PAA calibration standards employed for SEC molecular weight measurements aren't capable of providing accurate values due to the complexities of the block copolymers. It is difficult to analyse the exact molecular weight of polyelectrolytes due to the complexity in conformational changes. Therefore, values obtained from SEC should only be employed as a guide for complex species such as these block copolymers.

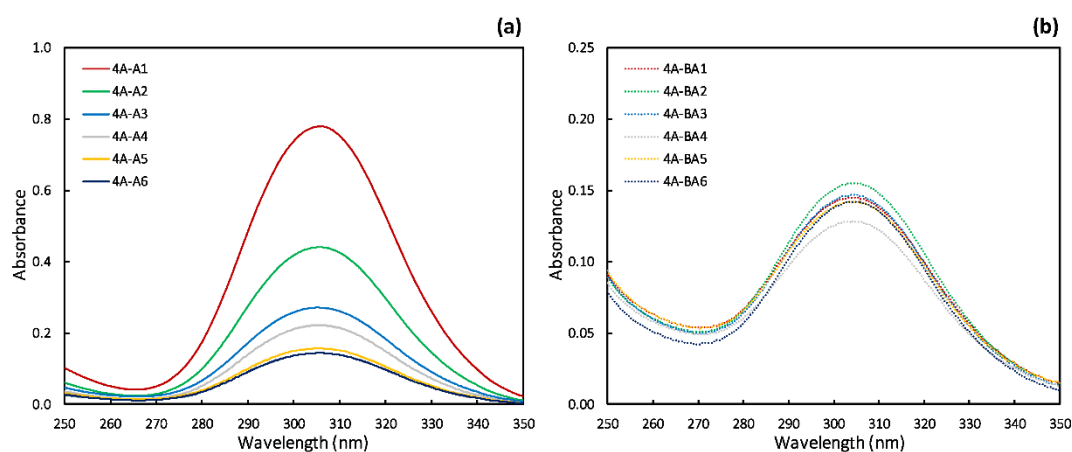


**Figure 2.** Overlay of UV-Vis spectra for (a) the macro-CTAs **4A-A1** – **4A-A6** at 0.25 wt% and (b) their respective star-shaped block copolymers **4A-BA1** – **4A-BA6** at 0.05 wt%.

**3.4. Cylinder settling tests.** The flocculation efficiency of the three control polymers (**PAA**, **PAM**, and **RAB**) and the six 4A-BA copolymers (**4A-BA1** – **4A-BA6**) were evaluated through a series of standard cylinder settling tests. Kaolin slurries were employed at a solid concentration of approximately 3 wt% for all cylinder settling tests. In addition, calcium chloride was added into the kaolin slurry at three different concentrations (0.05 M, 0.10 M, and 0.50 M) to generate the desired high ionic strength environment.

Two main factors were considered for the evaluation of the flocculation efficiency: settlement rate of the flocculated aggregates and the supernatant turbidity. These factors were measured and subsequently plotted as a function of flocculant dosage, which was introduced into the kaolin slurry at four different levels of 17, 33, 50, and 67 g/tds. The data obtained for the settlement rates and supernatant turbidity as a function of flocculant dosage is shown in Figure 3. These cylinder settling tests were performed with the best effort to maintain consistency by having the same operator and accurate concentrations of the kaolin solids and calcium salt. This was to lower the standard errors that were typically associated with these tests in previous studies, which may arise from variations in the solid concentrations and testing procedures, as well as other factors such as poor mixing.<sup>64, 65</sup> Cylinder settling test was mainly employed only as a guide for the comparison between polymeric flocculants with advanced architectures and those that are representative of current industry standards, and thus were deemed to be satisfactory for the purpose and hypothesis of this study. Further testings would be necessary prior to scale-up and implementation into industrial applications.

The settlement rate plots presented in Figure 3 were formatted at a similar scale across all three  $\text{Ca}^{2+}$  concentrations for ease of comparison. High settlement rate is desirable for most flocculation applications as this allows for faster and more efficient separation of the solid colloidal particles

from the slurry. The data obtained for the control polymers (**PAA**, **PAM**, and **RAB**) were represented by solid lines with circle markers, whilst **4A-BA1** – **4A-BA6** were represented by dashed lines with square markers. At the lowest multivalent cation concentration of 0.05 M, all six 4A-BA copolymers and **RAB** were capable of flocculating the kaolin slurry efficiently. A close-linear relationship between the settlement rate and the flocculant dosage was observed for all six 4A-BA copolymers, with **4A-BA4** – **4A-BA5** exhibiting higher settlement rates compared to **RAB** at dosages below 67 g/tds. However, **RAB** was still able to induce the highest settlement rate of approximately 8.5 m/h at a dosage of 67 g/tds. This indicated that **RAB** was unaffected by the initial level of  $\text{Ca}^{2+}$  within the slurry.

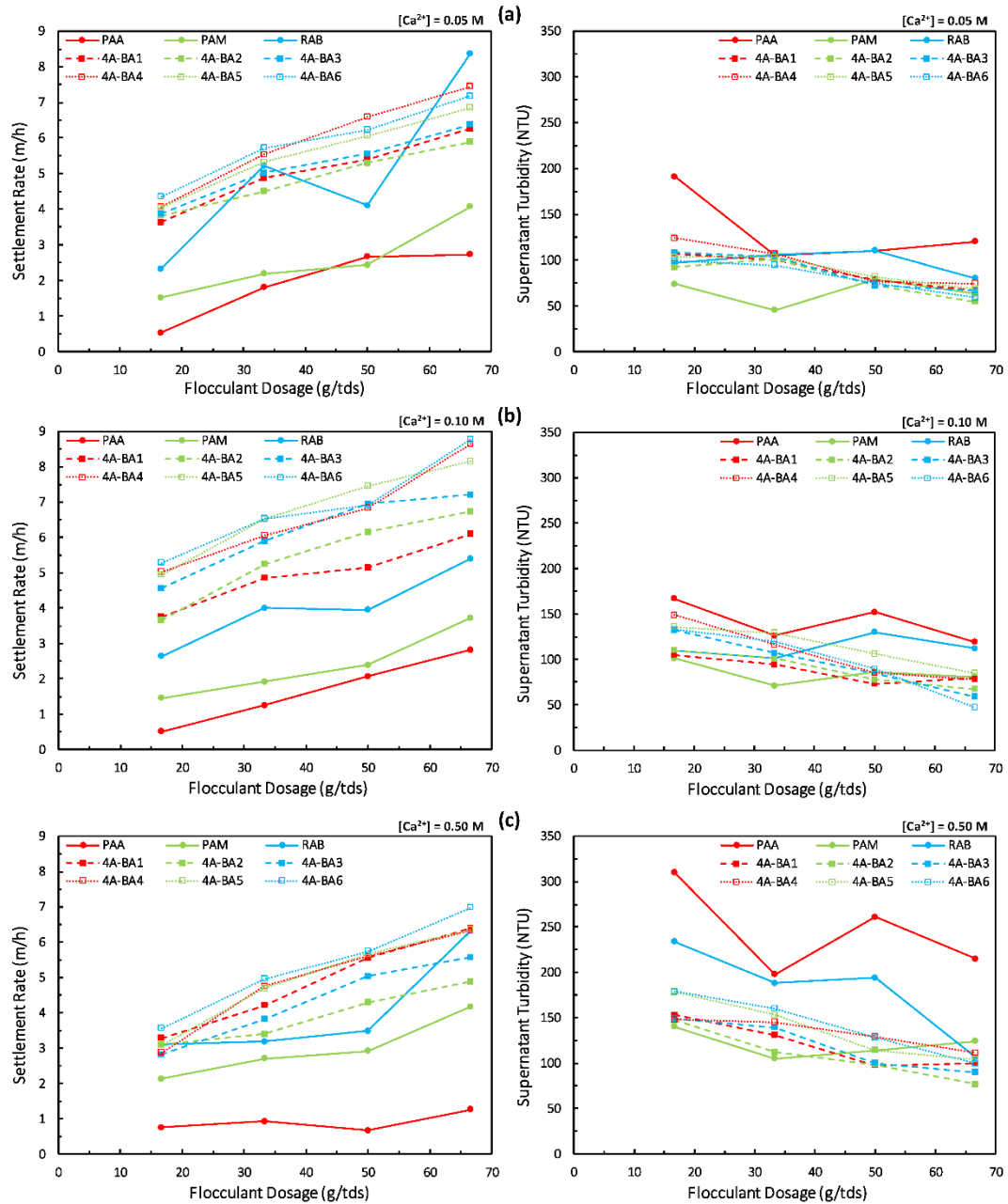


**Figure 3.** Data obtained from the cylinder settling tests with the settlement rate of the kaolin suspension (3 wt%) and the supernatant turbidity plotted as a function of flocculant dosage for the 4A-BA copolymers (4A-BA1 – 4A-BA6). Three different concentrations of  $\text{Ca}^{2+}$  cation were employed at (a) 0.05 M, (b) 0.10 M, and (c) 0.50 M.

Once the concentration of  $\text{Ca}^{2+}$  was doubled from 0.05 M, the settlement rates obtained by employing **RAB** were distinctively lower than all six of the 4A-BA copolymers across the range of flocculant dosages targeted. In contrast to this, the settlement rates obtained for the 4A-BA copolymers was observed to increase slightly, particularly more notable for the ones with longer A blocks (**4A-BA3** – **4A-BA6**). However, at the highest  $\text{Ca}^{2+}$  concentration employed, there was a drop in the settlement rates for the 4A-BA copolymers. This was most likely attributed to the excessive shielding of the terminal anionic blocks, which reduced the overall conformation of the polymer and thus led to less efficient polymer-particle bridging. Despite this, the flocculation performance of the 4A-BA copolymers was still generally superior compared to **RAB**.

A closer examination of the settlement rates amongst the 4A-BA copolymers indicated one clear trend. Polymers with longer terminal anionic A blocks such as **4A-BA4** – **4A-BA6** were able to generate flocs with faster settlement rates compared to polymers with shorter A blocks (**4A-BA1** – **4A-BA3**). The reason behind this was determined to be partly associated with the repulsion forces of the anionic groups. As mentioned previously, lower repulsion forces led to inadequate chain elongation and thus poorer polymer bridging. However, beyond a certain optimal concentration of anionic density, the flocculation efficiency will decrease significantly due to the collapse of polymer conformation, as observed in **PAA**.

The supernatant turbidity results were plotted as a function of dosage in Figure 3, and presented in the same format compared to the settlement rate plots for ease of following. The supernatant turbidity values obtained from using the 4A-BA copolymers and **RAB** were generally found to be in between the two extremes of **PAA** and **PAM**. **PAM** was able to induce the lowest turbidity at low flocculation dosages of 17 and 33 g/tds. of  $\text{Ca}^{2+}$ . It was determined that the presence of anionic functionalities played a major role in efficiently clarifying the kaolin slurry. **PAM** was one of the

best polymers at lowering the supernatant turbidity due to its lack of anionic group, and thus was not negatively affected by the presence of cations, while all other polymers were affected. However, the 4A-BA copolymers generally performed better in this regard at higher flocculation dosages of 50 g/tds and 67 g/tds across all three concentrations. In addition, the supernatant turbidity values were observed to decrease in a linear trend, and thus have the potential to be further lowered with higher polymer dosages.

A relatively plateau response curve was observed for **PAM**, whilst **PAA**'s response curve was relatively unstable. For example, at a  $\text{Ca}^{2+}$  concentration of 0.50 M, the turbidity obtained from **PAM** averaged at about 125 NTU whilst those obtained for **PAA** ranged between 190-310 NTU. As expected, this higher level of turbidity and poor stability was attributed to the negative effect of the multivalent cations within the slurry, which directly affected polymer conformation and hence its flocculation efficiency. Although stable response curves were obtained, the turbidity data obtained for **PAM** slightly increased with higher concentration of  $\text{Ca}^{2+}$ . The multivalent cations present in the solution most likely affected the particle edge surfaces, which would inhibit **PAM** adsorption through hydrogen bonding with the silanol and aluminol OH groups.

At the lowest  $\text{Ca}^{2+}$  concentration of 0.05 M, the supernatant turbidity obtained from using **RAB** was higher than all six 4A-BA copolymers above flocculant dosage of 17 g/tds. A relatively plateau response curve was obtained for **RAB**, whilst a clear and steady decline in the supernatant turbidity was observed for the 4A-BA copolymers as higher flocculant dosages were added. Similar declines in the supernatant turbidity were once again observed for the 4A-BA copolymers when the  $\text{Ca}^{2+}$  concentration was changed to 0.10 M and 0.50 M. These results provided a positive outlook for these 4A-BA copolymers as they remained stable throughout the large jump in the level of  $\text{Ca}^{2+}$ .

A further increase in the flocculant dosage would potentially result in better clarity for the supernatant.

Apart from an overall increase in the turbidity with higher  $\text{Ca}^{2+}$  concentration, a few other trends were observed amongst the 4A-BA copolymers. At 0.05 M of  $\text{Ca}^{2+}$ , minute differences in the turbidity were noted for the 4A-BA copolymers. However, as the concentration of  $\text{Ca}^{2+}$  was increased further to 0.10 M and 0.50 M, larger discrepancies between the 4A-BA copolymers were seen. Polymers with high anionic charge density (**4A-BA4** – **4A-BA6**) had poorer clarification performance compared to those with lower anionic charge densities (**4A-BA1** – **4A-BA3**). Despite this, the differences in clarification performance were deemed to be quite insignificant. In addition, the turbidity values obtained for the 4A-BA copolymers were generally lower than that of **RAB**, with high potential for being brought down further with higher flocculant dosages if necessary. To this end, the 4A-BA copolymers synthesized in this study have shown very promising flocculation efficiencies. The 4A-BA copolymers have evidently shown high potential as commercial flocculants due to their unique architecture that would allow them to withstand the high ionic strength environment.

#### 4. CONCLUSIONS

Six different star-shaped block copolymers (**4A-BA1** – **4A-BA6**) were successfully synthesized through the use of a two-stage aqueous RAFT polymerization process using a redox initiation system of APS/SFS. The aid of a 4-arm star RAFT agent (**4A-CTA**) was required in the first stage to synthesize the terminal anionic polymeric blocks from AA (**4A-A1** – **4A-A6**). The molecular weights of **4A-A1** – **4A-A6** were estimated to range from approximately 23.1 kDa to 173 kDa.

These polymers were subsequently used as the macro-CTAs in the second stage, where the chain was extended with AM to create the polymers **4A-BA1 – 4A-BA6**.

The 4A-BA copolymers and the three control copolymers (**PAA**, **PAM**, and **RAB**) were employed as the polymeric flocculants in a series of cylinder settling tests of kaolin slurries with three different concentrations of  $\text{Ca}^{2+}$  (0.05 M, 0.10 M, and 0.50 M). The flocculation efficiency of control polymer **RAB** diminished rapidly as the concentration of  $\text{Ca}^{2+}$  increased. In contrast, the 4A-BA copolymers showed a strong stability in the settlement rates of the flocs as well as the supernatant turbidity despite the excess levels of  $\text{Ca}^{2+}$ . Out of the six 4A-BA copolymers, **4A-BA6** was able to produce flocs with the fastest settlement rate, whilst **4A-BA1** was the most efficient at clarifying the slurry. To this end, the 4A-BA copolymers showed promising flocculation efficiency in high ionic strength slurries, and further optimizations and testings would possibly lead to the implementation of these polymers in current industrial applications of flocculation.

### ASSOCIATED CONTENT

**Supporting Information.** The Supporting Information is available free of charge on the ACS publication website at DOI: XXXX/XXXXXXX. Synthesis of **4A-A1 – 4A-A6** by RAFT Polymerisation of AA; Synthesis of **4A-BA1 – 4A-BA6** by RAFT Polymerisation of AM; SEC Overlays of RI- and UV-detected Molecular Weight Data for **4A-A1 – 4A-A6**; SEC Overlays of RI- and UV-detected Molecular Weight Data for **4A-BA1 – 4A-BA6**; Aminolysis of **4A-BA1**, SEC Chromatograms of the Controlled Polymers.

#### **AUTHOR INFORMATION**

**Corresponding Author.** \*E-mail: kei.saito@monash.edu. Phone: + 61 3 9905 4600. \*E-mail: neil.cameron@monash.edu. Phone: Tel: +61 3 9902 0774.

**Notes.** The authors declare no competing financial interest.

#### **ACKNOWLEDGEMENTS**

BASF Australia Ltd, and the Chemicals and Plastics Manufacturing Innovation Network and Training program (supported by Monash University, Chemistry Australia and the Victorian Government of Australia) are gratefully acknowledged for their financial supports. Dr Richard Macoun is gratefully acknowledged for his input into this project.

**REFERENCES**

1. Gregory, J.; Barany, S. Adsorption and flocculation by polymers and polymer mixtures. *Adv. Colloid Interface Sci.* **2011**, 169 (1), 1-12.
2. Bolto, B.; Gregory, J. Organic polyelectrolytes in water treatment. *Water Res.* **2007**, 41 (11), 2301-2324.
3. Dao, V. H.; Cameron, N. R.; Saito, K. Synthesis, properties and performance of organic polymers employed in flocculation applications. *Polym. Chem.* **2016**, 7, 11-25.
4. Konduri, M. K. R.; Fatehi, P. Influence of pH and ionic strength on flocculation of clay suspensions with cationic xylan copolymer. *Colloids Surf. A: Physicochem. Eng. Aspects* **2017**, 530, 20-32.
5. Burkert, H.; Hartmann, J. Flocculants. In *Ullmann's Encyclopedia of Industrial Chemistry*; Wiley-VCH Verlag GmbH & Co. KGaA: Federal Republic of Germany, 2000; Vol. 15, pp 199-210.
6. Moody, G. M. Chapter 6: Polymeric Flocculants. In *Handbook of Industrial Water Soluble Polymers*, Williams, P. A., Ed.; John Wiley & Sons: Oxford, The United Kingdom, 2008, pp 134-173.
7. Nasser, M. S.; James, A. E. The effect of polyacrylamide charge density and molecular weight on the flocculation and sedimentation behaviour of kaolinite suspensions. *Sep. Purif. Technol.* **2006**, 52 (2), 241-252.
8. Lu, L.; Pan, Z.; Hao, N.; Peng, W. A novel acrylamide-free flocculant and its application for sludge dewatering. *Water Res.* **2014**, 57, 304-312.

9. Moss, N. Flocculation: Theory and Application. *Mine and Quarry Journal* **1979**, 7 (5), 57-61.
10. Ji, Y.; Lu, Q.; Liu, Q.; Zeng, H. Effect of solution salinity on settling of mineral tailings by polymer flocculants. *Colloids Surf. A: Physicochem. Eng. Aspects* **2013**, 430, 29-38.
11. Pillai, J. Flocculants and Coagulants: The Keys to Water and Waste Management in Aggregate Production. Naperville, IL: Nalco Company (Stone Review) **1997**, 1-6.
12. Sabah, E.; Cengiz, I. An evaluation procedure for flocculation of coal preparation plant tailings. *Water Res.* **2004**, 38 (6), 1542-1549.
13. Greenlee, L. F.; Lawler, D. F.; Freeman, B. D.; Marrot, B.; Moulin, P. Reverse osmosis desalination: Water sources, technology, and today's challenges. *Water Res.* **2009**, 43 (9), 2317-2348.
14. Sabah, E.; Erkan, Z. E. Interaction mechanism of flocculants with coal waste slurry. *Fuel* **2006**, 85 (3), 350-359.
15. Feng, D.; van Deventer, J. S. J.; Aldrich, C. Removal of pollutants from acid mine wastewater using metallurgical by-product slags. *Sep. Purif. Technol.* **2004**, 40 (1), 61-67.
16. Witham, M. I.; Grabsch, A. F.; Owen, A. T.; Fawell, P. D. The effect of cations on the activity of anionic polyacrylamide flocculant solutions. *Int. J. Miner. Process.* **2012**, 114-117, 51-62.
17. Rogan, K. R. The variations of the configurational and solvency properties of low molecular weight sodium polyacrylate with ionic strength. *Colloid. Polym. Sci.* **1995**, 273 (4), 364-369.

18. Mortimer, D. A. Synthetic Polyelectrolytes - A Review. *Polym. Int.* **1991**, 25 (1), 29-41.
19. Kay, P. J.; Treloar, F. E. The Intrinsic Viscosity of Poly(acrylic acid) at Different Ionic Strengths: Random Coil and Rigid Rod Behaviour. *Die Makromolekulare Chemie* **1974**, 175 (11), 3207-3223.
20. Boisvert, J.-P.; Malgat, A.; Pochard, I.; Daneault, C. Influence of the counter-ion on the effective charge of polyacrylic acid in dilute condition. *Polymer* **2002**, 43 (1), 141-148.
21. Peng, F. F.; Di, P. Effect of Multivalent Salts - Calcium and Aluminum on the Flocculation of Kaolin Suspension with Anionic Polyacrylamide. *J. Colloid Interface Sci.* **1994**, 164 (1), 229-237.
22. Seright, R. S.; Campbell, A.; Mozley, P.; Han, P. Stability of Partially Hydrolyzed Polyacrylamides at Elevated Temperatures in the Absence of Divalent Cations. SPE-121460-PA **2010**, 15, 341-348.
23. Ghimici, L.; Constantin, M.; Fundueanu, G. Novel biodegradable flocculating agents based on pullulan. *J. Hazard. Mater.* **2010**, 181 (1-3), 351-358.
24. Liu, W.; Sun, W.; Hu, Y. Effects of water hardness on selective flocculation of diasporic bauxite. *Trans. Nonferrous. Met. Soc. China.* **2012**, 22 (9), 2248-2254.
25. Shipp, D. A. Reversible-Deactivation Radical Polymerizations. *Polymer Reviews* **2011**, 51 (2), 99-103.
26. Dao, V. H.; Cameron, N. R.; Saito, K. Synthesis of ultra-high molecular weight ABA triblock copolymers via aqueous RAFT-mediated gel polymerisation, end group modification and chain coupling. *Polym. Chem.* **2017**, 8 (44), 6834-6843.

27. Read, E.; Guinaudeau, A.; James Wilson, D.; Cadix, A.; Violleau, F.; Destarac, M. Low temperature RAFT/MADIX gel polymerisation: access to controlled ultra-high molar mass polyacrylamides. *Polym. Chem.* **2014**, *5* (7), 2202-2207.
28. Carmean, R. N.; Becker, T. E.; Sims, M. B.; Sumerlin, B. S. Ultra-High Molecular Weights via Aqueous Reversible-Deactivation Radical Polymerization. *Chem* **2017**, *2* (1), 93-101.
29. Despax, L.; Fitremann, J.; Destarac, M.; Harrisson, S. Low concentration thermoresponsive hydrogels from readily accessible triblock copolymers. *Polym. Chem.* **2016**, *7* (20), 3375-3377.
30. Mapas, J. K. D.; Thomay, T.; Cartwright, A. N.; Ilavsky, J.; Rzyayev, J. Ultrahigh Molecular Weight Linear Block Copolymers: Rapid Access by Reversible-Deactivation Radical Polymerization and Self-Assembly into Large Domain Nanostructures. *Macromolecules* **2016**, *49* (10), 3733-3738.
31. Rzyayev, J.; Penelle, J. HP-RAFT: A Free-Radical Polymerization Technique for Obtaining Living Polymers of Ultrahigh Molecular Weights. *Angew. Chem. Int. Ed.* **2004**, *43* (13), 1691-1694.
32. Xu, J.; Jung, K.; Atme, A.; Shanmugam, S.; Boyer, C. A Robust and Versatile Photoinduced Living Polymerization of Conjugated and Unconjugated Monomers and Its Oxygen Tolerance. *J. Am. Chem. Soc.* **2014**, *136* (14), 5508-5519.
33. Truong, N. P.; Dussert, M. V.; Whittaker, M. R.; Quinn, J. F.; Davis, T. P. Rapid synthesis of ultrahigh molecular weight and low polydispersity polystyrene diblock copolymers by RAFT-mediated emulsion polymerization. *Polym. Chem.* **2015**, *6* (20), 3865-3874.

34. Xue, L.; Agarwal, U. S.; Lemstra, P. J. High Molecular Weight PMMA by ATRP. *Macromolecules* **2002**, 35 (22), 8650-8652.
35. Mao, B. W.; Gan, L. H.; Gan, Y. Y. Ultra high molar mass poly[2-(dimethylamino)ethyl methacrylate] via atom transfer radical polymerization. *Polymer* **2006**, 47 (9), 3017-3020.
36. Simms, R. W.; Cunningham, M. F. High Molecular Weight Poly(butyl methacrylate) by Reverse Atom Transfer Radical Polymerization in Miniemulsion Initiated by a Redox System. *Macromolecules* **2007**, 40 (4), 860-866.
37. Arita, T.; Kayama, Y.; Ohno, K.; Tsujii, Y.; Fukuda, T. High-pressure atom transfer radical polymerization of methyl methacrylate for well-defined ultrahigh molecular-weight polymers. *Polymer* **2008**, 49 (10), 2426-2429.
38. Mueller, L.; Jakubowski, W.; Matyjaszewski, K.; Pietrasik, J.; Kwiatkowski, P.; Chaladaj, W.; Jurczak, J. Synthesis of high molecular weight polystyrene using AGET ATRP under high pressure. *Eur. Polym. J.* **2011**, 47 (4), 730-734.
39. Huang, Z.; Chen, J.; Zhang, L.; Cheng, Z.; Zhu, X. ICAR ATRP of Acrylonitrile under Ambient and High Pressure. *Polymers* **2016**, 8 (3), 59.
40. Percec, V.; Guliashvili, T.; Ladislaw, J. S.; Wistrand, A.; Stjerndahl, A.; Sienkowska, M. J.; Monteiro, M. J.; Sahoo, S. Ultrafast Synthesis of Ultrahigh Molar Mass Polymers by Metal-Catalyzed Living Radical Polymerization of Acrylates, Methacrylates, and Vinyl Chloride Mediated by SET at 25 °C. *J. Am. Chem. Soc.* **2006**, 128 (43), 14156-14165.
41. Lligadas, G.; Percec, V. Ultrafast SET-LRP of methyl acrylate at 25 °C in alcohols. *J. Polym. Sci., Part A: Polym. Chem.* **2008**, 46 (8), 2745-2754.

42. Nguyen, N. H.; Leng, X.; Percec, V. Synthesis of ultrahigh molar mass poly(2-hydroxyethyl methacrylate) by single-electron transfer living radical polymerization. *Polym. Chem.* **2013**, 4 (9), 2760-2766.
43. Mayadunne, R. T. A.; Jeffery, J.; Moad, G.; Rizzardo, E. Living Free Radical Polymerization with Reversible Addition–Fragmentation Chain Transfer (RAFT Polymerization): Approaches to Star Polymers. *Macromolecules* **2003**, 36 (5), 1505-1513.
44. Boschmann, D.; Vana, P. Z-RAFT Star Polymerizations of Acrylates: Star Coupling via Intermolecular Chain Transfer to Polymer. *Macromolecules* **2007**, 40 (8), 2683-2693.
45. Wang, R.; McCormick, C. L.; Lowe, A. B. Synthesis and Evaluation of New Dicarboxylic Acid Functional Trithiocarbonates: RAFT Synthesis of Telechelic Poly(n-butyl acrylate)s. *Macromolecules* **2005**, 38 (23), 9518-9525.
46. Moad, G.; Rizzardo, E.; Thang, S. H. Living Radical Polymerization by the RAFT Process. *Aust. J. Chem.* **2005**, 58 (6), 379-410.
47. Moad, G.; Rizzardo, E.; Thang, S. H. Living Radical Polymerization by the RAFT Process - A First Update. *Aust. J. Chem.* **2006**, 59 (10), 669-692.
48. Moad, G.; Rizzardo, E.; Thang, S. H. Living Radical Polymerization by the RAFT Process - A Second Update. *Aust. J. Chem.* **2009**, 62 (11), 1402-1472.
49. Moad, G.; Rizzardo, E.; Thang, S. H. Living Radical Polymerization by the RAFT Process - A Third Update. *Aust. J. Chem.* **2012**, 65 (8), 985-1076.

50. Wang, R.; Lowe, A. B. RAFT polymerization of styrenic-based phosphonium monomers and a new family of well-defined statistical and block polyampholytes. *J. Polym. Sci., Part A: Polym. Chem.* **2007**, 45 (12), 2468-2483.
51. Qi, G.; Eleazer, B.; Jones, C. W.; Schork, F. J. Mechanistic Aspects of Sterically Stabilized Controlled Radical Inverse Miniemulsion Polymerization. *Macromolecules* **2009**, 42 (12), 3906-3916.
52. Qi, G.; Jones, C. W.; Schork, F. J. RAFT Inverse Miniemulsion Polymerization of Acrylamide. *Macromol. Rapid Commun.* **2007**, 28 (9), 1010-1016.
53. Ouyang, L.; Wang, L.; Schork, F. J. Synthesis of Well-Defined Statistical and Diblock Copolymers of Acrylamide and Acrylic Acid by Inverse Miniemulsion Raft Polymerization. *Macromol. Chem. Phys.* **2010**, 211 (18), 1977-1983.
54. Ouyang, L.; Wang, L.; Schork, F. J. RAFT Inverse Miniemulsion Polymerization of Acrylic Acid and Sodium Acrylate. *Macromolecular Reaction Engineering* **2011**, 5 (3-4), 163-169.
55. Currie, D. J.; Dainton, F. S.; Watt, W. S. The effect of pH on the polymerization of acrylamide in water. *Polymer* **1965**, 6 (9), 451-453.
56. Hill, M. R.; Carmean, R. N.; Sumerlin, B. S. Expanding the Scope of RAFT Polymerization: Recent Advances and New Horizons. *Macromolecules* **2015**, 48 (16), 5459-5469.
57. Barner-Kowollik, C.; Buback, M.; Charleux, B.; Coote, M. L.; Drache, M.; Fukuda, T.; Goto, A.; Klumperman, B.; Lowe, A. B.; Mcleary, J. B.; Moad, G.; Monteiro, M. J.; Sanderson, R. D.; Tonge, M. P.; Vana, P. Mechanism and kinetics of dithiobenzoate-mediated RAFT

polymerization. I. The current situation. *J. Polym. Sci., Part A: Polym. Chem.* **2006**, 44 (20), 5809-5831.

58. Vana, P.; Davis, T. P.; Barner-Kowollik, C. Easy Access to Chain-Length-Dependent Termination Rate Coefficients Using RAFT Polymerization. *Macromol. Rapid Commun.* **2002**, 23 (16), 952-956.

59. Buback, M.; Junkers, T.; Vana, P. Laser Single Pulse Initiated RAFT Polymerization for Assessing Chain-Length Dependent Radical Termination Kinetics. *Macromol. Rapid Commun.* **2005**, 26 (10), 796-802.

60. Ren, J. M.; McKenzie, T. G.; Fu, Q.; Wong, E. H. H.; Xu, J.; An, Z.; Shanmugam, S.; Davis, T. P.; Boyer, C.; Qiao, G. G. Star Polymers. *Chem. Rev.* **2016**, 116 (12), 6743-6836.

61. Hu, J.; Qiao, R.; Whittaker, M. R.; Quinn, J. F.; Davis, T. P. Synthesis of Star Polymers by RAFT Polymerization as Versatile Nanoparticles for Biomedical Applications. *Aust. J. Chem.* **2017**, 70 (11), 1161-1170.

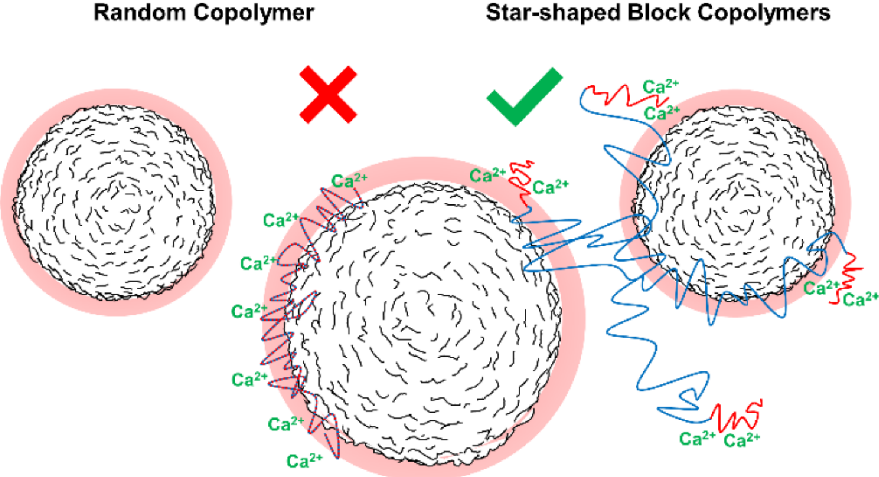
62. Willcock, H.; O'Reilly, R. K. End group removal and modification of RAFT polymers. *Polym. Chem.* **2010**, 1 (2), 149-157.

63. Swift, T.; Swanson, L.; Geoghegan, M.; Rimmer, S. The pH-responsive behaviour of poly(acrylic acid) in aqueous solution is dependent on molar mass. *Soft Matter* **2016**, 12 (9), 2542-2549.

64. Owen, A. T.; Fawell, P. D.; Swift, J. D.; Farrow, J. B. The impact of polyacrylamide flocculant solution age on flocculation performance. *Int. J. Miner. Process.* **2002**, 67 (1), 123-144.

65. Farrow, J. B.; Swift, J. D. A new procedure for assessing the performance of flocculants. *Int. J. Miner. Process.* **1996**, 46 (3), 263-275.

TABLE OF CONTENTS



### 4.3. Supporting Information

## Supporting Information

# Synthesis of UHMW Star-shaped AB Block Copolymers and their Flocculation Efficiency in High Ionic Strength Environments

*Vu H. Dao,<sup>a</sup> Neil R. Cameron,<sup>\*b,c</sup> and Kei Saito<sup>\*a</sup>*

<sup>a</sup> School of Chemistry, Monash University, Clayton, VIC 3800, Australia. E-mail:  
kei.saito@monash.edu, Tel: + 61 3 9905 4600

<sup>b</sup> Department of Materials Science and Engineering, Monash University, Clayton, VIC 3800,  
Australia. E-mail: neil.cameron@monash.edu, Tel: +61 3 9902 0774

<sup>c</sup> School of Engineering, University of Warwick, Coventry, CV4 7AL, United Kingdom

**In total 7 pages, 2 Tables and 4 Figures**

**Supporting Information.** Synthesis of 4A-A1 – 4A-A6 by RAFT Polymerisation of AA, Synthesis of 4A-BA1 – 4A-BA6 by RAFT Polymerisation of AM, SEC Overlays of RI- and UV-detected Molecular Weight Data for 4A-A1 – 4A-A6, SEC Overlays of RI- and UV-detected Molecular Weight Data for 4A-BA1 – 4A-BA6, Aminolysis of 4A-BA1, and SEC Chromatograms of Control Polymers.

**Synthesis of 4A-A1 – 4A-A6 by RAFT Polymerisation of AA**

The star-shaped macro chain transfer agents (macro-CTAs) **4A-A1 – 4A-A6** were synthesized by RAFT polymerization of AA according to the general procedure outlined in the main manuscript. The quantities of monomer, RAFT reagent **4A-CTA**, internal standard, solvent, and initiators employed for the synthesis of these polymers are detailed in Table S1.

**Table S1. Quantities of reagents and solvent used in the synthesis of 4A-A1 – 4A-A6**

	Polymer					
	4A-A1	4A-A2	4A-A3	4A-A4	4A-A5	4A-A6
AA	5.78 mL <sup>a</sup>					
	46.3 mmol					
4A-CTA	90.1 mg	45.1 mg	30.0 mg	22.5 mg	18.0 mg	15.0 mg
	0.083 mmol	0.042 mmol	0.028 mmol	0.021 mmol	0.017 mmol	0.014 mmol
DMF	0.30 mL <sup>b</sup>					
H <sub>2</sub> O	3.96 mL	4.09 mL	4.13 mL	4.15 mL	4.17 mL	4.18 mL
APS	158 μL <sup>d</sup>	79 μL <sup>d</sup>	53 μL <sup>d</sup>	40 μL <sup>d</sup>	32 μL <sup>d</sup>	26 μL <sup>d</sup>
	0.014 mmol	0.007 mmol	0.005 mmol	0.003 mmol	0.003 mmol	0.002 mmol
SFS	107 μL <sup>e</sup>	54 μL <sup>e</sup>	36 μL <sup>e</sup>	27 μL <sup>e</sup>	21 μL <sup>e</sup>	18 μL <sup>e</sup>
	0.014 mmol	0.007 mmol	0.005 mmol	0.003 mmol	0.003 mmol	0.002 mmol

<sup>a</sup> AA was prepared as a 57.6 wt% (8 M) stock solution in Milli-Q water and used as is for the synthesis of polymers **4A-A1 – 4A-A6**. <sup>b</sup> DMF was added into the reaction mixture as an internal standard for the analysis of monomer conversion. <sup>c</sup> APS was prepared as a 2.0 wt% stock solution in Milli-Q water prior to use as the redox initiator for the synthesis of **4A-A1 – 4A-A6**. <sup>d</sup> SFS was prepared as a 2.0 wt% stock solution in Milli-Q water prior to use as the redox initiator for the synthesis of **4A-A1 – 4A-A6**.

**Synthesis of 4A-BA1 – 4A-BA6 by RAFT Polymerisation of AM**

The star-shaped block copolymers **4A-BA1 – 4A-BA6** were synthesized by RAFT polymerization of AM according to the general procedure outlined in the main manuscript. The quantities of monomer, macro-CTA (**4A-A1 – 4A-A6**), internal standard, solvent, and initiators employed for the synthesis of these polymers are detailed in Table S2.

**Table S2. Quantities of reagents and solvent used in the synthesis of 4A-BA1 – 4A-BA6**

	Polymer					
	4A-BA1	4A-BA2	4A-BA3	4A-BA4	4A-BA5	4A-BA6
<b>AM</b>	5.86 mL <sup>a</sup>					
	46.9 mmol					
<b>Macro-CTA</b>	51.1 mg	113 mg	182 mg	251 mg	304 mg	384 mg
	0.002 mmol	0.002 mmol	0.002 mmol	0.002 mmol	0.002 mmol	0.002 mmol
<b>DMF</b>	0.30 mL <sup>b</sup>					
<b>H<sub>2</sub>O</b>	4.14 mL					
<b>APS</b>	8 μL <sup>d</sup>					
	0.37 μmol					
<b>SFS</b>	6 μL <sup>e</sup>					
	0.37 μmol					

<sup>a</sup> AM was prepared as a 56.9 wt% (8 M) stock solution in Milli-Q water and used as is for the synthesis of polymers **4A-BA1 – 4A-BA6**. <sup>b</sup> DMF was added into the reaction mixture as an internal standard for the analysis of monomer conversion. <sup>c</sup> APS was prepared as a 1.0 wt% stock solution in Milli-Q water prior to use as the redox initiator for the synthesis of **4A-BA1 – 4A-BA6**. <sup>d</sup> SFS was prepared as a 1.0 wt% stock solution in Milli-Q water prior to use as the redox initiator for the synthesis of **4A-BA1 – 4A-BA6**.

**SEC Overlays of RI- and UV-detected Molecular Weight Data for 4A-A1 – 4A-A6**

The chromatograms of **4A-A1 – 4A-A6** were obtained by SEC through RI- and UV-detection. The overlay of the RI SEC chromatograms for each **4A-A1 – 4A-A6** polymer and their corresponding chromatograms obtained by UV-detection at 305 nm is shown in Figure S1.

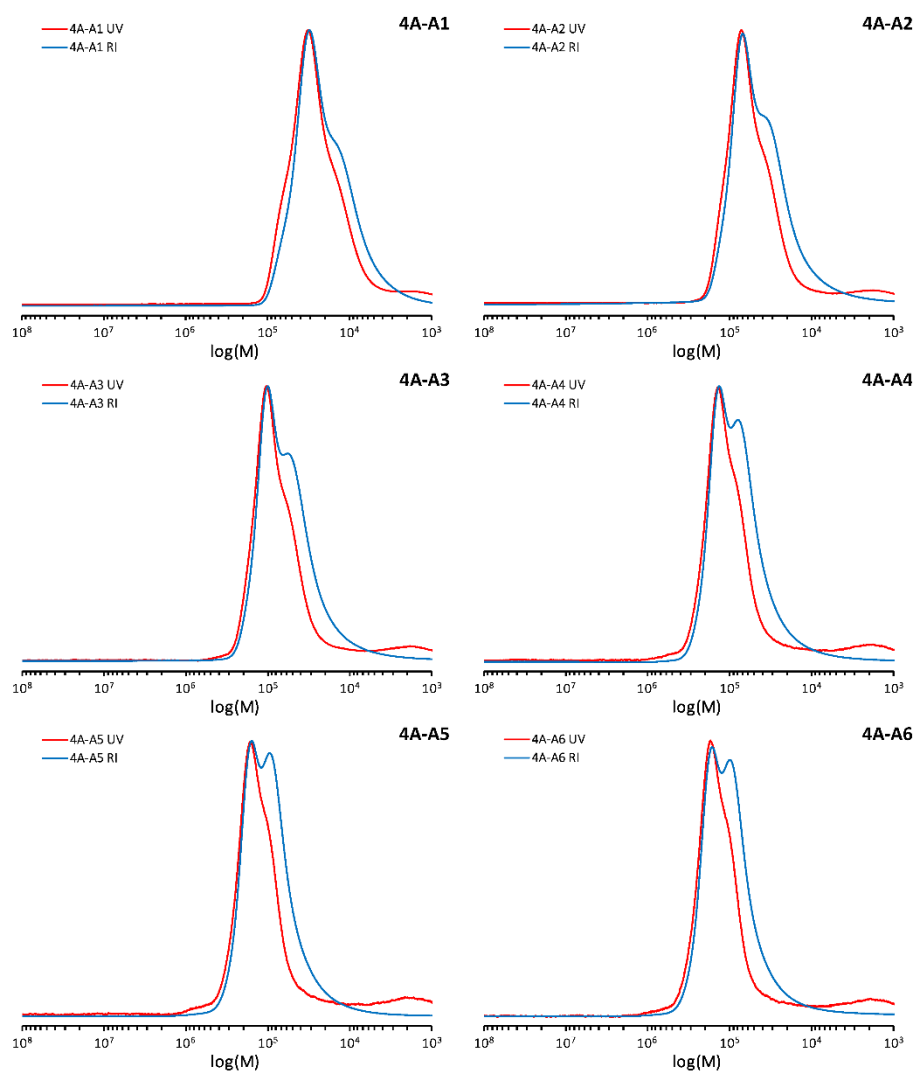


**Figure S1.** Overlays of SEC chromatograms obtained by RI- and UV-detection for the macro-CTAs **4A-A1 – 4A-A6**.

**SEC Overlays of RI- and UV-detected Molecular Weight Data for 4A-BA1 – 4A-BA6**

The chromatograms of **4A-BA1 – 4A-BA6** were also obtained by SEC through RI- and UV-detection. The overlay of the RI SEC chromatograms for each **4A-BA1 – 4A-BA6** copolymer and their corresponding chromatograms obtained by UV-detection at 305 nm is shown in Figure S2.

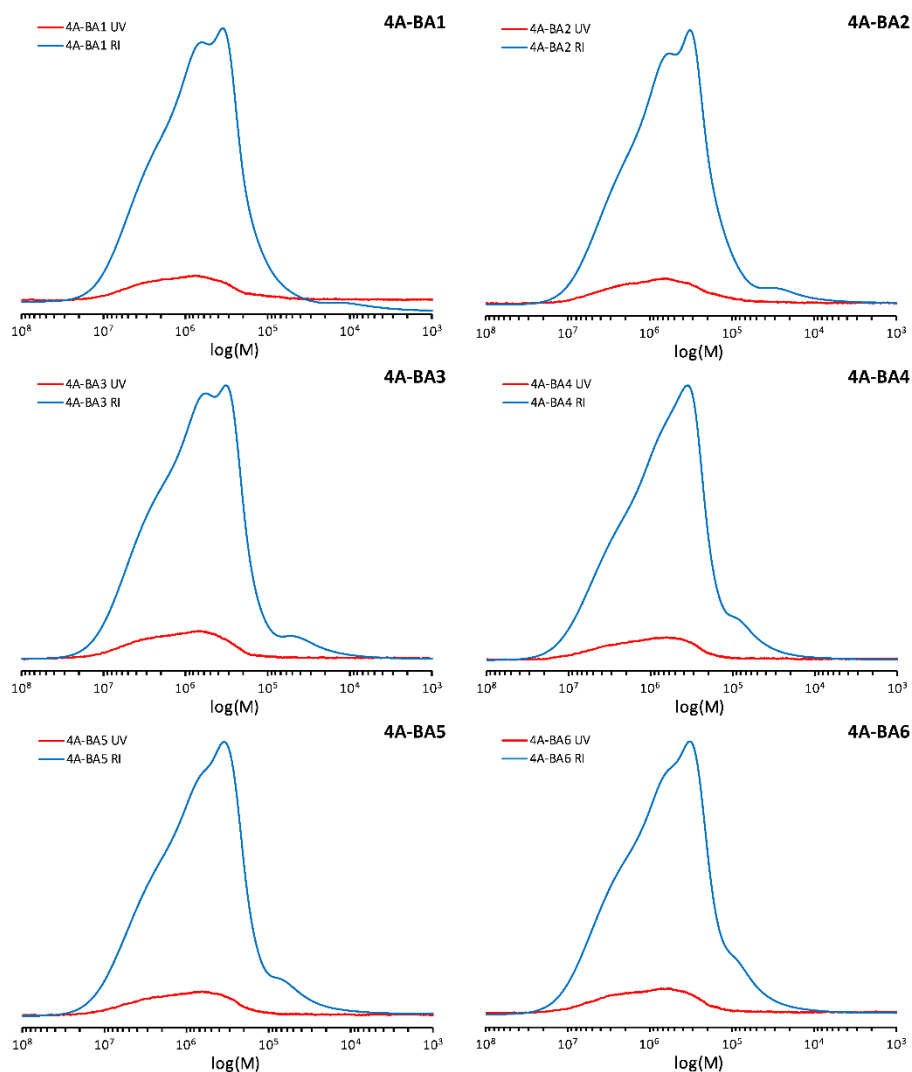


**Figure S2.** Overlays of SEC chromatograms obtained by RI- and UV-detection for the star-shaped block copolymers **4A-BA1 – 4A-BA6**.

### Aminolysis of 4A-BA1

Star-shaped polymer **4A-BA1** was subjected to an aminolysis process as a trial to determine whether there is a change in the molecular weight distribution. A 0.5 wt% loading of **4A-BA1** and a 0.5 wt% loading of tris(2-carboxyethyl)phosphine was prepared in Milli-Q water. This reaction mixture was subsequently degassed with argon bubbling for 30 minutes, immediately followed by the injection of *n*-butylamine (1 mL). The reaction was allowed to proceed under an inert atmosphere for 24 hour. At this point, a small fraction of the reaction mixture was analysed with SEC, and the SEC overlays of **4A-BA1** pre-aminolysis and post-aminolysis are shown in Figure S3.

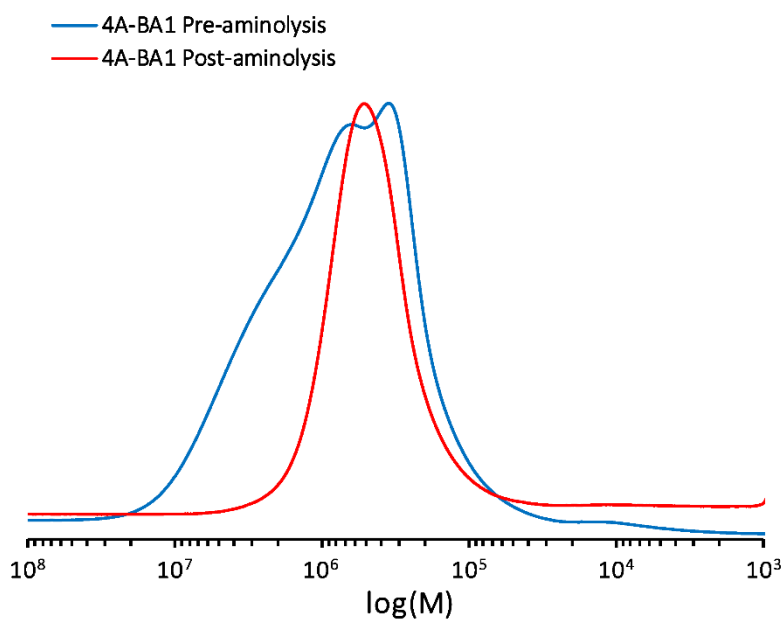


**Figure S3.** Overlays of SEC chromatograms for **4A-BA1** before (blue line) and after (red line) the aminolysis process.  $M_{n,SEC}$  of **4A-BA1** before and after aminolysis are 259 kDa ( $D = 3.76$ ) and 394 kDa ( $D = 1.41$ ), respectively.

## SEC Chromatograms of the Controlled Polymers

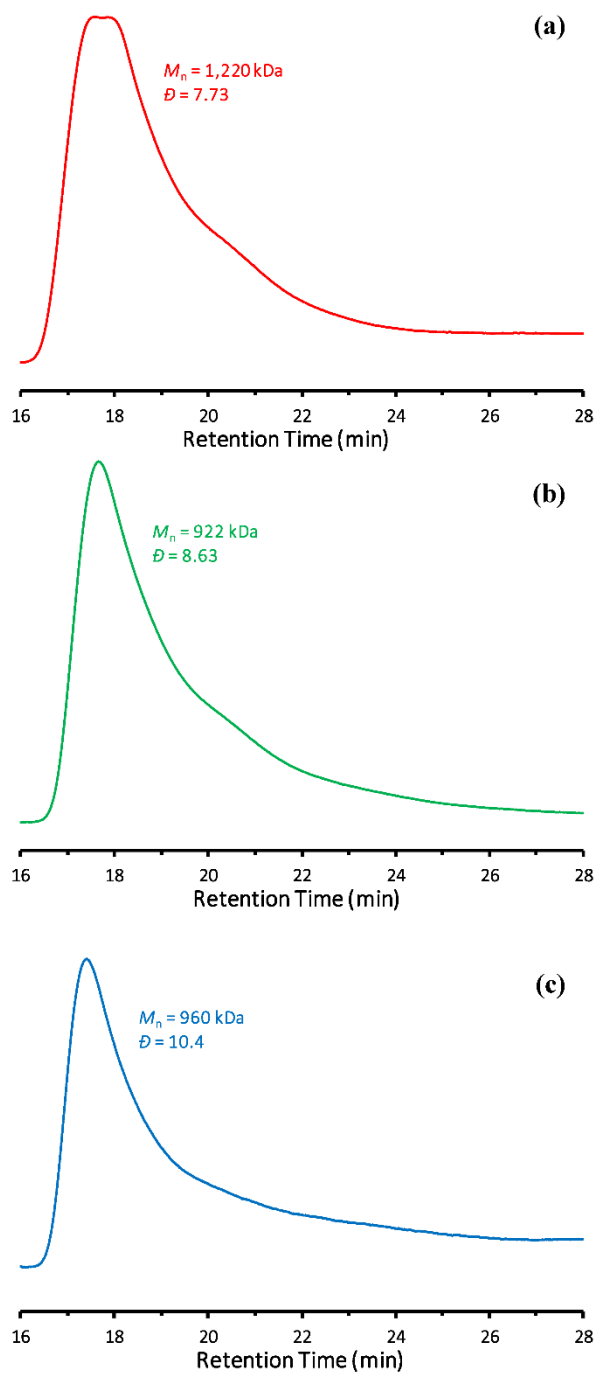


**Figure S4.** SEC chromatograms for control polymers (a) PAA, (b) PAM, and (c) RAB.

## 4.4. Appendix

Prior to the successful synthesis of the star-shaped block copolymers (**SAB1** – **SAB6**) using RAFT polymerisation with the aid of a 4-arm star-shaped chain transfer agent (**4A-CTA**), a series of other experiments were performed to create the star-shaped block copolymers by other methodologies. These employed the existing AB diblock copolymers (**AB1** – **AB8**) synthesised in Chapter 2 as the initial building block. The living terminal thiocarbonylthio functionality on the polymer chain was converted into a thiol moiety through a simple aminolysis procedure under inert conditions. The thiol-terminated AB diblock copolymer was then subjected to a coupling process with different 4-arm star polyethylene glycol (PEG) polymers bearing active terminal functionalities (Figure 4.1).

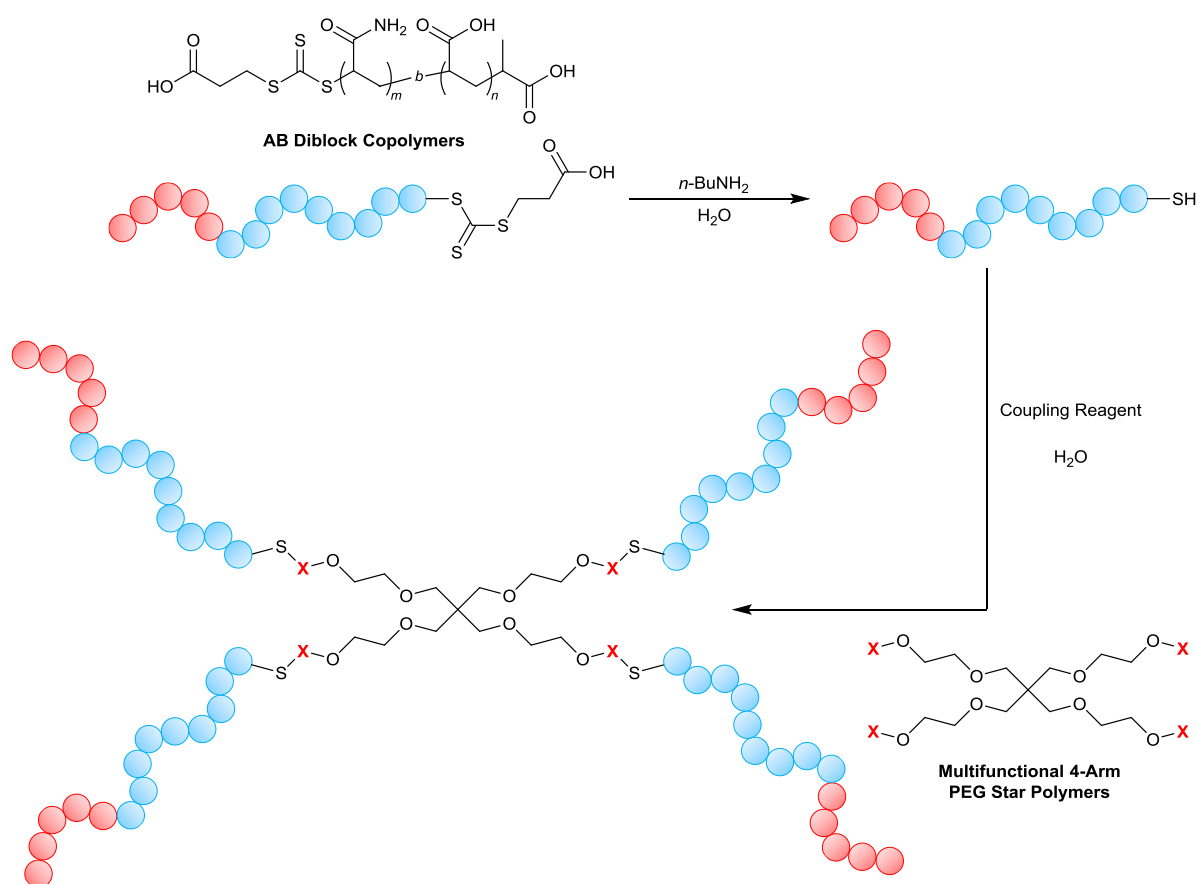


Figure 4.1. Schematic for the reaction between the AB diblock copolymers and multifunctional 4-arm PEG star polymers.

## Chapter 4

Three different synthetic pathways classified as thiol-ene, thiol-norbornene, and thiol-epoxy reactions were employed in an attempt to synthesise the desired 4-arm well-defined star-shaped copolymers. This general approach was selected as it was hypothesised to be an efficient pathway by utilising the pre-existing AB diblock copolymer. However, these types of reactions were proven to be difficult to achieve despite their high reactivities and fast reaction kinetics. This was primarily attributed to the steric hindrance due to the high molecular weight of the AB diblock copolymers and thus these methods were deemed to be unsatisfactory. This Appendix section outlined the prominent attempts of employing thiol-ene, thiol-norbornene, and thiol-epoxy methods to create the desired 4-arm star-shaped block copolymers.

### 4.4.1. Synthesis of 4-arm star-shaped copolymers *via* thiol-ene reactions

Prior to the coupling stage, the thiocarbonylthio functionality on the AB diblock copolymer chain was converted into a thiol *via* an aminolysis step under inert conditions to prevent disulfide couplings. Due to the weak sulfur-hydrogen bonding, this allows for fast couplings with other active functionalities under mild conditions. Thiol-ene click chemistry was initially selected for the synthesis of the desired star-shaped block copolymers due to its high efficiency and versatility. Once created, the thiol-terminated was then subjected to thiol-ene coupling by Michael-addition reaction with a commercially available 4-arm star PEG-acrylamide polymer (PEG-AM). The reaction schematic for this thiol-ene coupling process is shown in Figure 4.2.

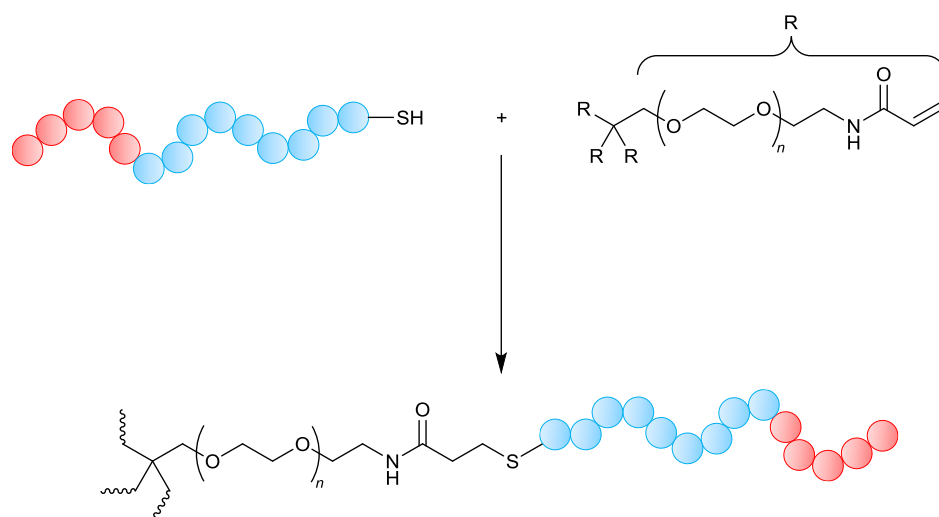


**Figure 4.2.** General reaction schematic for the synthesis of 4-arm star-shaped block copolymers *via* thiol-ene reaction.

Initial thiol-ene experiments were conducted using a trial AB diblock copolymer with molecular weight of approximately 50 kDa, rather than the pre-existing AB diblock copolymers synthesised in Chapter 2 (molecular weights of approximately 500 kDa). The reason behind this was to determine the rough reaction conditions to achieve optimal coupling. In addition, these test experiments would determine whether the Michael-addition reaction would be suitable for these high molecular weight polymers.

Several trial thiol-ene experiments were performed with varying reaction conditions. Both the aminolysis and coupling steps were performed concurrently as a one-pot synthesis initially. Due to its lack of success, the aminolysis and coupling steps were then performed sequentially in one-pot, as well as sequentially in two separate reaction flasks. However, one of the main undesired reactions that would occur with the aminolysis step was disulfide coupling. Therefore, in addition to deoxygenation by argon bubbling, tris(2-carboxyethyl)phosphine (TCEP) was employed to aid with the reduction of unwanted disulfide linkages. A summary of the noteworthy thiol-ene experiments is shown in Table 4.1.

Table 4.1. Thiol-ene couplings between thiol-terminated AB diblock copolymers and a 4-arm star PEG-acrylamide polymer ( $M_n = 2,000$  Da).

Entry	$M_{n,sec}$ of AB Diblock (kDa)	Type of Synthesis	[BuNH <sub>2</sub> ]:[C=S]	[TCEP]:[C=S]	Final $M_{n,sec}$ (kDa)
1	50.7 ( $\mathcal{D} = 1.37$ )	One-pot	20,000:1	100:1	58.2 ( $\mathcal{D} = 1.49$ )
2	50.7 ( $\mathcal{D} = 1.37$ )	Sequentially in one-pot	20,000:1	100:1	66.3 ( $\mathcal{D} = 1.38$ )
3	50.7 ( $\mathcal{D} = 1.37$ )	Sequentially in separate pots	20,000:1	100:1	54.7 ( $\mathcal{D} = 2.28$ )
4	4.07 ( $\mathcal{D} = 1.21$ )	One-pot	5:1	5:1	3.95 ( $\mathcal{D} = 1.29$ )
5	4.07 ( $\mathcal{D} = 1.21$ )	Sequentially in one-pot	5:1	5:1	3.97 ( $\mathcal{D} = 1.28$ )
6	4.07 ( $\mathcal{D} = 1.21$ )	Sequentially in separate pots	5:1	5:1	3.87 ( $\mathcal{D} = 1.30$ )

## Chapter 4

The thiol-ene coupling reactions were performed with an AB diblock copolymer loading of 0.5 wt%. This concentration was assigned to be similar to that of the aminolysis reactions for the synthesis of the ABA triblock copolymers (Chapter 2). The ratio between *n*-butylamine and the thiocarbonylthio functionality was fixed at an optimal ratio of 20,000:1 due to the high molecular weight of the thiol-terminated AB diblock copolymer (50.7 kDa). However, for the lower molecular weight species (4.07 kDa), this ratio was brought down to 5:1 as the excess quantity of *n*-butylamine was hypothesised to be unnecessary for optimal conversion. As for the ratio of TCEP to the thiocarbonylthio functionality, this ratio was also brought down from 100:1 to 5:1 with the decrease in the molecular weight of the AB diblock copolymer.

As observed in Table 4.1, the small changes in the molecular weight before and after the thiol-ene reaction indicated unsuccessful coupling. In the one-pot synthesis, the molecular weight increased to 58.2 kDa from 50.7 kDa. This increment was slightly better (up to 66.3 kDa) when the thiol-terminated polymer was synthesised first, prior to introducing PEG-AM in the same reaction mixture. When these two reactions were performed separately, only a slight increase the molecular weight was observed (54.7 kDa) alongside a broader molecular weight distribution.

When a lower molecular weight polymer was employed, all three types of reaction displayed minimal changes. These poor results were possibly attributed to the high molecular weight of the polymer. Coiling effects would result in shielding of the active functional groups on both the AB diblock copolymer and PEG-AM, which most likely inhibited the coupling reaction. In addition, results obtained from the lower molecular polymer indicated that this type of coupling was unsuitable, due to slow reaction kinetics.

### 4.4.2. Synthesis of 4-arm star-shaped copolymers *via* thiol-norbornene reactions

A different reaction pathway was sought out to synthesise the desired star-shaped copolymers. This involved the use of the highly reactive norbornene functionality. Light-mediated thiol-norbornene reactions have the potential to reach near-quantitative conversion due to relief of the norbornene ring

## Chapter 4

strain. Consequently, a coupling strategy between the AB diblock copolymers and the 4-arm star PEG-norbornene (PEG-NBN) was employed at various reaction conditions (Figure 4.3). Lithium phenyl-2,4,6-trimethylbenzoylphosphinate (LAP) was employed as the photoinitiator for this reaction.

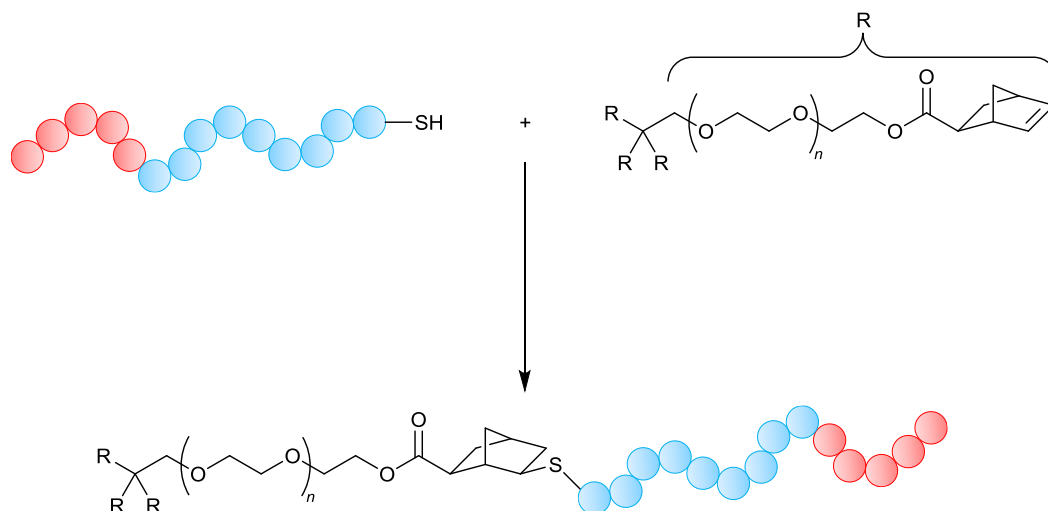


**Figure 4.3.** General reaction schematic for the synthesis of 4-arm star-shaped block copolymers *via* thiol-norbornene reaction.

The thiol-norbornene coupling was initially performed in a small UV-crosslinker with five 365 nm lamps. The reaction was later on performed in a larger UV-reactor with 16 365 nm lamps to see the effect of higher intensity on the coupling efficiency. Due to its high reactivity, a short initial irradiation time of 10 minutes was applied to the reaction mixture. Further irradiation was applied for another 20 minutes to allow for comparison between different irradiation times. The concentration of LAP was maintained at 2.2 mM in all the thiol-norbornene reactions as this concentration was optimal and typical in previous studies. A summary of the noteworthy thiol-norbornene experiments is shown in Table 4.2.

The thiol-norbornene reactions were conducted using thiol-terminated AB diblock copolymers produced from a separate aminolysis reaction. Unlike the thiol-ene reactions, the reactants (AB diblock copolymer and PEG-NBN) loading for the coupling was fixed at approximately 10 wt%. An initial trial experiment with a short chain polymer ( $M_{n,SEC}$  of 4.07 kDa) showed a drop in the overall molecular weight to 1.09 kDa after 10 minutes of irradiation. This decrease was a result of a high molecular weight

## Chapter 4

shoulder observed in the overall molecular weight distribution of the final product. The molecular weight of this shoulder was determined to be approximately four times larger than that of the AB diblock copolymer. It was suspected that this peak represented the coupled star product. However, the intensity of this peak was approximately one third compared to the original AB diblock copolymer, which indicated incomplete coupling. A further 20 minutes of irradiation did not change the molecular weight distribution. This implied that the initial 10 minutes of irradiation completely consumed the LAP photoinitiator present in the reaction mixture.

The same reaction conditions was applied to another AB diblock copolymer with slightly higher molecular weight ( $M_{n,SEC}$  of 7.50 kDa). This time, the overall molecular weight increased to 12.6 kDa. Similar molecular weight distributions were observed where a high molecular weight peak was obtained after irradiation. This peak was determined to be six times the original molecular weight of the AB diblock copolymer. However, the coupling efficiency was still low, and further irradiation did not affect this.

Table 4.2. Thiol-norbornene couplings between thiol-terminated AB diblock copolymers and a 4-arm star PEG-norbornene polymer ( $M_n = 5,000$  Da).

Entry	$M_{n,SEC}$ of AB Diblock (kDa)	Irradiation Intensity (W)	Irradiation Time (mins)	[LAP] (mM)	Final $M_{n,SEC}$ (kDa)
<b>7</b>	4.07 ( $\mathcal{D} = 1.21$ )	5 × 8 W	10	2.2	1.09 ( $\mathcal{D} = 7.89$ )
<b>8</b>	4.07 ( $\mathcal{D} = 1.21$ )	5 × 8 W	30	2.2	1.07 ( $\mathcal{D} = 8.03$ )
<b>9</b>	7.50 ( $\mathcal{D} = 1.25$ )	5 × 8 W	10	2.2	12.6 ( $\mathcal{D} = 2.00$ )
<b>10</b>	7.50 ( $\mathcal{D} = 1.25$ )	5 × 8 W	30	2.2	12.6 ( $\mathcal{D} = 2.02$ )
<b>11</b>	7.50 ( $\mathcal{D} = 1.25$ )	16 × 8 W	10	2.2	10.4 ( $\mathcal{D} = 1.73$ )
<b>12</b>	7.50 ( $\mathcal{D} = 1.25$ )	16 × 8 W	30	2.2	10.1 ( $\mathcal{D} = 1.84$ )

## Chapter 4

It was suspected that the intensity of the irradiation had an important role in this coupling process. Therefore, the same reaction was repeated in a large UV-reactor with triple the UV-intensity. However, despite the new set-up and the amplified irradiation intensity, minimal changes in the results were observed. This new set-up led to a smaller increase to the overall molecular weight. The relative intensity of the high molecular weight shoulder was observed to be less than one third compared to the AB diblock copolymer. Although there were improvements in the results with respect to thiol-ene, the coupling efficiency was still inadequate. This would also drastically decrease if the thiol-norbornene methodology was applied to a polymer with molecular weight of at least 500 kDa. Therefore, another coupling technique was employed to synthesise the desired star-shaped copolymers at higher efficiency.

### 4.4.3. Synthesis of 4-arm star-shaped copolymers *via* thiol-epoxy reactions

After the unsuccessful attempts with the thiol-norbornene strategy, a 4-arm star PEG-epoxide polymer (PEG-EPX) was employed. The thiol-epoxy method was selected due to its high yield and high regioselectivity under ambient conditions. This method did not require an photoinitiator like the thiol-norbornene method. Lithium hydroxide is typically used as the base catalyst in the thiol-epoxy reaction and thus it was employed in this study. Glutathione was initially employed to test the viability of this reaction, subsequently followed by higher molecular weight AB diblock copolymers (7.50 or 751 kDa). The overall schematic for the thiol-epoxy process is shown in Figure 4.4.

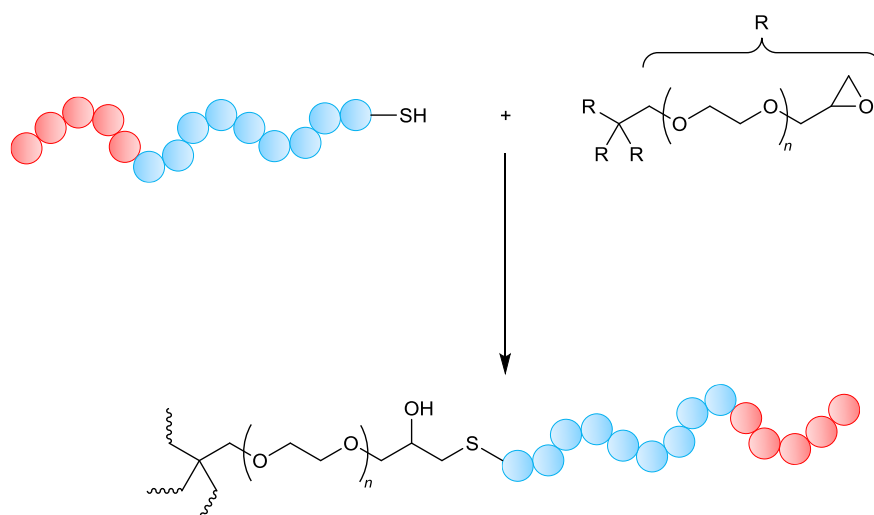


**Figure 4.4.** General schematic for the synthesis of 4-arm star-shaped block copolymers *via* thiol-epoxy reaction.

The thiol-epoxy reactions were conducted using thiol-terminated AB diblock copolymers produced from a separate aminolysis reaction. The concentration of the reactants (AB diblock copolymer and PEG-EPX) was initially maintained at 5 wt%. The ratio between lithium hydroxide and the thiol functionality was varied based on the molecular weight of the thiol-terminated species. A summary of the noteworthy thiol-epoxy experiments is shown in Table 4.3.

The initial trial experiment with glutathione and a short chain PEG-EPX ( $M_n$  of 600 Da) was successful.  $^1\text{H}$  NMR data confirmed successful coupling of all four terminals on the PEG-EPX to four molecules of glutathione. This reaction was performed at room temperature with a lithium hydroxide to thiol ratio of only 0.3:1. Based on this result, similar reaction conditions were employed for the coupling between a high molecular weight AB diblock copolymer ( $M_{n,\text{SEC}}$  of 7.50 kDa) and PEG-EPX ( $M_n$  of 2,000 Da). The ratio between lithium hydroxide to thiol was increased to 72:1 for two reasons. The high molecular weight of the AB diblock copolymer led to coiling effects on the polymer chain, which had the potential to shield the active thiol functionality from interacting with the base. In addition, the A block comprised of acidic carboxyl functionality which would also interact with the base. Therefore, the concentration of lithium hydroxide was increased in excess to counteract these problems.

## Chapter 4

As observed in Table 4.3, the overall molecular weight of the AB diblock copolymer increased from 7.50 kDa to 10.4 kDa after the coupling process. This final overall molecular weight was lower than what was theoretically expected due to a bimodal molecular weight distribution. The high molecular weight peak had a slightly lower intensity compared to that of the low molecular weight, which indicated incomplete coupling. Consequently, the concentration of the reactants were subsequently reduced to 1 wt% from 5 w % to reduce any negative effects associated with the viscosity of the reaction mixture.

Table 4.3. Thiol-epoxy coupling reactions between thiol-terminated AB diblock copolymers and 4-arm star PEG-epoxide polymers ( $M_n = 600$  or  $2,000$  Da).

Entry	$M_{n,SEC}$ of AB Diblock (kDa)	Concentration of Reactants (wt%)	Reaction Temperature (°C)	[LiOH]:[SH]	Final $M_{n,SEC}$ (kDa)
<b>13</b>	Glutathione (MW = 307 Da)	5	25	0.3:1	N/A
<b>14</b>	7.50 ( $\bar{D} = 1.25$ )	5	25	72:1	10.4 ( $\bar{D} = 1.75$ )
<b>15</b>	7.50 ( $\bar{D} = 1.25$ )	1	25	72:1	14.6 ( $\bar{D} = 1.50$ )
<b>16</b>	751 ( $\bar{D} = 1.25$ )	1	25	20,000:1	892 ( $\bar{D} = 2.01$ )

## Chapter 4

With a decrease in the concentration of the reactants, a slightly larger increase in the overall molecular weight was observed. This corresponded to a final overall molecular weight of approximately 14.6 kDa rather than 10.4 kDa when 5 wt% of reactants were employed. A bimodal molecular weight distribution was still present. However, the intensity of the higher molecular weight peak was higher compared to that of the lower molecular weight species. Theoretical calculations based on the  $^1\text{H}$  NMR data was also indicative of this. At a reactants concentration of 5 wt%, the ratio of attachment of the AB diblock copolymer onto the PEG-EPX core was determined to be only approximately 1.3:1. With a lower reactants concentration of 1 wt%, this ratio increased to 1.7:1. This indicated that the coupling was slightly more successful with this decrease in the reactant concentration. Despite this, the coupling efficiency was still inadequate.

The thiol-epoxy method was also employed on an AB diblock copolymer with  $M_{n,SEC}$  of 751 kDa. The reactants concentration was maintained at 1 wt%. This reaction led to an increase in the overall molecular weight up to 892 kDa. Based on the  $^1\text{H}$  NMR data, the attachment ratio between the AB diblock copolymer and the PEG-EPX was determined to be 1.3:1. These results confirmed that coupling was significantly more difficult when the AB diblock copolymer had a larger molecular weight. Despite best efforts at attaching the thiol-terminated AB diblock copolymer onto a multifunctional star-shaped core, the coupling efficiency was inadequate throughout all three different methods. The molecular weights of the final products were insufficient for flocculation comparison with the ABA triblock copolymers. Therefore, these three methodologies were determined to be unsuccessful. The high molecular weight of the pre-existing AB diblock copolymers made it difficult for coupling. Consequently, it was determined that better success would be achieved if the star-shaped copolymers were synthesised from the very beginning.

This page is intentionally left blank.

# Chapter 5

Conclusions and Outlooks

This page is intentionally left blank.

# Chapter 5

## Conclusions and Outlooks

---

### 5.1. Project Conclusions

This thesis has presented and discussed the developments and flocculation testings of several well-defined ultra-high molecular weight (UHMW) anionic polymers with advanced architectures, which were derived from acrylic acid (AA) and acrylamide (AM) monomers. Two different types of architectures were targeted: ABA triblock copolymers and star-shaped AB block copolymers. The anionic A block was designed to be located at the terminals, while the non-ionic B block remained at the centre or core of the polymer chain.

Eight different UHMW ABA triblock copolymers (**ABA1 – ABA8**) were synthesised and characterised as discussed in Chapter 2. The overall molecular weights of these ABA triblock copolymers were targeted to be approximately 1 MDa. These ABA triblock copolymers were synthesised in a three-stage process. The first of which employed an aqueous RAFT-mediated gel polymerisation process, where eight different living homopolymers of AA were created with molecular weights ranging from 5.21 kDa to 173 kDa ( $\bar{D} < 1.20$ ). The second stage used the same RAFT polymerisation process and the living homopolymers as the macro chain transfer agent to extend the polymer chain with AM. Several reaction conditions were employed to achieve optimal growth in the molecular weight, due to inefficient chain extension associated with the macro-CTAs possessing high molecular weights. Consequently, this led to the synthesis of eight different UHMW AB diblock copolymers with molecular weights of approximately 500 kDa ( $\bar{D} < 1.50$ ).

## Chapter 5

RAFT polymerisation was once again employed to incorporate a third block onto the polymer chain. However, due to the high molecular weight of the AB diblock copolymers, the chain extension efficiency was inadequate. Therefore, an aminolysis process was utilised to convert the thiocarbonylthio functionality on the polymer chain into a thiol. Under optimal oxidation conditions, these thiol functionalities coupled to form the desired ABA triblock copolymers with molecular weights ranging from 967 kDa to 1.21 MDa ( $D < 1.70$ ).

In Chapter 3, the novel UHMW ABA triblock copolymers were tested for their flocculation efficiencies in high ionic strength kaolin slurries, where three different concentrations of  $\text{Ca}^{2+}$  (0.05 M, 0.10 M, and 0.50 M) were employed. Three control polymers (homopolymer of AA, **PAA**; homopolymer of AM, **PAM**; and random copolymer of AA and AM, **RAB**) were also synthesised. Polymer **RAB** possessed an architecture that is comparable to that of commercial flocculants and thus was created and utilised for direct flocculation comparison with the ABA triblock copolymers.

Cylinder settling tests were performed initially where the settlement rates and the supernatant turbidity were evaluated as the flocculant dosage increased from 17 to 67 g/tds. The ABA triblock copolymers were able to flocculate the kaolin suspension consistently even with a high concentration of  $\text{Ca}^{2+}$ , whereas the flocculation efficiency of **RAB** deteriorated rapidly with the same increase in the level of  $\text{Ca}^{2+}$ . In addition, the ABA triblock copolymers were able to clarify the colloidal suspension efficiently, where the supernatant turbidity values obtained were lower than those of **RAB** across all three concentrations of  $\text{Ca}^{2+}$  employed. Consequently, turbulent pipe flow with an in-line FBRM probe was utilised as a supplementary method to gain a better understanding of the flocculation mechanism and the aggregate profile. It was observed that the aggregation induced by **RAB** was significantly affected by the excess level of cations, whereas the ABA copolymers were relatively unaffected. In addition, the aggregate profile showed that these ABA triblock copolymers targeted smaller colloidal particles, which consequently led to better clarification of the slurry.

## Chapter 5

Deviating away from ABA triblock copolymer architecture, Chapter 4 focused on the synthesis and flocculation analysis of six 4-arm star-shaped AB block copolymers (**SAB1** – **SAB6**). A three-stage procedure was required to synthesise these polymers. A 4-arm star RAFT agent (**4A-CTA**) was synthesised and used as the initial chain transfer agent. The star-shaped block copolymers were subsequently created using the same aqueous RAFT-mediated gel polymerisation process employed for the synthesis of the ABA triblock copolymers. Cylinder settling tests in high ionic strength kaolin slurry ( $\text{Ca}^{2+}$  concentrations of 0.05 M, 0.10 M, and 0.50 M) were once again performed with flocculant dosages ranging from 17 to 67 g/tds. The flocculation efficiencies of the star-shaped block copolymers were also directly compared to those of the control polymers **PAA**, **PAM**, and **RAB**. While the flocculation efficiency of **RAB** diminished rapidly with the increase in the concentration of  $\text{Ca}^{2+}$ , the star-shaped block copolymers also exhibited strong stability under high ionic strength environments.

To this end, the well-defined UHMW ABA triblock and star-shaped copolymers developed in this project showed promising efficiencies as polymeric flocculants in high ionic strength environments. With further developments and flocculation testings, these polymers could have the potential to be implemented into current industrial applications of flocculation.

### 5.2. Project Outlooks

The effect of multivalent cations on the flocculation efficiency of anionic polymer flocculants is well studied. However, little work has been done to develop a solution that can comprehensively address this problem. There are several potential pathways this project could adopt in the future to further narrow the research gaps associated with this challenge.

All of the polymers developed in this project had molecular weights of approximately 1 MDa. While this is considered as UHMW, polymers currently being employed in commercial applications can have molecular weights going up to 20 MDa. The synthesis of ultra-high molecular weight polymers using reversible-deactivation radical polymerisation (RDRP) processes is currently known to be challenging, particularly for those with complex architectures. However, if polymers with well-defined advanced architectures can be developed at high molecular weights (ranging from 5 to 20 MDa), this would unlock promising potentials for the field of flocculation, while also advancing the field of controlled radical polymerisation. RDRP processes can also be employed to create similar molecular weight polymeric flocculants with low ( $\mathcal{D} \approx 1-2$ ), medium ( $\mathcal{D} \approx 4-5$ ), and high dispersity ( $\mathcal{D} > 10$ ). This would allow for a comprehensive study on the effect of dispersity on the flocculation efficiency of block copolymers.

In addition to higher molecular weights, other monomers can be explored in the synthesis of the ABA triblock copolymers and the star-shaped AB block copolymers. For example, polyethylene oxide can be used to substitute for acrylamide, whilst 2-acrylamido-2-methylpropane sulfonic acid can substitute for acrylic acid. This would allow for comparison with the polymers discussed in this thesis and determine whether the change in monomers have a positive or negative impact on the flocculation efficiency in high ionic strength environments.

RDRP techniques have the potential to create polymers with complex architectures. Apart from the ABA triblock and star-shaped block architectures targeted in this project, polymers with more advanced architecture can be synthesised and tested for flocculation efficiency. The proposed architectures can

## Chapter 5

include graft copolymer, multi-arm star-shaped block copolymers, and hyperbranched block copolymers. In addition, the anionic blocks currently located at the terminals of the polymer chain can be redistributed in smaller portions throughout the whole polymer chain to see the effect this has on the flocculation efficiency. While this has a similar architecture compared to that of random copolymers, the blocks would be well-defined and designed to allow for maximum solubility in high ionic strength environment.

The flocculation analysis techniques could be further improved by employing advanced automated systems where the settling rate and supernatant turbidity are quantified under well-controlled and consistent environment. As this technique and the scientific results progress, a small-scale pipe reactor can be employed to gain further data that could lead to the implementation of these well-defined UHMW polymers in industrial applications of flocculation.

This page is intentionally left blank.